Existe-t-il un lien entre complexité génomique et évolution clinique dans les tumeurs musculaires lisses utérines ?

Sabrina Croce

N°d'ordre NNT : 2020LYSE1071

THESE de DOCTORAT DE L'UNIVERSITE DE LYON

opérée au sein de

l'Université Claude Bernard Lyon 1

Ecole Doctorale 340

Biologie Moléculaire Intégrative et Cellulaire

Spécialité de doctorat : Cancérologie

Soutenue publiquement

Le 6 Mai 2020

par :

Sabrina Croce

« Existe-t-il un lien entre complexité génomique et évolution clinique dans les tumeurs musculaires lisses utérines ? »

Devant le jury composé de :

Madame Florence DUFFAUD, PU-PH, Université Aix-Marseille	*Rapporteure*
Monsieur Philippe MORICE, PU-PH, Université Paris Sud	*Rapporteur*
Madame Isabelle RAY-COQUART, PU-PH, Université Lyon1	*Examinatrice*
Madame Sophie LE GUELLEC, PH, Oncopole Toulouse	*Examinatrice*
Monsieur Germain GILLET, PU-PH, Université Lyon 1, BMIC	*Examinateur*
Monsieur Philippe ROCHAIX, PH, Oncopole Toulouse	*Examinateur*
Monsieur Laurent ARNOULD, PH, Centre anticancéreux Dijon	*Examinateur*

Madame Mojgan DEVOUASSOUX-SHISHEBORAN, PU-PH, Université Lyon1 Directrice de thèse

Monsieur Frédéric CHIBON, DR2, CRCT Toulouse Co-directeur de thèse

τὸν φρονεῖν βροτοὺς ὁδώσαντα,
τὸν πάθει μάθος
θέντα κυρίω ἔχειν. *Αγαμεμνων–Αισχυλος*

Il [Zeus] conduit les hommes dans la voie de la sagesse, et il a décrété qu'ils posséderaient la science par la douleur.

Agamemnon-Eschyle- de Leconte de Lisle

REMERCIEMENTS

Je tiens tout d'abord à remercier les rapporteurs, Pr Florence Duffaud et Pr Philippe Morice et les membres du jury, Pr Isabelle Ray-Coquard, Dr Sophie Le Guellec, Pr Germain Gillet, Dr Philippe Rochaix qui ont accepté d'évaluer mon travail en particulier dans les circonstances actuelles difficiles dues à la pandémie en cours.

Un remerciement particulier à mes deux Directeurs de Thèse Mojgan et Fred qui m'ont encouragée, soutenue et guidée avec corrections et conseils avisés au long des trois années de thèse et bien avant.

La collaboration avec Fred a débuté il y a neuf ans et continue avec plusieurs projets en cours qui termineront, je l'espère, pas avant nos respectives retraites. En plus qu'une riche et fructueuse collaboration scientifique une amitié et une estime profonde de ma part s'est établie.

Mojgan, je te remercie pour m'avoir incluse dans ton EPU, de m'avoir impliquée dans tes projets scientifiques et d'avoir déplacé mers et montagnes pour que je puisse m'inscrire, suivre et terminer le doctorat, je n'y crois pas encore. Le doctorat n'est, j'espère, que le début de notre collaboration avec plein de projets ensemble !

Germain, je vous remercie pour le soutien, votre amabilité et empathie quand je naviguais dans les méandres administratifs de l'Ecole doctorale.

Isabelle, je te remercie pour ta disponibilité et amabilité et patience en particuliers lors des comité de suivi de thèse.

Philippe, je te remercie d'avoir accepté d'être juré et de la sympathie avec laquelle tu m'a accueillie dans ton laboratoire.

Sophie, la pathologie nous a fait nous rencontrer, le trail notre passion nous unit et une profonde amitié nous soude.

Laurent, je te remercie de la sympathie et de la jovialité avec la quelle tu m'accueilles lors de nos réunions de relecture.

Je remercie les personnes que j'ai rencontré en chemin et qui m'ont aidé avec leur compétence, disponibilité et empathie : Tom Lesluyes, Gaëlle Pérot, Valérie Velasco, Isabelle Hostein mais la liste est longue et je m'excuse par avance si je ne peux pas tous les mentionner.

Enfin je tiens à remercier qui me soutiennent au quotidien dans la vie depuis 16 ans ou depuis toujours : Jean-François (Topo), Maïa, Udo, mes parents et Marie-Claude. Le quotidien avec une épouse, une mère, une fille ou belle-fille comme moi peut être dur...

RESUME

Les sarcomes à génomique complexe sont caractérisés par un génome remanié en l'absence d'un évènement génomique récurrent connu et les léïomyosarcomes (LMS) font partie de ce groupe. Les tumeurs musculaires lisses utérines se divisent selon l'évolution clinique en léiomyomes (LM) et LMS et selon la morphologie en fusocellulaires, épithélioïdes et myxoïdes avec des critères diagnostiques distincts. Si ces critères sont suffisants pour un diagnostic lésionnel correct dans la majorité des cas, ils ne permettent pas la distinction entre un LM et un LMS dans un faible pourcentage de tumeurs. Dans ces cas la tumeur est dénommée « tumeur musculaire lisse utérine à potentiel de malignité incertain » (STUMP) posant un problème de prise en charge clinique. Certains variants comme le léiomyome à Noyaux Bizarres (LM-BN) pose un véritable problème diagnostique. D'évolution clinique bénigne, il présente un profil génomique hétérogène pouvant être complexe. L'analyse de la complexité du profil génomique basée sur le calcul du Genomic Index (GI) issu de la signature CINSARC (Complexity INdex in SARComas) a démontré sa valeur pronostique dans les sarcomes des tissus mous à génomique complexe, mais également dans les GIST. Notre hypothèse est qu'à l'instar des sarcomes des tissus mous le degré de complexité génomique est corrélé à l'évolution clinique dans les tumeurs musculaires lisses utérines. Le but de ce travail de thèse était d'étudier sur plusieurs tumeurs musculaires lisses utérines, bénignes, malignes et STUMP, de type fusiforme et les variantes à noyaux bizarres et épithélioïdes, le profil génomique par CGH-array et la signature d'expression CINSARC en utilisant la technique de Nanostring, en corrélation avec l'évolution clinique. Une première étude publiée a permis de confirmer que la complexité génomique est liée à l'évolution des tumeurs musculaires lisses utérines et peut être un outil diagnostique complémentaire à l'analyse morphologique. Nous avons testé cette hypothèse sur une série de 70 tumeurs musculaires lisses utérines et démontrer que le GI au seuil de 10 distingue les tumeurs sans récidive (LM) des tumeurs avec risque accru de récidive et d'évolution létale (LMS) en démembrant la catégorie de STUMP. Avec l'application de la signature CINSARC au matériel fixé en formol, par technologie Nanostring nous avons démontré sur une série de 60 LMS que cette signature est pronostique en survie globale et libre de maladie. De plus la signature CINSARC NANOCIND a montré sa valeur pronostique dans les LMS utérins de stade I pour lesquels la chimiothérapie adjuvante est discutée, sans efficacité prouvée. La signature CINSARC Nanocind® se propose comme un outil de randomisation dans les essais cliniques à venir. Nous avons par ailleurs analysé les profiles génomiques par array-CGH d'une série de 69 LM-BN et démontré que le LM-BN est une entité séparée du LM et du LMS identifiant 3 sous-types distincts de LM-BN : un groupe *FH*-déficient, un associé aux altérations de *TP53* avec un génome plus remanié et un groupe sans altérations récurrentes. Notre étude souligne l´importance de l'intégration des données génomiques au contexte morphologique et clinique. Pour terminer nous avons validé le seuil du GI sur une plateforme génomique (AGILENT 180K) différente de celle d'origine (AGILENT 60K) et nous avons exploré le GI dans le variant à cellules épithélioïdes. Ainsi, la complexité génomique est corrélée à l'évolution clinique et l'étude du profil génomique des tumeurs musculaires lisses de l'utérus est utilisable en pratique quotidienne dans les lésions où la morphologie seule ne permet pas la distinction d'une tumeur bénigne d'une tumeur avec un potentiel évolutif, à condition d'intégrer ces données dans le contexte clinique et morphologique. La signature CINSARC dans les LMS de stade I peut permettre une meilleure prise en charge des patientes.

ABSTRACT

Sarcomas with complex genomics such as leiomyosarcomas (LMS) are characterized by an altered genome in the absence of a known recurrent "driver" genomic event. According to their clinical outcome, smooth muscle uterine tumours are divided into leiomyomas (LM) and LMS, and as spindle, epithelioid and myxoid variants with distinct diagnostic criteria depending on their morphology. The morphologic criteria are efficient but with some exceptions. In these cases, the tumour should be termed « smooth muscle tumour with uncertain malignant potential" (STUMP) and only the outcome can confirm its benign or malignant nature. Moreover, for some LM variants such as Bizarre Nuclei leiomyoma (BN-LM), the diagnosis may be particularly difficult. Even though BN-LM has a favourable outcome, it can harbour a complex genomic profile. The analysis of the complexity of a tumour's genomic profile based on its Genomic Index (GI) obtained with the CINSARC (Complexity INdex in SARComas) signature has demonstrated its prognostic value, not only in genomically complex soft tissue sarcomas but also in GIST. We hypothesized that, as in soft tissue sarcomas, the degree of genomic complexity in uterine smooth muscle tumours correlates with their clinical outcome. The aim of this PhD dissertation using array-CGH and the CINSARC signature by Nanostring was to study the genomic profile of several series of benign and malignant uterine tumours and STUMP tumours with spindle, epithelioid and Bizarre Nuclei variants and to correlate the results with clinical outcome.

In our first paper, we demonstrated that the genomic complexity of uterine smooth muscle tumours is related to their clinical outcome and that genomic analysis by array-CGH is a useful diagnostic tool complementary to the morphological approach. We subsequently demonstrated in a larger series of 70 tumours that the GI at the threshold of 10 splits STUMP into two groups: those without recurrence and with a similar behaviour to LM, and a second group with a rate of recurrence and death akin to LMS but more indolent. We demonstrated the prognostic value of the CINSARC Nanocind® signature by Nanostring technology on 60 formalin-fixed, paraffin-embedded uterine LMS for overall and disease-free survival. These results were confirmed even on stage I LMS, for which the efficacy of adjuvant chemotherapy remains to be proven. The CINSARC Nanocind® signature could be a useful tool for randomization in future clinical trials evaluating the benefit of adjuvant treatment on uterine LMS, in particular at an early stage. We also analysed the genomic profiles of 69 BN-LM by array-CGH and demonstrated that BN-LM is an entity different from LM and LMS. We identified 3 distinct BN-LM subtypes: an *FH*-deficient group, a group associated to *TP53* alterations with chromosomal instability. And a third without recurrent alterations. Our results highlight the importance of integrating genomic data into the morphological and clinical context. Finally, we validated the GI threshold on a genomic platform (AGILENT 180K) different from the original one (AGILENT 60K) and We explored genomic profiles also for the epithelioid variant. Thus, genomic complexity correlates with outcome so genome profile analysis is a diagnostic tool complementary to morphology for distinguishing benign tumours from tumours with a risk of recurrence. The CINSARC signature may allow better patient management, especially in stage I LMS.

AVANT PROPOS

Le sujet de ma thèse nait d'une part d'un besoin clinique et anatomopathologique urgent que j'ai vécu et que je vis au quotidien avec passion : le diagnostic des tumeurs musculaires lisses utérines dans un centre expert des sarcomes et de gynécologie et d'autre part de ma curiosité et du besoin de pousser mes connaissances (ou pour mieux dire de repousser mon ignorance) sur ces tumeurs et sur le plus vaste sujet des mécanismes de la tumorigenèse des lésions mésenchymateuses gynécologiques. En effet sur le plan anatomopathologique le diagnostic histologique de la majorité des tumeurs musculaires lisses utérines ne pose pas de problème et les critères morphologiques à la base du diagnostic sont efficients. Il existe néanmoins un pourcentage de cas (qui peut être important dans les centres experts à qui ces cas sont adressés pour deuxième ou troisième avis) où les critères diagnostiques ne permettent pas aux pathologistes de distinguer une lésion musculaire lisse bénigne (léiomyome, LM) d'une tumeur musculaire lisse maligne (léiomyosarcome, LMS). Dans ces cas, la tumeur est dénommée Tumeur Musculaire Lisse Utérine à Potentiel de Malignité Incertain (STUMP), qui n'est pas un diagnostic en soi et pose un réel problème de prise en charge clinique avec le risque de sous ou sur traitement et un stress psychologique chez la patiente. Par ailleurs il existe des exemples de tumeurs sans critère de malignité morphologique mais qui réservent une évolution clinique défavorable [1]. Un problème diagnostique majeur est représenté également par une variante de tumeur musculaire lisse cliniquement bénigne, le léiomyome à Noyaux Bizarres (LM-BN) [2], qui représente une vraie énigme aussi bien sur le plan diagnostique que biologique [3, 4].

J'ai la chance de collaborer depuis environ 9 ans avec le Dr Frédéric Chibon et son équipe, travaillant principalement sur l'étude des sarcome à génomique complexe le thème conducteur de ses recherches et depuis environ 5 ans avec le Pr Mojgan Devouassoux, pathologiste expert national et international en gynécopathologie et référent dans les réseaux TMRO (tumeur rares de l'ovaire) et RRePS (Réseau de Référence en Pathologie des Sarcomes des tissus mous et des viscères) gynécologique.

Dans cet environnement clinico-scientifique, associant la morphologie, l'analyse des profils génomiques des tumeurs musculaires lisses utérines et l'évolution clinique, nous avons formulé l'hypothèse que le pronostic des patientes présentant une tumeur musculaire lisse utérine est corrélé à la complexité génomique. Par conséquent l'étude génomique de ces tumeurs peut représenter un véritable outil diagnostique, en complément de la morphologie.

L'ensemble de ma thèse vise à démontrer cette hypothèse.

TABLE DES MATIERES

LISTE DES FIGURES

LISTE DES TABLEAU

1. INTRODUCTION

1. 1.1Généralité : La complexité génomique et le cancer

La modification du génome est le point commun à toute cellule cancéreuse, indépendamment de son histotype. La transformation d'une cellule normale en cellule tumorale nécessite la mutation ponctuelle, « driver » et non passagère (c'est à dire que la mutation est impliquée dans l'oncogenèse et donne un avantage sélectif à la cellule en favorisant sa croissance). Cette transformation nécessite des variations structurales des chromosomes et des modifications du nombre de copie des gènes car les mutations ponctuelles à elles seules ne sont pas suffisantes au développement d'une tumeur[5]. Les altérations varient de la modification nucléotidique (mutation) jusqu'aux réarrangements impliquant la totalité du génome (aneuploïdie). Une condition favorable pour que les altérations structurales des chromosomes aient lieu est l'instabilité chromosomique qui correspond à un état dynamique dans lequel la cellule gagne ou perd des chromosomes [6]. Le rôle de l'instabilité chromosomique dans les cancers est complexe et pas univoque. Si elle semble jouer un rôle pro-tumoral sur la cellule et concourir au développement des métastases [7] et corrèle avec la résistance aux traitements [8], elle prédispose à la chimiosensibilité comme démontré dans les carcinomes mammaires [9] et rectaux [10].

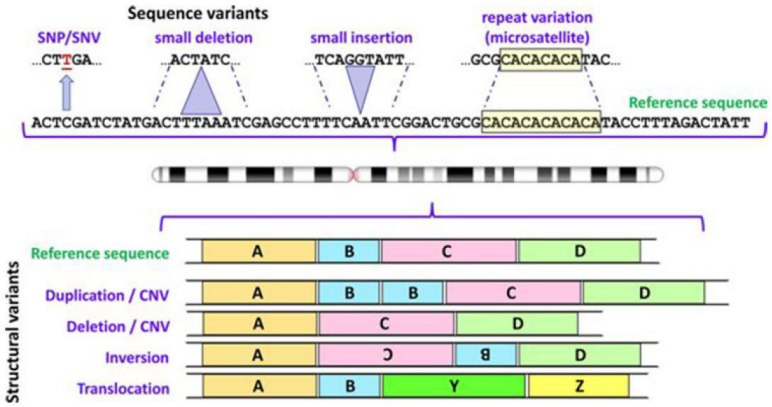

Figure 1. Altérations retrouvées dans les génomes humains.

En haut : Variations de un ou quelques nucléotides.
En bas : variations structurales
The genetic basis of the disease. Jackson M et al *Essays in Biochemistry* (2018)

Parmi les altérations structurales des chromosomes on dénombre les translocations, les délétions, les inversions et les duplications[11, 12](Fig 1). Les réarrangements équilibrés donnent lieu à des altérations sans gain ou perte de matériel chromosomique, sous la forme de translocations réciproques, inversions et insertions et ont pour conséquence la surexpression d'un gène inclus dans un point de cassure ou la création d'un gène hybride par la fusion des deux gènes de part et d'autre des points de cassure [13]. Ce mécanisme est central (driver) dans la pathogenèse d' environ 20% des sarcomes qu'on appelle «à génomique simple » c'est-à-dire que ces réarrangements équilibrés sont associés dans la majorité des cellules à une translocation [13] dont la cascade protéique qui en découle induit le sarcome, et la détection du réarrangement est intégrée dans les critères diagnostiques [14]. Parmi les tumeurs mésenchymateuses utérines les sarcomes du stroma endométrial de bas grade sont associés aux réarrangements de *JAZF1, PHF1, EPC1*[15, 16], et ceux de haut grade associés aux fusions impliquant les gènes *YWHAE et BCOR*[17-20]. D'autres entités comme les UTROSCT (Tumeurs utérines ressemblants aux tumeurs des cordons sexuels de l'ovaire) dans lesquelles des nouveaux réarrangements récurrents ont été récemment décrits (*GREB1, ESR1, NCOA*)[21, 22.23] seront probablement reclassées et mieux identifiées dans les années futures à la lumières des analyses génomiques à haut débit.

Les réarrangements non équilibrés entrainent la perte ou le gain de matériel génétique (ex duplications, délétions, translocations non réciproques)(Fig 1). En particulier les pertes de copies impactent plus fréquemment les gènes suppresseurs de tumeurs et les gains impactent les oncogènes par un mécanisme de haplo-insuffisance des gènes suppresseurs de tumeur et une triplo-sensitivité des oncogènes [24].

Selon le modèle de cancérogenèse reconnu, le cancer est constitué d'une accumulation d'événements génomiques séquentiels qui amènent à une complexité génomique dans la cellule (modèle de cancérogenèse multistep). La chromothripsis (du grec χρῶμασῶμα=chromosome, c'est-à-dire corps coloré et θρίψις/ τρίβω =réduire en miettes, râper) représente une exception à cette règle.

La chromothripsis consiste dans une fragmentation chromosomique produite par un nombre important de cassures double brins simultanées, suivie par un réassemblage aléatoire, le tout en un seul événement catastrophique, en brulant les étapes de l'évolution graduelle du génome[25](Fig 2). Le phénomène est limité à un ou deux chromosomes, car, s'il était étendu, il serait incompatible avec la survie de la cellule. A la base de la chromosthripsis il y aurait, parmi les mécanismes promoteurs, un défaut de ségrégation durant la mitose qui amène à la formation d'un micronoyau au moment de la télophase avec comme conséquence la pulvérisation des chromosomes pas complétement répliqués dans le micronoyau. Des mutations aux niveaux des proto-oncogènes et des onco-suppresseurs tels que *FBXW7* et *TP53* peuvent induire la formation de micronoyaux et donc favoriser la chromothripsis [26, 27]. Ce phénomène a été observé dans 2-3% des cancers mais jusqu'à 25% des cancers de l'os (ostéosarcomes et chordomes) et considéré comme signe de malignité[28, 29].

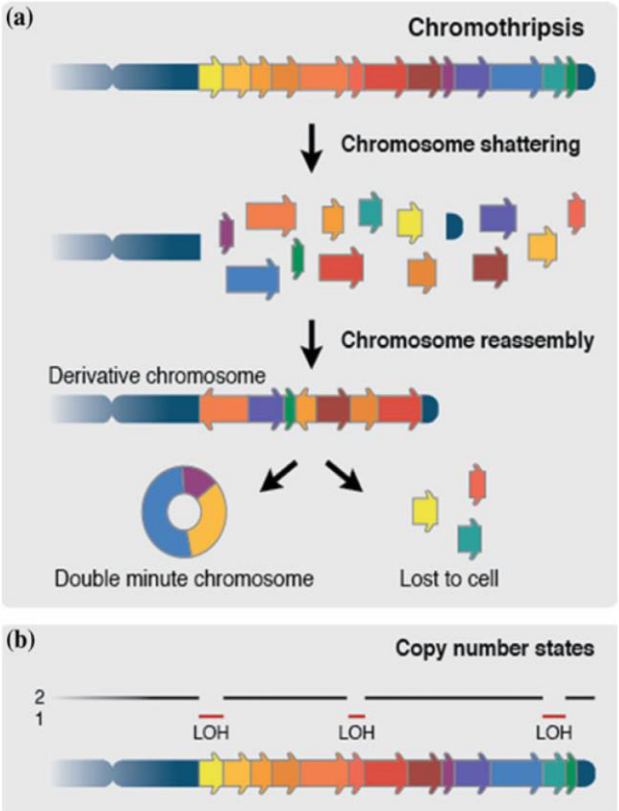

Figure 2. Chromothripsis

A. Morcèlement d'un chromosome suivi d'un rassemblement random le tout dans un seul événement catastrophique.
B. La chromothripsis provoque des changement du nombre des copies et résulte dans la perte d'hétérozygozie (LOH)

D'après Mirjam S. de Pagter and Wigard P. Kloosterman 2015

En 2013 l'équipe finlandaise de Mehine a pu mettre en évidence, grâce à l'analyse par whole genome, sur une série de 38 LM utérins, la présence de réarrangements complexes de type chromothripsis et démontrer que ce mécanisme représente la cause principale des instabilités chromosomiques dans les LM utérins et qui peut expliquer également la survenue des tumeurs bénignes[30].

Un autre événement prédisposant l'évolution tumorale est le dédoublement de l'ensemble des chromosomes ou tétraploïdisation, d'incidence variable dans les cancers (de 11% dans les glioblastomes à 62% des carcinomes vésicaux)[31] et qui représenterait une étape intermédiaire entre un état diploïde pré-tumoral et aneuploïde tumoral comme observé dans le carcinome du col utérin[32]. La tétraploïdisation amènerait à l'instabilité chromosomique et à une hétérogénéité génomique parmi les cellules favorisant la survie en condition de stress environnementaux[32].

L'index d'altérations génomiques et de variation de nombre de copies des gènes a montré sa valeur pronostique de survie globale dans plusieurs histotypes et dans différents organes, du carcinome prostatique[33] aux carcinomes ovariens[34], endométriaux[35] et aux sarcomes[36].

1.1.2 LES SARCOMES ET LE REMANIEMENT GENOMIQUE

Les sarcomes à génomique complexe (des tissus mous ainsi que gynécologiques) sont caractérisés, à la différence des sarcomes à génomique simple (associés à une translocation ou à une mutation activatrice) par un génome remanié à caryotype complexe[14, 56] avec des variabilités à l'intérieur du même histotype (ex entre deux cas différents de LMS utérins). A l'analyse morphologique les atypies sont diffuses et souvent associées à un aspect pléomorphe. Dans les tissus mous ces sarcomes sont les UPS (sarcomes pléomorphes indifférenciés), les myxofibrosarcomes, les liposarcomes dédifférenciés et les LMS. Par ailleurs, les LMS utérins montrent des analogies avec les LMS retro-péritonéaux ou profonds qui se différencient des LMS superficiels et des membres par leur profil génomique et leur évolution clinique [57].

1. 1.3 MECANISMES IMPLIQUES DANS LE GENESE DES LEIOMYOMES UTERINS

Nonobstant des multiples altérations géniques ont été récemment rapportées dans les LM utérins, les mécanismes à la base de la léiomyomagenèse demeurent encore peu connus. Le LM nait d'une seule cellule souche somatique transformée [37-39] tandis que multiples tumeurs concomitantes ont une origine clonale commune avec des clones secondaires distincts[40, 41](cf Fig 3).

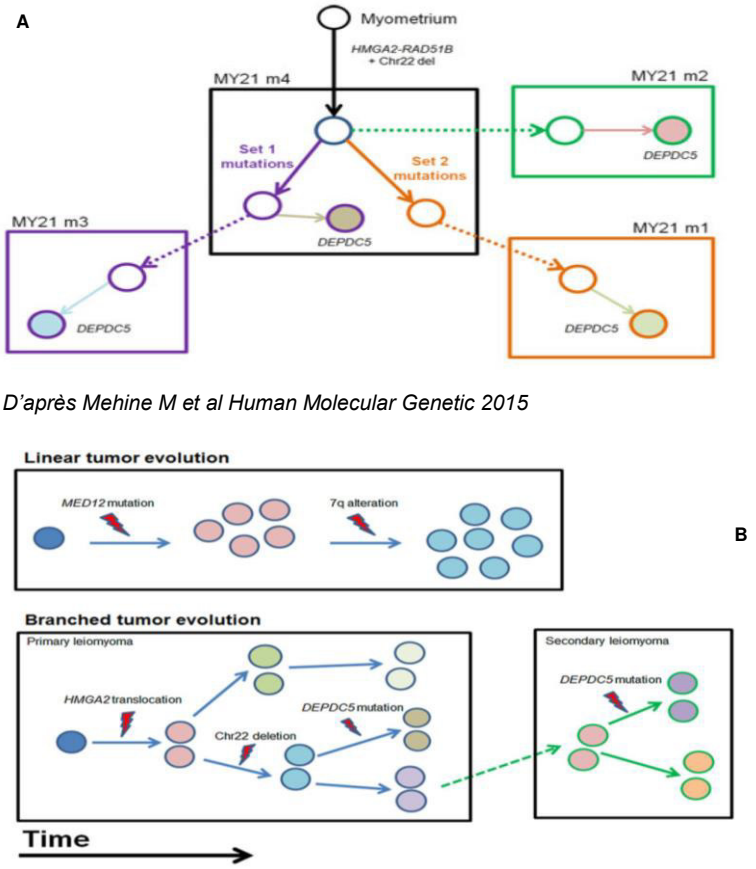

D'après Mehine M et al Human Molecular Genetic 2015

Figure 3. Origine clonale des multiples LM.

A. Les LM m1, m3 et probablement m2 naissent de différents sous-clones qui ont tous comme origine commune m4. Chaque LM acquiert des nouvelles mutations « privées ». La tumeur m4 contient différentes populations « sous-clones » génétiquement distinctes.

B. Modèles alternatifs de développement de LM.

L'expansion d'une seule population cellulaire in multiples sous-clones suit des mécanismes différents et alternatifs. Les altérations impliquant *MED12* et *HMGA2* sont mutuellement exclusives et représentent les plus communes à la différence des délétions du 7q et les mutations de *DEPDC5* qui semblent être des événements secondaires reléguées à une sous-population cellulaire.

Il existe une importante hétérogénéité morphologique et génomique parmi les léiomyomes [42]. Sur la base d'une clusterisation hiérarchique basée sur les profils d'expression des différents types de LM (conventionnel, cellulaire, à noyaux bizarres et mitotiquement actif) et après étude bio-informatique d'enrichissement des gènes impliqués dans les différentes voies de signalisation, 4 types moléculaires de LM ont étés décrits[42, 43] (Fig 4) :

1. le groupe de LM associés aux mutations des exons1 et 2 de *MED12* (chr Xq13.1) [44-46],
2. le groupe associé aux réarrangements de *HMGA2* (chr 12q15) avec surexpression de HMGA2[42, 43, 47-49]
3. le groupe associé à l'inactivation biallélique (mutation et LOH) du *FH* (chr 1q43) [50]
4. le groupe associé aux délétions de *COL4A5* et *COL4A6 (chr Xq22)*

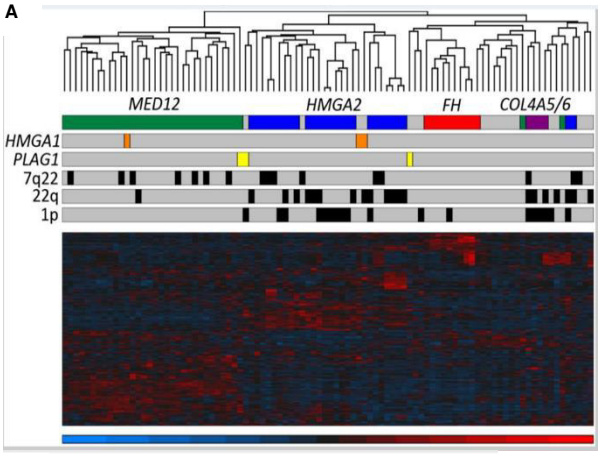

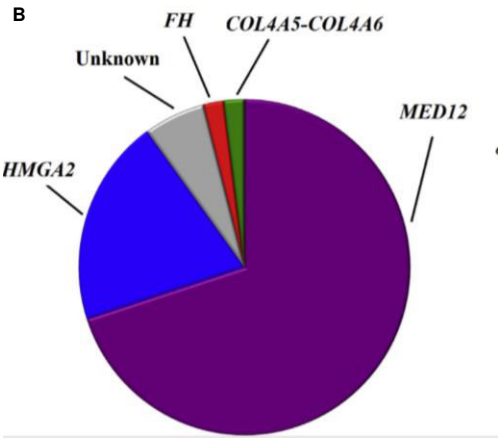

Figure 4. La répartition des LM selon les altérés.

A. Sur la base des 1% des gènes les plus variés le groupe hétérogène de léiomyomes a pu être démembré en 4 catégories : le groupe ***MED12* muté** (vert), le groupe ***HMGA2* réarrangé** (bleu), le groupe ***FH* délété** (rouge) et le groupe ***COL4A5-COL4A6* délété** (violet) (d'après Mehine M et al PNAS 2015). D'après *Mehine M et al Human Molecular Genetics 2015*

B. Fréquence des altérations génétiques dans les LM. *D'après Mehine M et al Fertility and sterility 2014*

1) Les LM associés aux mutations du gène MED12 (chr Xq13) (cf Fig 4,5,6)
Dans la série de Méhine [42] ce groupe est le plus fréquent (34/94 LM, 36%) mais ce taux de mutation arrive à des fréquences bien plus élevées (70%)[44, 51-53]. Le gène le plus surexprimé et de façon unique dans ce groupe est *RAD51B* (issu d'un transcrit non codant de *RAD51B*) associé au *SFRP1* (secreted frizzled-related protein 1), ce dernier impliqué dans l'inhibition de la voie de signalisation WNT et beta-caténine, et à *ADAM12* [42]. Ce dernier est surexprimé durant le développement placentaire et inhibe IGFBP-5[42] qui contrôle négativement la prolifération et la migration.
Basé sur les différents hystotypes des LM (conventionnel, cellulaire et très cellulaire, mitotiquement actif et à noyaux bizarres) le pourcentage de mutation de *MED12* varie. Elle est maximale dans les LM conventionnels (57%)[43] pour diminuer dans les LM mitotiquement actif (36%)[43] et cellulaire (16%) et très cellulaire (8%), il est rare (25%)[54, 55]voire absent dans les LM-BN[43].
2) Les LM associés aux réarrangements de HMGA2 (ch 12q15) (cf Fig 4,5,6)
Ce groupe suit par fréquence celui avec les mutations de MED12 (25-29%)[42, 43]. Sa fréquence varie dans les différents histotypes de LM : 32% dans le LM cellulaire, 4% dans le LM mitotiquement actif, 17% dans le LM-BN[43]. Parmi les gènes les plus surexprimés dans ce groupe de LM, on identifie un inhibiteur de la voie Wnt WIF1 (Wnt inhibitory factor 1) et *PLAG1* (pleomorphic adenoma gene 1) qui contrôle positivement IGF2 (Insulin growth factor 2). IGF2BP2 (Insulin-like growth factor 2 mRNA binding protein 1) ainsi que PAPPA2 (Pappalysin 2) liée à l'IGF2 sont surexprimés.
3) Les LM associés à l'inactivation biallélique (mutation et LOH) du *FH* (chr 1q43) (cf Fig 4,5,6)
Cet évènement se concentre particulièrement dans l'histotype LM-BN (33%)[43]. Le gène exclusivement exprimé par ce groupe de LM est le *AKR1B10* (aldokétoreductase family 1). L'accumulation intracellulaire de fumarate due à

l'absence d'enzyme fumarate hydratase inhibe la dégradation de HIF1alpha (hypoxia inductible factor 1alpha) et inhibe le gène *KEAP1* responsable de la régulation négative du gène *NRF2* (Nuclear factor erythroid 2 related factor 2) qui est donc surexprimé dans ce groupe de LM tout comme dans différents types de cancers.

4) Les LM associés aux délétions de *COL4A5* et *COL4A6 (chr Xq22)* (cf Fig 4,5,6)
Il s'agit de l'altération la moins fréquente, estimée à 4%[42].
Le gène le plus fréquemment exprimé et de façon unique par rapport aux autres LM est le insulin receptor substrate-4 (IRS4), un gène adjacent à COL4A5[42] qui induit la prolifération cellulaire via IGF1.

Enfin, les délétions de 7q22 (15%), 22q (21%) et 1p (19%)[42], sont des mécanismes minoritaires de léiomyomagenèse et peuvent se surajouter aux autres événements driver.

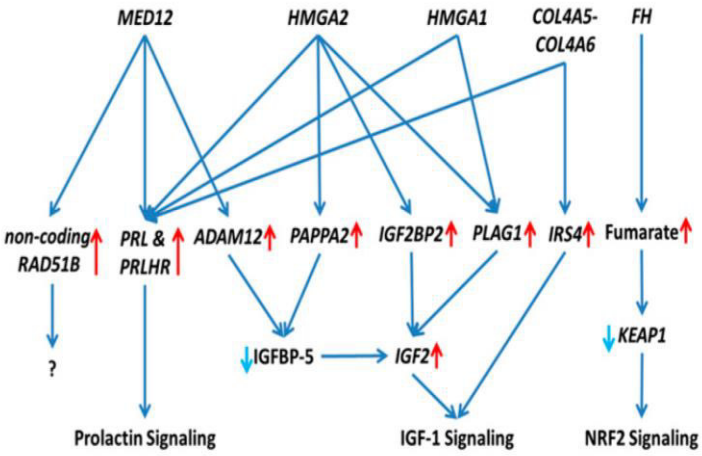

D'après Mehine M, PNAS 2015

Figure 5. Schéma des voies à la base du développement et de la croissance du LM.

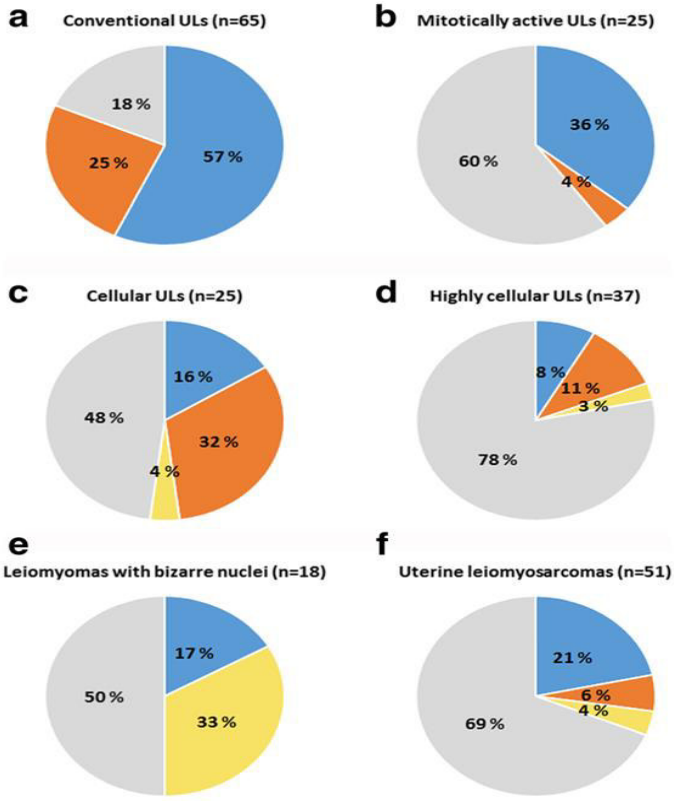

Figure 6. Les différents sous-types de LM sont biologiquement distincts.

En bleu : mutations de MED12
En orange : réarrangements de HMGA2
En jaune : inactivation de FH
En gris : événements inconnus
Ainsi la mutation de MED12 est plus fréquemment retrouvée dans le LM conventionnel et moins fréquemment dans le LM-BN (17%) et dans le LM très cellulaire (8%).
Les translocations de HMGA2, rapportée dans 32% des LM cellulaires est rare dans les LM mitotiquement actifs et presque absente dans les LM-BN.
L'inactivation biallélique de FH atteigne 32% des LM-BN alors qu'elle est rare dans les LM conventionnels.
D'après Mâkinen N Molecular Cancer 2017

Le Tableau 1 résume les principales altérations somatiques et les prédispositions génétiques à la base de la pathogénèse des LM utérins.

Tableau 1. Les altérations impliquées dans la genèse des léiomyomes

Léiomyomes utérins : Génotypes et Phénotypes

Altérations constitutionnelles

Syndrome de REED/ HLRCC
Mutation germinale autosomique dominante du gène *FH* (Fumarate Hydratase) 1q43

Syndrome de Alport
Léiomyomatose diffuse
Délétion germinale dominante des gènes *COL4A5 et COL4A6* (Xq22)

Etudes d'associations pangénomiques dans les populations

- Femmes Japonaises (10q24.33, 22q13.1, 11p15.5)
- Femmes Caucasiennes (17q25.3, gène *FASN* (synthétase des acides gras))

Altérations somatiques

Aberrations chromosomiques
(structure des chromosomes)
40%

- **Réarrangements *HMGA2*** (ch 12q15) (10%) et ***HMGA1*** (ch 6q21)(<10%) avec ***RAD51B*** (ch14q24)
- **Délétion du ch 7q (gène CUX1)**
- **Délétions du gène FH** (ch 1q43)
- **Délétions des gènes COL4A5 et COL4A6** (ch Xq22)
- **Autres Délétions chromosomiques** 1p36, 10q22 (AT6B), 17q et 22q

Altérations au niveau nucléotidique
(Mutations) 70%

Mutations de **MED12** (ch X 13.1)

Altérations épigénétiques

Analyse de la Méthylation du génome et de l'expression de l'ARN

- **Inhibition de *KLF11*, *DLEC1*, *KRT19*** dans le léiomyome par rapport au myomètre sain
- **↑miR-21** associé à ↓ du gene ***PDCD-4*** (programmed cell death 4)

D'après Ordolu Z Clin Obstet Gynecol. 2017

1. 1.4.MECANISMES IMPLIQUES DANS LE GENESE DES LEIOMYOSARCOMES UTERINS

Les LMS utérins font partie des sarcomes à génomique complexe. Dans l'état actuel de nos connaissances il n'existe pas d'altération moléculaire dominante et commune à tous les LMS qui puisse à elle seule expliquer la genèse de ces tumeurs et avoir une valeur diagnostique. En effet chaque LMS présente des altérations chromosomiques complexes « privées », c'est à dire propres à chaque cas [58]. De plus dans les séries d'analyse TCGA rapportées dans la littérature, les LMS utérins représentent un groupe minoritaire souvent noyé dans les LMS des tissus mous[59, 60]. A titre d'exemple des 53 LMS reportés dans la série TCGA en 2017[60] et des 39 de la série publiée en 2018[59] respectivement 27 et 10 étaient utérins.

Les LMS sont caractérisés par une faible charge mutationnelle (entre 1.06 et 3.9 mutations per Mb) et par un haut nombre de cassures intrachromosomiques (130-180 cassures non équilibrées)[59]. Les gènes le plus souvent mutés sont *TP53* (49%), *RB1* (27%) suivis de ATRX (24%). Si on considère les mutations et les délétions, le gène *TP53* est altéré dans 92% des LMS et RB1 dans 94% [59, 61]. *RB1* et *TP53* représentent les deux centres névralgiques qui contrôlent à leur tour des gènes reliés à la réponse aux dommages de l'ADN et à la maintenance des télomères (ex *TOPORS, ATR, TP53BP1, TELO2*), au contrôle du cycle cellulaire et de l'apoptose (*PSDM11, CASP7, XPO1*), aux mécanismes de régulation épigénétique (*HIST3H3, SETD7, KMT2C*), à la régulation de la prolifération musculaire (*MAPK14, DUSP10, MEF2C*) et à la régulation de la stabilité de l'ARN messager (*ZFP36L1, SRSF5*)[62]. Les régions chromosomiques le plus souvent perdues sont 13q14 incluant *RB1*, 17p12 incluant *TP53*, 10q incluant *PTEN* et 16q. Sur ce dernier chromosome il n'a pas été identifié de gène qui puisse avoir un rôle dans la cancérogenèse [61, 63](Fig7). Un mécanisme alternatif aux inactivations bi alléliques de *RB1* et *TP53* (détecté dans 94 et 92% des cas respectivement), observé dans quelques cas, est la perte du *CDKN2A* (ch 9p, codant pour la protéine p16) et la surexpression de *CCDN1*[59].

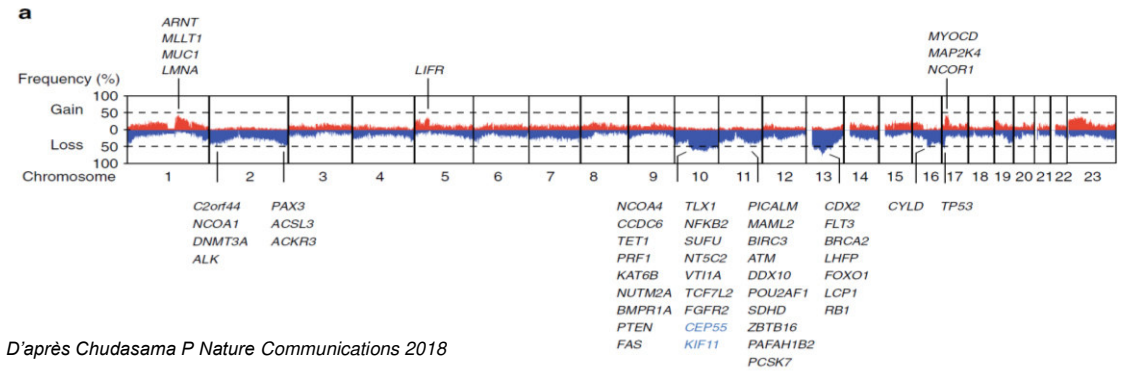

D'après Chudasama P Nature Communications 2018

Figure 7.Principales altérations chromosomiques (gains, pertes), variations du nombre de copie des gènes (CNV) dans les LMS (tissus mous et utérins).

La mutation du gène *MED12* retrouvée jusqu'à 70% des LM[43, 50, 64], est beaucoup moins fréquente dans le LMS[4, 43, 45, 46, 65]. L'analyse par whole genome des larges series de LMS (des tissus mous et utérins) a mis en évidence que la genèse des LMS est plus basée sur la combinaison d'altérations de la structure chromosomique que par des mutations ponctuelles activant un oncogène ou inactivant un gène suppresseur de tumeur [58]. Une altération récurrente dans les LMS du retropéritoine est l'amplification de MYOCD[66]. Ce gène code la Myocardine, un cofacteur de transcription du *SRF* (*Serum Response Factor*) qui régule la différenciation musculaire lisse[67].

Les LMS utérins sont distincts des autres LMS des tissus mous par des profils transcriptomiques et génomiques différents et par un pronostic plus agressif[68]. Des altérations des gènes impliqués dans la recombinaison homologue ont été détectées *: PTEN* (57%), *BRCA2* (53%), *ATM* (22%),*CHEK1* (22%), *XRCC3* (18%), *CHEK2* (12%), *BRCA1* (10%), *RAD51* (10%), *FANCA* (27%) and *FANCD2* (10%)[59]. L'altération des gènes impliqués dans la recombinaison homologue peut représenter le rationnel pour les thérapies anti-PARP. Récemment dans une série de LMS des tissus mous il a été mis en évidence un réarrangement impliquant le gène *ALK*[69]. Néanmoins dans cet article les auteurs ne précisent pas le profil génomique des LMS associés au réarrangement de *ALK*. En pathologie utérine un réarrangement de *ALK* significativement présent dans la population tumorale reclassifie la lésion en tumeur myofibroblastique inflammatoire [70-73].

1. 1.5. MECANISMES IMPLIQUES DANS LE GENESE DES STUMP UTERINES

A l'analyse CGH-array ces tumeurs montrent des profils génomiques hétérogènes : certaines de ces tumeurs montrent des profils génomiques très simples, et pour cela proches des LM, d'autres plus complexes, semblables aux LMS [71, 74] mais présentant moins fréquemment des gains par rapport à ces derniers (cf chapitre suivant). Les mutations MED12 surviennent dans 10% de ces tumeurs [45, 46, 75].

1.2 TUMEURS MESENCHYMATEUSES UTERINES : GENERALITE (CLASSIFICATION OMS 2020)

Ce sont des tumeurs dérivées des tissus mésodermiques ou des tissus se différenciant vers du mésoderme. On distingue une différentiation homologue selon les constituants du corps utérin : muscle lisse et chorion cytogène et une hétérologue vers du tissu mésenchymateux normalement absents de l'utérus : muscle strié, cartilage, os, tissu adipeux etc. L'utérus, dérivé des canaux Mülleriens, se divise en une couche interne correspondant à l'endomètre et à une couche externe correspondant au myomètre[76] qui est constitué de cellules musculaires lisses associées à un réseau vasculaire complexe fait de gros vaisseaux ainsi que de lymphatiques[77]. La couche interne correspond à l'endomètre composé de l'épithélium luminal, glandulaire et du stroma cytogène[77].

Selon l'OMS 2014 et 2020[78, 79] on distingue donc parmi les tumeurs mésenchymateuses de l'utérus par ordre de fréquence (Tableau 2):

Les tumeurs musculaires lisses

- Bénignes : léiomyome (LM) et variants
- Malignes : léïomyosarcome (LMS) et variants
- A potentiel de malignité Incertain (STUMP)

Les tumeurs Stromales de l'Endomètre

- Bénignes : le Nodule du stroma Endométrial
- Malignes :
  - le Sarcome du Stroma Endométrial de Bas grade
  - le Sarcome du Stroma Endométrial de Haut grade
  - le sarcome Utérin Indifférencié

Tumeurs Mésenchymateuses Diverses

- PECome
- Tumeur Myofibroblastique Inflammatoire
- UTROSCT (Tumeurs Utérines ressemblant aux tumeurs des cordons sexuels de l'ovaire)
- Rhabdomyosarcome
- Sarcome Alveolaire des Parties Molles
- Tumeur Fibreuse Solitaire
- Sarcomes *NTRK* réarrangés
- Sarcomes *COL1A1-PDGFB* réarrangés
- Sarcomes *SMARCA4* déficients
- Tumeur adipocytaire
- Tumeur maligne des gaines nerveuses périphériques (MPNST)

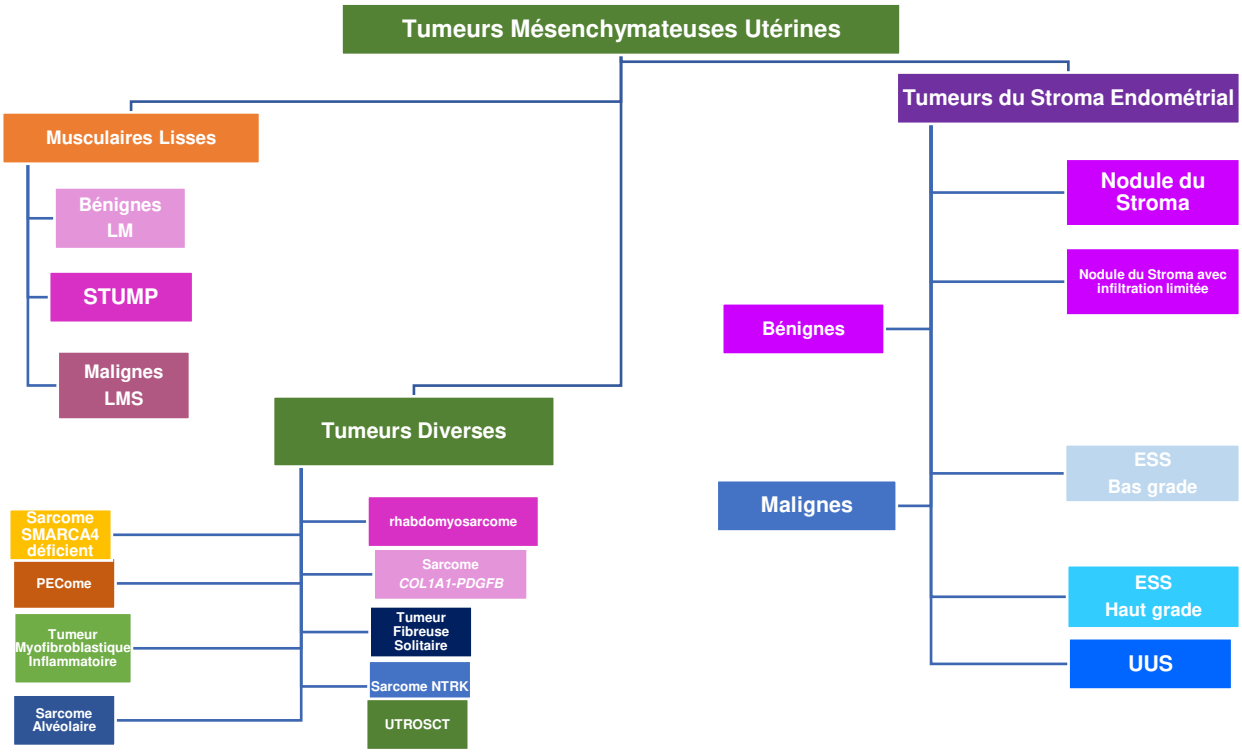

Tableau 2. Synopsis des tumeurs mésenchymateuses utérines selon OMS 2020

1. 2.1 LES TUMEURS MUSCULAIRES LISSES DE L'UTERUS

Principales tumeurs conjonctives du corps utérin, les tumeurs musculaires lisses naissent du myomètre et se définissent comme une prolifération de cellules présentant une différenciation musculaire lisse[79].

1. 2.2 TUMEURS MUSCULAIRES LISSES BENIGNES : LE LEIOMYOME (LM) ET SES VARIANTES

Définition (OMS 2020)[79] :Tumeur mésenchymateuse bénigne dérivant du muscle lisse avec un large spectre de variantes morphologiques (Tableau 3).

Epidémiologie : le LM est la tumeur utérine la plus fréquente touchant 70% des femmes (plus de 80% chez les femmes d'origine africaine)[80] avec un pic entre trente et cinquante ans. Le LM est 800 fois plus fréquent que le LMS[81].

Clinique : Un tiers des LM est symptomatique avec des manifestations cliniques variables selon le nombre, la taille du LM et la localisation (sous-muqueuse, intramurale ou sous-séreuse) allant de la ménométrorragie à la sensation de poids abdominal (syndrome de masse) jusqu'à l'ascite (syndrome de Meigs)[82]. Une particularité rare est l'atteinte vasculaire (cardiaque et pulmonaire) dans le cadre du LM bénin métastasant constitué d'un embole de LM qui atteint via la veine cave inférieure, le cœur et les veines pulmonnaires[83] .

Prédispositions et possibles causes (Tableau 1): la survenue des LM est liée au statut hormonal[84], n'étant pas observé chez les filles prépubères et étant rare chez les adolescentes [85]. L'incidence augmente durant l'âge fertile jusqu'à la ménopause où l'incidence baisse drastiquement[86]. Paradoxalement les LM diminuent leur taille, voire disparaissent durant la grossesse[87], nonobstant le niveaux d'œstrogènes et progestérone très élevés [88], probablement en raison d'un effet combiné entre le niveau hormonal et la réorganisation utérine du post-partum [89].L'ethnicité joue un rôle également important dans le développement des LM utérins. En effet les femmes d'ethnie africaine ont 2 à 3 fois plus tendance à développer des symptômes cliniques et à un plus jeune âge probablement en

relation à la taille des LM [80]. Une incidence accrue des LM est associée à différents syndromes génétiques : le syndrome de Alport [90](associé aux mutations des gènes *COL4A5-COL4A6*), syndrome de Proteus[91] (altération du gène *AKT1*), syndrome de Cowden[92] (mutations du gène *PTEN*) et le syndrome de Reed[93, 94 95](HLRCC, hereditary leiomyomatosis and renal cell cancer, associé à la mutation du gène *FH*). Dans ce dernier syndrome l'insurgence de multiples LM symptomatiques à un âge jeune, voire très jeune (20-30 ans) doit faire suspecter un syndrome de Reed.

Les études d'association génique ont identifié un polymorphisme du 17q25.3 responsable de la surexpression de FAS dans les populations Caucasiennes [96], et trois loci (10q24.33, 22q13.1 et 11p15.5) chez les Asiatiques, prédisposant à une susceptibilité accrue pour les LM [97].

Léiomyome (usuel) et ses variantes histologiques (Tableau 3)

Variantes histologiques du LM	
-Léiomyome cellulaire (dont la variante hautement cellulaire)	- Léiomyome à Noyaux Bizarres
- Léiomyome mitotiquement actif	- Léiomyome hydropique
- Léiomyome apoplectique	- Lipoléiomyome
- Léiomyome épithélioïde	- Léiomyome myxoïde
- Léiomyome disséquant ou "cotylédonoïde"	- Léiomyomatose diffuse
- Léiomyomatose intraveineuse (ou intravasculaire)	- Léiomyome (bénin) métastasant
-Léiomyome *FH*-déficient	

1.2.3.1 LEIOMYOME USUEL

Macroscopie : Unique ou multiple, sous-muqueux, intramural ou sous-séreux il apparait le plus souvent comme une masse bien circonscrite de couleur blanchâtre, fibreuse, de consistance variable, de rénitente à dure calcifiée (Fig1).

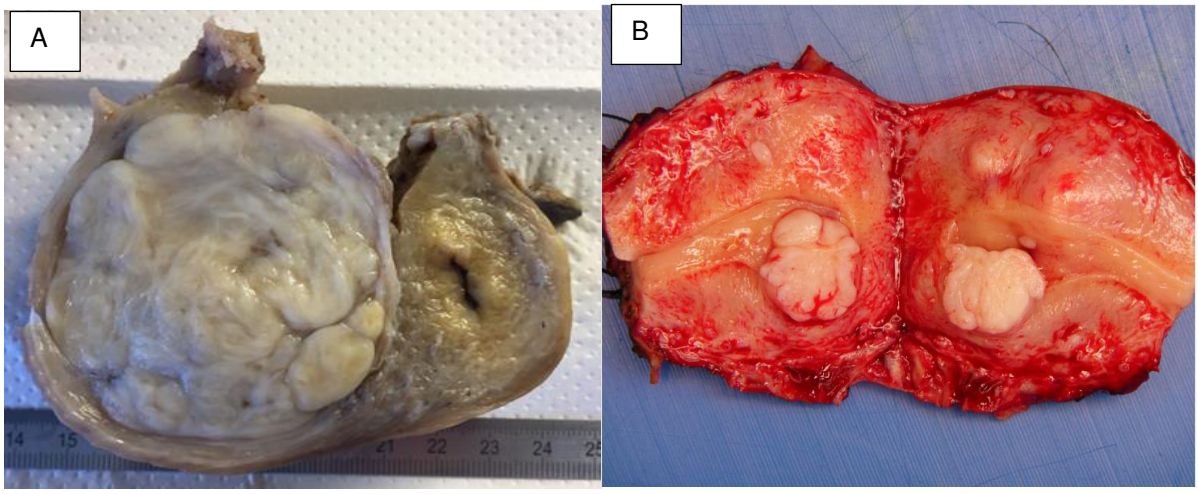

Figure 8. Aspects macroscopiques des LM de type usuel. La lésion est bien limitée par rapport au myomètre adjacent (A). Elle apparait fasciculée, blanchâtre, rénitente à la coupe. Le LM peut être unique ou multiple, sous-muqueux, sous-séreux ou interstitiel (B).

Microscopie : le LM conventionnel est constitué de cellules fusiformes disposées en faisceaux entrecroisés (Fig 9). Il est le plus souvent peu cellulaire ou normo cellulaire à cause de la déposition de collagène donnant un aspect éosinophile et hyalin parfois calcifié (LM ancien). Les mitoses sont <10 mitoses/10 champs à fort grossissement. Des remaniements nécrotiques (nécrose ischémique, non tumorale) peuvent coexister.

Immunohistochimie : le LM exprime les marqueurs musculaires lisses : actine, desmine, H-caldesmone, transgéline et les récepteurs hormonaux.

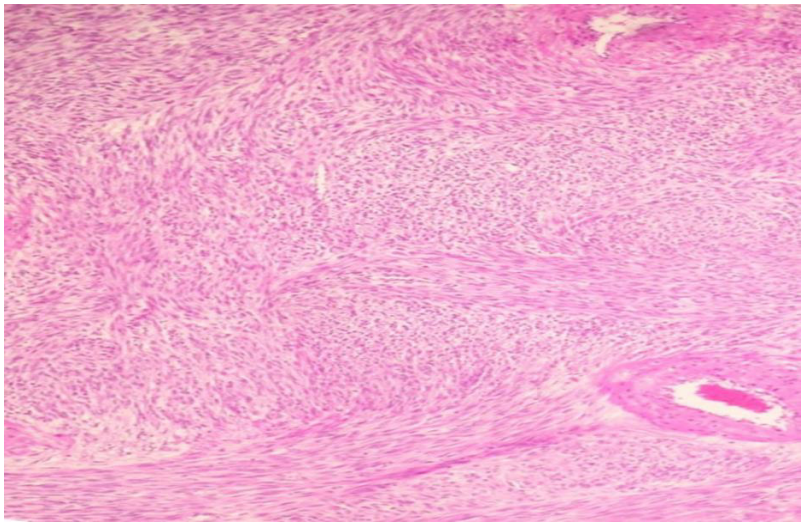

Figure 9. Aspect morphologique microscopique d'un LM usuel.

A noter les vaisseaux de calibre augmenté, à paroi épaissie. Les cellules fusiformes s'organisent en faisceaux.

1.2.3.2 LEIOMYOME A NOYAUX BIZARRES

Il s'agit d'un LM par ailleurs conventionnel qui contient des cellules géantes multinuclées en quantité variable le plus souvent agencées en groupes[2, 78, 79, 98-100].

Macroscopie : Masse bien circonscrite, le plus souvent jaunâtre (Fig 10).

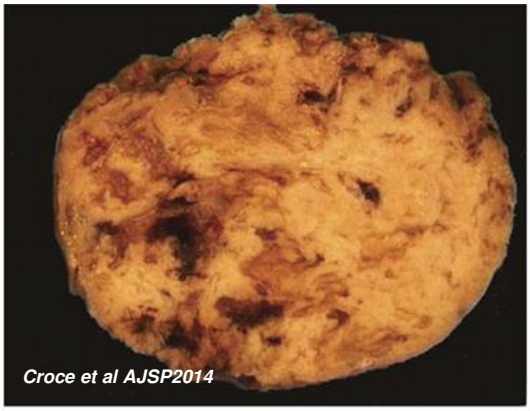

Figure 10. Aspect macroscopique d'un LM à Noyaux Bizarre.

A noter l'aspect jaunâtre ponctué de foyers hémorragiques.

Microscopie (Fig 11 et 12) : Le diagnostic peut s'avérer particulièrement ardu pour sa ressemblance avec un LMS en particulier pour l'aspect faussement atypique des noyaux bizarres et la présence de kharyorrexis qui peuvent être interprétées à tort comme des mitoses atypiques[2]. Les clefs diagnostiques reposent dans le compte mitotique inférieur à 10 mitoses/10 champs à fort grossissement (jusqu'à 7 mitoses ont été rapportées)[2, 100] et dans l'absence d'atypie dans les cellules fusiformes qui entourent les noyaux bizarres (Fig 11).

La tumeur montre des vaisseaux à paroi épaissie siège d'une nécrose fibrinoïde inflammatoire et des images d'oblitération suggérant un contexte de souffrance hypoxique. Une partie des LM à Noyaux Bizarres montre des aspect morphologiques décrits dans les LM FH-déficient[2, 100, 101] : noyaux cabossés avec nucléole proéminent et orangiophile, halo clair perinucléolaire, inclusions rhabdoïdes intra-cytoplasmiques, vascularisation hémangioéricytaire. Dans 55% des cas il existe une altération du gène *FH*[100]. Une inactivation biallélique de *FH* a été mise en évidence dans 33% des LM à noyaux bizarres[43]. Certains auteurs ont subdivisé les LM-BN en deux types : type I associé morphologiquement au LM *FH* déficient *MED12* muté, le plus souvent *TP53* wild type et le type II sans aspect *FH*-déficient souvent *HMGA* réarrangé et qui comporterait plus fréquemment des mutations du gène *TP53*[102].

Immunohistochimie : n'est pas utile dans le diagnostic différentiel entre un LM à Noyaux Bizarres et un LMS. En effet selon les études le KI-67 dans les LM à Noyaux Bizarres varie entre 5 et 25%[103-105] et dans une étude 30% des LM à Noyaux Bizarres ont montré un KI-67>20% alors que 30% des LMS ont montré un KI-67 <20%[103]. La protéine p16 peut être exprimée dans les LM-BN (entre 25 et 100% selon les séries)[104, 106].

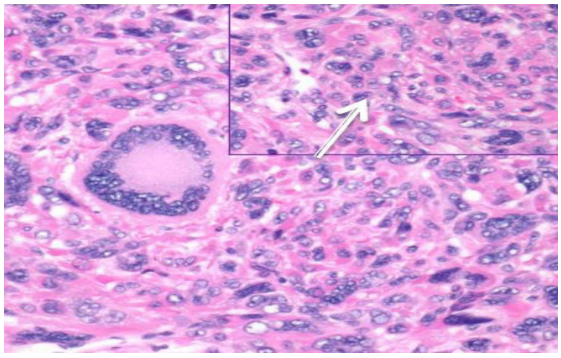

Figure 11. Les clefs diagnostiques d'un LM à Noyaux Bizarres : l'absence d'atypie au niveau des cellules fusiformes (flèche) et le compte mitotique <10 mitoses/CFG (champs à fort grossissement).

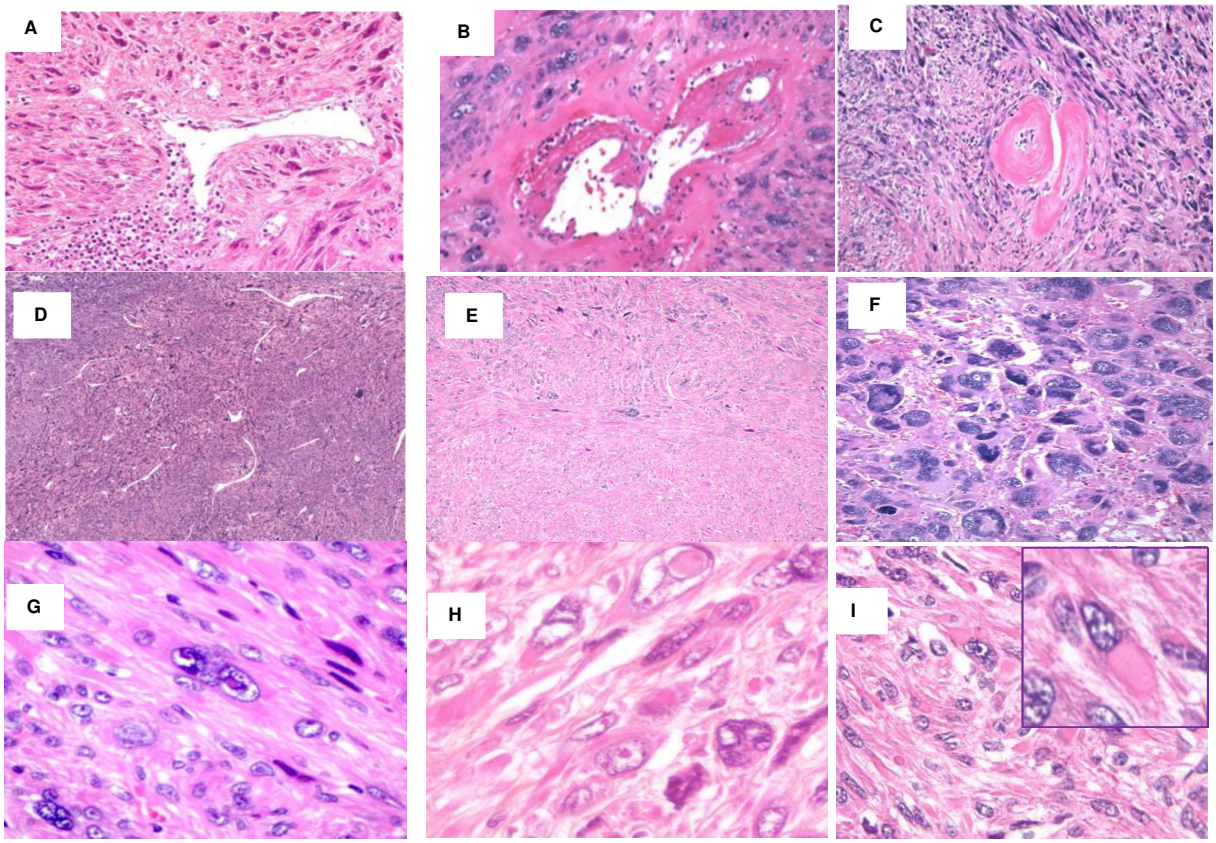

Figure 12. Caractéristiques des LM à Noyaux Bizarres. Vaisseaux à paroi épaissie (A) siège d'une nécrose fibrinoïde inflammatoire (B) et des images d'oblitération (C). Parfois la vascularisation est de type hémangiopéricytaire ou en « bois de cerfs » (staghorn vessels) (D). Les « Noyaux Bizarres » peuvent avoir une distribution focale, dispersés en bouquets (E) ou diffuse (F). Les noyaux peuvent montrer des inclusions (G), des nucléoles orangiophiles et des halos clairs perinucléolaires (H) comme observé dans les LM FH-déficients. Par places les cytoplasmes montrent des inclusions éosinophiles d'allure rhabdoïde (I).

1.2.3.3 LEIOMYOME EPITHELIOÏDE

C'est un LM constitué de cellules rondes ou polygonales de morphologie épithélioïde à cytoplasme éosinophile ou clair[78, 107, 108](Fig 13). La tumeur montre une architecture cordoniforme, trabéculaire ou diffuse. Si la taille est inférieure à 1 cm, on parle de « plexiform tumorlets ». Le compte mitotique doit être inférieur à 2 mitoses/ 10 champs

à fort grossissement et la nécrose doit être absente[79]. Il s'agit d'une variante peu décrite dans la littérature avec de séries de petite taille[107, 108].

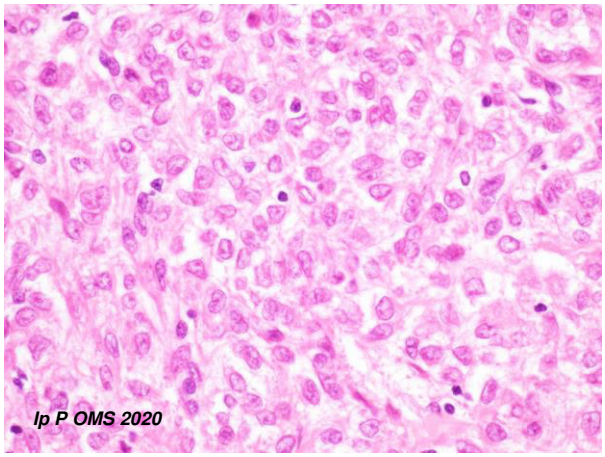

Figure 13. LM épithélioïde. Les noyaux sont ronds ou polygonales sans atypie. Les cytoplasmes quand visibles sont éosinophiles ou clairs.

1.2.3.4 LEIOMYOME MYXOÏDE

C'est un LM hypocellulaire dont les cellules sont séparées par un stroma myxoïde (Bleu Alcian positif). Les cellules tumorales ne montrent pas de mitoses ou les mitoses sont exceptionnelles et toujours inférieures à 2 mitoses/ 10 champs à fort grossissement (Fig 14). En dehors de l'absence d'atypie et de nécrose, l'élément diagnostic clef est la bonne limitation de la tumeur par rapport au myomètre adjacent. La limitation est proposée comme le critère diagnostique premier auquel s'ajoutent l'absence d'atypie et nécrose et <2 mitoses [109, 110] (Tableau 4).

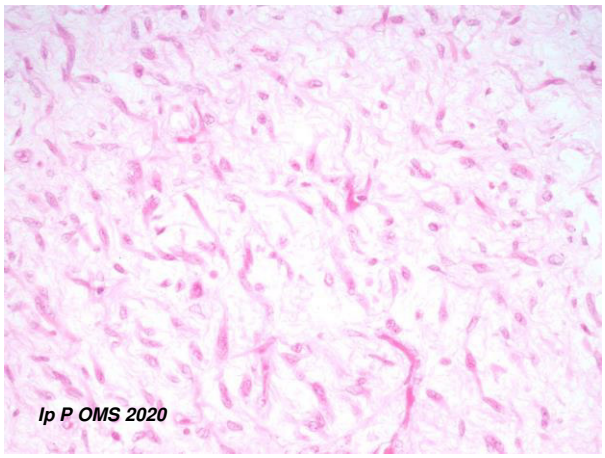

Figure 14. LM myxoïde

Cellules fusiformes séparées par un stroma myxoïde. Absence d'atypie et au maximum 1 mitose/10 CFG

Tableau 4. Algorithme diagnostique pour une tumeur musculaire lisse myxoïde *(selon Busca A et al)*[37]

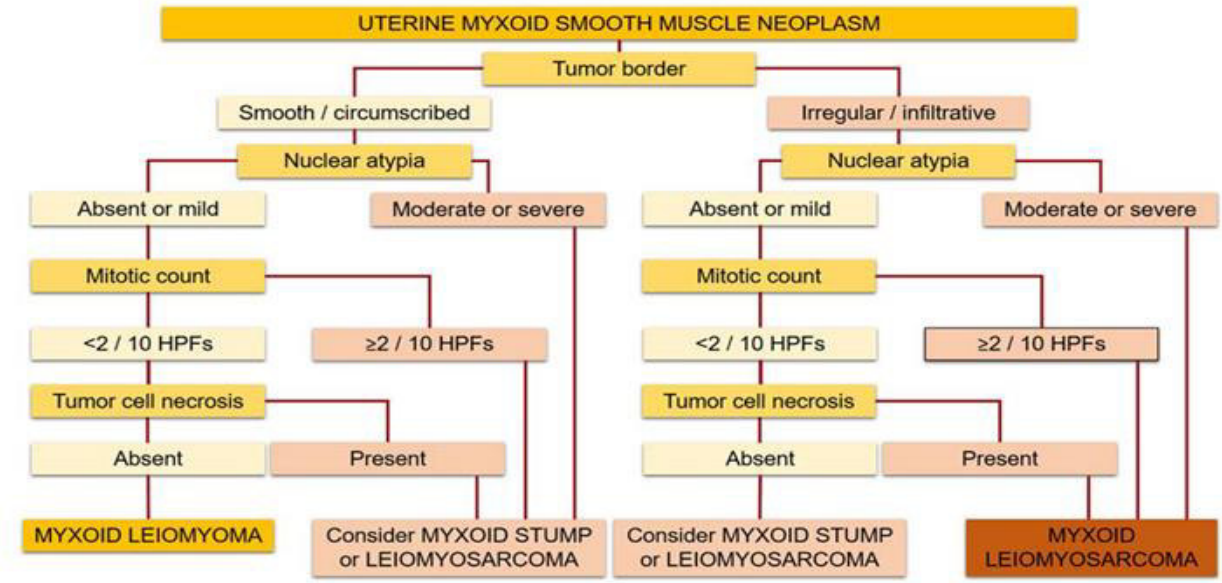

1.2.3.5 LEIOMYOME MITOTIQUEMENT ACTIF

Il s'agit d'un LM comportant plus de 5 mitoses/ 10 champs à fort grossissement selon certains auteurs[98] ou >10 mais moins de 15, sans autre critère péjoratif [78]. L'activité mitotique plus élevée est souvent mise en relation à un traitement hormonal ou à une imprégnation hormonale observée le plus souvent chez les patientes jeunes.

1.2.3.6 LEIOMYOME APOPLECTIQUE

C'est un LM comportant des zones de nécrose ischémique et hémorragique.

Macroscopie : LM avec zone cicatricielle, hémorragique centrale (Fig 15 A). Plus rarement plusieurs zones hémorragiques peuvent coexister.

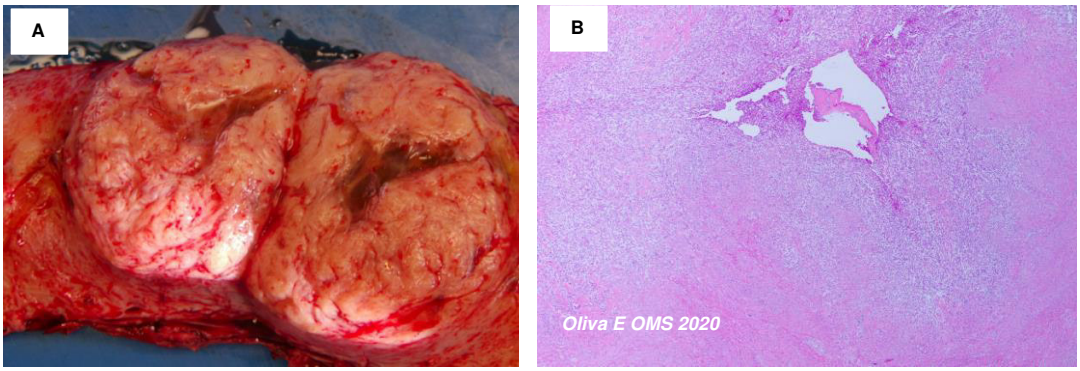

Figure 15. Aspect macroscopique (A) et microscopique (B) d'un LM apoplectique. A noter la cicatrice hémorragique centrale (A). La cellularité est augmentée autour de la nécrose centrale (B).

Microscopie : LM avec zone de nécrose ischémico-hémorragique en différentes phases d'évolution : la nécrose est remplacée par un tissu fibreux réorganisé si l'ischémie n'est pas récente (Fig 8B). A la périphérie de la zone nécrotique les cellules peuvent être plus éosinophiles, montrer des modifications réactionnelles et pseudo-atypies ainsi qu'une activité mitotique plus élevée et des marqueurs du cycle cellulaire augmentés notamment la p16, troublant l'interprétation diagnostique[111].

1.2.3.7 LEIOMYOME HYDROPIQUE

LM remanié par un important œdème qui dissocie les fibres musculaires et alterne des territoires hypocellulaires, « alvéolaires » rappelant les alvéoles pulmonaires, à zones normo ou hypercellulaires.

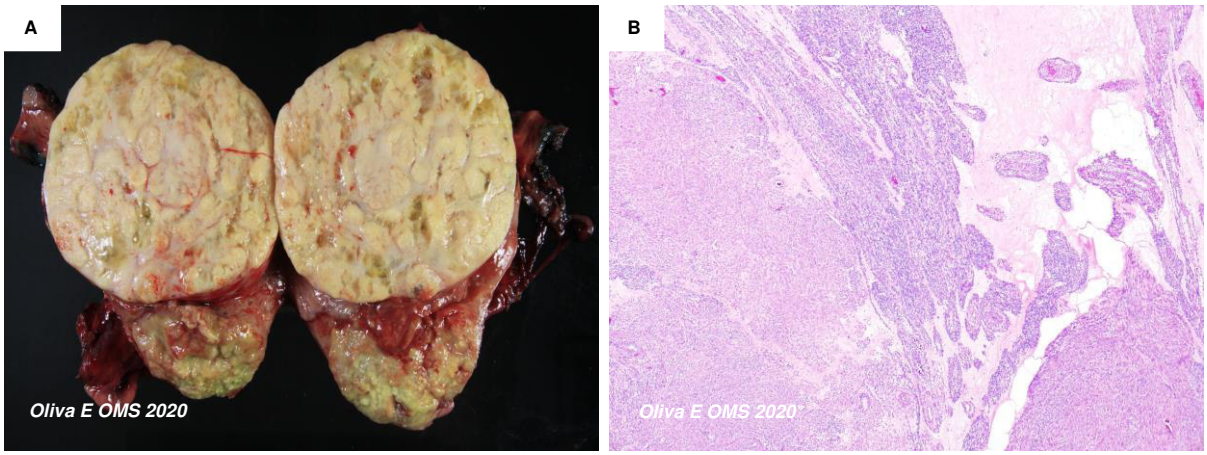

Figure 16. Aspect macroscopique (A) et microscopique (B) d'un LM hydropique. A noter l'alternance de territoires hypo-cellulaires occupés par de l'œdème avec territoires plus cellulaires.

1.2.3.8 LEIOMYOME CELLULAIRE

Macroscopie : LM de consistance mollasse et de couleur jaune en raison de la forte cellularité.

Microscopie : LM montre une cellularité augmentée (Fig 17), conférant un aspect bleu à petit grossissement. Les cellules sont fusiformes et le cytoplasme est peu abondant. Il peut mimer une tumeur du stroma endométrial. La clef du diagnostic est la présence de gros vaisseaux à paroi épaissie. Les atypies sont absentes et les mitoses sont rares.

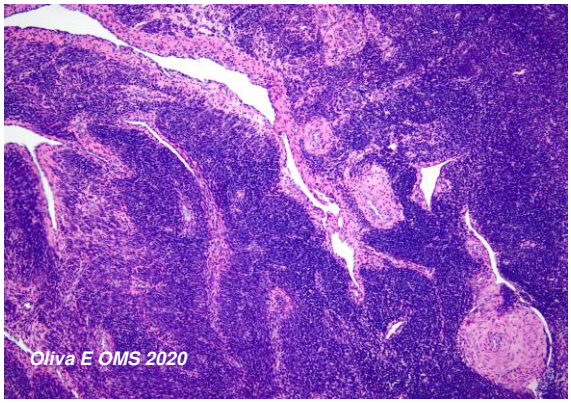

Figure 17. Léiomyome (très)cellulaire. A noter l'aspect « bleu » de la lésion qui traduit la forte densité cellulaire. Les cellules ont des cytoplasmes peu abondants ou inapparents.

1.2.3.9 LEIOMYOME *FH*-DEFICIENT

Il s'agit d'une définition à la fois morphologique, immunophénotypique et moléculaire. C'est un LM montrant une vascularisation en « bois de cerf » ou hémangyopericytaire montrant des remaniements hydropiques (œdème alvéolaire) et des noyaux caractéristiques : cabossés avec un renforcement de la membrane nucléaire, un nucléole orangiophile proéminent, un halo clair perinucléolaire et des inclusions cytoplasmiques rhabdoïdes[101]. En immunohistochimie ces LM perdent l'expression de l'enzyme Fumarate Hydratase[112, 113] et montrent une accumulation de 2SC (2Succynil cystéine)[101]. Sur le plan moléculaire plus de 1% des LM montrent une mutation somatique au niveau du gène *FH* [113]. Pour ce qui concerne la mutation germinale de *FH* responsable du syndrome HLRCC, la morphologie et l'immunohistochimie ne sont pas fiables pour prédire l'existence d'une mutation germinale[113, 114]. L'aspect de LM-FH déficient est retrouvé également dans bon nombre des LM à Noyaux Bizarres [100,

[102, 115, 116]. Au point de vue moléculaire une inactivation biallélique (une mutation et un LOH étant les événements plus fréquents) de *FH* a été rapportée dans 33%[43]à 50%[100] des LM à Noyaux Bizarres.

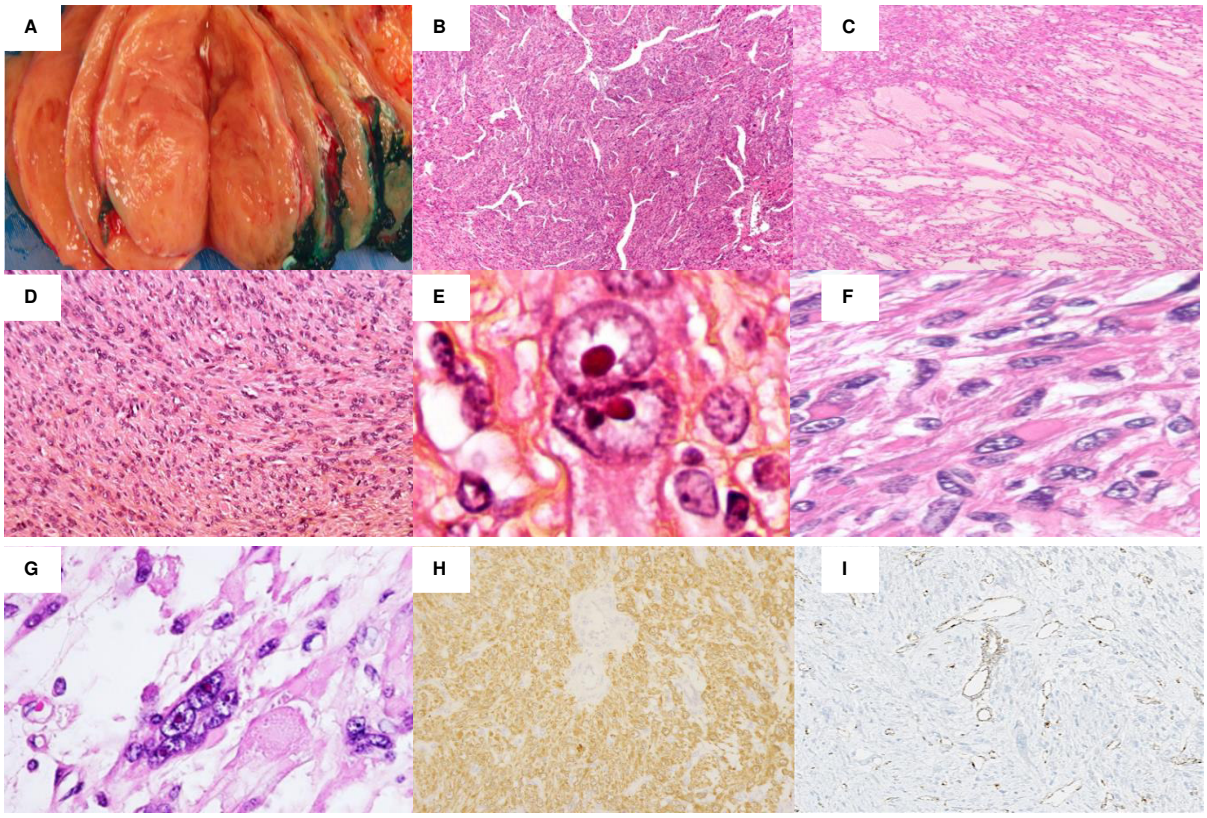

Figure 18. Figure synoptique des LM-FH déficient. Aspect macroscopique charnu et moins fasciculé qu'un LM habituel (A). Vascularisation hémangiopéricytaire (staghorn vessels- vaisseaux en bois de cerf) (B) ; œdème alvéolaire (C) ; territoires à cellularité augmentée (D) avec noyaux cabossés de façon diffuse, faussement atypiques ; nucléole orangiophile, halo clair peri-nucléolaire (E) ; inclusions cytoplasmiques rhabdoïdes (F) ; cellules géantes multinuclées (G) ; perte d'expression de l'enzyme fumarate hydratase (H) ; accumulation cytoplasmique de 2SC(2 succynil-cystéine) (I).

1.3.10 LEIOMYOME DISSEQUANT OU COTYLEDONOÏDE

Macroscopie : LM sous la forme de multiples nodules « en grappe » (Fig 19).

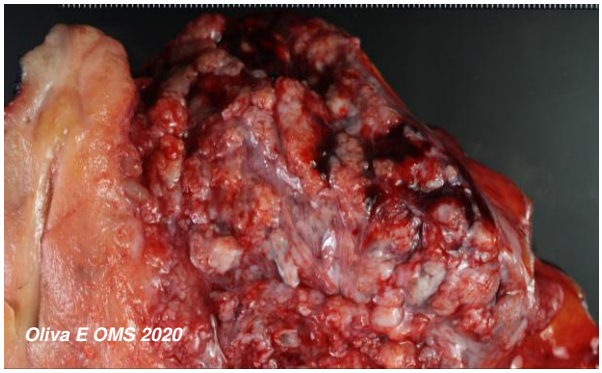

Figure 19. Aspect macroscopique d'un LM cotylédonoïde.

A noter la croissance exophytique qui rappelle un placenta.

Microscopie : ce LM montre des cellules qui infiltrent la paroi du myomètre dissociant les fibres du myomètre comme un placenta [117, 118]. Le LM peut s'étendre au-delà de l'utérus. Le compte mitotique est faible, l'atypie et la nécrose sont absents. On peut observer des remaniements hydropiques.

1.3.11 LEIOMYOMATOSE INTRAVEINEUSE ET LEIOMYOMATOSE DIFFUSE

La léiomyomatose intraveineuse (LIV) correspond à la présence d'une tumeur musculaire lisse à l'intérieur d'un vaisseau externe au LM qui fréquemment s'associe à une extension extra-utérine (pelvienne ou péritonéale)[119]. La léiomyomatose diffuse (utérine ou péritonéale) correspond à la présence de multiples nodules tumoraux épars dont les contours sont souvent difficiles à distinguer car ils ont tendance à fusionner entre eux et avec le myomètre adjacent [120, 121]. Les cellules ne présentent ni d'atypie ni de nécrose et le compte mitotique est inférieur à 10 mitoses/ 10 champs à fort grossissement.

Macroscopie : la léiomyomatose intravasculaire se présente sous la forme de multiples protrusions vasculaires vermiformes (Fig 20). Sa détection peut être macroscopique (à un œil entrainé) ou de découverte microscopique. En macroscopie elle est indistinguable d'un sarcome du stroma endométrial.

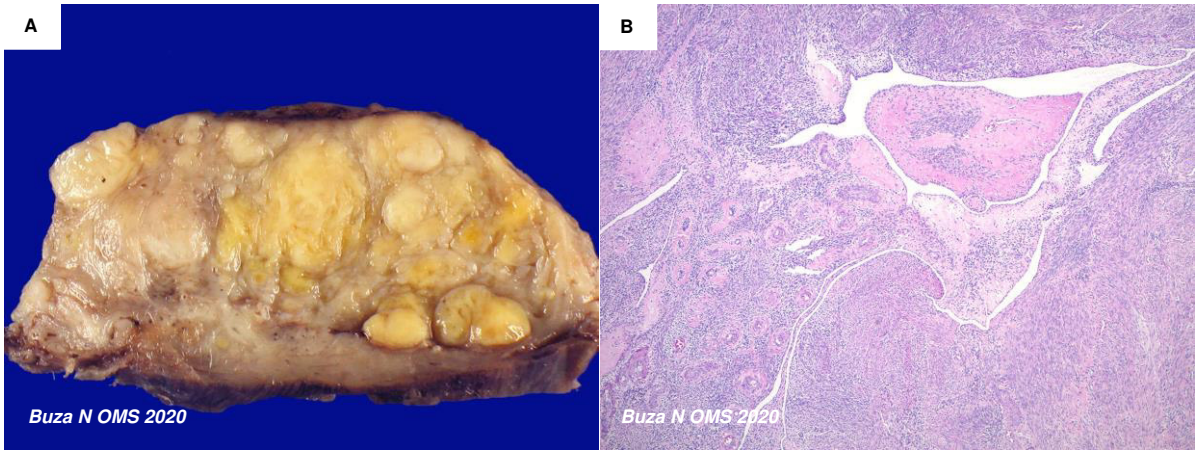

Figure 20. Léiomyomatose. Multiples nodules sortant à la pression, en dehors ou sans nodule de LM (A). Localisation intraveineuse d'une tumeur musculaire lisse sans atypie (B).

Microscopie : la LIV consiste en multiples protrusions musculaires lisses dans les vaisseaux en dehors des limites d'un LM. Ces tumeurs sont souvent hydropiques et intimement liées aux vaisseaux (Fig 13). Les cellules ne montrent pas d'atypie et les mitoses sont rares[122].

Evolution et pronostic : la diffusion au-delà de l'utérus est rapportée dans 30% des cas avec extension dans les veines pelviennes, la veine cave inférieure et rarement au cœur et vaisseaux pulmonaires. Le risque de récidive est estimé à 10%[123].

1.3.12 LEIOMYOME BENIN METASTASANT

Il s'agit d'un LM usuel mais il est retrouvé dans le parenchyme pulmonaire d'une patiente aux antécédents de LM utérin. La lésion à distance et la lésion utérine sont clonalement reliées[124].

Macroscopie : nodule(s) bien circonscrit(s) de taille variable entre 2 et 5 mm [125]

Microscopie : prolifération fusocellulaire disposée en faisceaux entrecroisés avec cytoplasmes éosinophiles, atypies discrètes avec activité mitotique minime ou absente[126] et distribution peri-bronchiolaire et périphérique dans le poumon[127] (Fig 21). Le LM peut s'associer à du tissu adipeux. Le LM métastasant exprime les récepteurs hormonaux [128].

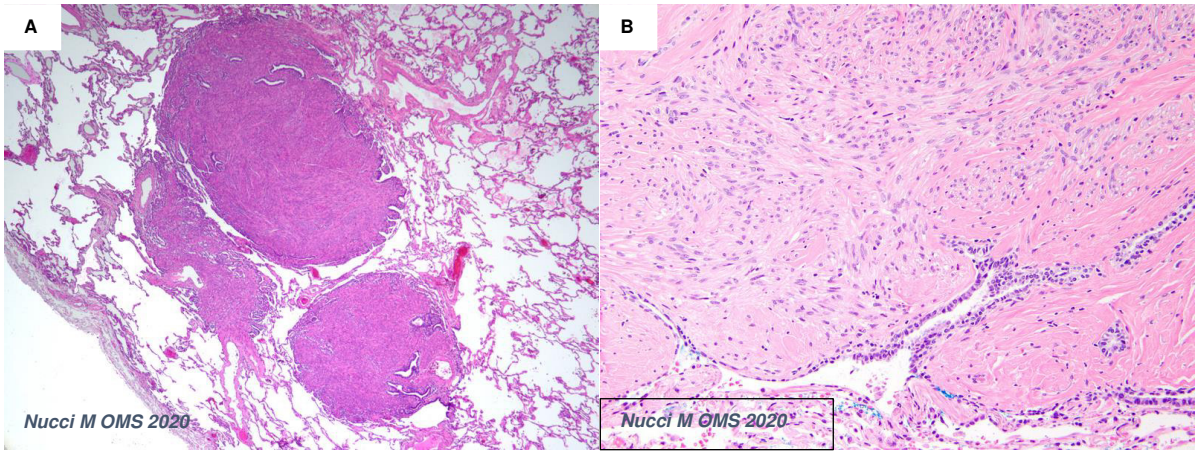

Figure 21. LM bénin métastasant au poumon. Les nodules sont périphériques et montrent une distribution peri-bronchiolaire (A). Les atypies sont discrètes (B).

Pathogénèse

Les LM métastasants montrent plus fréquemment des délétions des bras longs des chromosomes 19 et 22[127].

Evolution et pronostic

L'évolution est indolente à l'exception des cas avec diffusion extensive, responsable de l'insuffisance respiratoire et du décès [83]. Les « métastases » répondent à la thérapie hormonale [129]

1.2.4 LES TUMEURS MUSCULAIRES LISSES UTERINES MALIGNES. LEIOMYOSARCOMES UTERINS (LMS)

Tumeur mésenchymateuse maligne dérivant du muscle lisse myométrial avec morphologie fusiforme ou épithélioïde ou myxoïde (OMS 2020)[130].

Définition :Il s'agit du sarcome utérin le plus fréquent (40-50%) mais il représente seulement le 1% des tumeurs malignes de l'utérus [131]. Les patientes sont en général d'âge supérieur à 50 ans.

Macroscopie : Masse le plus souvent unique, en général de taille > 5cm, de consistance charnue à la coupe, souvent d'aspect nécrotique et hémorragique. Les bords sont aussi bien arrondis que irréguliers[132].

Critères diagnostiques

Ils sont différents selon les différent histotypes (cf Tableau 5)

Tableau 5. Critères diagnostiques des LMS utérins, selon le sous-type histologique

Léïomyosarcomes utérins		
LMS à cellules fusiformes/ LMS conventionnel	LMS Epithélioïde	LMS Myxoïde
Deux ou plus de ces critères	Deux ou plus de ces critères	Un ou plus de ces critères
Atypie nucléaire* (2+/3+)	Atypie nucléaire (2+/3+)	Atypie nucléaire (2+/3+)
Nécrose tumorale	Nécrose tumorale	Nécrose tumorale
≥10 mitoses/10CFG* (2.4mm2)	≥4 mitoses/10 CFG* (2.4mm2)	>1 mitose/10 CFG* (2.4mm2)
		Bords mal limités/infiltration

*: atypie évaluée à l'objectif x10

Macroscopie : Masse uterine, le plus souvent unique, plus rarement multiple, d'aspect charnu (cf Fig 22A) souvent ponctuée de nécrose et de remaniements hémorragiques de diamètre moyen de 10 cm. Les LMS myxoïdes sont souvent gélatineux.

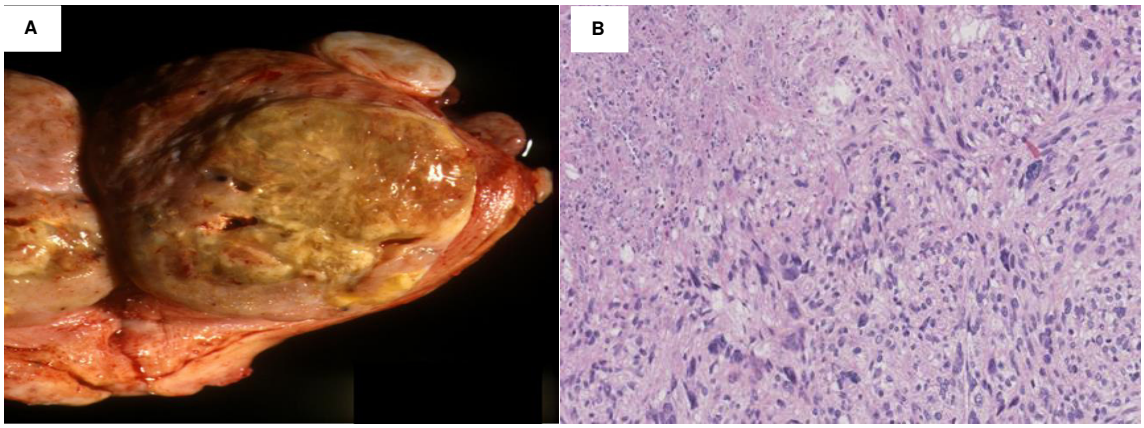

Figure 22. LMS fusiforme. Masse avec mode de croissance expansif « pushing », d'aspect charnu et nécrotique (A). Cellules fusiformes avec atypies modérées à marquées. A noter en haut à gauche la nécrose tumorale (B).

Microscopie :

1.2.4.1 LMS CONVENTIONNEL/A CELLULES FUSIFORMES (cf Fig 22B): Tumeur constituée de cellules fusiformes agencées en faisceaux, avec cytoplasme éosinophile abondant, noyaux fusiformes, hyperchromatiques et nucléoles évidents. Le pléomorphisme nucléaire peut être marqué avec présence de cellules géantes

multinucléées. L'infiltration du myomètre peut être de type « pushing » ou arrondie ou infiltrative et destructive mais ceci n'est pas un critère diagnostique pour ce sous-type.

1.2.4.2 LMS EPITHELIOÏDE : Le LMS épithélioïde est constitué de cellules épithélioïdes pour au moins 50% de la tumeur. Les cellules épithélioïdes sont rondes ou polygonales, avec cytoplasme éosinophile ou clarifié. Les cellules sont agencées en nids, en travées en cordes (cf Fig 23).

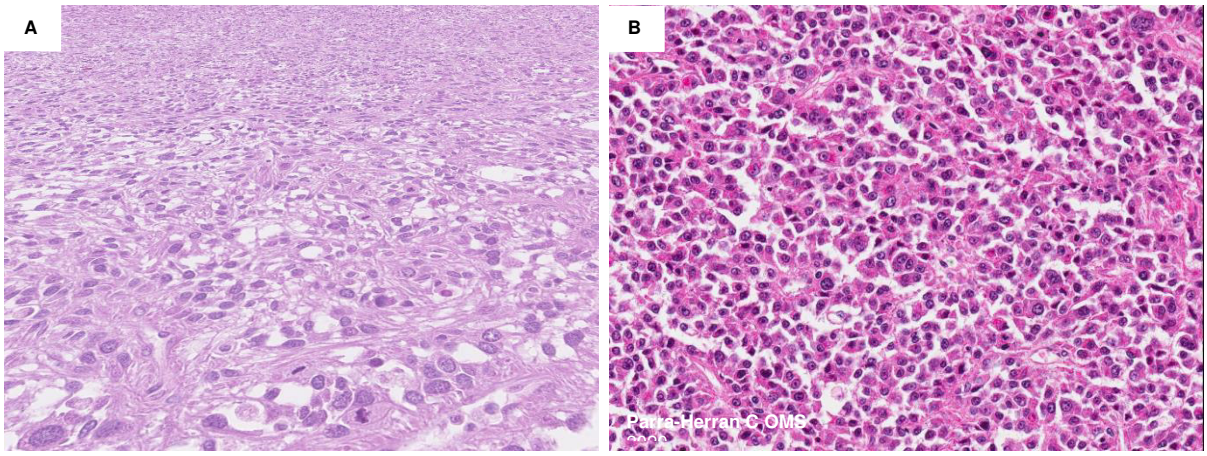

Figure 23. LMS épithélioide. Noyaux arrondis hyperchromatiques avec cytoplasmes clarifiés (A) ou éosinophiles (B).

1.2.4.3 LMS MYXOÏDE :Il s'agit d'une variante de LMS avec une riche composante myxoïde (30 à 60% de la tumeur selon les auteurs), qui apparait macroscopiquement gélatineuse. Les cellules sont fusiformes ou étoilées (Fig 24A). Le critère diagnostique plus important pour ces tumeurs est la limitation par rapport au myomètre adjacent[109, 110](Fig 24B, Tableau 4).

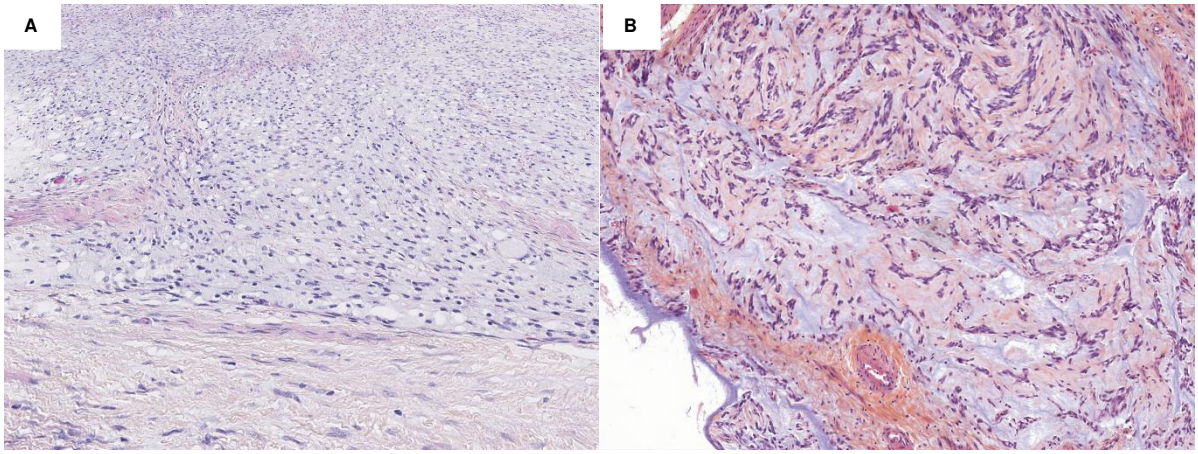

Figure 24. LMS myxoïde. Cellules fusiformes entourées d'une matrice myxoïde (A). Bords tumoraux mal limités (B).

Immunohistochimie des LMS: Les LMS expriment de façon variable les marqueurs musculaires lisses (desmine, H-caldesmone et transgéline). Les LMS épithélioides peuvent exprimer les kératines et être faiblement positifs pour les marqueurs musculaires lisses, tout comme les LMS myxoïdes. Les LMS fusiformes expriment souvent les RE (récepteurs aux œstrogènes) et les RP(récepteurs à la progestérone). Ils peuvent surexprimer la p16 et la p53[110].

Biologie moléculaire des LMS : une partie (35%) des LMS épithélioides a montré la présence d'un réarrangement intéressant le gène *PGR* [133](codant pour le RP) qui se

traduit par une surexpression des RE et RP. Le réarrangement du gène *PLAG1* a été mis en évidence dans 25% des LMS myxoïdes[134].

Pronostic : La survie globale à 5 ans est de 41%, tout stade confondu [135], 51% au stade I, 25% au stade II, sans survie à 5 ans quand la tumeur est étendue au-delà du pelvis[136]. La réponse à la chimiothérapie est faible[131].

1.2.5 STUMP (SMOOTH MUSCLE TUMORS OF UNCERTAIN MALIGNANT POTENTIAL) TUMEUR MUSCULAIRE LISSE A POTENTIEL DE MALIGNITE INCERTAIN

Définition : Tumeur musculaire lisse qui ne peut pas être diagnostiquée comme LMS mais qui ne rentre pas dans les critères diagnostiques d'un LM ou de ses variants et qui a une évolution maligne seulement dans une minorité de cas (OMS 2020)[137].

Il s'agit d'un diagnostic d'exclusion.

L'âge moyen est de 43 ans ,10 ans plus jeunes que les patientes atteintes de LMS[138]. Les patientes qui ont récidivé sont 10 ans plus jeunes par rapport aux patientes sans récidive[138-140].

Macroscopie Les STUMP ont le même aspect macroscopique que les LM. Les STUMP qui ont récidivé ont le plus souvent montré des bords irréguliers, mal limités par rapport au myomètre adjacent [138].

Critères diagnostiques : Ils sont différents selon les différents histotypes (Tableau 6)

1.2.5.1 STUMP (TUMEUR FUSOCELLULAIRE/ CONVENTIONNELLE)(CF FIG 25)

Tableau 6. Critères diagnostiques des STUMP fusiformes (selon OMS 2020)

Atypie	Nécrose	Mitoses	diagnostic	récidive
Présente	absente	<10mitoses/10 CFG*	STUMP	12-17%
Absente	présente	<10 mitoses/10 CFG	STUMP	28%
Absente	absente	≥15 mitoses/10 CFG	STUMP	0
Présente	absente	Compte mitotique incertain dû aux caryorrhexis	STUMP	

CFG : champs à fort grossissement

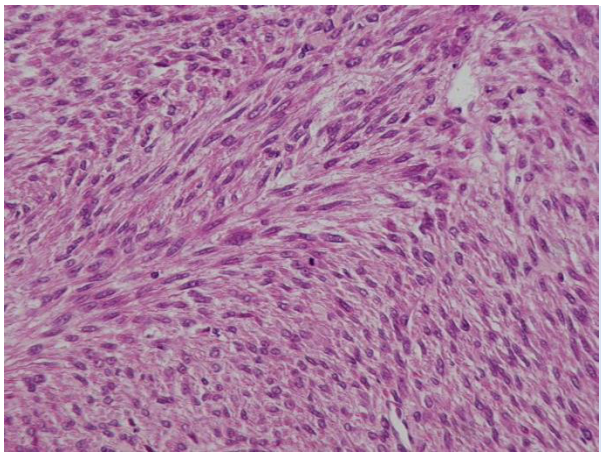

Figure 25. STUMP fusiforme.

Tumeur musculaire lisse sans nécrose avec atypies diffuses, modérées mais avec moins de 10 mitoses.

1.2.5.2 STUMP EPITHELIOÏDE : Tumeur musculaire lisse épithélioïde avec atypies ou 2 à 3 mitoses/10 HPF ou nécrose[107, 141].

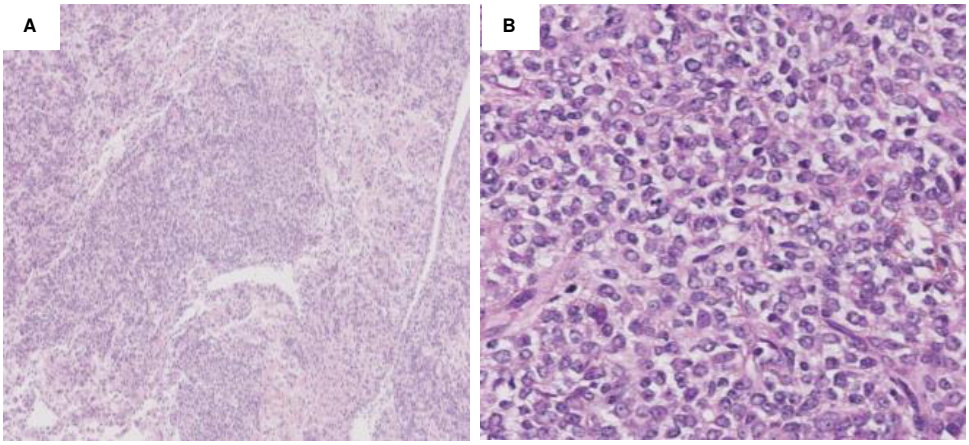

Figure 26. STUMP épithélioïde. Territoires peu cellulaires alternant avec des territoires très cellulaires (A). Cellules épithélioïdes avec atypie (B).

1.2.5.3 STUMP MYXOÏDE : Tumeur musculaire lisse myxoïde à bords infiltrants ou mal limités ou atypies ou 2 mitoses/10 HPF[109, 110].
Pronostic :Le taux de récidive des STUMP varie entre 7et 28% selon les critères utilisés (cf Tableau 5). Les sous-types épithélioïde et myxoïde tendent à récidiver plus fréquemment[142] mais l'évolution est plus indolente par rapport au LMS (en moyenne 47 mois). Les récidives peuvent présenter la même morphologie ou celle d'un LMS. La survie moyenne après récidive est de 5 ans[140].
Les marqueurs immunohistochimiques tels que p16, p53, ki-67, p21, bcl-2, ER and PR n'ont pas montré de valeur pronostique [103, 104, 111]. La perte d'expression de *ATRX* ou *DAXX* a été associée avec un pronostic péjoratif dans les STUMP et LMS [143, 144]

1.3 TUMEURS MUSCULAIRES LISSES UTÉRINES ET COMPARATIVE GENOMIC HYBRIDIZATION ARRAY (CGH ARRAY)

L´étude cytogénétique des altérations somatiques du nombre de copies (somatic copy number alteration/SCNA) a mis en évidence le caractère inhérent des anomalies structurelles à l´échelle chromosomique au sein des cancers. L´enjeu étant de faire la part des choses entre les altérations ciblant des gènes « driver », susceptibles de devenir un outil diagnostique ou une cible thérapeutique, et les nombreuses altérations apparemment aléatoires qui s´accumulent au décours de la tumorigénèse. Les altérations les plus focales, segmentaires, « ciblées », semblent être les pistes les plus prometteuses à emprunter afin de traquer les gènes les plus pertinents.[145]

Dès la fin des années 1980, des tentatives de classifications caryotypiques des LM[146-148] et LMS [149, 150 151] utérins et de corrélations à l´aspect morphologique sont rapportées. Les efforts afin d´extraire de profils génomiques complexes de ces tumeurs, les éléments les plus pertinents permettant d´améliorer la prise en charge thérapeutique se poursuivent jusqu´à aujourd´hui.

Avec l'arrivée de la CGH-array (Comparative Genomic Hybridization), technique qui détecte à une forte résolution (par rapport au caryotype) la variation du nombre de copie (CNV) de segments chromosomiques sur tout le génome, a ouvert la voie à la recherche des événements chromosomiques récurrents dans les cancers tels que les gains, les amplifications, les pertes hétérozygotes et homozygotes, les translocations non équilibrées et la chromotripsis[152].

Technique CGH . La technique varie selon la technologie utilisée (AGILENT versus AFFYMETRIX les deux plateformes plus répandues) et la résolution des puces.

Il s'agit d'une hybridation génomique comparative (CGH). Cela implique que l'ADN de l'échantillon tumoral est comparé avec un ADN de référence (Fig 27).

Dans la plateforme AGILENT l'hybridation est physique : cela veut dire que l'ADN test et l'ADN référence sont hybridés. L'ADN d'un échantillon tumoral est marqué avec un fluorochrome et est co-hybridé sur une puce à ADN avec de l'ADN normal marqué avec un autre fluorochrome. La puce est ensuite scannée et la fluorescence des 2 fluorochromes au niveau de chaque sonde de la puce est mesurée. Les données obtenues sont les ratios de fluorescence ADN tumoral/ADN normal en log 2 pour chaque sonde de la puce.

Pour une puce AGILENT 60K environ 60 000 sondes sont hybridées et ces dernières correspondent à des oligonucléotides de 60 pb.

La puce permet d'hybrider sur une même lame jusqu'à 8 échantillons et présente une sonde toutes les 41 kb de manière générale et toutes les 33 kb dans les gènes Refseq.

Différent est l'approche de la technologie AFFYMETRIX (Fig 28) selon laquelle l'ADN à tester est hybridé avec la puce et non pas avec l'ADN test. Les données obtenues sur la puce sont comparées via les algorithmes du logiciel ChAS à des librairies de références obtenues sur des tissus sains. Pour la puce ONCOSCAN ChAS le modèle de référence est obtenu d'environ 400 ADN obtenues de tissus sains et tissus peri-tumoraux fixés en formol et inclus en paraffine (FFPE) provenant d'une 20aine de sources couvrant une large sélection de zones géographiques, de sites collecteurs, d'âge de blocs, de types de cancer et de sexe. Elle contient au total 217454 sondes pratiquement toutes polymorphes (moins de 1000 sondes non polymorphes). Les sondes sont des oligonucléotides de 25 pb synthétisées sur la lame par photolithographie, chaque sonde correspond à des milliers d'oligonucléotides identiques. La puce est en silicium. Elle présente une résolution de 50 kb à 125 kb sur 900 gènes décrits comme étant impliqués dans des cancers. En dehors de ces gènes, 90% du génome présente une résolution de 300-310 kb et 97% du génome présente une résolution d'au moins 380 kb. La résolution des LOH à travers le génome est =10

MB. Si la fraction de cellules présentant l'anomalie est grande la résolution augmente jusqu'à 3 à 5 MB.
Cette dernière technologie remplace de plus en plus la plateforme AGILENT, du moins en cancérologie et sur matériel FFPE.

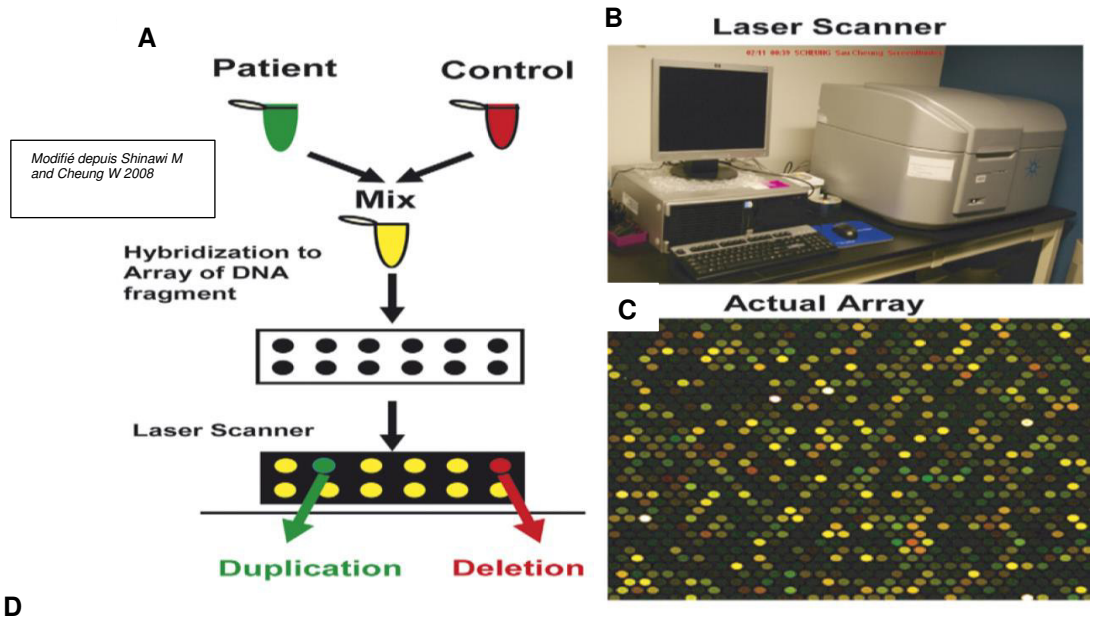

D

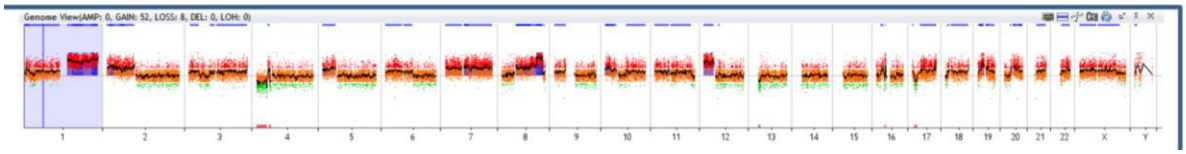

Figure 27. Principe d'analyse génomique comparative selon technologie Agilent
L'ADN à tester est marqué avec fluorochrome vert (Cy 3), l'ADN de référence est marqué en rouge (Cy 5). Les deux ADN sont mis à hybrider sur une plaque contenant les puces. Les lames sont scannées Le microarray avec les spots avec différente intensité de fluorescence qui correspond à un ratio entre ADN tumoral et ADN de référence. Les données sont analysées par un logiciel qui en sort un profil.

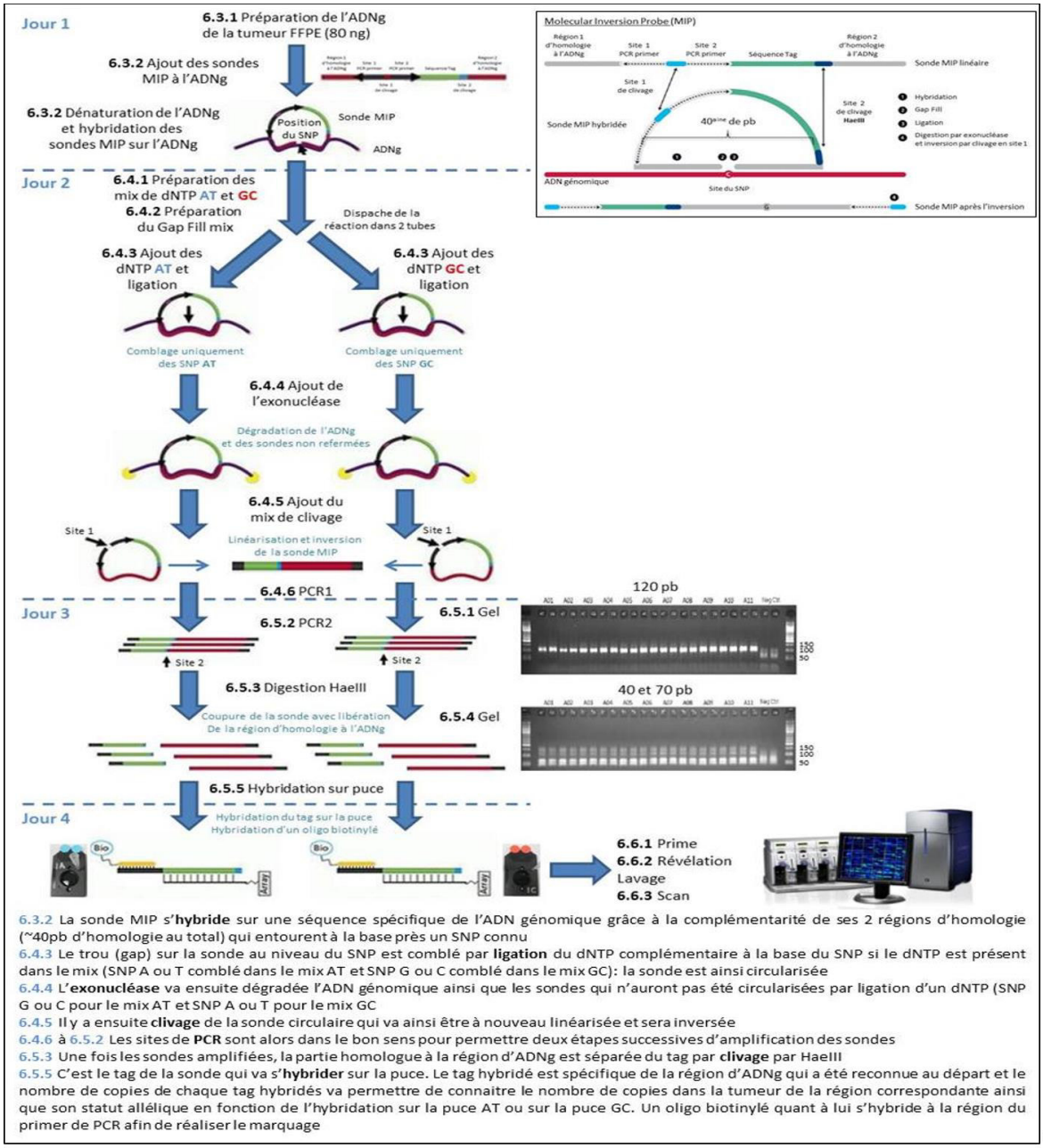

Figure 28. Principe d'analyse génomique comparative selon technologie Affymetrix

Schéma de la méthode Oncoscan CNV_ Adapté du Oncoscan CNV Assay Userguide/ Affymetrix

En 2010 l´équipe de Frédéric Chibon a développé la signature pronostique CINSARC (Complexity INdex in SARComas) qui a permis de discriminer au sein des sarcomes à génomique complexe (autres qu´à translocation), deux groupes pronostiques distincts dont l´issue clinique corrélait avec la complexité génomique et cela avec plus d´exactitude que ne le faisaient les grades histopronostiques jusqu´alors utilisés[36]. Cette signature a par la suite été validée au sein des GIST (Gastro Intestinal Stromal Tumor) notamment au sein des GIST classées en risque intermédiaire selon les classifications histopathologiques. Elle a permis de discriminer parmi ces dernières, celles à plus haut risque métastatique, susceptibles de tirer un véritable profit d´une thérapie adjuvante[153]. Cette expérience dans le groupe des GIST a également permis d´extraire de la signature CINSARC son corollaire, l´indice génomique (Genomic Index/GI) témoin de la complexité structurelle de la tumeur à l´échelle chromosomique. Ce dernier est calculé sur base des analyses de CGH Array comme suit :

$GI = A^2 / C$

où A correspond au nombre d´altérations (gains et délétions segmentaires) et C au nombre de chromosomes altérés[154].

1.4 L'ANALYSE DU PROFIL GENOMIQUE PAR CGH-ARRAY ET SES APPLICATIONS AUX TUMEURS MUSCULAIRES LISSES UTERINES : PREMIER ESSAIS ENCOURAGEANTS ET L'ETUDE SUR LES STUMP

En analogie à l'exemple des GIST les tumeurs musculaires lisses utérines ont été analysées en CGH. Les résultats ont été encourageants : les 10 LM testés ont montré un génome très peu remanié (profil plat ou peu remanié). Les 10 LMS au contraire ont montré un génome instable avec de nombreuses cassures intrachromosomiques, des chromostripsis (profil remanié ou très remanié) (Fig 29).En se basant sur cette observation qui confirme l'hypothèse du départ, à la base de la thèse, selon laquelle la complexité chromosomique au sein des tumeurs musculaires lisses est liée d'une part à l'évolution et d'autre part identifie des catégories diagnostiques séparées, l'étape suivante a été de tester les STUMPs. L´Indice Génomique au cut off de 10, permet de discriminer un groupe à faible risque de récurrence dont le comportement biologique se rapproche de celui des LM, et un groupe à haut risque de récurrence représentant probablement une forme de LMS de bas grade[74] (Fig 30).

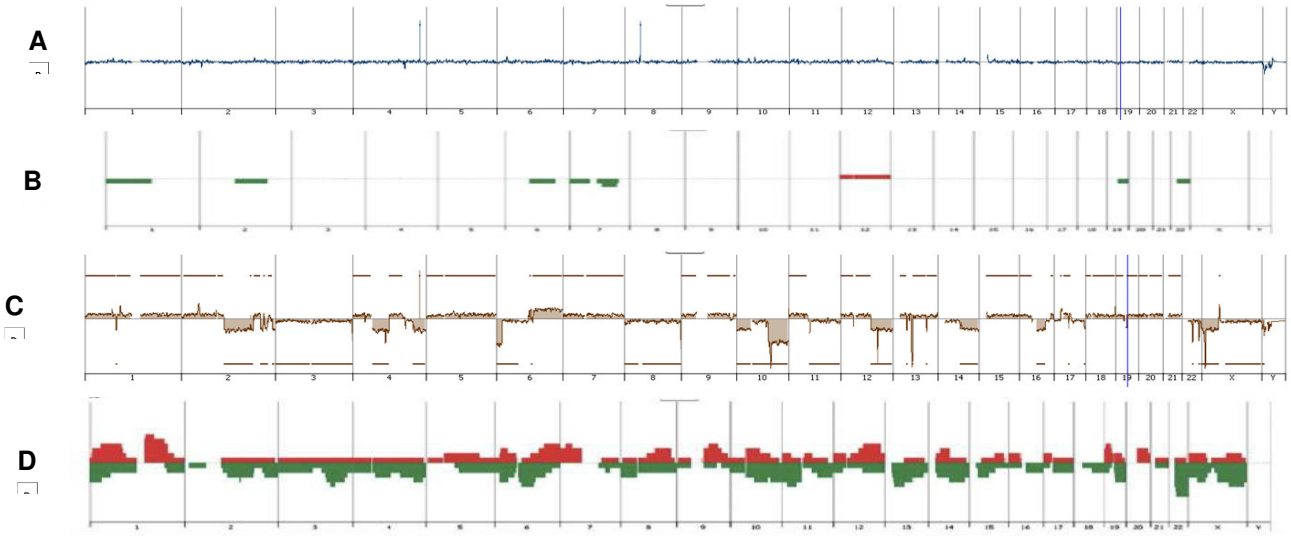

Figure 29. Différence génomique entre LM et LMS. *En* A le profil d'un LM et en B le penetrance plot de 10 cas. Les LM montrent des profils plats ou très peu remaniés. En C le profil d'un LMS en D le penetrance plot de 10 LMS. Les LMS montrent des profils remaniés ou très remaniés. *Modifié depuis Croce et al 2015[74]*

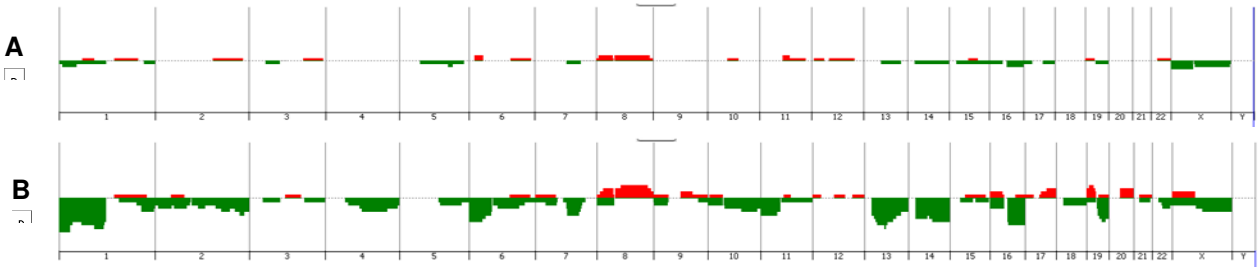

Figure 30. Genomic Index dans les STUMP. Le groupe de STUMP a été séparé selon le Genomic Index au cut off de 10 en un groupe peu remanié, proche des LM, sans récidive (13/29) (A) et en un groupe remanié, proche des LMS avec récidives et décès (16/29).*Modifié depuis Croce et al 2015[74]*

1.5 LA SIGNATURE D'EXPRESSION CINSARC NANOCIND®

Complexity INdex in SARComas est une signature transcriptomique, issue de l'expression de 67 gènes impliqués dans la biogenèse, le contrôle de la mitose et de la ségrégation chromosomique(Fig 31) obtenue de la combinaison des gènes différemment exprimés dans les sarcomes des tissus mous de grade 3 versus 1 et 2 selon le grade FNLCC[36, 155] et sélectionnés par la significativité statistique (Fig 32).
Cette signature est le reflet de l'instabilité chromosomique des tumeurs mais les gènes surexprimés dans cette signature le sont sans passer par des altérations chromosomiques telles que l'amplification/gain ou altérations structurales des loci qui les abritent. Ces gènes sont sous le contrôle de facteurs de transcription tels que *NFY* et *E2F1* [156]. La signature CINSARC a démontré sa valeur pronostique dans 21 des 39 cancers testés, se montrant supérieure aux 15000 autres signatures évaluées[157]. La principale limitation de la signature, qui avait été mise au point sur matériel congelé, a été, jusqu'à il y a deux ans, le faible rendement sur matériel fixé en formol et inclus en paraffine (FFPE) qui représente la routine diagnostique. En effet la signature CINSARC à partir de matériel FFPE avec technologie de RNA-seq total est efficace dans moins de 60% des cas[158]. La combinaison de la signature CINSARC avec la technique Nanostring®(Fig 33) méthode qui ne nécessite pas de retro-transcription (RT-PCR) et d'amplification du cDNA mais qui quantifie directement la quantité de transcrit[159], a permis d'appliquer la signature sur matériel FFPE, que ce soit sur pièce opératoire ou sur microbiopsie[160].

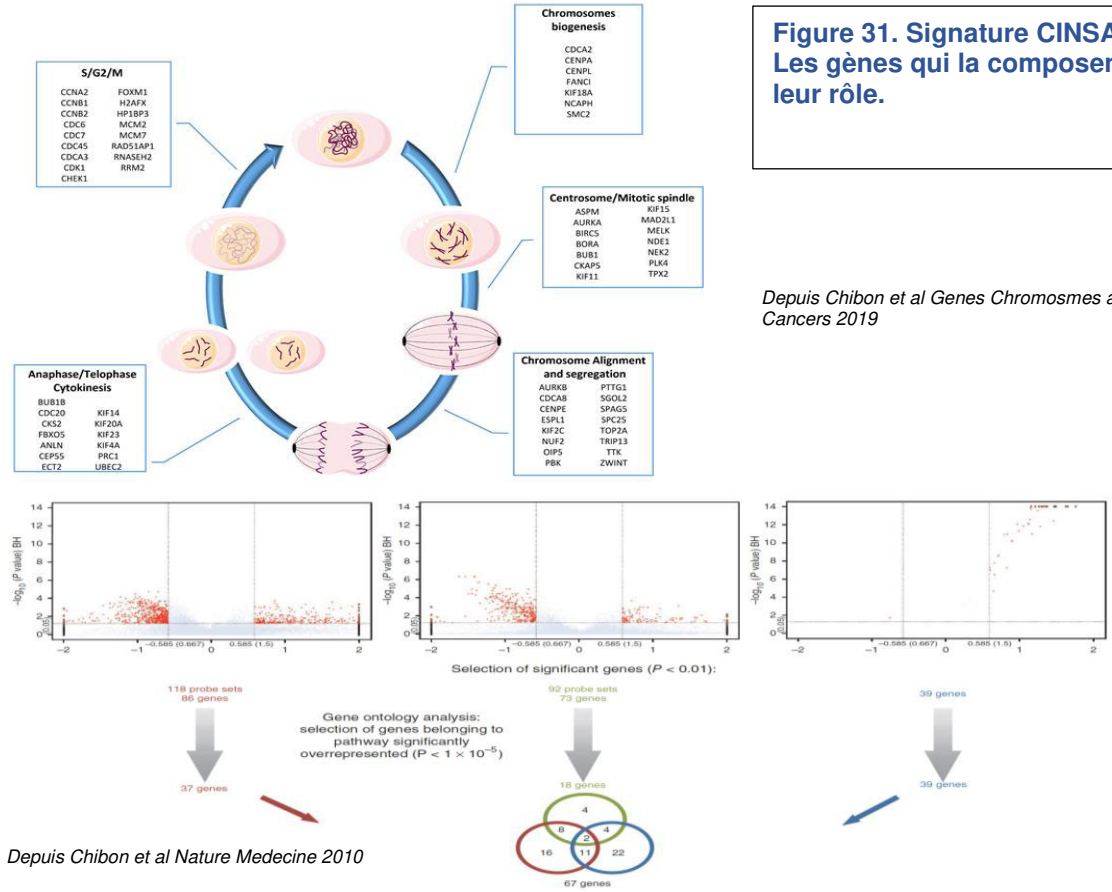

Figure 31. Signature CINSARC. Les gènes qui la composent et leur rôle.

Depuis Chibon et al Genes Chromosmes and Cancers 2019

Depuis Chibon et al Nature Medecine 2010

Figure 32.Schéma du processus de création de la signature CINSARC. Les profils d'expression ont été comparés (test de Welch) selon les groupes des tumeurs obtenu selon l'altération du nombre des copie par CGH (gauche), le grade FNLCC (au centre) et une signature d'expression d'instabilité chromosomique (à droite).

La signature de 67 gènes CINSARC est issue de l'analyse par enrichissement par Gene Ontology qui a permi d'identifier les voies impliquées dans les gènes altérés. Le

diagramme de Venn montre les gènes communs aux analyses et les gènes non partagés.

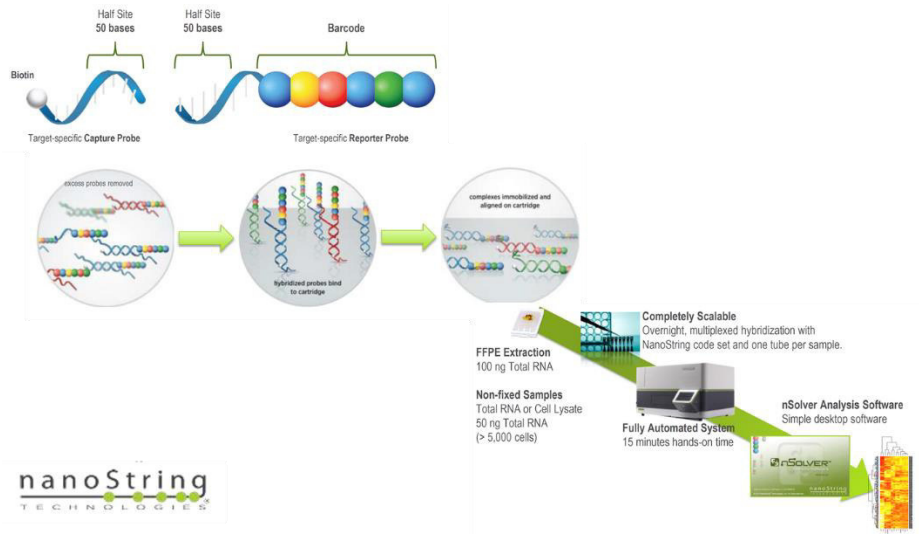

Figure 33. Schéma de la méthode Nanostring®.

Deux sondes sont employées pour fixer les transcrits ciblés, incluant une sonde avec une succession de 6 fluorochromes qui servira de code barre et une sonde biotinylée permettant la fixation au support. Après l'étape d'hybridation et purification, les complexes hybridés sont liés à la surface de la plaque de comptage et immobilisés et alignés prêts à être scannés. Les données sont élaborées par le logiciel nSolver.

2 RATIONNEL DE L'ETUDE ET HYPOTHESE DE TRAVAIL

L'hypothèse qui est le fil conducteur et qui anime ma thèse est la suivante :

il existe un lien entre la complexité génomique des tumeurs musculaires lisses utérines et la structuration des catégories diagnostiques d'une part et (intrinsèquement lié au premier volet) l'évolution clinique de ces tumeurs d'autre part.

Après avoir démontré l'utilité diagnostique du profil génomique évalué par CGH-array dans les tumeurs musculaires lisses de l'utérus, essentiellement de type fusiforme et la valeur pronostique du GI dans les STUMP au cours d'un premier travail publié[74] et discuté en introduction, nous avons entrepris une série de travaux au cours de ce travail de thèse qui ont pour objectifs :

1- De démontrer la valeur pronostique du GI dans les LMS utérins à cellules fusiformes (article publié)
2- De démontrer la valeur pronostique de la signature CINSARC dans les LMS utérins surtout de stade I (article publié)
3- D'évaluer l'utilité clinique et pronostique du profil génomique et du GI dans les variants des tumeurs musculaires lisses de l'utérus à cellules épithélioides (article en cours de publication) et à noyaux bizarres (article en cours de publication)

3 RESULTATS

3.1 LE RISQUE POTENTIEL DE RECIDIVE DES TUMEURS MUSCULAIRES LISSES UTERINES CONVENTIONNELLES (FUSIFORMES) EST CORRELE AVEC LE GENOMIC INDEX (GI)

Le rationnel de l'étude et le besoin clinique

Les LMS utérins représentent 1 à 3% des tumeurs malignes utérines[161] et les sarcomes utérins les plus fréquents (50 à 60% des sarcomes utérins)[136]. L'incidence annuelle est estimée entre 0,36[162] et 0.8[163] cas pour 100000 femmes et 0.5 à 2 per 100000 femmes entre 35-64 ans [164]. Le diagnostic est souvent de découverte fortuite sur une pièce d'hystérectomie réalisée pour « myome », ce qui implique que le type de chirurgie est souvent inadapté et dans la majorité des cas le seul matériel disponible pour les analyses consiste en un matériel FFPE. Le pronostic est sévère et le stade demeure le facteur pronostique le plus important. Plus de 50% des patientes sont diagnostiquées au stade I (tumeur limitée à l'utérus), néanmoins même à un stade précoce le taux de récidive est élevé et seulement 28% des patientes sont indemnes de maladie à 5 ans. Actuellement la prise en charge des LMS utérins ne prévoit pas de traitement adjuvant après l'exérèse chirurgicale (en dehors d'essais clinique) sauf au stade avancé et pour cela le stade FIGO reste le facteur pronostique majeur, même s'il ne permet pas d'identifier les patients susceptibles d'évoluer rapidement. En particulier pour les LMS au stade I (limités à l'utérus) il n'est pas possible d'identifier les patientes qui pourraient bénéficier d'une chimiothérapie adjuvante. Le grade histopronostique des sarcomes (grade FLNCC) qui est le facteur principal de prédiction des métastases et de la survie globale dans les sarcomes des tissus mous n'a pas montré de valeur pronostique dans les LMS utérins [165]. Un nomogramme prédictif de la survie globale à 5 ans (exprimée en % de survie globale) a été publié [166]. Les paramètres avec une valeur pondérale forte dans ce nomogramme sont néanmoins liés au stade et il intègre la valeur grade qui n'est pas consensuel.

Identifier les patientes avec LMS avec risque élevé de récidive au moment du diagnostic est essentiel dans la décision thérapeutique

Série et méthodes. Analyse du profil génomique par CGH-array plateforme Agilent (8x60K) d'une série de 77 tumeurs musculaires lisses utérines (19 LM, 14 STUMP, 44 LMS) avec données clinico-pathologiques annotées.

Résultats et Discussion. Nous avons confirmé sur une série plus large ce que nous avions précédemment publié[74] : le GI au seuil de 10 est un outil diagnostique qui permet de distinguer parmi les STUMP, les tumeurs bénignes et malignes. Nous avons de plus démontré que le GI au seuil de 35 est un facteur de mauvais pronostic dans les LMS. En particulier pour les LMS au stade I de GI ≥35, le gain du chromosome 5p (comportant *RICTOR*), la perte du chr 13 (emportant *RB-1*), le gain de 17p (emportant *MYOCD*) sont des facteurs pronostiques péjoratifs. Ces données pourront être prises en compte dans la randomisation des patientes lors des essais cliniques qui comparent le bénéfice de la chimiothérapie adjuvante versus pas de chimiothérapie dans les LMS utérins au stade I.

MODERN PATHOLOGY (2018), 1–13

Genome profiling is an efficient tool to avoid the STUMP classification of uterine smooth muscle lesions: a comprehensive array-genomic hybridization analysis of 77 tumors

Sabrina Croce[1,2,22], Agnès Ducoulombier[3,4,22], Agnès Ribeiro[1], Tom Lesluyes[2,5], Jean-Christophe Noel[6], Frédéric Amant[7,8], Louis Guillou[9,10], Eberhard Stoeckle[11], Mojgan Devouassoux-Shisheboran[12], Nicolas Penel[3], Anne Floquet[13], Laurent Arnould[14], Frédéric Guyon[11], Florence Mishellany[15], Camille Chakiba[13], Tine Cuppens[7], Michal Zikan[16], Agnès Leroux[17], Eric Frouin[18], Isabelle Farre[19], Catherine Genestie[20], Isabelle Valo[21], Gaëtan MacGrogan[1] and Frédéric Chibon[1,2]

[1]Department of Biopathology, Institut Bergonié, Comprehensive Cancer Centre, Bordeaux, France; [2]Institut National de la Santé et de la Recherche Medicale (INSERM) U1218, Bordeaux, France; [3]Oncology Department, Centre Oscar Lambret, Comprehensive Cancer Centre, Lille, France; [4]Oncology Department, Centre Antoine Lacassagne, Comprehensive Cancer Centre, Nice, France; [5]University of Bordeaux, Bordeaux, France; [6]Department of Pathology, Clinic of Gynecopathology and Senology, Erasme University Hospital, Brussels, Belgium; [7]KU Leuven - University of Leuven, Department of Oncology, Gynaecologic Oncology; University Hospitals Leuven, Department of Obstetrics and Gynaecology, Leuven, Belgium; [8]Centre for Gynecologic Oncology Amsterdam (CGOA), Antoni Van Leeuwenhoek - Netherlands Cancer Institute, Amsterdam, The Netherlands; [9]Argot-Lab, Lausanne, Switzerland; [10]Institut Universitaire de Pathologie, Lausanne, Switzerland; [11]Department of Surgery, Institut Bergonié, Comprehensive Cancer Centre, Bordeaux, France; [12]Department of Pathology, Hôpital Universitaire Lyon Sud, Pierre Benite, France; [13]Department of Medical Oncology, Institut Bergonié, Comprehensive Cancer Centre, Bordeaux, France; [14]Department of Pathology, Centre JF Leclerc, Comprehensive Cancer Centre, Dijon, France; [15]Department of Pathology, Centre Jean Perrin, Comprehensive Cancer Centre, Clermont-Ferrand, France; [16]Gynaecological Oncology Center, Department of Obstetrics and Gynaecology, Charles University in Prague – First Faculty of Medicine and General University Hospital, Prague, Czech Republic; [17]Department of Pathology, Centre Alexis Vautrin, Comprehensive Cancer Centre, Vandoeuvre-les Nancy, France; [18]Department of Pathology, University Hospital, Poitiers, France; [19]Department of Pathology, Centre Oscar Lambret, Comprehensive Cancer Centre, Lille, France; [20]Department of Pathology, Institut Gustave Roussy, Comprehensive Cancer Centre, Villejuif, France and [21]Department of Pathology, ICO Site Paul Papin, Comprehensive Cancer Centre, Angers, France

The diagnosis of a uterine smooth muscle lesion is, in the majority of cases, straightforward. However, in a small number of cases, the morphological criteria used in such lesions cannot differentiate with certainty a benign from a malignant lesion and a diagnosis of smooth muscle tumor with uncertain malignant potential (STUMP) is made. Uterine leiomyosarcomas are often easy to diagnose but it is difficult or even impossible to identify a prognostic factor at the moment of the diagnosis with the exception of the stage. We hypothesize, for uterine smooth muscle lesions, that there is a gradient of genomic complexity that correlates to outcome. We first tested this hypothesis on STUMP lesions in a previous study and demonstrated that this 'gray category' could be split according to genomic index into two groups. A benign group, with a low to moderate alteration rate without recurrence and a malignant group, with a highly rearranged profile akin to uterine leiomyosarcomas. Here, we analyzed a large series of 77 uterine smooth muscle lesions (from 76 patients) morphologically classified as 19 leiomyomas, 14 STUMP and 44 leiomyosarcomas with clinicopathological and genomic correlations. We

Correspondence: Dr S Croce, MD, Department of Pathology, Institut Bergonie, 229 cours de l'Argonne, Bordeaux F-33000, France.
E-mail: s.croce@bordeaux.unicancer.fr
[22]These authors contributed equally to this work.
Received 13 July 2017; revised 10 November 2017; accepted 12 November 2017; published online 12 January 2018

confirmed that genomic index with a cut-off = 10 is a predictor of recurrence ($P < 0.0001$) and with a cut-off = 35 is a marker for poor overall survival ($P = 0.035$). For the tumors confined to the uterus, stage as a prognostic factor was not useful in survival prediction. At stage I, among the tumors reclassified as molecular leiomyosarcomas (ie, genomic index ≥ 10), the poor prognostic markers were: 5p gain (overall survival $P = 0.0008$), genomic index at cut-off = 35 (overall survival $P = 0.0193$), 13p loss including *RB1* (overall survival $P = 0.0096$) and 17p gain including *MYOCD* gain (overall survival $P = 0.0425$). Based on these findings (and the feasibility of genomic profiling by array-comparative genomic hybridization), genomic index, 5p and 17p gains prognostic value could be evaluated in future prospective chemotherapy trials.
Modern Pathology dvance online publication, 12 January 2018; doi:10.1038/modpathol.2017.185

Uterine sarcomas are rare neoplasms accounting for 4% of all uterine tumors with an estimated incidence of 0.86 per 100 000 women.[1] Uterine smooth muscle lesions include very common benign tumors such as leiomyomas and malignant as leiomyosarcomas.[2] The overall incidence of leiomyomas is 70–80% by 50 years of age.[3] Leiomyomas have a benign behavior despite the benign metastasizing leiomyoma and leiomyomatoses, whereas leiomyosarcomas eventually lead to death through recurrences in up to 75% of cases.[4,5]

The diagnosis of uterine smooth muscle lesions, based on the Stanford criteria (three morphological features: presence of cytologic atypia, mitotic count and tumor cell necrosis),[6] is straightforward in the majority of the cases. However, sometimes morphology is confusing and introduces a degree of subjectivity in the interpretation of these criteria. External factors such as prior treatments (hormonal therapies) or a non-optimal fixation of the sample may pose diagnostic challenges. Hence, such lesions are usually classified as smooth muscle tumors of uncertain malignant potential (STUMP).[2] This classification could result in a risk of under or over diagnosis with clinical consequences for the treatment that could impact the patient.

The FIGO stage is still the most important uterine leiomyosarcomas prognostic factor and forms the basis of the therapeutic strategy.[4,7–9] However, FIGO staging fails to identify patients with high risk of death who could potentially be eligible for chemotherapy.[10–13] Even if this disease is clinically very aggressive,[5] it is difficult to predict the outcome especially when the diagnosis is made at stage I (confined to the uterus). Recently, a specific uterine leiomyosarcomas nomogram for predicting post-resection 5-year overall survival using seven clinicopathological items (age, tumor size, tumor grade, cervical involvement, loco-regional metastases, distant metastases and mitotic index) was published[14] and was subsequently validated on an independent series.[15] In this nomogram, the mitotic index and the tumor grade were taken into account as biological parameters. Nevertheless, the tumor grading in uterine leiomyosarcomas is controversial because by definition leiomyosarcomas diagnosed on the basis of Stanford criteria[6] are of high grade. Contrary to other soft tissue sarcomas, the tumor grade does not show a prognostic value in uterine leiomyosarcomas.[16] Among the seven parameters, three (presence of regional metastasis, distant metastasis and size) are strictly linked to the FIGO stage.[14]

Hence, there is a need to clarify these prognostic strategies. A few years ago, we published a new classification method based on genomic profiling complementary to the morphology able to distinguish within the STUMP category those uterine smooth muscle lesions with a risk of recurrence and poor outcomes from benign lesions.[17]

In this study, we analyzed the genomic profile by array-comparative genomic hybridization in a series of 77 uterine smooth muscle lesions (44 leiomyosarcomas, 14 STUMP and 19 leiomyomas) to validate the power of genomic index as a recurrence predictor. Furthermore, we set out to improve our previous results by studying a larger series with a broader follow-up and to identify overall survival prognostic factors in uterine leiomyosarcomas.

Materials and methods

Tumor Samples

Seventy-seven formalin-fixed and paraffin-embedded uterine smooth muscle lesions from 76 patients (for one patient, both the primary tumor and the recurrence were examined) were collected in France through the French sarcoma network (RRePS and GYN RRePS) (Institut Bergonié of Bordeaux, Centre Oscar Lambret of Lille, Hôpitaux Universitaires Lyon Sud, Centre JF LeClerc, Dijon, Hôpital Universitaire of Poitiers, Centre Jean Perrin, Clermont-Ferrand, Centre Alexis Vautrin, Vandouevre-les Nancy, Institut Gustave Roussy, ICO, Paul Papin, Angers), from Belgium (Hopitaux Universitaires de Bruxelles, Catholic University of Leuven), Czech Republic (University Hospital from Prague) and Switzerland (Hôpitaux Universitaires and Argot-Lab of Lausanne). Fourteen uterine tumors diagnosed as STUMP along with 19 uterine leiomyomas previously published[17] were included in the series. The tumors were diagnosed between 1977 and 2013. For each patient, 1–8 slides were available (mean: 2 slides). All cases were centrally reviewed by one of the authors (SC) and classified according to Stanford

criteria[6] and 2014 WHO guidelines for female reproductive organs.[2] Cytologic atypia was evaluated at medium power magnification (objective ×10) according to the presence of high nuclear size or nuclear pleomorphism and hyperchromatism,[18] the mitotic count was evaluated on 10 high-power fields (objective ×40, field diameter 0.53 mm) and the tumor cell necrosis defined by an abrupt transition from necrotic to non-necrotic areas without interposed granulation tissue.[18] The mitotic cut-off was 10 mitoses/10 power fields for spindle cell smooth muscle tumors, ≥4 mitoses for epithelioid and ≥2 mitoses for myxoid tumors.[2,18]

Frozen material was available for five samples. The samples from the tumor archives of each participating department were centralized in the Biological Resources Center of Institut Bergonié, which the French authorities authorized for scientific research (AC-2008-812).

DNA Extraction

Genomic DNA was extracted from formalin-fixed and paraffin-embedded tissues according to the protocol for DNA isolation from formalin-fixed and paraffin-embedded tissues (http://www.chem-agilent.com/pdf/G441090020v3_1_CGH_ULS_Protocol.pdf) (Agilent Technologies, Santa Clara, CA, USA). A cut-off of 50% of cellularity in tumor samples was set for the analysis.

Array-Comparative Genomic Hybridization Analysis

DNA was hybridized onto 8×60 K whole-genome arrays (G4450A; Agilent Technologies) according to the manufacturer's protocol. Microarray slides were scanned using a DNA Microarray Scanner, images were analyzed by Feature Extraction V10.1.1.1 followed by Agilent Cytogenomic software 4.0. The ADM-2 algorithm of the Comparative Genomic Hybridization Analytics v4.0.76 software (Agilent Technologies) was used to identify the DNA copy number anomalies at the probe level. A low-level copy number gain was defined as a log 2 ratio >0.25 and a copy number loss was defined as a log 2 ratio <0.25. A high-level gain or amplification was defined as a log 2 ratio >1.5 and a homozygous deletion was suspected when the ratio was <-1. The range for derivative log ratio spread cut-off was fixed to 0.50. Genomic index was calculated for each profile as follows: genomic index = A^2/C, where A is the total number of alterations (segmental gains and losses) and C is the number of involved chromosomes.[19,17]

Statistical Analysis

Metastasis-free survival was calculated by the Kaplan–Meier method from the date of initial diagnosis to the date of first metastasis or last follow-up. Overall survival, using the Kaplan–Meier method, was calculated from the date of diagnosis to death or last follow-up. Survival curves were compared with the log-rank test. Univariate survival analyses were performed by using the R software version 3.4.0 (R Development Core Team, Vienna, Austria, 2009) and the 'survival' package (A Package for Survival Analysis in S; Terry Therneau, February 2002; R package, version 2.40-1). To test whether gene alterations (losses or gains) are enriched in groups of tumors classified by the genomic index, Fisher's exact tests were performed. Multivariate survival analyses were performed using Cox regression with Firth's correction with the 'coxphf' package (Georg Heinze and Meinhard Ploner, 2016, version 1.12).

Results

Pathologic Features

After centralized pathological review, the series comprised 19 leiomyomas, 14 STUMP and 44 leiomyosarcomas. Morphologically, all leiomyomas but one case of bizarre nuclei leiomyoma, showed conventional spindle cell morphology. Spindle cell features were observed in the STUMP group (all 14 tumors).

Among the 44 leiomyosarcomas (43 patients), 29/44 tumors showed a spindle cell morphology, 10/44 epithelioid, 4/44 pleomorphic with giant osteoclastic cells (with negative stains for melanocytic markers) and 1/44 myxoid (Figure 1). The clinicopathological data are summarized in Table 1.

Genomic Data and Clinical Correlations

Genome complexity evaluation by genomic index assessment (quantitative approach) and prognostic value. Array-comparative genomic hybridization was analyzable in all 77 tumors. Follow-up data were available for all but two patients with leiomyomas (mean follow-up: 63.6 months, range: 9–232 months). The genomic profiling split the present series of uterine smooth muscle lesions in two groups according to the cut-off defined in our previous paper (genomic index = 10):[17] a group with genomic index <10 (19/74) and a second group with genomic index ≥10 (55/74; Figure 2a).

The first group (genomic index <10) is characterized by a low level of chromosomal rearrangements (Figure 3a; mean genomic index: 2.3, range: 0–9.14) in contrast with the second group (genomic index ≥10) harboring complex genomic profiles (mean genomic index: 51.8, range: 11–180; Figure 3b).

The Kaplan–Meier analysis demonstrated a significant difference in clinical outcome with no recurrence in the group with genomic index <10

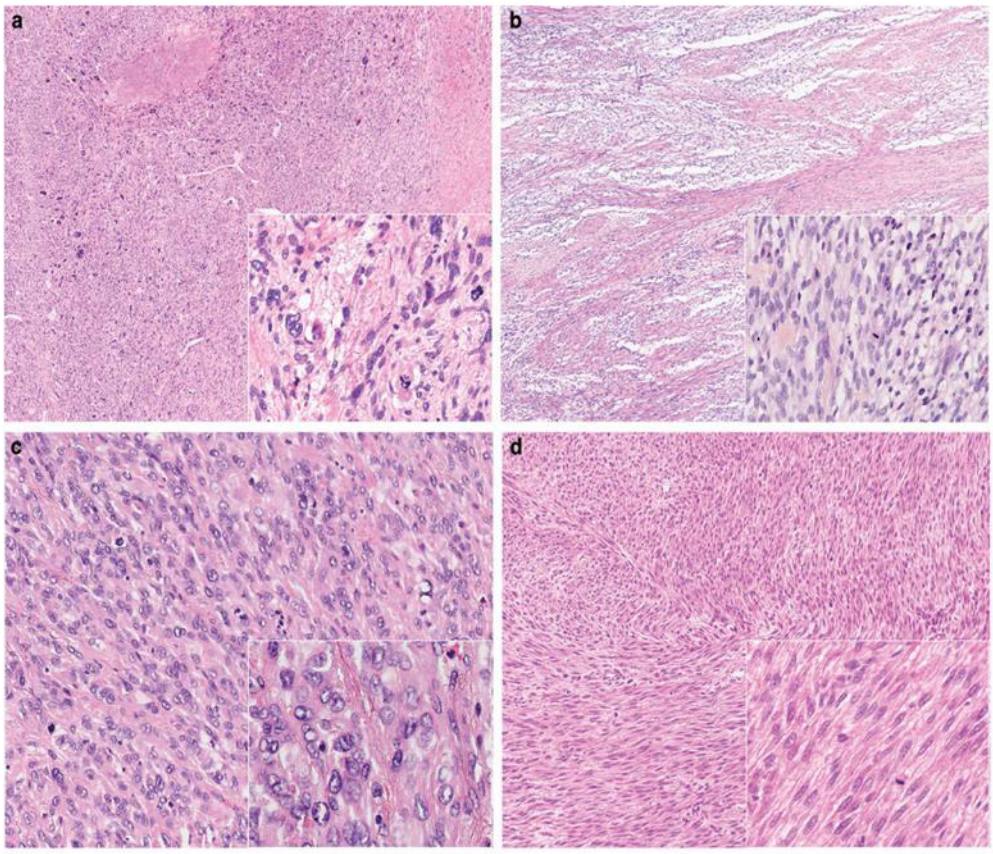

Figure 1 A representation of the morphological features of uterine smooth muscle lesions. (**a**) Uterine leiomyosarcoma with spindle cells, pleomorphic and osteoclastic features and atypical mitoses, stage FIGO IB and genomic index = 84. The patient developed lung metastases and died 32.4 months after the diagnosis (patient 68). (**b**) Myxoid leiomyosarcoma with infiltration of myometrial wall. Some areas are highly cellular with four mitoses, stage FIGO 2B and genomic index = 13.5 (patient 47). (**c**) Epithelioid leiomyosarcoma with genomic index = 27. The patient died of disease 26 months after the diagnosis with peritoneal metastases (patient 48). (**d**) Smooth muscle lesion with mild atypia, 20 mitoses (STUMP) with genomic index = 14.3. The patient had multiple peritoneal and retroperitoneal recurrences and she is alive after 103.2 months (patient 33).

and recurrences and deaths in the second group (Figure 2b), confirming our previous results.[17]

Morphologically, the first group included all leiomyomas, two STUMPs and no leiomyosarcomas. The second group included all leiomyosarcomas and 12 STUMPs. Only four patients with leiomyosarcomas did not recur (of note, one patient died of pulmonary embolism 9 days after surgery) and among the 12 STUMPs with genomic index ≥ 10, seven recurred (Table 1).

All leiomyomas showed a flat or very simple profile (mean genomic index: 1.9, range: 0–9.1). The leiomyosarcomas group showed a complex, rearranged chromosome profile with numerous intrachromosomal breaks (gains and losses). The mean genomic index in the leiomyosarcomas group was 55 (range: 13.5–180). The STUMP group was then split into two groups according to genomic index. Owing to the clinical aggressiveness and outcome of the tumors with genomic index ≥ 10, they were thereafter considered as leiomyosarcomas.

Therefore, the second step was to identify a death predictor in this newly defined group of leiomyosarcomas. Different genomic index cut-offs (five for each step) were tested and a cut-off of genomic index = 35 was identified as an efficient predictor of death ($P = 0.035$, HR = 2.18 (1.04–4.58); Figure 2c).

In order to identify specific chromosomal alterations (qualitative approach) related to prognostic value, we analyzed differential penetrance plots among the patients alive, whose tumor had genomic index ≥ 10 (19/55) and patients who died of the disease (36/55). We identified five frequent alterations, in addition to genomic index ≥ 35 (Figure 2c), associated with overall survival: 5p gain (Figure 2d, Table 2a), 1p gain, 13q loss (including *RB1*) and 17p gain including *MYOCD* (Table 2a). Staging being the gold standard for clinical/pathological prognosis, all

Table 1

Clinical data												*Genomic data*									
Patient	*FU status*	*Age*	*RFS months*	*OS months*	*Recurrence*	*Type of recurrence*	*FIGO stage*	*Size cm*	*Location*	*Type of surgery*	*Centralized diagnosis*	*Morphology*	*FH features*	*5p gain*	*1p gain*	*17p gain*	*17p loss*	*13 loss*	*GI*
1	A-NOS	40	53.6	53.6	No			4	Uterus	Hysterectomy R0	LM	Spindle	No	0	0	0	0	0	0
2	A-NOS	49	75.3	75.3	No			3.7	Uterus	Hysterectomy R0	LM	Spindle	No	0	0	0	0	0	1
3	A-NED	50	68.6	68.6	No			5.5	Uterus	Hysterectomy R0	LM	Spindle	Yes	0	0	0	0	0	0
4	A-NOS	63	37	37	No			1.4	Uterus	Hysterectomy R0	LM	Spindle	No	0	0	0	0	0	0
5	Lost	45						3.5	Pelvis/ peritoneum	Total resection R0	LM	Spindle	No	0	0	0	0	0	4
6	A-NED	46	58.4	58.4	No			4	Uterus	Total hysterectomy R0	LM	Spindle	Yes	0	0	0	0	0	2
7	A-NED	48	53	53	No			15	Uterus	Total hysterectomy R0	LM	Spindle	Yes	0	0	0	0	0	2
8	A-NED	49	72.9	72.9	No			6.5	Uterus	Total hysterectomy R0	LM	Spindle	Yes	0	0	0	0	0	0
9	DOC	67	21.3	21.3	No			7	Large ligament	Total resection R0	LM	Spindle	No	0	0	0	0	0	2
10	Lost	48						5.5	Uterus	Total hysterectomy R0	LM	Spindle cellular	Yes	0	0	0	0	0	5
11	A-NED	32	101.5	101.5	No			6.5	Uterus	Myomectomy R0	LM	Spindle	Yes	0	0	0	0	0	0
12	A-NED	44	102	102	No			4.5	Uterus	Total hysterectomy R0	LM	Spindle	No	0	0	0	0	0	0
13	A-NED	67	102.1	102.1	No			1.5	Uterus	Total hysterectomy R0	LM	Spindle	No	0	0	0	0	0	0
14	A-NED	68	102.2	102.2	No			1.2	Uterus	Total hysterectomy R0	LM	Spindle	Yes	0	0	0	0	0	0
15	A-NED	40	137.8	137.8	No			4.5	Uterus	Total hysterectomy R0	LM	Spindle	Yes	0	0	0	0	0	1
16	A-NED	36	137.2	137.2	No			15	Uterus	Myomectomy R0	LM	Spindle	Yes	0	0	0	0	0	1
17	A-NED	44	175.2	175.2	No			4.5	Uterus	Total hysterectomy R0	LM	Spindle	Yes	0	0	0	0	0	1
19	A-NED	80	93.8	93.8	No	Residual disease	ND	15	Pelvis/ uterus	Total hysterectomy R1	STUMP	Spindle	Yes	0	0	0	0	0	3
20	A-NED	36	84.2	84.2	No			7	Uterus	Total hysterectomy R0	LM	BN-LM	Yes	0	0	0	-2 TP53	-2 RB1	9
21	A-NED	34	128.9	128.9	No		ND	NA	Uterus	Myomectomy R0	STUMP	Spindle	Yes	0	0	0	0	0	8.3
22	A-NED	47	99.9	99.9	No			6	Uterus	Total hysterectomy R0	LM	Spindle	No	0	0	0	0	0	9.14
23	A-NED	63	51.6	51.6	No		IB	7	Uterus	Total hysterectomy	STUMP	Spindle	Yes	0	0	0	0	0	56.81
24	A-NED	42	NA	61.2	No		IB	8	Uterus	Subtotal hysterectomy	STUMP	Spindle	No	0	0	0	0	0	32.6
25	A-NED	47	NA	99.6	No		IB	7	Uterus	Total hysterectomy	STUMP	Spindle	Yes	0	0	0	0	0	14.28
26	AWD	48	36	162.0	Yes	Bladder, rectum, omentum, para-aortic LN, lung	IB	7	Uterus	Total hysterectomy	STUMP	Spindle	Yes	0	0	0	0	-1RB1	16.9

Table 1 (Continued)

Clinical data											*Genomic data*										
Patient	*FU status*	*Age*	*RFS months*	*OS months*	*Recurrence*	*Type of recurrence*	*FIGO stage*	*Size cm*	*Location*	*Type of surgery*	*Centralized diagnosis*	*Morphology*	*FH features*	*5p gain*	*1p gain*	*17p gain*	*17p loss*	*13 loss*	*GI*
27	AWD	50	57	104.4	Yes	Paravertebral soft tissue, bone	I	NA	Uterus	Total hysterectomy	STUMP	Epithelioid	No	0	0	0	-1 no TP53	-1 RB1	22.23
28	A-NOS	77	17	25.2	Yes	Peritoneum, ileum, vagina, pelvis	IB	11	Uterus	Total hysterectomy	STUMP	Spindle	No	0	1	0	0	-2 RB1	48
29	A-NED	60	NA	42.0	No		IA	2	Uterus	Myomectomy	STUMP	Spindle	No	0	1	2 ampl MYOC	0	-2 RB1	52
30	DOD	66	55	55.2	Yes	Vagina	IB	8	Uterus	Total hysterectomy	STUMP	Spindle	Yes	0	0	0	0	-1 RB1	21.33
31	A-NED	85	NA	106.8	No		IB	11	Uterus	Total hysterectomy	STUMP	Epithelioid	No	0	1	0	0	-1 RB1	94.1
32	DOD	43	10	15.6	Yes	Bone	IB	20	Uterus	Total hysterectomy	STUMP	Spindle	Yes	0	1	2 ampl MYOC	-1 TP53	-1 RB1	100
33	A-NED	46	35	103.2	Yes	Peritoneum, right ovary, retroperitoneum	IA	5	Uterus	Total hysterectomy	STUMP	Spindle	Yes	0	0	0	0	0	14.3
34	A-NED	48	12	147.6	Yes	Uterine cervix, peritoneum, soft tissue (leg and arm)	I	NA	Uterus	Total hysterectomy	STUMP	Spindle	Yes	0	0	0	0	0	11
35	DOD	55	26.4	56.4	Yes	Pelvis, peritoneum	III	NA	Uterus	Total hysterectomy	LMS	Spindle	Yes	0	0	0	0	0	44.64
36	DOD	51	26.4	61.2	Yes	Soft tissue, bone, lung	IB	9	Uterus	Total hysterectomy	LMS	Epithelioid	Yes	0	0	0	0	-2 RB1	156
37	DOD	56	136.8	171.6	Yes	Lung	IA	1.8	Uterus	Total hysterectomy	LMS	Epithelioid	No	0	1	0	-1 TP53	-2 RB1	18
38	DOD	50	19.2	57.6	Yes	Lung	IB	7	Uterus	Total hysterectomy	LMS	Spindle	Yes	0	0	0	-2TP53	-2 RB1	22
39	DOD	59	21.6	48	Yes	Lung	IA	3	Uterus	Total hysterectomy	LMS	Spindle	Yes	0	0	1 MYOCD	-1 TP53	-2RB1	52.26
40	AWD	40	72	110.4	Yes	Clavicular LN, lung, pancreas	IB	19	Uterus	Total hysterectomy	LMS	Spindle	Yes	0	0	1 MYOCD	-2TP53	-1 RB1	25
40	AWD	45	NA	NA	—		NA	NA	Uterus	Total hysterectomy	LMS	Spindle	No	0	0	1 MYOCD	-2TP53	-1 RB1	69
41	DOD	40	0	13.2	Yes	Lung	IVB	8	Uterus	Total hysterectomy	LMS	Spindle	Yes	0	1	0	-1 TP53	-1 RB1	28.9
42	DOD	63	8.5	27.6	Yes	Lung	IB	7	Uterus	Total hysterectomy	LMS	Spindle	No	0	1	0	0	-2 RB1	19.6
43	DOD	53	9	27.6	Yes	Lung	III	2.8	Uterus	Total hysterectomy	LMS	Spindle	No	1	1	1 MYOCD	- 1 TP53	-1 RB1	69
44	DOD	62	1.6	34.8	Yes		IA	4.5	Uterus	Total hysterectomy	LMS	Spindle	Yes	1	0	2MYOCD	-1 TP53	-2 RB1	40
45	AWD	63	1.2	84	Yes	Lung	IB	10	Uterus	Total hysterectomy	LMS	Spindle	No	0	0	0	0	-2 RB1	15.12
46	DOD	68	ND	6	ND	ND	IIB	12	Uterus	Total hysterectomy	LMS	Epithelioid	Yes	0	1	1 MYOCD	0	-1RB1	46
47	DOC pulmonary embolism	62	NA	0 9 days	No		IIB	8	Uterus	Total hysterectomy	LMS	Myxoid	No	0	0	0	0	0	13.5
48	DOD	71	13.2	26	Yes	Peritoneum	III	12	Uterus	Total hysterectomy	LMS	Epithelioid	No	0	0	2 ampl MYOC	-2 TP53	-1RB1	27

Table 1 (Continued)

	Clinical data											*Genomic data*										
	Patient FU status	*Age*	*RFS months*	*OS months*	*Recurrence*	*Type of recurrence*	*FIGO stage*	*Size cm*	*Location*	*Type of surgery*	*Centralized diagnosis*	*Morphology*	*FH features*	*5p gain*	*1p gain*	*17p gain*	*17p loss*	*13 loss*	*GI*
49	DOD	57	19.2	23	Yes	Lung	IB	7.5	Uterus	Total hysterectomy	LMS	Spindle	No	0	0	0	0	-1RB1	36
50	DOD	38	27.6	ND	Yes	Lung	IB	7.5	Uterus	Total hysterectomy	LMS	Spindle	No	0	0	1MYOCD	0	-1RB1	41.66
51	DOD	47	12	32	Yes	Vagina, bladder, rectum	I	NA	Uterus	Total hysterectomy	LMS	Spindle	No	0	0	1MYOCD	0	0	44
52	DOD	59	0	3	Yes	Lung	IVB	23	Uterus	Total hysterectomy	LMS	Spindle	Yes	0	0	0	0	0	33
53	DOD	87	1.6	3.2	Yes	Peritoneum, ileum	IIB	11	Uterus	Total hysterectomy	LMS	Epithelioid	No	1	1	1MYOCD	0	-2 RB1	38.4
54	DOD	58	0	2.9	Yes	Lung	IVB	6	Uterus	Total hysterectomy	LMS	Spindle	No	1	1	1 no MYOCD	0	-1RB1	24.9
55	DOD	26	25.2	48	Yes	Soft tissue, lung	IA	4	Uterus	Total hysterectomy	LMS	Spindle	No	1	1	1MYOCD	- 1 TP53	-2 RB1	141
56	DOD	60	0	ND	Yes	Peritoneum, omentum	III	15	Uterus	Total hysterectomy	LMS	Pleomorphic osteoclastic	No	1	1	0	0	-1RB1	35
57	DOD	63	2.8	8.2	Yes	Lung, peritoneum, brain	IB	10	Uterus	Total hysterectomy	LMS	Pleomorphic osteoclastic	Yes	0	1	0	0	-1RB1	24.9
58	A-NED	76	NA	104.4	No		IA	2	Uterus	Total hysterectomy	LMS	Epithelioid	No	0	0	0	0	0	18.7
59	DOD	67	7	12	Yes	Peritoneum	III	20	Uterus	Total hysterectomy	LMS	Spindle	No	0	0	0	0	-1 RB1	17.28
60	DOD	27	12	19.2	Yes	Peritoneum	IIB	8	Uterus	Total hysterectomy	LMS	Spindle	Yes	0	0	1MYOCD	-2 TP53	-2RB	39.7
61	DOD	44	0	13.2	Yes	Lung, peritoneum	IVB	16	Uterus	Total hysterectomy	LMS	Spindle	No	1	1	1 no MYOCD	- 1 TP53	- 1 RB1	88.47
62	DOD	54	73.2	102	Yes	Lung	IB	7.5	Uterus	Total hysterectomy	LMS	Spindle	No	0	0	0	- 1 TP53	- 1 RB1	60
63	AWD	59	14.4	75.6	Yes	Lung, liver, peritoneum	IVA	6	Uterus	Total hysterectomy	LMS	Spindle	Yes	0	0	1 no MYOCD	-2 TP53	-2 RB1	115
64	DOD	58	50.4	232.8	Yes	Lung	I	NA	Uterus	Total hysterectomy	LMS	Spindle	Yes	0	0	1 no MYOCD	0	0	48
65	DOD	36	2.9	9.4	Yes	Vagina, peritoneum	IB	6	Uterus	Total hysterectomy	LMS	Spindle	No	1	0	2 MYOCD	-2 TP53	-2RB	82
66	A-NED	53	NA	57.6	No		IB	6	Uterus	Total hysterectomy	LMS	Spindle	No	0	0	0	- 1 TP53	-2RB	45
67	DOD	63	10.6	18	Yes	Lung, bone, pelvis	IB	10	Uterus	Total hysterectomy	LMS	Spindle	No	1	0	1MYOCD	0	-2 RB1	101
68	DOD	60	1.1	32.4	Yes	Lung	IB	9	Uterus	Total hysterectomy	LMS	Pleomorphic osteoclastic	No	1	1	1MYOCD	0	- 1 RB1	84
69	A-NED	43	NA	42	No		IB	6.5	Uterus	Total hysterectomy	LMS	Epithelioid	Yes	0	0	0	0	0	32
70	DOD	58	1.1	3.4	Yes	Peritoneum	IVA	14	Uterus	Total hysterectomy	LMS	Epithelioid	Yes	1	1	1MYOCD	0	- 1 RB1	72.2
71	DOD	76	2.3	2.6	Yes	Lung, peritoneum	III	7	Uterus	Total hysterectomy	LMS	Spindle	Yes	1	1	1MYOCD	- 1 TP53	-2RB	64.69
72	A-NED	69	4.5	96	Yes	Lung	IB	30	Uterus	Total hysterectomy	LMS	Epithelioid	Yes	0	0	1MYOCD	0	- 1 RB1	180
73	AWD	69	21.6	58.8	Yes	Lung	III	13	Uterus	Total hysterectomy	LMS	Spindle	No	0	0	0	0	- 1 RB1	33.9

Table 1 (Continued)

Clinical data												*Genomic data*									
Patient	*FU status*	*Age*	*RFS months*	*OS months*	*Recurrence*	*Type of recurrence*	*FIGO stage*	*Size cm*	*Location*	*Type of surgery*	*Centralized diagnosis*	*Morphology*	*FH features*	*5p gain*	*1p gain*	*17p gain*	*17p loss*	*13 loss*	*GI*
74	DOD	80	1.3	2.6	Yes	Peritoneum, bone, lung	III	14	Uterus	Total hysterectomy	LMS	Epithelioid	Yes	1	1	1 no MYOCD	- 1 TP53	- 1 RB1	114.33
75	DOD	55	NA	39.6	ND	ND	IB	10	Uterus	Total hysterectomy	LMS	Spindle	Yes	0	0	0	0	-2 RB1	56.81
76	DOD	57	48	78.0	Yes	Pelvis, peritoneum, ureter	IB	7	Uterus	Total hysterectomy	LMS	Spindle	Yes	0	0	1MYOCD	0	- 1 RB1	42.88
77	DOD	53	8.1	57.6	Yes	Peritoneum, liver, lung	IB	13	Uterus	Total hysterectomy	LMS	Pleomorphic osteoclastic	Yes	1	0	1MYOCD	0	- 1 RB1	60.84

Abbreviations: A-NED: alive not evidence of disease; A-NOS: alive not otherwise specified; AWD: alive with disease; DOD: dead of disease; DOC: dead of other disease; GI: genomic index; MYOCD: myocardin gene; OS: overall survival; RB1: retinoblastoma gene; RFS: relapse-free survival; -1 heterozygous loss; -2 homozygous loss. 1 gain; +2 amplification.

markers (including genomic index ≥35) were tested for independency against the stage in a multivariate analysis. Stage and 5p gain were shown to be statistically independent prognostic factors at multivariate analysis (stage: $P<0.001$, HR=4.36 (1.82–10.42), 5p gain: $P=0.04$, HR=3.24 (1.04–10.04); Table 2a). Given that stage I tumors can have a risk of metastasis, we then further refined staging by testing molecular prognostic factors within stage. Among the tumors with genomic index ≥10 and stage I (37/55 patients), four overall survival prognostic factors were still significant: 5p gain ($P<0.001$, HR=4.88 (1.74–13.7); Figure 2e), genomic index at the cut-off of 35 ($P=0.0193$, HR=3.2 (1.15–8.92); Figure 2f), 13 chromosome loss including *RB1* ($P=0.0096$, HR=9.04 (1.2–67.81)) (Supplementary Figure 1A) and 17p gain including *MYOCD* ($P=0.0425$, HR=2.45 (1–5.97)) (Supplementary Figure 1B).

Among the other clinicomorphological parameters tested, the presence of moderate and marked atypia (Fisher's $P=0.043$), the presence of tumor necrosis (Fisher's $P=0,001$) and a mitotic index (cut-off ≥20; *t*-test $P<0.001$) were poor prognostic markers for overall survival (Table 2b,Supplementary Figure 1C). For these parameters, multivariate analysis showed that genomic index ≥35 remained significantly independent ($P=0.0333$; Table 2c).

Correlation Between Chromosomal Alterations and Morphology

No correlation was found between genomic index and morphology of the tumor (spindle, epithelioid or myxoid). No correlation was observed between any specific genomic alteration (5p gain, 17p loss, 13 loss, 17p gain) and tumor morphology (spindle *vs* epithelioid).

Discussion

In the last 5 years, many analyses based on whole-genome approaches have improved our knowledge of uterine smooth muscle lesion biology.[20–22] Nevertheless, the routine diagnostic practice lacks complementary diagnostic tools. For uterine leiomyosarcomas, despite very aggressive clinical features,[5] it is difficult to predict the outcome, especially when the diagnosis is made at stage I (tumor confined to the uterus).

According to the literature,[8,10,23] adjuvant treatment of a stage I uterine leiomyosarcomas is an option without evidence of benefit. There is a need for clinical trials to highlight the benefit of chemotherapy in terms of overall survival and relapse-free survival. In absence of clinical prognostic markers, the identification of new genomic prognostic markers appears critical for setting up clinical trials aiming to evaluate new treatments in uterine leiomyosarcomas. Genomic prognostic markers

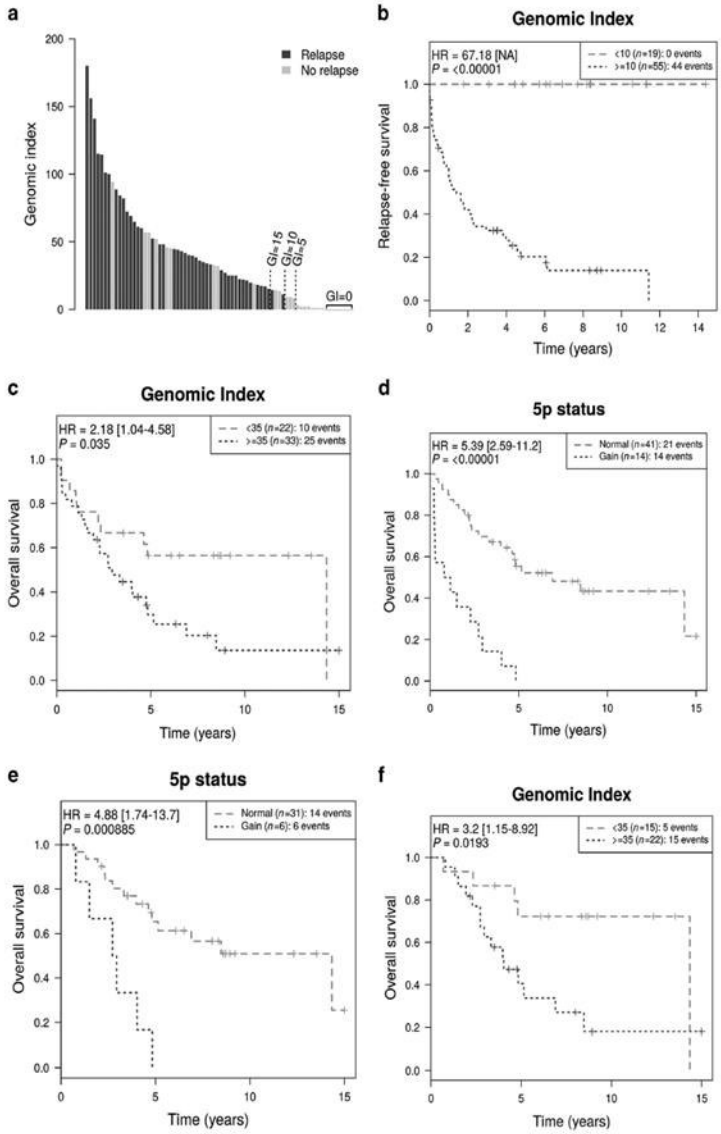

Figure 2 Genomic index and genomic alterations and clinical outcome. (**a**) Histogram. The number of patients with relapse (black bar) and without relapse (gray bar) shown in *x* axis; the genomic index level in *y* axis. The genomic index at the cut-off of 10 splits the population of 74 patients with uterine smooth muscle lesion in a group of 19 patients without metastases and a group of 55 patients with 44 metastatic events. (**b**) Kaplan-Meier relapse-free survival analysis of 74 uterine smooth muscle tumors according the genomic index at the cut-off of 10. (**c**) Kaplan-Meier for overall survival according to genomic index at the cut-off of 35 in the subgroup with genomic index ≥ 10 (genomic leiomyosarcomas). (**d**) Kaplan-Meier analysis of overall survival in the group with genomic index ≥ 10 (genomic leiomyosarcomas) with 5p gain. (**e**) Kaplan-Meier analysis of overall survival in the group with genomic index ≥ 10 (genomic leiomyosarcomas) with 5p gain with tumors limited to the uterus (stage I). (**f**) Kaplan-Meier analysis of overall survival in the group with genomic index ≥ 10 (genomic leiomyosarcomas) with tumors limited to the uterus (stage I) according to genomic index at the cut-off of 35.

could have an essential role in deciding on adjuvant chemotherapy for stage I uterine leiomyosarcomas. In our series of 37 molecular leiomyosarcomas (genomic index ≥ 10) at stage I, four genomic prognostic markers correctly separated the outcomes for patients alive or dead: 5p gain, chromosome 13 loss including *RB1*, proximal 17p gain with *MYOCD* and genomic index ≥ 35.

Figure 3 Penetrance plots of the different subgroups classified according to genomic index. (**a**) Penetrance plot of the tumors with genomic index <10 (benign tumors: all leiomyomas and two STUMPs). (**b**) Penetrance plot of tumors with genomic index >10 (malignant tumors: all leiomyosarcomas and 12 STUMPs). (**c**) Penetrance plot of tumors with genomic index >10 (malignant tumors: all leiomyosarcomas and 12 STUMPs) of patients alive. (**d**) Penetrance plot of tumors with genomic index >10 (malignant tumors: all leiomyosarcomas and 12 STUMPs) of patients dead of disease.

Further analyses are required to understand whether this is due to a chromosomal mechanism (specific or general) or due to genes located in these regions that are specifically overexpressed as a consequence of a chromosomal gain. The 5p gain was previously reported in extra-uterine[24] and uterine leiomyosarcomas[25] but no association with outcome was observed. The 17p proximal gain, including the *MYOCD* gene, was previously reported in literature in soft tissue leiomyosarcomas[24,26–28] and in uterine leiomyosarcomas.[25] *MYOCD* gene induces smooth muscle differentiation and promotes cell migration.[27] In a human uterine leiomyosarcomas cell line, *MYOCD* induced a phenotypic cell switch from a dedifferentiated to a differentiated smooth muscle phenotype.[29] MYOCD expression level controls smooth muscle differentiation protein expression and has an impact on cell migration in soft tissue leiomyosarcomas.[27] Furthermore, it confers aggressive outcome in soft tissue sarcomas.[30]

Hu et al[25] found a gain of 17p in 38% of the uterine leiomyosarcomas and interestingly, no 17p gain was found in alive patients (4/19). Chromosome 13 was lost in 80% of the leiomyosarcomas in our

Table 2 Statistical data: univariate and multivariate analyses for OS of the subgroup with GI >10 (malignant tumors)

	Univariate		*Multivariate*	
OS	***P-value***	***HR***	***P-value***	***HR***
Stage	**<0.001**	**4.32 (2.03–9.2)**	**<0.001**	**4.36 (1.82–10.42)**
5p gain	**<0.001**	**5.39 (2.59–11.2)**	**0.0042**	**3.24 (1.04–10.04)**
1p gain	**<0.001**	**3.3 (1.66–6.56)**	0.2989	1.61 (0.66–3.96)
GI ≥35	**0.0349**	**2.18 (1.04–4.58)**	0.8419	1.10 (0.44–2.71)
17p loss TP53	0.1119	**1.72 (0.87–3.36)**	0.4807	0.75 (0.33–1.68)
13 loss RB1	**0.0103**	**4.19 (1.28–13.77)**	0.1860	2.44 (0.65–9.19)
17p gain MYOCD	**0.0054**	**2.57 (1.29–5.13)**	0.6188	1.29 (0.48–3.47)

Abbreviations: GI: genomic index; HR: hazard ratio; OS: overall survival.
Bold values signify the significant results.

Table 2B Univariate analysis for RFS and OS of the subgroup with GI >10 (malignant tumors)

	RFS	*OS*
Atypia	***P*=0.04918**	***P*=0.04345**
Mitoses cut-off 20	***P*<0.001**	***P*<0.001**
Necrosis	*P*=0.0963	*P*=0.001

Abbreviations: GI: genomic index; OS: overall survival; RFS: relapse-free survival.
Bold values signify the significant results.

Table 2C Multivariate analysis for OS for stage I LMS

OS	P-*value*	*HR*
GI ≥35	**0.0333**	**3.10 (1.09–10.78)**
Atypia	0.0837	10.89 (0.77–>100)
Mitoses cut-off 20	0.128	0.48 (0.09–1.63)
Necrosis	0.263	0.48 (0.09–1.63)

Abbreviation: OS: overall survival.
Bold values signify the significant results.

series and is the most common genomic event in uterine (76%) [25] and extra-uterine leiomyosarcomas (ranging from 54% [28,24] to 71% [26]) and in the majority of the cases, correlation between this event and follow-up was not established.

The morphological analysis based on the presence of atypia, mitotic count and tumor cell necrosis correlated to a poor outcome in our series. The prognostic value of cytological atypia,[31,32] as well the mitotic count[5,33,34] was reported in previous publications. However, atypia and mitoses could be difficult to assess and there is only a moderate inter-observer agreement on tumor cell necrosis in uterine smooth muscle lesions among gynecological pathologists.[35] Genomic index assessment could be a useful tool, as highlighted in our multivariate analysis (Table 2c), to avoid such diagnostic discrepancies.

In our series, the genomic index cut-off of 10 splits the STUMP group into two: a flat or very simple genomic profile group akin to leiomyomas and a group of tumors with complex genomic profile similar to leiomyosarcomas (with recurrences and deaths) thereby erasing the STUMP category. In the benign lesions group with genomic index <10 (all leiomyomas and two STUMP), there were no chromosomal alterations such as *RB1* and *TP53* loss (Table 1). One exception is the bizarre nuclei leiomyoma case, with a borderline genomic index = 9, which showed chromosome 13 loss including the *RB1* gene and chromosome 17p loss including the*TP53* gene. These alterations have already been reported in these benign lesions.[36–39] In fact, some bizarre nuclei leiomyomas inexplicably show rearranged profiles (in our experience lower than leiomyosarcomas) and a good outcome. Furthermore, the origin of this subtype of leiomyoma is not clear either.

Genomic profiling by array-comparative genomic hybridization on formalin-fixed and paraffin-embedded samples is a useful, easy and accessible tool complementary to the morphological approach. It is a diagnostic tool that splits the STUMP category into benign (leiomyoma) and malignant (leiomyosarcomas) tumors. It is a prognostic marker and a predictor of overall survival in stage I uterine leiomyosarcomas. Indeed, all the comparative genomic hybridization analyses on our series were performed on formalin-fixed and paraffin-embedded and -extracted DNA, with 100% feasibility. Genomic profiling could be used even on a limited amount of material such as pre-operative biopsies in order to guide surgical intervention (hysterectomy *vs* myomectomy or a minimally invasive surgery).

In conclusion, we have demonstrated that STUMP classification could be overcome by utilizing genomic index at the cut-off of 10. The 5p gain as genomic event and the stage as clinical parameter are poor overall survival prognostic factors in uterine leiomyosarcomas. In stage I tumors, the 5p gain, 17p gain, chromosome 13 loss and genomic index at the cut-off of 35 are poor prognostic factors of overall survival and therefore they could be potential parameters for randomization in prospective clinical trials. This approach opens the way to new insights into uterine and other gynecological smooth muscle lesions and would allow reclassification of lesions

according to genomic complexity. In fact, there is a continuum gradient of genomic complexity and instability correlating with tumor aggressiveness. As genomic profiling by array-comparative genomic hybridization on formalin fixed and paraffin embedded is feasible and accessible in hospital laboratories, this approach could be used in routine practice as a complement to histology.

Acknowledgments

This study was supported by the grants from ARC and la Ligue Régionale contre le cancer. We thank Dr Ravi Nookala of Institut Bergonié for the medical writing service and Magali Philip, Quitterie Fontanges, Patrick Murat and Virginie Duvignau for photographs. FA is senior researcher for the Research Fund Flanders (F.W.O.).

Disclosure/conflict of interest

The authors declare no conflict of interest.

References

1 Skorstad M, Kent A, Lieng M. Uterine leiomyosarcoma - incidence, treatment, and the impact of morcellation. A nationwide cohort study. Acta Obstet Gynecol Scand 2016;95:984–990.
2 Oliva E, Carcangiu ML, Carinelli SG, *et al.* Mesenchymal tumours. Smooth muscle tumour of uncertain malignant potential. In: Kurman RJ CM, Herrington CS, Young RH (eds). WHO Classification of Tumours of Female Reproductive Organs, 2014, pp 135–147.
3 Baird DD, Dunson DB, Hill MC, *et al.* High cumulative incidence of uterine leiomyoma in black and white women: ultrasound evidence. Am J Obstet Gynecol 2003;188:100–107.
4 Ricci S, Stone RL, Fader AN. Uterine leiomyosarcoma: epidemiology, contemporary treatment strategies and the impact of uterine morcellation. Gynecol Oncol 2017;145:208–216.
5 Garcia C, Kubat JS, Fulton RS, *et al.* Clinical outcomes and prognostic markers in uterine leiomyosarcoma: a population-based cohort. Int J Gynecol Cancer 2015;25:622–628.
6 Bell SW, Kempson RL, Hendrickson MR. Problematic uterine smooth muscle neoplasms. A clinicopathologic study of 213 cases. Am J Surg Pathol 1994;18:535–558.
7 Amant F, Coosemans A, Debiec-Rychter M, *et al.* Clinical management of uterine sarcomas. Lancet Oncol 2009;10:1188–1198.
8 Hensley ML, Ishill N, Soslow R, *et al.* Adjuvant gemcitabine plus docetaxel for completely resected stages I-IV high grade uterine leiomyosarcoma: results of a prospective study. Gynecol Oncol 2009;112:563–567.
9 Amant F, Lorusso D, Mustea A, *et al.* Management strategies in advanced uterine leiomyosarcoma: focus on trabectedin. Sarcoma 2015;2015:704124.
10 Omura GA, Blessing JA, Major F, *et al.* A randomized clinical trial of adjuvant adriamycin in uterine sarcomas: a Gynecologic Oncology Group Study. J Clin Oncol 1985;3:1240–1245.
11 Reed NS, Mangioni C, Malmstrom H, *et al.* Phase III randomised study to evaluate the role of adjuvant pelvic radiotherapy in the treatment of uterine sarcomas stages I and II: an European Organisation for Research and Treatment of Cancer Gynaecological Cancer Group Study (protocol 55874). Eur J Cancer 2008;44:808–818.
12 Rose PG, Boutselis JG, Sachs L. Adjuvant therapy for stage I uterine sarcoma. Am J Obstet Gynecol 1987;156:660–662.
13 Sorbe B, Johansson B. Prophylactic pelvic irradiation as part of primary therapy in uterine sarcomas. Int J Oncol 2008;32:1111–1117.
14 Zivanovic O, Jacks LM, Iasonos A, *et al.* A nomogram to predict postresection 5-year overall survival for patients with uterine leiomyosarcoma. Cancer 2012;118:660–669.
15 Iasonos A, Keung EZ, Zivanovic O, *et al.* External validation of a prognostic nomogram for overall survival in women with uterine leiomyosarcoma. Cancer 2013;119:1816–1822.
16 Pautier P, Genestie C, Rey A, *et al.* Analysis of clinicopathologic prognostic factors for 157 uterine sarcomas and evaluation of a grading score validated for soft tissue sarcoma. Cancer 2000;88:1425–1431.
17 Croce S, Ribeiro A, Brulard C, *et al.* Uterine smooth muscle tumor analysis by comparative genomic hybridization: a useful diagnostic tool in challenging lesions. Mod Pathol 2015;28:1001–1010.
18 Oliva E. Practical issues in uterine pathology from banal to bewildering: the remarkable spectrum of smooth muscle neoplasia. Mod Pathol 2016;29(Suppl 1):S104–S120.
19 Lagarde P, Perot G, Kauffmann A, *et al.* Mitotic checkpoints and chromosome instability are strong predictors of clinical outcome in gastrointestinal stromal tumors. Clin Cancer Res 2012;18:826–838.
20 Mehine M, Kaasinen E, Makinen N, *et al.* Characterization of uterine leiomyomas by whole-genome sequencing. N Engl J Med 2013;369:43–53.
21 Mehine M, Kaasinen E, Aaltonen LA. Chromothripsis in uterine leiomyomas. N Engl J Med 2013;369:2160–2161.
22 Makinen N, Aavikko M, Heikkinen T, *et al.* Exome sequencing of uterine leiomyosarcomas identifies frequent mutations in TP53, ATRX, and MED12. PLoS Genet 2016;12:e1005850.
23 Hempling RE, Piver MS, Baker TR. Impact on progression-free survival of adjuvant cyclophosphamide, vincristine, doxorubicin (adriamycin), and dacarbazine (CYVADIC) chemotherapy for stage I uterine sarcoma. A prospective trial. Am J Clin Oncol 1995;18:282–286.
24 El-Rifai W, Sarlomo-Rikala M, Knuutila S, *et al.* DNA copy number changes in development and progression in leiomyosarcomas of soft tissues. Am J Pathol 1998;153:985–990.
25 Hu J, Khanna V, Jones M, *et al.* Genomic alterations in uterine leiomyosarcomas: potential markers for clinical diagnosis and prognosis. Genes Chromosomes Cancer 2001;31:117–124.
26 Larramendy ML, Kaur S, Svarvar C, *et al.* Gene copy number profiling of soft-tissue leiomyosarcomas by array-comparative genomic hybridization. Cancer Genet Cytogenet 2006;169:94–101.
27 Perot G, Derre J, Coindre JM, *et al.* Strong smooth muscle differentiation is dependent on myocardin gene amplification in most human retroperitoneal leiomyosarcomas. Cancer Res 2009;69:2269–2278.

28 Agaram NP, Zhang L, LeLoarer F, *et al.* Targeted exome sequencing profiles genetic alterations in leiomyosarcoma. Genes Chromosomes Cancer 2016;55:124–130.
29 Kimura Y, Morita T, Hayashi K, *et al.* Myocardin functions as an effective inducer of growth arrest and differentiation in human uterine leiomyosarcoma cells. Cancer Res 2010;70:501–511.
30 Perot G, Mendiboure J, Brouste V, *et al.* Smooth muscle differentiation identifies two classes of poorly differentiated pleomorphic sarcomas with distinct outcome. Mod Pathol 2014;27:840–850.
31 Nordal RR, Kristensen GB, Kaern J, *et al.* The prognostic significance of stage, tumor size, cellular atypia and DNA ploidy in uterine leiomyosarcoma. Acta Oncol 1995;34:797–802.
32 Wang WL, Soslow R, Hensley M, *et al.* Histopathologic prognostic factors in stage I leiomyosarcoma of the uterus: a detailed analysis of 27 cases. Am J Surg Pathol 2011;35:522–529.
33 Pelmus M, Penault-Llorca F, Guillou L, *et al.* Prognostic factors in early-stage leiomyosarcoma of the uterus. Int J Gynecol Cancer 2009;19:385–390.
34 Davidson B, Kjaereng ML, Forsund M, *et al.* Progesterone receptor expression is an independent prognosticator in FIGO stage I uterine leiomyosarcoma. Am J Clin Pathol 2016;145:449–458.
35 Lim D, Alvarez T, Nucci MR, *et al.* Interobserver variability in the interpretation of tumor cell necrosis in uterine leiomyosarcoma. Am J Surg Pathol 2013;37:650–658.
36 Downes KA, Hart WR. Bizarre leiomyomas of the uterus: a comprehensive pathologic study of 24 cases with long-term follow-up. Am J Surg Pathol 1997;21:1261–1270.
37 Croce S, Young RH, Oliva E. Uterine leiomyomas with bizarre nuclei: a clinicopathologic study of 59 cases. Am J Surg Pathol 2014;38:1330–1339.
38 Liegl-Atzwanger B, Heitzer E, Flicker K, *et al.* Exploring chromosomal abnormalities and genetic changes in uterine smooth muscle tumors. Mod Pathol 2016;29:1262–1277.
39 Zhang Q, Ubago J, Li L, *et al.* Molecular analyses of 6 different types of uterine smooth muscle tumors: emphasis in atypical leiomyoma. Cancer 2014;120:3165–3177.

Supplementary Information accompanies the paper on Modern Pathology website (http://www.nature.com/modpathol)

3.2 LA SIGNATURE CINSARC PRONOSTIQUE DE SURVIE GLOBALE ET LIBRE DE MALADIE DANS LES LMS UTERINS EN PARTICULIERS AU STADE I. APPLICATIONS CLINIQUES

L'application de la signature transcriptomique CINSARC, depuis peu réalisable sur matériel FFPE par technologie Nanostring, représente une méthode alternative à l'estimation du Genomic Index(GI) et elle représente son évolution.

Cette signature a l'avantage, par rapport au GI, d'analyser des gènes plus directement impliqués dans le cycle cellulaire et dans la progression tumorale car issus d'une sélection par Gene Ontology[155].

D'autre part l'analyse du GI par CGH-array présente, parmi ses limites, le fait d'être plateforme dépendant (selon la méthode d'analyse AGILENT ou AFFYMETRIX, selon la puissance des puces et le logiciel d'analyse) et risque de ne pas être reproductible sur les différentes plateformes.

La méthode CINSARC Nanocind® garantit la reproductibilité et par conséquent la fiabilité des résultats. En effet, cette méthode utilise une plateforme Nanostring, très répandue, avec des protocoles standardisés quel que soit le laboratoire et centralise les données sur un seul site qui élabore les données selon un seul algorithme.

La signature en classant les LMS utérins en deux groupes C1 (centroïde 1) et C2 (centroïde 2) distingue deux groupes de LMS avec une survie globale et libre de maladie significativement différentes.

En particulier au stade I (tumeur limitée à l'utérus) représentant 60% des LMS utérins, la signature CINSARC distingue deux groupes distincts en survie globale et en survie libre de maladie. Cette donnée est extrêmement intéressante avec des retombées cliniques de première importance.

En effet les essais cliniques qui visent à évaluer le bénéfice de la chimiothérapie adjuvante dans la stratégie thérapeutique des LMS au stade I n'ont pas été contributifs[167].

Sur la base des résultats de notre article la signature Cinsarc Nanocind® est l'outil de randomisation optimal pour les futurs essais cliniques.

Ces données vont dans le sens de l'hypothèse de la thèse en démontrant la présence d'une corrélation entre expression des gènes liés à l'instabilité chromosomique, au remaniement génomique et à la progression du cycle cellulaire et l'évolution clinique.

Published OnlineFirst December 3, 2019; DOI: 10.1158/1078-0432.CCR-19-2891

The Nanocind Signature Is an Independent Prognosticator of Recurrence and Death in Uterine Leiomyosarcomas

Sabrina Croce[1,2], Tom Lesluyes[3,4,5], Carine Valle[10], Loubna M'Hamdi[5], Noémie Thébault[4], Gaëlle Pérot[4,5], Eberhard Stoeckle[6], Jean-Christophe Noël[7], Quitterie Fontanges[7], Mojgan Devouassoux-Shisheboran[8], Denis Querleu[6], Frédéric Guyon[6], Anne Floquet[9], Camille Chakiba[9], Laetitia Mayeur[1], Flora Rebier[1], Gaëtan Marie MacGrogan[1], Isabelle Soubeyran[1,2], Sophie Le Guellec[4,5], and Frédéric Chibon[4,5]

ABSTRACT

Purpose: Uterine leiomyosarcoma, which accounts for 7% of all soft-tissue sarcomas and 1%–3% of all uterine malignancies, is an aggressive tumor responsible for a significant proportion of uterine cancer–related deaths. While Federation Internationale des Gynaecologistes et Obstetristes (FIGO) stage is the most important prognostic factor, metastatic and relapse rates at stage I exceed 50% so it is currently impossible to predict the clinical outcome of stage I leiomyosarcomas. In 2010, our team published a transcriptomic signature composed of 67 genes related to chromosome biogenesis, mitosis control, and chromosome segregation. It has demonstrated its prognostic value in many cancer types and was recently successfully applied to formalin-fixed, paraffin-embedded sarcomas by NanoCind on NanoString technology, making another step forward toward its use in routine practice.

Experimental Design: Sixty uterine leiomyosarcomas at any stage, including 40 localized in the uterus (stage I), were analyzed with the NanoCind (CINSARC with NanoString) signature. Its prognostic value was evaluated for overall survival and relapse-free survival and compared in multivariate analysis with other prognostic markers like FIGO staging and genomic index.

Results: The NanoCind signature was able to split the heterogeneous group of uterine leiomyosarcomas of any stage including stage I into two distinct groups with different relapse-free survival and overall survival. These results were validated on an independent cohort of uterine leiomyosarcomas in The Cancer Genome Atlas consortium.

Conclusions: The NanoCind signature is a powerful prognosticator that outperforms FIGO staging and the genomic index. The CINSARC signature is platform independent and "ready to use" and should now be used for randomization in future therapeutic trials.

Introduction

Uterine leiomyosarcoma is a rare tumor accounting for 7% of all soft-tissue sarcomas (STS; refs. 1, 2) and 1%–3% of uterine malignancies (3, 4), but it is the most frequent subtype representing 57%–60% of all uterine sarcomas (4). Owing to its aggressiveness, 5-year overall survival (OS) is 41% for all stages (5), 51% at stage I, 25% at stage II, and no survival at 5 years in patients with tumor spread outside the pelvis (4). Furthermore, uterine leiomyosarcoma accounts for a significant proportion of uterine cancer–related deaths (3, 4) with an annual incidence estimated between 0.36 (1) and 0.8 (6) per 100,000 women-year and 0.5 to two per 100,000 women-year in the age group 35–64 years (7).

Among the prognostic factors, FIGO stage is still the most important prognosticator in uterine leiomyosarcoma and guides the therapeutic strategy (8–10). Because most uterine leiomyosarcoma are diagnosed at stage I (4, 5), that is, confined to the uterus, it is impossible to distinguish the patients who will recur and die of the tumor from those with a long survival. A specific uterine leiomyosarcoma nomogram for predicting postresection 5-year OS was published recently (11, 12). The items of the nomogram are based on clinicopathologic parameters such as age, tumor size, tumor grade, cervical involvement, loco regional metastases, distant metastases, and mitotic index (11). One of its limitations is the value of tumor grade, as there is no recognized tumor grade according to the 2014 World Health Organization (WHO) classification of the gynecologic and reproductive organs (13), and uterine leiomyosarcoma diagnosed according to the Stanford criteria (14) are by definition of high grade (15).

As stated by Pautier and colleagues on a series of 157 uterine sarcomas, the Fédération Nationale des Centres de Lutte Contre le Cancer (FNLCC) grading score could not be used as a prognostic indicator for uterine leiomyosarcoma (16).

The analysis of chromosome complexity in uterine leiomyosarcoma by comparative genomic hybridization (CGH) array recently demonstrated the prognostic value of the genomic index (GI) at the cutoff of

[1]Department of Biopathology, Institut Bergonié, Comprehensive Cancer Center, Bordeaux, France. [2]INSERM U1218, Bordeaux, France. [3]University of Bordeaux, Bordeaux, France. [4]Oncosarc, INSERM UMR1037, Cancer Research Center of Toulouse, Toulouse, France. [5]Department of Pathology, Institut Claudius Regaud, IUCT-Oncopole, Toulouse France. [6]Department of Surgery, Institut Bergonié, Comprehensive Cancer Center, Bordeaux, France. [7]Department of Pathology, Clinic of Gynecopathology and Senology, Erasme University Hospital, Brussels, Belgium. [8]Department of Pathology, CHU Lyon Sud, Pierrebenite, France. [9]Department of Oncology, Institut Bergonié, Comprehensive Cancer Center, Bordeaux, France. [10]Plateau Génomique et Transcriptomique, INSERM U1037, Cancer Research Center of Toulouse, Toulouse, France.

Note: Supplementary data for this article are available at Clinical Cancer Research Online (http://clincancerres.aacrjournals.org/).

Corresponding Author: Sabrina Croce, Institut Bergonié, 228 cours de l'Argonne, Bordeaux F-33000, France. Phone: 3306-6688-9941; Fax: 3305-5633-0438; E-mail: s.croce@bordeaux.unicancer.fr

Clin Cancer Res 2020;XX:XX–XX

doi: 10.1158/1078-0432.CCR-19-2891

Translational Relevance

Uterine leiomyosarcoma is one of the most aggressive uterine cancers with a risk of recurrence superior to 50% at stage I. Despite the high risk of recurrence there is not an evidence of benefit of adjuvant treatment. We are convinced that to demonstrate a benefit from the new drugs in early stage uterine leiomyosarcoma we need to find the pertinent tools of randomization. In this study, we demonstrated for the first time the strong prognostic value of CINSARC NanoCind signature in uterine leiomyosarcoma outperforming the stage. The feasibility and robustness of CINSARC NanoCind signature was recently demonstrated on formalin-fixed, paraffin-embedded sarcomas, even on biopsy material. Our data were validated on an external series of uterine leiomyosarcoma published on The Cancer Genome Atlas. CINSARC NanoCind signature could be a useful and pertinent tool of randomization in the future clinical trials evaluating the benefit of adjuvant treatment on uterine leiomyosarcoma, in particular at early stage.

35 for OS but not relapse-free survival (RFS; ref. 17). In 2010, our team published a prognostic transcriptomic signature obtained by a combination of differentially expressed genes in FNLCC grade 3 versus one and two STS, and in highly rearranged tumors versus those with a low level of chromosome rearrangements and complexity (18). This 67-gene signature composed of genes belonging to significantly enriched pathways related to chromosome biogenesis, mitosis control, and chromosome segregation (18, 19) has demonstrated its prognostic value in 21 of 39 cancer types, outperforming more than 15,000 different signatures (20). Recently, the CINSARC signature was successfully applied to formalin-fixed, paraffin-embedded (FFPE) sarcomas by NanoCind, a NanoString Technology, with a similar risk-group classification on frozen, as well as FFPE tumor, and even on biopsy material (21). Given the limitations of prognostication devices currently applied or foreseen for uterine leiomyosarcoma, we tested whether the NanoCind prognostic signature could improve prognostication in uterine sarcomas.

Materials and Methods

Tumor samples

The series of 56 uterine leiomyosarcoma and five Smooth muscle Tumors of Uncertain Malignant Potential (STUMP), centrally reviewed and diagnosed according to Stanford criteria (13–15), were classified in 61 uterine leiomyosarcoma after GI analysis at a cutoff of 10, as reported previously (17, 22). Follow-up and clinical data were obtained for each case.

The samples from the tumor archives were centralized in the Biological Resources Center of Institut Bergonié, which the French authorities authorized for scientific research (AC-2008-812).

Clinical data

Among the 60 interpretable uterine leiomyosarcoma (one sample not interpretable for CINSARC/NanoCind analysis), 40 (67%) were at stage I, (six at stage IA, 30 at stage IB, and 4 at stage I without other specification), three (5%) at stage II, six (10%) at stage III, nine (15%) at stage IV, and for two (3%) the stage was not known.

Regarding the modalities of surgery, it was not possible to specify whether any of the patients included in the study had morcellation procedure for resection of the tumor.

At follow-up, only 12 patients (20%) were alive without evidence of disease (mean, 6.66 years; median, 6.5 years; minimum, 2.2 years; maximum, 9.7 years). Among them, two had a peritoneal relapse at 35 months and a lung metastasis at 4.5 months after the first surgery but were alive without evidence of disease at last control. Nine of 60 (15%) were alive with evidence of disease at last follow-up (mean, 7.3 years; median, 6.4 years; minimum, 3.2 years; maximum, 12.6 years) and 39 of 60 (65%) had died of disease (mean, 3.2 years; median, 2.4 years; minimum, 0.2 years; maximum, 19.7 years).

CGH analysis

DNA extraction and CGH array from 45 uterine leiomyosarcomas and five STUMPs published before (17), as well 11 new uterine leiomyosarcoma were performed as described previously (17, 22).

NanoCind signature

RNA extraction and the analysis on the nCounter code set (NanoCind, patent number EP18305190·3; panel of 75 probes targeting 67 distinct CINSARC genes and eight housekeeping genes) were performed as described previously (21).

Results

Clinicopathologic, genomic, and transcriptomic data are presented in Supplementary Table S1. We carried out the CINSARC signature analysis on the series composed of 61 genomic uterine leiomyosarcomas of all stages. All, but one, were interpretable (final series: 60 uterine leiomyosarcomas).

CINSARC NanoCind signature predicts uterine leiomyosarcoma patients' outcome

The CINSARC signature split the heterogeneous population of uterine leiomyosarcoma at any stage into a group with high risk of relapse and metastases [RFS; $P = 6.7 \times 10^{-4}$; HR = 3.71 (1·65–8·32); **Fig. 1A**] as well as shorter OS [OS; $P = 7.56 \times 10^{-4}$; HR = 5.97 (1·83–19·48); **Fig. 1B**] and a group with long survival and lower risk of recurrence (**Table 1**). We thus compared the prognostic value of CINSARC to that of GI. Among the 60 tumors of the series (previously reported, refs. 17, 22), one was not analyzed by CGH array because there was not enough material and three were not interpretable. All the 56 interpretable tumors had a GI > 10 (genomic uterine leiomyosarcoma; from 11 to 180).

By applying a cutoff of 35 as defined previously (17), GI was prognostic for OS at all stages [OS; $P = 1.48 \times 10^{-2}$; HR = 2.39 (1.16–4.91); **Fig. 1C**] and at stage I (OS; $P = 6.9 \times 10^{-3}$; HR = 4.16 (1.36–12.74); **Fig. 2C**] but not for RFS ($P = 6.03 \times 10^{-1}$). Multivariate analysis showed that the CINSARC NanoCind signature outperformed GI by CGH array because the prognostic value of GI was no longer significant for OS (CINSARC: $P = 1.91 \times 10^{-3}$, HR = 4.41 (1.64–16.43); GI: $P = 9.03 \times 10^{-2}$, HR = 1.84 (0.91–3.96)]. RFS was not tested because GI was not significant at univariate analysis.

CINSARC NanoCind signature predicts stage I FIGO uterine leiomyosarcoma patients' outcome

Even if no clinical or histologic criteria can discriminate poor prognosis patients within FIGO stage I tumors (localized and accordingly considered as patients with good prognosis), the CINSARC signature showed its prognostic value for these stage I uterine leiomyosarcoma by identifying patients with low RFS [$P = 3.38 \times 10^{-3}$; HR = 3.83 (1.46–10.08); **Fig. 2A**] and OS (OS; $P = 9.89 \times 10^{-3}$; HR = 5.51 (1.28–23.69); **Fig. 2B**]. Indeed, among the 27 of 40 (67.5%) stage I

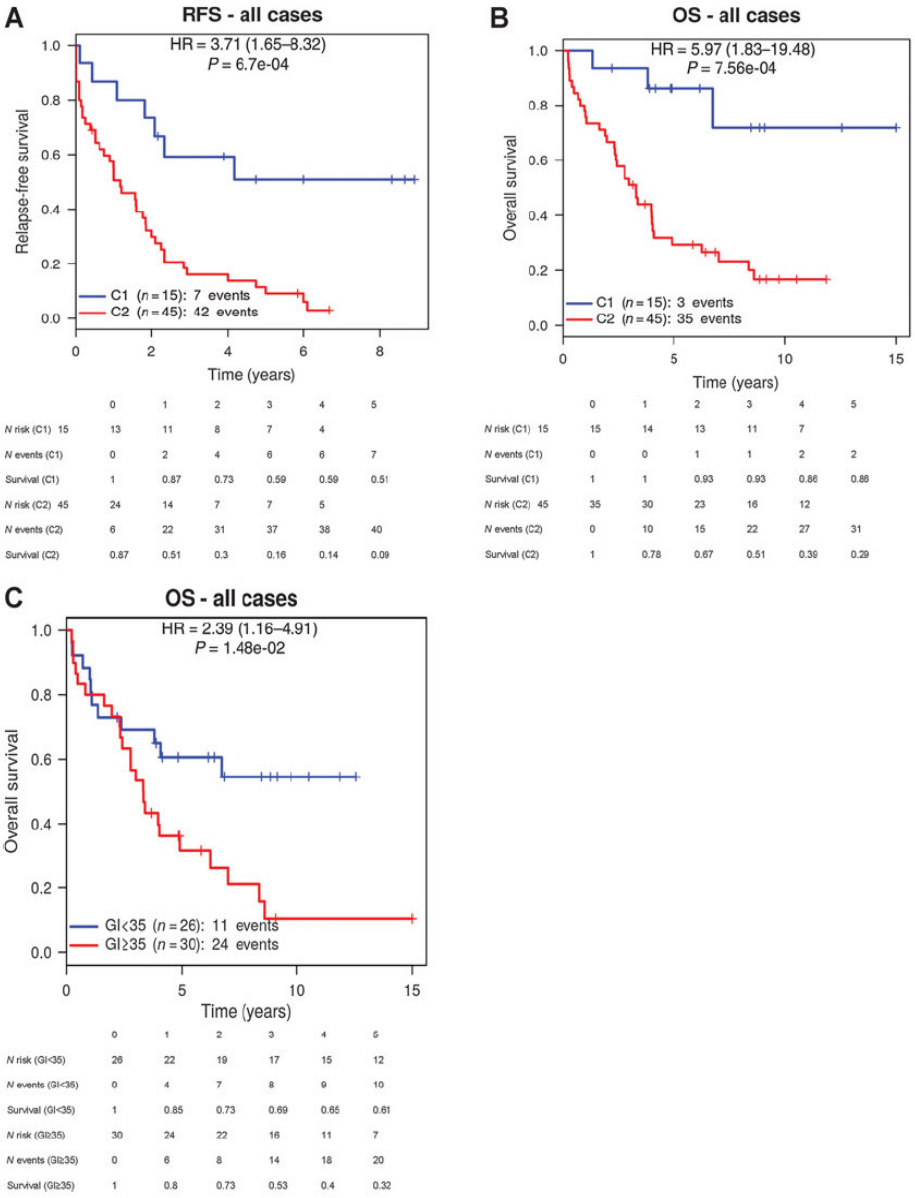

Figure 1.

RFS (**A**) and OS (**B**) analysis according to CINSARC signature for uterine leiomyosarcomas at any stage. **C,** OS analysis according to GI at the cutoff of 35 for any stage uterine leiomyosarcoma.

uterine leiomyosarcoma classified by the signature as having a high risk of recurrence and death (C2, for centroid 2), 85% had a dismal outcome: 19 of 27 (70.3%) died of disease and four of 27 (14.7%) were alive with disease (Supplementary Table S1). On the other hand, among the 13 (32.5%) uterine leiomyosarcoma at stage I classified as low risk (C1, for centroid 1), eight of 13 (62%) were alive without evidence of disease, two of 13 (15%) alive with disease, and three of 13 (23%) had died of disease.

At morphologic analysis, the C2 (high-risk) group of uterine leiomyosarcoma had a higher mitotic count ($P = 3.5 \times 10^{-7}$; Wilcoxon test), and more frequently harbored tumor cell necrosis ($P = 0.036$; Fisher exact test) compared with C1 patients (low-risk group). No statistically significant difference was observed between the C1 and C2 groups for the presence of atypia ($P = 0.6$; χ^2 test). At univariate analysis, the presence of atypia was correlated with low survival (OS: $P = 4.27 \times 10^{-2}$; HR = 2.03 (1·01–4·12)] but not with

Table 1. Prognostic analysis of the cohort.

Total patients	61	DOD	AWD	NED	OS	HR (95% CI)	RFS	HR (95% CI)
CINSARC NanoCind interpretable	60							
All stages	60							
C1	15	4	3	8	$P = 7.56 \times 10^{-4}$	5.97 (1.83–19.48)	$P = 6.7 \times 10^{-4}$	3.71 (1.65–8.32)
C2	45	35	6	4				
Stage I	40							
C1	13	3	2	8	$P = 9.89 \times 10^{-3}$	5.51 (1.28–23.69)	$P = 3.38 \times 10^{-3}$	3.83 (1.46–10.08)
C2	27	19	4	4				
Array-CGH interpretable	56							
All stages	56							
≤35	21	8	6	7	$P = 1.48 \times 10^{-2}$	2.39 (1.6–4.91)	$P = 6.03 \times 10^{-1}$	
≥35	35	28	2	5				
Stage I	36							
≤35	14	0	0	7	$P = 6.96 \times 10^{-3}$	4.16 (1.36–12.74)	$P = 3.79 \times 10^{-1}$	
≥35	22	17	0	5				
Multivariate analysis								
CINSARC NanoCind interpretable					$P = 1.91 \times 10^{-3}$	4.41 (1.64–16.43)		
GI					$P = 9.03 \times 10^{-2}$	1.84 (0.91–3.96)		
CINSARC NanoCind interpretable					$P = 3.14 \times 10^{-4}$	5.13 (1.95–18.90)		
Atypia					$P = 4.85 \times 10^{-2}$	1.96 (1–4.08)		

Note: Clinicopathologic data and correlation with CINSARC NanoCind signature and GI.
Abbreviations: A-NED, alive with no evidence of disease; AWD, alive with disease; CI, confidence interval; DOD, dead of disease.

RFS ($P = 3.07 \times 10^{-1}$; HR = 1.37 (0.76–2.48)]. At multivariate analysis, CINSARC and atypia for OS were both statistically significant although CINSARC had the strongest value [CINSARC: $P = 3.14 \times 10^{-4}$; HR = 5.13 (1.95-18.90); Atypia: $P = 4.85 \times 10^{-2}$; HR = 1.96 (1-4.08)].

Validation on an independent cohort

CINSARC NanoCind signature was applied to an independent series of 32 uterine leiomyosarcoma (23). Our signature was again predictive of metastasis [metastases-free survival (MFS) $P = 4.5 \times 10^{-2}$; HR = 3.2 (0.97–10.6)] and death [OS $P = 1.61 \times 10^{-2}$; HR = 8.46 (1.05–67.92); Fig. 3A and B].

Discussion

The strongest prognostic factor currently used in uterine leiomyosarcoma on the basis of therapeutic strategy is the stage (24). Most patients are diagnosed at stage I (localized, corresponding to a good prognosis). Nevertheless even at this stage, the metastatic relapse rate exceeds 50% (2). Until now, it has not been possible to distinguish, among patients with stage I uterine leiomyosarcoma, who will relapse and die of disease from those with long survival (9, 10).

Until now (2, 25–28), there is no clear evidence of the benefit of adjuvant chemotherapy in early stage uterine leiomyosarcoma. The FNLCC grading system failed to predict the outcome in uterine leiomyosarcoma (16). In 2014, the WHO was unable to recognize any grading system for uterine leiomyosarcoma as being universally acceptable for prognostic purposes, and the difficulty of proving the possible benefits of chemotherapy likely contributed to this overall uncertainty. These data weaken the value of the nomograms based on current histologic grading.

However, accurate prognostic factors in early stage uterine leiomyosarcoma are needed for guiding randomization in future chemotherapy and targeted therapy trials.

NanoCind signature: a powerful prognostic tool in uterine leiomyosarcoma

Our signature differentiates uterine leiomyosarcoma at any stage into a group with high risk of RFS and poor OS and another with better prognosis. Moreover, in clinical practice with stage I uterine leiomyosarcoma, which represents 60% of newly diagnosed tumors and for which there is no indication for adjuvant chemotherapy (8–10, 29–31), the CINSARC NanoCind signature identifies a group of patients (C2; ref. 32; 67.5% of this series) with a high risk of relapse and death, with 85.2% of death from disease and relapse. The strength of these data has been confirmed by the validation on an external series of uterine leiomyosarcoma from The Cancer Genome Atlas (TCGA) bioportal (ref. 27). These patients could be offered an adjuvant treatment and could be enrolled in the chemotherapy arm in ongoing and future clinical trials. On the other hand, those in the low-risk group (C1, 32.5% of the series) showing 61.5% of RFS could benefit from a prudential "wait-and-watch" strategy. This signature adequately identify the high-risk group (C2) but is less performant in the identification of low-risk group (C1) as five of 13 patients in the good prognostic group relapsed.

These findings are particularly interesting in an era in which the pertinence and utility of adjuvant chemotherapy for early stage tumors limited to the uterus are questioned (29, 30).

GI assessment by CGH array is a simple tool with a prognostic value, as we recently reported (17). Nevertheless, when one compares the prognostic power of the NanoCind signature with the GI, the former outperforms the latter in several aspects. First, NanoCind signature is prognostic not only for OS but also for RFS. Because relapse and the risk of metastasis are criteria used to decide upon adjuvant treatment, transcriptomic analysis is more informative than genomic profiling.

Second, the CINSARC signature is platform independent, as it has been tested with efficient and reproducible results on arrays (Affymetrix and Agilent), RNA-seq, and on NanoString Technology (19, 21, 32, 33). In addition, NanoString is far less influenced than RNA-seq by the poor quality of RNA extracted from FFPE blocks (21).

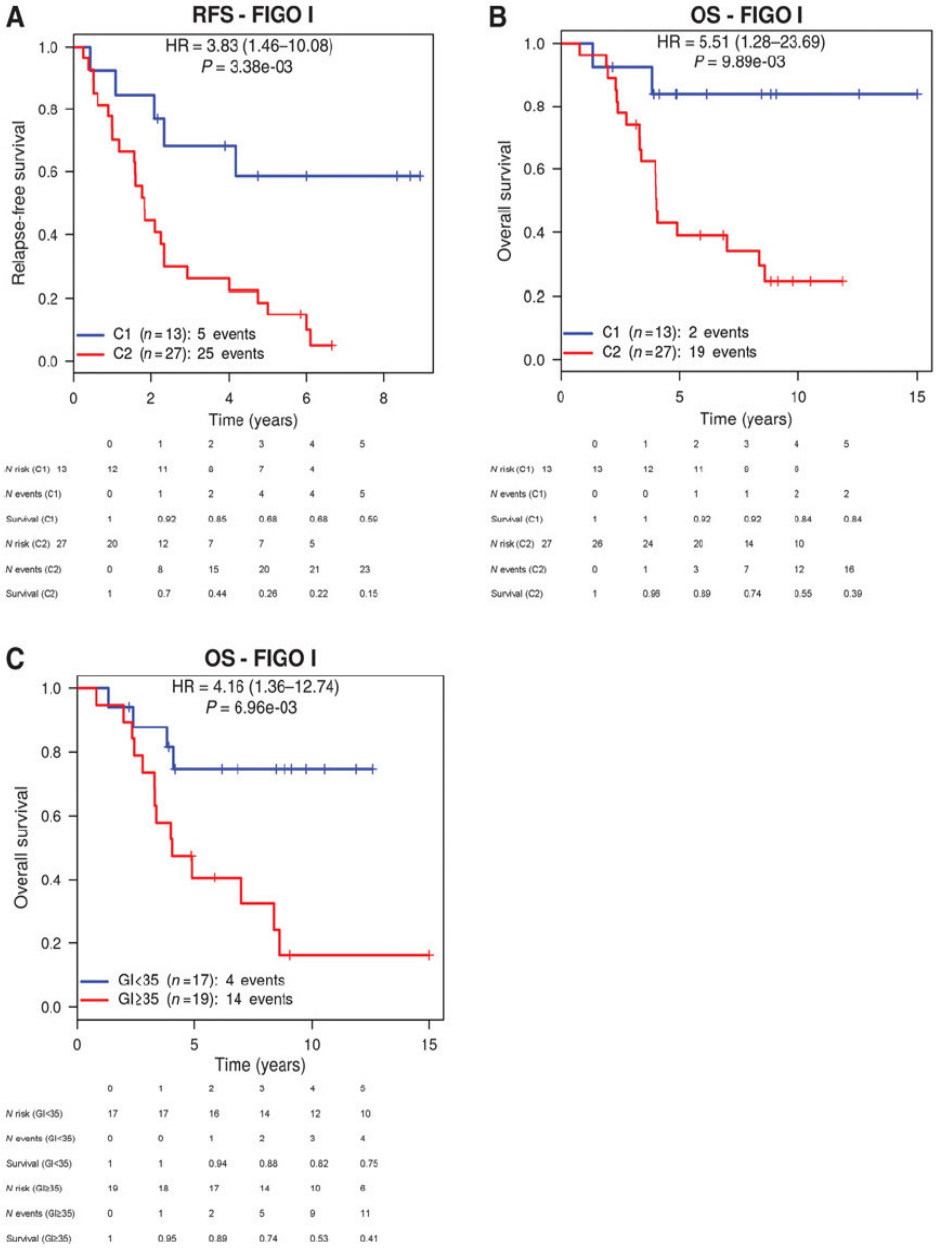

Figure 2.

RFS (**A**) and OS (**B**) for stage I uterine leiomyosarcoma according to CINSARC signature. **C,** OS for stage I uterine leiomyosarcoma according to GI at the cutoff of 35.

Unlike NanoCind, the GI is platform dependent, being strictly related to the resolution of the array. In our previous article, we established the cutoff of 35 on an Agilent platform of 8 × 60K (17). This value could change if the number of probes is higher (e.g., 4 × 180K) or the method for genomic hybridization is different (e.g., Agilent vs. Affymetrix Technology), and it needs to be validated on any new platform. Furthermore, NanoCind has the huge advantage of being ready to use. With the acquisition of NanoString technologies in many laboratories and molecular biology platforms, it will become more accessible.

Within the framework of a clinical trial led by the French Sarcoma group to evaluate prospectively the impact of NanoCind on patients' outcome, we have set up a network of NanoString users trained in CINSARC analysis and are developing a secure website where

Published OnlineFirst December 3, 2019; DOI: 10.1158/1078-0432.CCR-19-2891

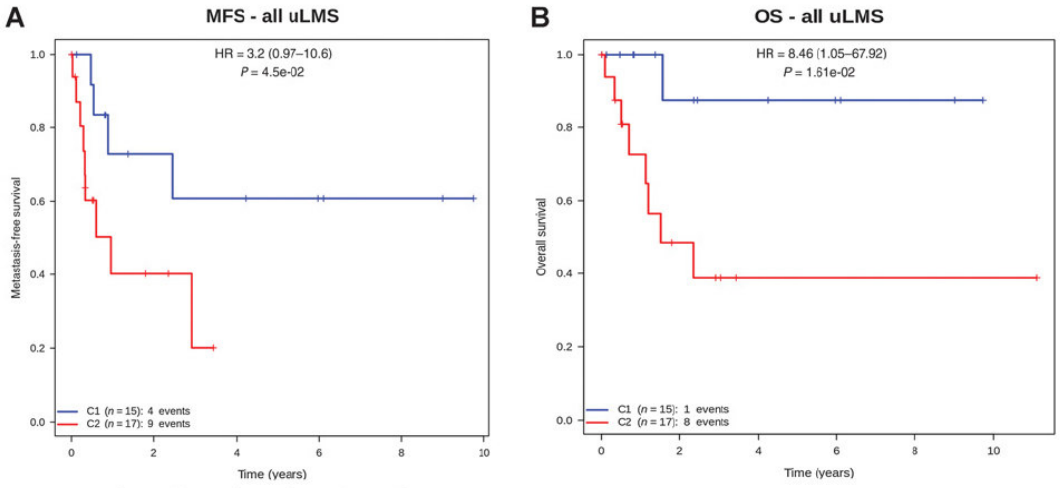

	0	1	2	3	4	5
N risk (C1)	15	7	6	5	5	4
N events (C1)	0	3	3	4	4	4
Survival (C1)	1	0.73	0.73	0.61	0.61	0.61
N risk (C2)	17	4	3	1	NA	NA
N events (C2)	0	8	8	9	NA	NA
Survival (C2)	1	0.4	0.4	0.2	NA	NA

	0	1	2	3	4	5
N risk (C1)	15	9	7	5	5	4
N events (C1)	0	0	1	1	1	1
Survival (C1)	1	1	0.88	0.88	0.88	0.88
N risk (C2)	17	9	5	3	1	1
N events (C2)	0	4	7	8	8	8
Survival (C2)	1	0.73	0.48	0.39	0.39	0.39

Figure 3.
MFS (**A**) and OS (**B**) for uterine leiomyosarcoma (uLMS) cohort from TCGA according to CINSARC signature.

clinicians will be invited to upload their NanoCind data and will receive the corresponding CINSARC classification. To accompany this evolution, these findings should now be confirmed in a larger independent cohort and even in a prospective setting.

The CINSARC NanoCind signature has now demonstrated its powerful prognostic value in a retrospective cohort of 60 uterine leiomyosarcoma (67% of whom presented at stage I) in RFS and OS at all stages including stage I by outperforming FIGO staging and GI assessment by CGH array. These data have been validated on an external cohort from TCGA data. It should therefore now be considered as the best prognostic tool for randomization in future clinical trials evaluating adjuvant treatment in stage I uterine leiomyosarcoma. The adjuvant arm could be offered to patients in the high-risk (C2) groups, while the observation arm could include low-risk (C1) patients.

Disclosure of Potential Conflicts of Interest

D. Querleu is a paid consultant for Arquer Diagnostic. No potential conflicts of interest were disclosed by the other authors.

Authors' Contributions

Conception and design: S. Croce, S.L. Guellec, F. Chibon
Development of methodology: T. Lesluyes, L. Mayeur, F. Rebier, S.L. Guellec, F. Chibon
Acquisition of data (provided animals, acquired and managed patients, provided facilities, etc.): S. Croce, C. Valle, L. M'Hamdi, G. Pérot, E. Stoeckle, Q. Fontanges, M. Devouassoux-Shisheboran, F. Guyon, A. Floquet, G. MacGrogan, I. Soubeyran
Analysis and interpretation of data (e.g., statistical analysis, biostatistics, computational analysis): T. Lesluyes, N. Thébault, E. Stoeckle, C. Chakiba, L. Mayeur, F. Rebier, S.L. Guellec
Writing, review, and/or revision of the manuscript: S. Croce, T. Lesluyes, E. Stoeckle, J.-C. Noël, D. Querleu, A. Floquet, C. Chakiba, G. MacGrogan, S.L. Guellec, F. Chibon
Administrative, technical, or material support (i.e., reporting or organizing data, constructing databases): S. Croce, L. M'Hamdi, L. Mayeur, F. Rebier, S.L. Guellec
Study supervision: F. Chibon

Acknowledgments

This work was supported by "Association pour Corentin" and "Phil'antrop." We thank Dr Ray Cooke for the medical writing service.

The costs of publication of this article were defrayed in part by the payment of page charges. This article must therefore be hereby marked *advertisement* in accordance with 18 U.S.C. Section 1734 solely to indicate this fact.

Received September 3, 2019; revised October 18, 2019; accepted November 26, 2019; published first December 3, 2019.

References

1. Toro JR, Travis LB, Wu HJ, Zhu K, Fletcher CD, Devesa SS. Incidence patterns of soft tissue sarcomas, regardless of primary site, in the surveillance, epidemiology and end results program, 1978-2001: an analysis of 26,758 cases. Int J Cancer 2006;119:2922–30.

2. Seagle BL, Sobecki-Rausch J, Strohl AE, Shilpi A, Grace A, Shahabi S. Prognosis and treatment of uterine leiomyosarcoma: a National Cancer Database study. Gynecol Oncol 2017;145:61–70.
3. D'Angelo E, Prat J. Uterine sarcomas: a review. Gynecol Oncol 2010;116: 131–9.
4. Abeler VM, Royne O, Thoresen S, Danielsen HE, Nesland JM, Kristensen GB. Uterine sarcomas in Norway. A histopathological and prognostic survey of a total population from 1970 to 2000 including 419 patients. Histopathology 2009; 54:355–64.
5. Burghaus S, Halmen S, Gass P, Mehlhorn G, Schrauder MG, Lux MP. Outcome and prognosis in uterine sarcoma and malignant mixed Mullerian tumor. Arch Gynecol Obstet 2016;294:343–51.
6. Skorstad M, Kent A, Lieng M. Uterine leiomyosarcoma - incidence, treatment, and the impact of morcellation. A nationwide cohort study. Acta Obstet Gynecol Scand 2016;95:984–90.
7. Brooks SE, Zhan M, Cote T, Baquet CR. Surveillance, epidemiology, and end results analysis of 2677 cases of uterine sarcoma 1989–1999. Gynecol Oncol 2004;93:204–8.
8. Ricci S, Stone RL, Fader AN. Uterine leiomyosarcoma: epidemiology, contemporary treatment strategies and the impact of uterine morcellation. Gynecol Oncol 2017;145:208–16.
9. Amant F, Coosemans A, Debiec-Rychter M, Timmerman D, Vergote I. Clinical management of uterine sarcomas. Lancet Oncol 2009;10:1188–98.
10. Amant F, Lorusso D, Mustea A, Duffaud F, Pautier P. Management strategies in advanced uterine leiomyosarcoma: focus on trabectedin. Sarcoma 2015;2015: 704124.
11. Zivanovic O, Jacks LM, Iasonos A, Leitao MM Jr, Soslow RA, Veras E, et al. A nomogram to predict postresection 5-year overall survival for patients with uterine leiomyosarcoma. Cancer 2012;118:660–9.
12. Iasonos A, Keung EZ, Zivanovic O, Mancari R, Peiretti M, Nucci M, et al. External validation of a prognostic nomogram for overall survival in women with uterine leiomyosarcoma. Cancer 2013;119:1816–22.
13. Oliva E, Carcangiu ML, Carinelli SG, IP P, Loening T, Longacre TA, et al. Mesenchymal tumours. Smooth muscle tumour of uncertain malignant potential. In: Kurman RJ, Carcangiu ML, Herrington CS, Young RH, editors. WHO classification of tumours of female reproductive organs. Lyon, France: IARC; 2014. p. 135–47.
14. Bell SW, Kempson RL, Hendrickson MR. Problematic uterine smooth muscle neoplasms. A clinicopathologic study of 213 cases. Am J Surg Pathol 1994;18: 535–58.
15. Oliva E. Practical issues in uterine pathology from banal to bewildering: the remarkable spectrum of smooth muscle neoplasia. Mod Pathol 2016;29: S104–20.
16. Pautier P, Genestie C, Rey A, Morice P, Roche B, Lhomme C, et al. Analysis of clinicopathologic prognostic factors for 157 uterine sarcomas and evaluation of a grading score validated for soft tissue sarcoma. Cancer 2000;88: 1425–31.
17. Croce S, Ducoulombier A, Ribeiro A, Lesluyes T, Noel JC, Amant F, et al. Genome profiling is an efficient tool to avoid the STUMP classification of uterine smooth muscle lesions: a comprehensive array-genomic hybridization analysis of 77 tumors. Mod Pathol 2018;31:816–28.
18. Chibon F, Lagarde P, Salas S, Perot G, Brouste V, Tirode F, et al. Validated prediction of clinical outcome in sarcomas and multiple types of cancer on the basis of a gene expression signature related to genome complexity. Nat Med 2010;16:781–7.
19. Chibon F, Lesluyes T, Valentin T, Le Guellec S. Cinsarc signature as a prognostic marker for clinical outcome in sarcomas and beyond. Genes Chromosomes Cancer 2019;58:124–9.
20. Lesluyes T, Delespaul L, Coindre JM, Chibon F. The CINSARC signature as a prognostic marker for clinical outcome in multiple neoplasms. Sci Rep 2017;7:5480.
21. Le Guellec S, Lesluyes T, Sarot E, Valle C, Filleron T, Rochaix P, et al. Validation of the Complexity INdex in SARComas prognostic signature on formalin-fixed, paraffin-embedded, soft-tissue sarcomas. Ann Oncol 2018;29:1828–35.
22. Croce S, Ribeiro A, Brulard C, Noel JC, Amant F, Stoeckle E, et al. Uterine smooth muscle tumor analysis by comparative genomic hybridization: a useful diagnostic tool in challenging lesions. Mod Pathol 2015;28:1001–10.
23. Cancer Genome Atlas Research Network, Abeshouse A, Adebamowo C, Adebamowo SN, Akbani R, Akeredolu T, et al. Genome atlas research network. Comprehensive and integrated genomic characterization of adult soft tissue sarcomas. Cell 2017;171:950–65.
24. Kapp DS, Shin JY, Chan JK. Prognostic factors and survival in 1396 patients with uterine leiomyosarcomas: emphasis on impact of lymphadenectomy and oophorectomy. Cancer 2008;112:820–30.
25. Greer BE, Koh WJ, Abu-Rustum N, Bookman MA, Bristow RE, Campos SM, et al. Uterine neoplasms. Clinical practice guidelines in oncology. J Natl Compr Canc Netw 2009;7:498–531.
26. Omura GA, Blessing JA, Major F, Lifshitz S, Ehrlich CE, Mangan C, et al. A randomized clinical trial of adjuvant adriamycin in uterine sarcomas: a Gynecologic Oncology Group Study. J Clin Oncol 1985;3:1240–5.
27. Hensley ML, Enserro D, Hatcher H, Ottevanger PB, Krarup-Hansen A, Blay JY, et al. Adjuvant gemcitabine plus docetaxel followed by doxorubicin versus observation for high-grade uterine leiomyosarcoma: a phase III NRG Oncology/Gynecologic Oncology Group Study. J Clin Oncol 2018;36:3324–30.
28. Bogani G, Fuca G, Maltese G, Ditto A, Martinelli F, Signorelli M, et al. Efficacy of adjuvant chemotherapy in early stage uterine leiomyosarcoma: a systematic review and meta-analysis. Gynecol Oncol 2016;143:443–7.
29. Friedman CF, Hensley ML. Options for adjuvant therapy for uterine leiomyosarcoma. Curr Treat Options Oncol 2018;19:7.
30. George S, Serrano C, Hensley ML, Ray-Coquard I. Soft tissue and uterine leiomyosarcoma. J Clin Oncol 2018;36:144–50.
31. Roberts ME, Aynardi JT, Chu CS. Uterine leiomyosarcoma: a review of the literature and update on management options. Gynecol Oncol 2018;151:562–72.
32. Lesluyes T, Perot G, Largeau MR, Brulard C, Lagarde P, Dapremont V, et al. RNA sequencing validation of the complexity INdex in SARComas prognostic signature. Eur J Cancer 2016;57:104–11.
33. Valentin T, Lesluyes T, Le Guellec S, Chibon F. Chemotherapy in localized soft tissue sarcoma: will we soon have to treat grade 1 tumours? Update on CINSARC performances. Ann Oncol 2019;30:153–5.

*3.*3 L'ANALYSE DU PROFIL GENOMIQUE PAR CGH-ARRAY EST APPLICABLE AUX TUMEURS MUSCULAIRES LISSES UTERINES DE TYPE EPITHELIOIDES

Le rationnel de l'étude et le besoin clinique

Ce travail a eu un double objectif. Premièrement réaliser une étude de validation du Genomic Index (GI) sur deux plateformes génomiques différentes : AGILENT x60K (sur laquelle les seuils du GI ont été calculés) et AGILENT x180 qui est plus fréquemment diffuse dans les services de cytogénétique.

Deuxièmement tester les seuils du GI sur un variant rare de tumeurs musculaires lisses de l'utérus : le variant épithélioide qui est distinct sur le plan morphologique par des critères diagnostiques à part, in particulier par un seuil mitotique plus bas par rapport au variant fusocellulaire. Peu de données ont été jusqu'à maintenant publiées en littérature et les altérations génomiques sous-jacentes à ces tumeurs sont inconnues.

Série et méthodes. Pour tester la correspondance des valeurs du GI nous avons analysé sur la plateforme AGILENTx180. une série de 11 cas (7 LM et 4 LMS) à partir de la série qui avait servi à établir le GI sur la plateforme x60.

La série d'étude a été composée de 32 tumeurs musculaires lisses de l'utérus de type épithélioides ainsi distribuées : 7 E-LM, 13 E-LMS et 12 E-STUMP et collectée de 5 centres français impliqués dans le réseau national RRePS (réseau de référence en pathologie des sarcomes). L'analyse du profil génomique des tumeurs a été réalisée sur les deux plateformes, une fois établie la concordance des résultats.

Résultats et discussion

Nous observé des résultats concordants entre les deux plateformes, et nous avons établi le seuil diagnostique de 10 qui sépare les LM des LMS. Tous les E-LMS ont montré un GI>10 (GI moyen 69.7, médian : 36 variable entre 14.4 et 180). Des 7 E-LM 5 ont montré un GI<10 et deux un GI borderline (10.1 et11.6). parmi les 12 E-STUMP ont montré un GI<10 (entre 2 et 8,1) et 5>10 (entre 16 à 49). L'analyse de courbes de survie Kaplan-Meier a montré une tendance entre le GI (au seuil de 10) et la survie globale sans être statistiquement significatif. Les E-STUMP de notre série, sous réserve d'un nombre réduit d'effectifs et d'un suivi clinique court (suivi moyen des E-STUMP : 2,25 ans, médian 1,8) semblent montrer un décours favorable.

Epithelioid smooth muscle tumours of the uterus. A comprehensive Genomic profile analysis by CGH-array of 32 tumors.

Sabrina Croce[1,2], Evelyne Callet Bauchu[3], Laetitia Mayeur[1], Flora Rebier[1], Claire Larmonnier[1], Catherine Genestie[4], Laurent Arnould[5], Pierre-Alexandre Just[6,7], Patricia Pautier[8], Béatrice Grange[3], Isabelle Soubeyran[1], Gaëlle Pérot[9], Frédéric Chibon[9,10*] and Mojgan Devouassoux-Shisheboran[11*]

1. Department of Biopathology, Institut Bergonié, Comprehensive Cancer Center, Bordeaux, France
2. INSERM U1218, Bordeaux
3. Cytogenetics and Molecular Biology Department, Hospices Civils de Lyon, Lyon-Sud Hospital, Pierre Bénite, France
4. Department of Pathology, University Paris-Saclay, Gustave Roussy Cancer Center, Villejuif, France.
5. Department of Pathology, Centre JF Leclerc, Comprehensive Cancer Centre, F- Dijon, France
6. Department of Pathology, Cochin Hospital, Hôpitaux Universitaires Paris Centre, Assistance Publique-Hôpitaux de Paris, 75014 Paris, France.
7. Faculty of Medicine, Paris Descartes University, 75006 Paris, France
8. Department of Oncology, University Paris-Saclay, Gustave Roussy Cancer Center, Villejuif, France.
9. Oncosarc, INSERM UMR1037, Cancer Research Center of Toulouse, Toulouse, France
10. Department of Pathology, Institut Claudius Regaud, IUCT-Oncopole, Toulouse France
11. Department of Pathology, Hospices Civils de Lyon, Lyon-Sud Hospital, Pierre Bénite, France

* both authors equally contributed

Running title

Epithelioid uterine smooth muscle tumors and array-CGH

Corresponding author

Dr Sabrina Croce

Biopathology Department, Institut Bergonié

229 cours de l'Argonne F-33000

Bordeaux, France

s.croce@bordeaux.unicancer.fr

Abstract

Epithelioid smooth muscle tumours of the uterus are a rare variant of uterine tumours with distinct diagnostic morphologic criteria, and in particular with a more restrictive mitotic threshold. Few data on limited series have been published in literature so far and the genomic events associated to this variant are unknown.

In this study we validate the Genomic Index on a platform (AGILENT X180K) with higher resolution of the array compared to the original one (AGILENT x60). After the array-validation, We analyzed by array-CGH a series of 32 epithelioid uterine smooth muscle tumors (7 leiomyomas, 12 STUMP and 13 leiomyosarcomas) collected from 5 centers in France involved in national network of sarcoma. All epithelioid leiomyosarcomas had a Genomic index >10 (mean GI value : 69.7; median 36, from 14.4 to 180). Among the epithelioid leiomyomas 5/7 had a GI<10 and two 10.1 and 11.6)and among the STUMP 5/12 had a GI<10 (between 2 and 8.1) and 5 >10 (between 16 and 49). Kaplan-Meyer analysis highlights a trend between the overall survival and GI at the cut off of 10, though it was not statistically significant. The STUMP tumours, under limitation of weak number of cases and limited follow up (mean follow up of STUMP: mean 2,25, median1,8y) in our series, seems to have a favorable outcome.

In conclusion we validate the GI at the threshold of 10 on two different genomic platforms with different array resolutions (180K versus 60K) and we describe the genomic profiles of a series of 32 epithelioid smooth muscle tumors of the uterus.

Introduction

The large majority of uterine smooth muscle tumors are spindle cells tumors[78]. Epithelioid type is uncommon and has been subject of only few papers[141 107, 133, 168].

Epithelioid smooth muscle tumors display round to polygonal cells with granular or clear cytoplasms and “epithelial-like appearance” with alveolar, nested, trabecular or diffuse architecture [98]. In a leiomyosarcoma (LMS) the epithelioid component has to be at least 50% of the tumor [78]. According to 2014WHO the diagnostic criteria include moderate to severe cytologic atypia and/or tumor cell necrosis or ≥4 mitoses/10 HPFs (2.4 mm2)[107 78, 98]. For the epithelioid smooth muscle tumors with uncertain malignant potential (STUMP) diagnostic criteria include any degree of cytologic atypia and 2 to 3 mitoses or tumor cell necrosis[107].

The morphological criteria of malignancy in the epithelioid subtype are more problematic than those for the spindle cell variant of uterine smooth muscle tumors, because of short mitotic cut off (≥4 mitoses instead of ≥10 for spindle subtype) and because of the rarity of the histotype which makes the pathologist less confident.

Some years ago we published 2 studies on spindle cell smooth muscle tumors of the uterus and array-CGH[74, 169] demonstrating the presence of a gradient of genomic complexity correlating with clinical outcome. Hence we have employed array-CGH analysis as complementary tool to morphology in the diagnosis of complex uterine smooth muscle tumors.

The results of array-CGH analyses and the cuts off of genomic Index (diagnostic cut off GI≥10 and prognostic cut off GI≥35) were established on 60K[74, 169]array from AGILENT platform We routinely use the array-CGH analyses with these published diagnostic and prognostic cut-off in problematic uterine smooth muscle tumors. However, the initial studies have been based on spindle cell variant and their accuracy in epithelioid subtype of smooth muscle tumor is totally unknown.

In this study we ought to analyze the genomic profiles by array-CGH of a series of epithelioid uterine smooth muscle tumors and perform a technical validation of Genomic Index thresholds on a 180K AGILENT platform with higher resolution compared to the 60K AGILENT platform where the GI where originally defined.

Materials and Methods

Tumors Samples

Thirty-two epithelioid uterine smooth muscle tumors from 5 centers in France (Departments of Pathology of Hospices Civils de Lyon, Institut Bergonié of Bordeaux, Institut Gustave Roussy of Villejuif, Hopital Cochin of Paris, Centre Leclerc of Dijon) involved in the French network of sarcomas RRePS (Réseau de Référence en Pathologie des Sarcomes des tissus mous et des viscères) were collected. The series was thus composed of 12 epithelioid STUMP (E-STUMP) along with 13 E-LMS and 7 epithelioid leiomyomas (E-LM) .

In order to compare AGILENT 180K versus AGILENT 60K, 11 spindle smooth muscle tumors of the uterus (7 LM and 4 LMS) which were part of the original series that served for assess the GI cut off[74] were tested on two platforms.

For each patient, 1-10 slides were collected and all cases were centrally reviewed by two of the authors (SC and MDS) and classified according the 2014 WHO classification of tumors of female reproductive organs[78, 98]. Cytologic atypia was evaluated at the objective 10 according the presence of high nuclear size or nuclear pleomorphism and hyperchromatism[98]. The mitotic count was evaluated on 10 high power fields (objective x40, field diameter 0,55) and the tumor cell necrosis defined by an abrupt transition from necrotic to non-necrotic areas without interposed granulation tissue [98]. Mitotic cut off was ≥4 mitoses/10 HPF.

The samples were centralized in Biological Resources Center of Institut Bergonié and HCL (French authorization for scientific research (AC-2008-812).Once validated the GI threshold on the platform AGILENT x180, 14/32 tumors were analyzed on the genomic platform AGILENT X180 and the other on the AGILENT x60.

DNA extraction

Genomic DNA was extracted from formalin-fixed and paraffin-embedded (FFPE) tissues according to the protocol for DNA isolation from FFPE (https://www.qiagen.com/kr/products/diagnostics-and-clinical-research/solutions-for-laboratory-developed-tests/qiaamp-dsp-dna-ffpe-tissue-kit/#orderinginformation) with improvements such 1 h of incubation at 90°C,an RNA-ase treatment (4µL for 2 minutes) and the second wash buffer replaced by ethanol 80%.

A cut off of 50% of cellularity in tumor samples was set for the analysis.

Array-Comparative Genomic Hybridization Analysis

For the analyses two platforms were available: a 8x60K whole-genome arrays (SurePrint G3 Human CGH 8x60k bundle Agilent G5923A) and a 4x180K whole genome arrays (Sureprint G3 Human CGH Microarray 4x180K) according to the manufacturer's protocol. Microarray slides were scanned using a DNA Microarray Scanner, images were analyzed by Agilent DNA Microarray Scanner USK0057446 followed by Agilent® Cytogenomic software 4.0.3.12.

A low-level copy number gain was defined as a log 2 ratio >0.25 and a copy number loss was defined as a log 2 ratio <0.25. A high-level gain or amplification was defined as a log 2 ratio >1.5 and a homozygous deletion was suspected when the ratio was <-1. The range for Derivative Log ratio (DLR) spread cut-off was fixed to 0.50. Genomic Index was calculated for each profile as follows: Genomic Index (GI) = A^2/C, where A is the total number of alterations (segmental gains and losses) and C is the number of involved chromosomes [154 74].

In particular in the assessment of GI as previously described the X chromosome was not evaluated and the losses or the gains involving the entire chromosome, on either

side of centromere were counted as two events (e.g. loss of *p* and *q* arms of chromosome). We tested on the series three different methods of counting :1) the GI as previously published [74, 154, 169] 2) GI counting the loss or gain of the entire chromosome as one event 3) GI counting the loss or gain of the entire chromosome as one event and the chromosomal events on X chromosome. Chromomal breaks were calculated by the number of breaks flanking each intrachromosomal gain or loss.

Statistical Analysis

Overall survival, using the Kaplan–Meier method, was calculated from the date of diagnosis to death or last follow-up. Survival curves were compared with the log-rank test. Univariate survival analyses were performed by using the R software version 3.4.0 (R Development Core Team, Vienna, Austria, 2009) and the 'survival' package (A Package for Survival Analysis in S; Terry Therneau, February 2002; R package, version 2.40-1).

Results

In order to compare the Genomic Index on the two platforms: AGILENT 60K[74] and AGILENT 180K we selected a test series of 7 spindle cell uterine LM and 4 spindle cell uterine LMS that we tested in parallel on both platform. These tumours belonged to the original test series that served for establish the thresholds[74].

As we observed minor differences not influent on the Genomic Index assessment (cf Table 1) we retained the cut off of 10 for the diagnosis in LMS on the two platforms and.

The clinico-pathologic and genomic data are summarized in Table 2.

Clinical data

Clinical follow up was available for all patients but 4 (recent cases). All the 12 patients diagnosed with E-STUMP were alive and well (mean 2,25, median1,8y from 0.1 to 5,9 y). One patient (case 7 cf Table 2) had concurrently a stage 2 follicular B cell lymphoma treated by chemotherapy. Among the 7 patients with E-LM 6 were alive without evidence of disease (mean:4,4 y; median: 4,6 y from 0.3 to 6.5) and one was a recent case. Five out of 13 E-LMS were dead of disease, 2 alive with metastases, 2 alive and well and 3 were recent cases. One patient (case 22) had a lung metastases 2 years after the hysterectomy, treated by radiofrequency and she is alive without evidence of disease. The mean follow up for E-LMS was 3.4 y, varying from 0.2 to 11.2 y. Hysterectomy was performed in 25 cases, myomectomy in 4, curetting in 2 and one patient was operated by posterior pelvectomy.

The mean size of E-LMS was 10.3 cm (median 9; from 4 to 23 cm), 5 cm for E-STUMP (median 6; from 1.1 to 10 cm) and 10.4 cm for E-LM (median 10; from 6 to 15 cm).

Morphologic analysis

When the data was available, the margins were well limited in all E-STUMP but one (case 12) showing irregular borders and in all E-LM. Three of E-LMS showed well limited borders but 8 had infiltrative margins. In the E-LM atypia and necrosis were absent and mitotic count was low (from 1 to 3, mean 1.7, median 1). All E-LMS showed diffuse atypia. Six of them had tumor cell necrosis, and the mean mitotic count was 23.1 (median 20, from 4 to 48). Among the E-STUMP 4 showed atypia, in one tumor the tumor cell necrosis was doubtful and in one was present and mean mitotic count was 3.5 (median 2, from 1 to 14). Figure 1 illustrates some examples of E-LM, E-STUMP and E-LMS.

Genomic results

The GI assessment on two different genomic platforms resulted equivalent, despite the variations related to the different resolution of the arrays. In fact the GI was < 10 in all LM with a deviation of 1.2 and 3 between the two platforms (Table 1). In LMS the GI differences were more marked because of the higher number of alterations (complex genomics tumors) with deviations varying from 3 to 20,5. Nevertheless all LMS had a GI>10. The prognostic threshold of 35[169] was concordant in all LMS but one (LMS 3 , cf Table 1)) (

The group of E-LM had a quite simple genomic profiles with a GI varying from 2 to 11.6 (mean GI: 7.11, median: 7) and mean number of chromosomic breaks of 4.5 (median 5, from 0 to 8). Three out seven LM group harbored *RB1* deletions in a heterozygous manner and 1/7 *TP53* heterozygous deletion. Heterozygous *FH* deletion was observed only in 1/7 LM.

E-LMS showed complex genomic profiles as evidenced by a mean GI of 69.7 (median 36, from 14.4 to 180) and by mean chromosomic breaks of 27.9 (median value: 21,

from 4 to 92). Four out 13 E-LMS harbored a heterozygous *FH* deletion (in 2 cases the loss was included in a large chromosomal region). *RB1* was the most frequent deleted gene (11/13 tumors), 8 in heterozygous manner and 3 homozygous. *TP53* was lost in 3/13 E-LMS. Interestingly one E-LMS (case 23) harbored a homozygous deletion of *TP53* and *RB1* and the patient died of disease 2.5 y after the initial diagnosis. We did not observe a statistically significant difference between the E-LMS and the other LMS (from the series previously published[169] p =0.79). Compared to clinical outcome, the lower GI in E-LMS associated to death or persistent disease is 23.3. Minimal GI associated to good outcome is 14.4.

The E-STUMP group showed heterogeneous genomic profiles with a mean GI of 16.9 (median GI: 16,3 ; from 2 to 49) and mean chromosomic breaks of 6.1 (median 5.5 ; from 2 to 12). Three out of 12 E-STUMP harbored a *TP53* or *RB1* losses and none a *FH* deletion.

According to the GI at the cut off of 10 all E-LMS showed a GI>10 (mean 69.7). Among the E-LM 5 had a GI<10 (3,4,4.5,6,8) and 2 were >10 (10.1 and 11.6) with chromosomal breaks of 5 and 8 respectively. Among the heterogeneous group of E-STUMP 7 had a GI>10 (from 16 to 49; mean chromosomal breaks: 6; from 2 to 12) and 5 had a GI<10 (from 2 to 8; mean chromosomal breaks: 6.2 from 2 to 11).

. E-STUMP's genomic profiles in our series are quite heterogeneous as mirrored by variable GI values. The genomic events in E-STUMP in our series encompass losses or gains or both alterations of whole chromosome or large part of their arms without chromothripsis or very complex genomic event with the exception of a tumour (case 7) harboring 7 losses all localized on chromosome 11 without other chromosomal event. The patient was alive without recurrence but with a B cell follicular lymphoma. Three out 12 E-STUMP (cases 10,11,12) showed as genetic event only chromosomal gains (mean GI 18.2), 6 (cases 7,8,9) only chromosomal losses (mean GI 11.7) and 3 (cases 3,4,5) both gains and losses (mean Gi 23.1).

Kaplan-Meier analysis on 32 tumors of the series highlights a trend correlating the GI value at the cut off of 10 and overall survival but not a statisticaly significant correlation, probably because of low number of events (cf Fig 4).

Discussion

Epithelioid smooth-muscle tumors of the uterus are rare neoplasms defined by the presence of almost 50% of round, epithelioid, polygonal cells with clear or eosinophilic cytoplasms and nested, trabecular or solid architecture[107, 141] often associated to other areas of conventional, spindle smooth muscle tumor[141]. Only two series of 18 and 26 patients of epithelioid smooth muscle tumors of the uterus have been reported until now[107, 141] and on the basis of these descriptions the diagnostic criteria (in particular the cut off of 4 mitoses/10 high power field (HPF) at the field diameter of 0.47 mm) have been assessed. Nevertheless multi-institutional studies enrolling a consequent number of patients with long follow up are necessary in order to define their clinical behavior and firmly establish the diagnostic criteria which have been proposed.

Based on the assumption that clinical outcome of uterine smooth muscle tumors is related to genomic complexity, we previously demonstrated the diagnostic and prognostic value of Genomic Index by array-CGH on spindle cell smooth muscle lesions at the diagnostic threshold of 10, separating LM from LMS and at the cut off of 35, distinguishing the LMS with a lower recurrence-free survival [74, 169].

We first validate the GI at the threshold of 10 of the diagnostic value, separating the LM from LMS using the series that originally served to assess the GI[74] and then we run the epithelioid series.

Then we tested the validity of this hypothesis on 12 E-STUMP, 7 E-LM and 13 E-LMS, using a genomic platform (AGILENT x180K) with higher resolution of the array compared to the original genomic platform (AGILENT x60K) on which the GI thresholds (of 10 and 35) were assessed[74, 169].

we observed a link between the genomic complexity and the clinical outcome of uterine smooth muscle tumours of epithelioid variant even if, limited by the weak number of events in our series (5 death on 32 tumours, 13 E-LMS) the association between the GI at the cut off of 10 and the overall survival was not statistically significant. In fact in our series all the E-LMS had a GI>10 and 5 out of 7 E-LM had a GI<10. Two out of 12 E-LM had a borderline GI (10.1 and 11.6) without recurrence at 4.5 years and 3 months of follow up.

Our study has two caveats. First the absence of clinical event in E-STUMP and the limited size of the series and for that point more studies including larger series with consequent clinical follow up are needed. The second one is the lack of allelic status data informing about the tumor ploidy. Indeed this data is not available on these platforms unlike Affymetrix technology.

E-STUMP's Genomic profiles in our series are different from the profiles of STUMP of spindle type[74]. In fact E-STUMP show gains and/or losses of whole chromosome or of large part of chromosomal arm without chromothripsis (except one case showing multiple losses on one chromosome) or multiple events which are evidence of genomic complexity. This observation together with the scarce *TP53* and *RB1* deletions suggests that E-STUMP are different morphologically and genomically. from spindle STUMP .

Because of eosinophilic cytoplasmic inclusion Fumarate Hydratase-deficient LM could be in differential diagnosis of a E-LM and even E-STUMP. In our series we did not detect the morphologic features associated to FH-deficiency (hemangiopericytoma-like vascularization, alveolar edema, orangyophilic nucleolus and halo clear perinucleolar, rhabdoid inclusions) and only one out of 7 E-LM and none of the E-STUMP harbored a FH deletion detectable at array-CGH analysis. Four out of 13 E-LMS harbored an heterozygous deletion of FH but in these cases the morphology did not supported either the diagnosis of FH-deficient tumour. In light of powerful

prognostic value in recurrence-free survival and metastasis-free survival recently proved on uterine LMS[170] patients diagnosed with E-LMS could benefit of Nanocind signature in order to better assess the therapeutic strategy.

In conclusion we validate the GI at the threshold of 10 on two different genomic platforms with different array resolutions. We have thereafter analyzed by array-CGH a series of epithelioid smooth muscle tumours of the uterus observing a trend between the genomic complexity and the clinical outcome that was not statistically significant (p=0.11) because of low number of events and patients.

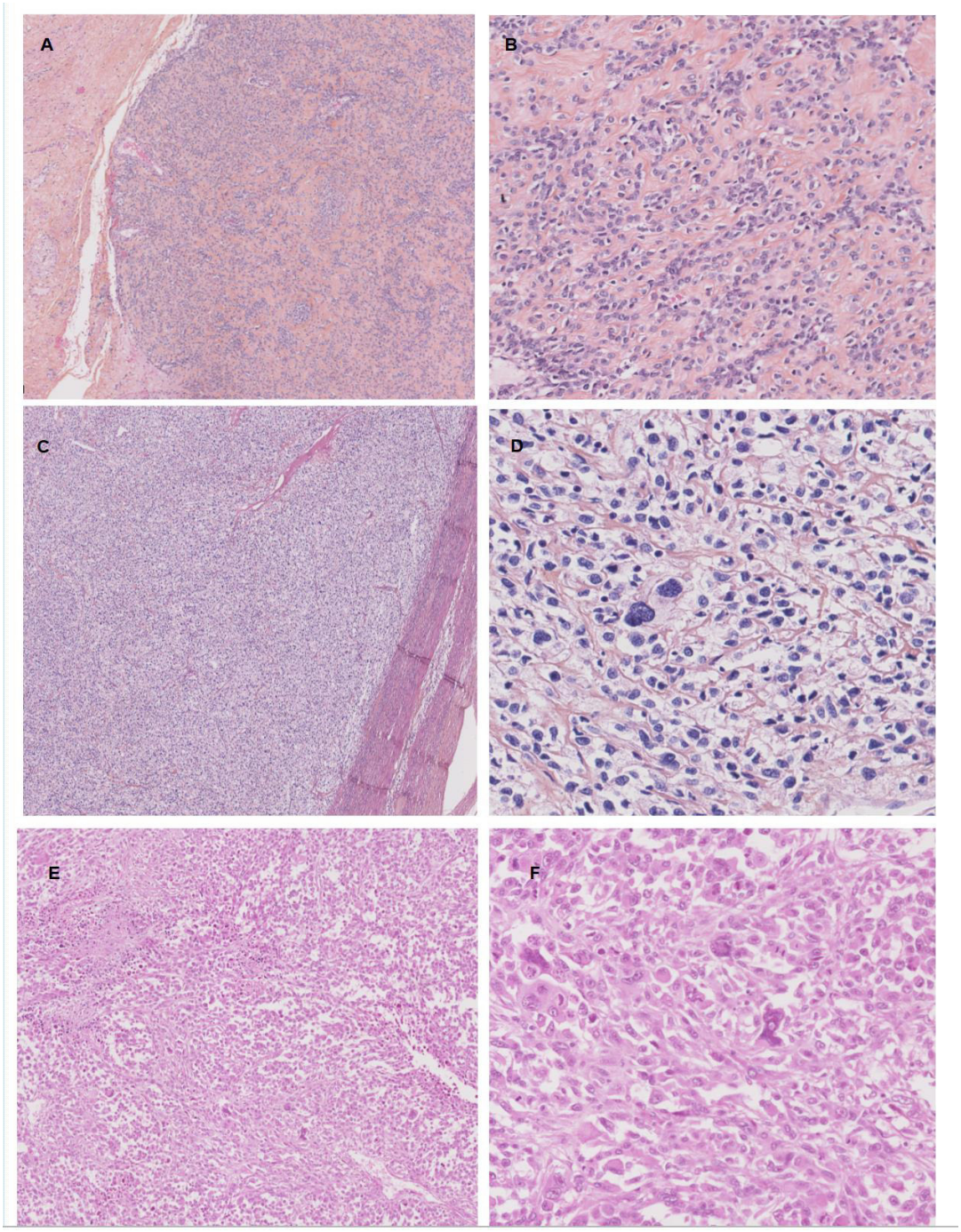

Figure 1

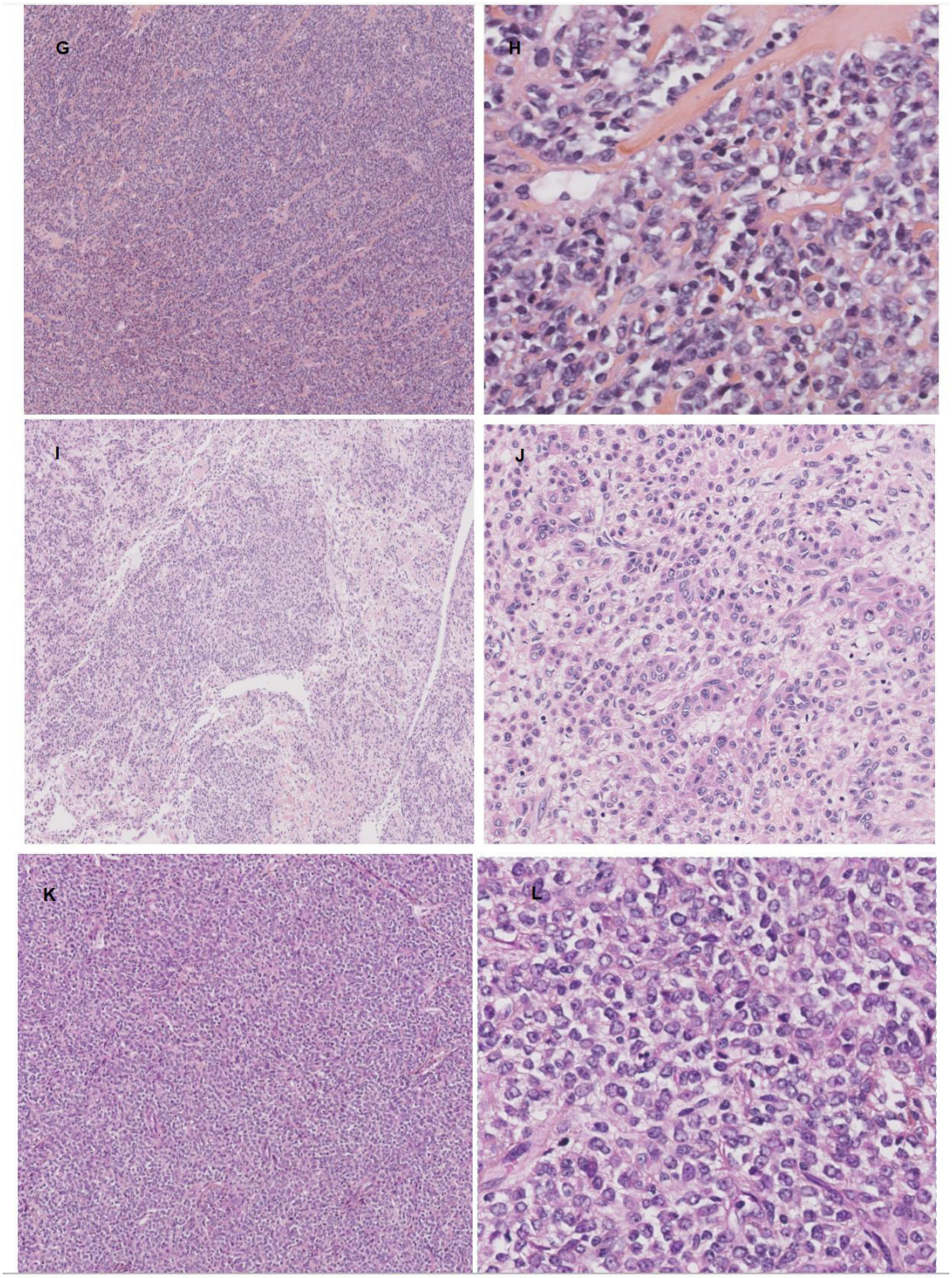

Figure 1

Figure 2

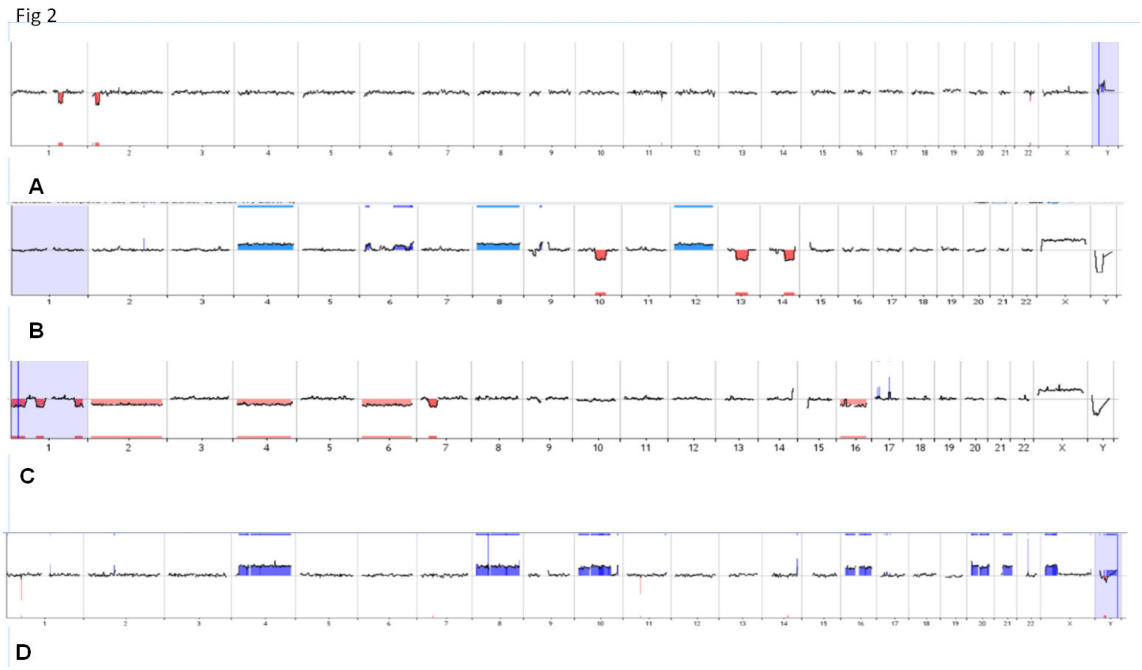

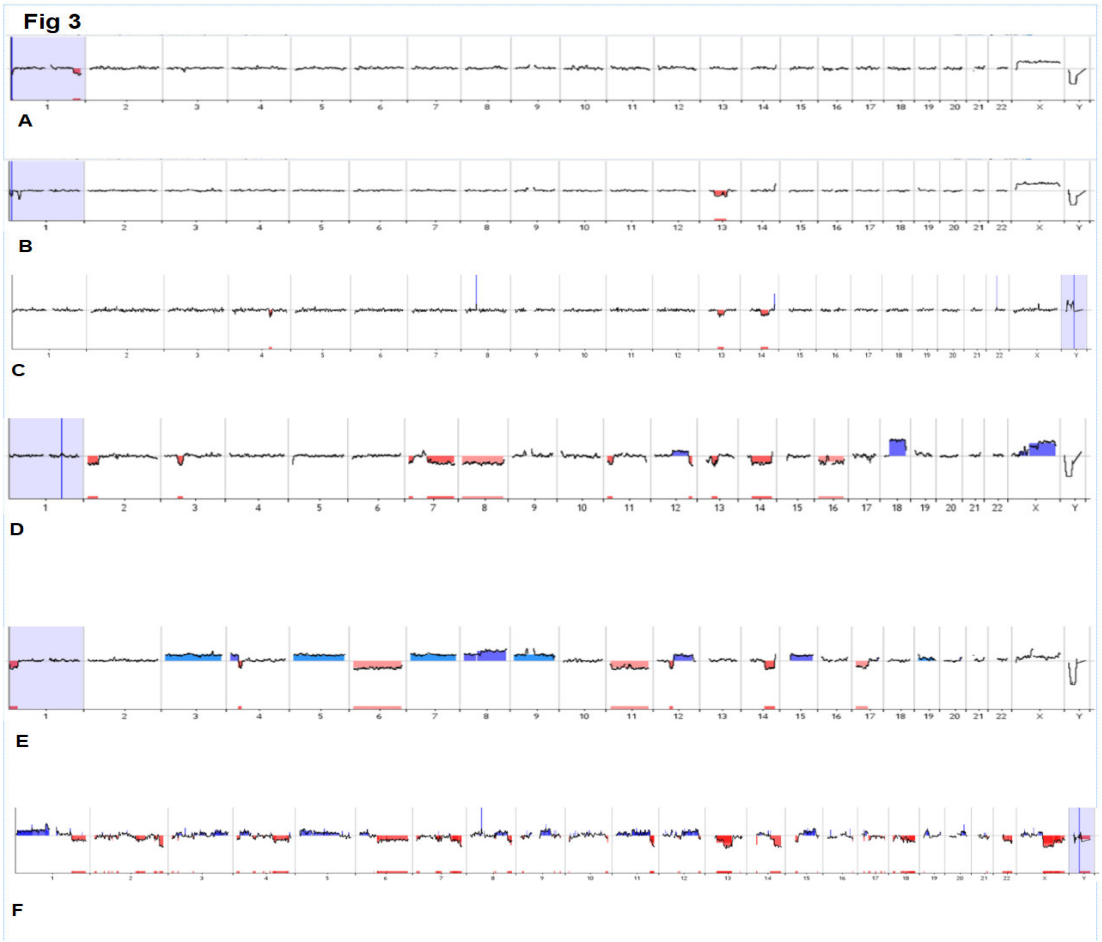

Figure 3

Figure 4

Fig 4

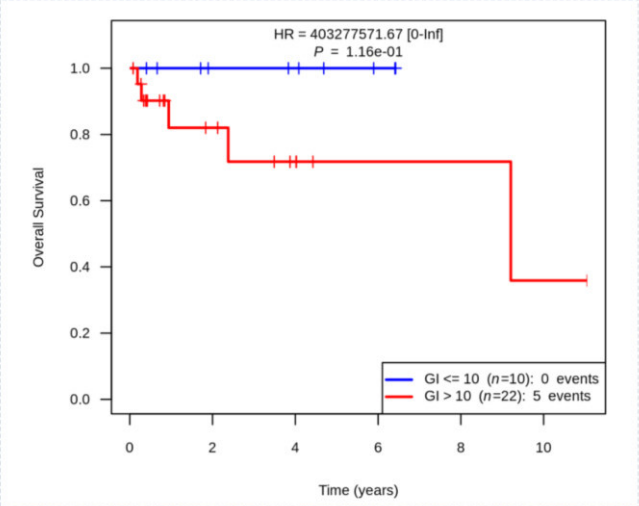

Figure legends

Figure 1. Morphologic features of some epithelioid uterine smooth muscle tumors of the series

Epithelioid LM (case 27) with well limited borders (A), moderate cellularity and round epithelioid cells without atypia (B).

Epithelioid LMS (case 25). Highly cellular tumor with pushing borders (C), diffuse atypia, polygonal clear cells (D).

Epithelioid LMS (case 16). Discoesive epithelial tumor with foci of necrosis (E), pleomorphic cells and high mitotic rate (F).

Epitheloid STUMP (case 8). Highly cellular tumor with trabecular and solid architecture (G) composed of epithelioid cells with scant cytoplasm (H). (Case 7) heterogeneous architecture alternating low and high cellular areas (I) with some atypia (J).(Case2) highly cellular tumor with dense architecture (K), epithelioid cells with scan cytoplams, irregular nuclei and 2 mitoses (L).

Figure 2. Genomic profiles of E-STUMP

Simple genomic profile with a GI =6.25 (case 6) akin to a profile observed in spindle cell leiomyoma (A).

More complex genomic profiles showing gains and losses with a GI= 18.7 (case 5)(B) and GI=32 (case 4) (C). STUMP with a profile harboring only gains without deletions and a GI=24 (case 10).

Figure 3. Genomic profiles of E-LM and E-LMS

E-LM show simple genomic profiles

A (Case 29) E-LM with GI=4. The patient is alive and well (4.5 y of follow up). B (Case 28) E-LM with GI=4.5. The patient is alive and well (6.5 y of follow up). C (Case 32) E-LM with GI= 3. The patient is alive and well (6.5 y of follow up).

E-LMS harbor very complex genomic profiles

D (Case 14) E-LMS with GI=23.3. The patient died of disease 9 months after the diagnosis.

E (Case15) E-LMS with GI=41. The patient died of disease 9.3y after the diagnosis.

F (Case 16) E-LMS with GI=149. The patient died of disease 3 months after the diagnosis.

Figure 4. Kaplan-Meyer curbs of 32 patients with Genomic Index at the cut off of 10.

Table 1. Comparative analysis of a test series of LM and LMS on two different platforms with 3 different methods of Genomic Index assessment

Table 2. Clinico-pathologic and genomic data of the series

Table 1. Comparative analysis of a test series of LM and LMS on two different platforms with 3 different methods of Genomic Index assessment

Test case	Platform AGILENT 8x60K *GI*	Platform AGILENT 4x180K	Intrachromosomal Breaks
LM1	0	0	0
LM2	8.3	5.3	3
LM3	5.3	5.3	3
LM4	6	7.2	5
LM5	5	4	5
LM6	0	0	0
LM7	0	0	0
LMS1	64	84.5	34
LMS2	96	93	34
LMS3	40	57.6	14
LMS4	84	88.8	25

Legend: GI: Genomic Index; LM : leiomyoma; LMS : leiomyosarcoma

Table 2. Clinico-pathologic and genomic data of the series

Patient	diagnosis	age	FU status	FU years	GI	N chr breaks	p17	q13	1q43	mitoses	Necrosis	Atypia	size (cm)	Type of Surgery	borders
1	E-STUMP	48	NED	4.1	8.1	11	0	-1	0	2	no	yes	2	hysterectomy	well limited
2	E-STUMP	65	NED	5.9	2	4	0	0	0	2	no	no	NA	hysterectomy	well limited
3	E-STUMP	47	NED	4	18.7	5	-1*	-1*	0	2	no	no	1,1	hysterectomy	NA
4	E-STUMP	52	NED	0.9	32	12	0	0	0	1	no	yes	9	hysterectomy	NA
5	E-STUMP	74	NED	2.1	18,7	6	-1	0	0	14	no	no	7	hysterectomy	well limited
6	E-STUMP	64	NED	1.9	6,25	10	0	0	0	2	yes	no	6	hysterectomy	well limited
7	E-STUMP	66	NED #	0.8	49	8	0	0	0	1	no	yes	2,5	hysterectomy	well limited
8	E-STUMP	72	NED	1.7	3	4	0	0	0	5	no	no	6	hysterectomy	well limited
9	E-STUMP	29	NED	0.6	2	2	0	0	0	5	no	no	10	myomectomy	NA
10	E-STUMP	85	NED	0.3	24	6	0	0	0	5	doubt	no	6,4	hysterectomy	well limited
11	E-STUMP	69	NED	4.1	16,6	3	0	0	0	1	no	yes	3,5	hysterectomy	well limited
12	E-STUMP	68	NED	0.1	16	2	0	0	0	2	no	no	2	hysterectomy	irregular
13	E-LMS	43	NED	1.8	14.4	8	0	-1	0	4	no	yes mild	17	posterior pelvectomy	infiltrating rectum
14	E-LMS	52	DOD	0.9	23.3	10	0	-1	0	46	yes	yes	9	hysterectomy	infiltrative
15	E-LMS	45	DOD	9.3	41.6	12	-1	0	0	8	no	yes	4	hysterectomy	well limited
16	E-LMS	58	DOD	0.3	149.33	63	0	-1	-1*	40	yes	yes	14	hysterectomy	infiltrative
17	E-LMS	97	DOD	0.2	60.8	16	0	-2	-1	18	yes	yes	11	hysterectomy	infiltrative
18	E-LMS	72	AWD	0.7	46.7	31	-1	-1	-1	39	no	yes	4,5	hysterectomy	infiltrative
19	E-LMS	48	recent case		32,1	11	0	-1	0	22	no	yes	NA	curetting	NA
20	E-LMS	49	NED	3.5	36	22	0	0	-1*	4	doubt	yes	4	hysterectomy	infiltrative

21	E-LMS	53	recent case		16	4	0	-1*	0	14	no	yes	14	hysterectomy	well limited
22	E-LMS	69	A-NED but lung mts in 2010 traited by radiofrequency	11.2	180	92	0	-1	0	20	yes	yes	30	hysterectomy	NA
23	E-LMS	65	DOD	2.4	30	21	-2	-2	0	48	no	yes	NA morcellated	hysterectomy morcellated	infiltrative
24	E-LMS	69	recent case		56	26	0	-1	0	22	yes	yes	6,5	hysterectomy	infiltrative
25	E-LMS	73	AWD	3.9	138	47	0	-2	0	15	yes	yes	6	hysterectomy	well limited
26	E-LM	43	NED	3.9	6	4	0	-1	0	1	no	no	14	myomectomy	NA
27	E-LM	51	NED	4.5	10,1	5	0	0	0	2	no	no	6	hysterectomy	well limited
28	E-LM	48	NED	6.5	4.5	7	0	-1	0	3	no	no	8	hysterectomy	well limited
29	E-LM	36	NED	4.8	4	2	0	0	-1	3	no	no	12	myomectomy	NA
30	E-LM	32	recent case		8	0	0	0	0	1	no	no	NA	curetting	NA
31	E-LM	51	NED	0.9	11,6	8	-1	-1*	0	1	no	no	15	hysterectomy morcellated	well limited
32	E-LM	32	NED	6.5	3	6	0	0	0	1	no	no	7,5	myomectomy	NA

Table 2 Legend. *: LOH not specific of the gene but loss of all harm; FU: Follow up; NED: not evidence of disease; AWD : alive with disease; DOD: dead of disease; NA: data not available; 0 : normal status; -1 : heterologous deletion ; -2 : homozygous deletion # other disease : follicular B cell lymphoma stage 2

Bibliography

[1] Oliva E CM, Carinelli SG, et al: Mesenchymal tumours. Smooth muscle tumour of uncertain malignant potential. WHO Classification of Tumours of Female Reproductive Organs. Edited by Kurman RJ CM, Herrington CS, Young RH. 2014. pp. pp 135–47.
[2] Kurman RJ, Norris HJ: Mesenchymal tumors of the uterus. VI. Epithelioid smooth muscle tumors including leiomyoblastoma and clear-cell leiomyoma: a clinical and pathologic analysis of 26 cases. Cancer 1976, 37:1853-65.
[3] Prayson RA, Goldblum JR, Hart WR: Epithelioid smooth-muscle tumors of the uterus: a clinicopathologic study of 18 patients. Am J Surg Pathol 1997, 21:383-91.
[4] Silva EG, Deavers MT, Bodurka DC, Malpica A: Uterine epithelioid leiomyosarcomas with clear cells: reactivity with HMB-45 and the concept of PEComa. Am J Surg Pathol 2004, 28:244-9.
[5] Chiang S, Samore W, Zhang L, Sung YS, Turashvili G, Murali R, Soslow RA, Hensley ML, Swanson D, Dickson BC, Stewart CJR, Oliva E, Antonescu CR: PGR Gene Fusions Identify a Molecular Subset of Uterine Epithelioid Leiomyosarcoma With Rhabdoid Features. Am J Surg Pathol 2019, 43:810-8.
[6] Oliva E: Practical issues in uterine pathology from banal to bewildering: the remarkable spectrum of smooth muscle neoplasia. Mod Pathol 2016, 29 Suppl 1:S104-20.
[7] Croce S, Ribeiro A, Brulard C, Noel JC, Amant F, Stoeckle E, Devouassoux-Shisheborah M, Floquet A, Arnould L, Guyon F, Mishellany F, Garbay D, Cuppens T, Zikan M, Leroux A, Frouin E, Duvillard P, Terrier P, Farre I, Valo I, MacGrogan GM, Chibon F: Uterine smooth muscle tumor analysis by comparative genomic hybridization: a useful diagnostic tool in challenging lesions. Mod Pathol 2015, 28:1001-10.
[8] Croce S, Ducoulombier A, Ribeiro A, Lesluyes T, Noel JC, Amant F, Guillou L, Stoeckle E, Devouassoux-Shisheboran M, Penel N, Floquet A, Arnould L, Guyon F, Mishellany F, Chakiba C, Cuppens T, Zikan M, Leroux A, Frouin E, Farre I, Genestie C, Valo I, MacGrogan G, Chibon F: Genome profiling is an efficient tool to avoid the STUMP classification of uterine smooth muscle lesions: a comprehensive array-genomic hybridization analysis of 77 tumors. Mod Pathol 2018.
[9] Lagarde P, Perot G, Kauffmann A, Brulard C, Dapremont V, Hostein I, Neuville A, Wozniak A, Sciot R, Schoffski P, Aurias A, Coindre JM, Debiec-Rychter M, Chibon F: Mitotic checkpoints and chromosome instability are strong predictors of clinical outcome in gastrointestinal stromal tumors. Clin Cancer Res 2012, 18:826-38.
[10] Croce S, Lesluyes T, Valle C, M'Hamdi L, Thebault N, Perot G, Stoeckle E, Noel JC, Fontanges Q, Devouassoux-Shisheboran M, Querleu D, Guyon F, Floquet A, Chakiba C, Mayeur L, Rebier F, MacGrogan GM, Soubeyran I, Le Guellec S, Chibon F: The Nanocind Signature Is an Independent Prognosticator of Recurrence and Death in Uterine Leiomyosarcomas. Clin Cancer Res 2019.

3.4 L'ANALYSE DU PROFIL GENOMIQUE PAR CGH-ARRAY COUPLEE A L'ETUDE MUTATIOINNEL DES LEIOMYOMES A NOYAUX BIZARRES PROPOSE LES LEIOMYOMES A NOYAUX BIZARRES COMME GROUPE GENOMIQUE A PART

Le contexte. Le LM-BN représente une variante rare de LM qui, du fait de la présence de noyaux monstrueux « faussement atypiques » et surtout de noyaux karryorectiques pose le problème du diagnostic différentiel avec les LMS. Confrontée avec ce diagnostic surtout dans le contexte des relectures et avis je me suis investie dans l'étude de cette entité en faisant le sujet de publication pendant mon séjour au Massachussetts General Hospital sous la direction de Esther Oliva (ref de ton article). Si cliniquement le LM-BN correspond à une tumeur bénigne, l'analyse du profil génomique laisse des doutes quant à sa bénignité. J'ai commencé les premières analyses CGH sur ces tumeurs en 2014, pour effectuer le travail en 2018 dirigeant le mémoire de Quitterie Fontanges, interne de médecine de l'université Erasme à Bruxelles qui était venue comme « fellow » dans le département de Biopathologie de l'instit Bergonié en 2018. J'ai coordonné le travail de relecture, analyse morphologique et immunohistochimique, interprétation CGH, intégration des donnés mutationnelles ayant abouti à une publication (ref). La difficulté de ce travail a été pour moi l'intégration des données moléculaires « inquiétantes » avec la clinique bénigne de cette entité : comment surpasser l'apparente contradiction de ces données par rapport à notre hypothèse selon laquelle le remaniement du génome corrèle avec le pronostic. En d'autres termes, les données de ce travail risquait de mettre en discussion nos précédents résultats [74, 169].

Méthodes et Résultats. Nous avons étudié 69 LM-BN de 68 patientes. Pour les 44 patientes avec suivi clinique disponible il n'y a pas eu de récidive, confirmant une fois de plus l'évolution bénigne. Le Genomic Index moyen était de 18,17 (GI médian 10,6, de 1 à 77) statistiquement plus bas que le GI moyen des LMS (GI moyen 51.8, p=1,5 $x10^{-9}$). Les événements génomiques récurrents étaient : 1) perte de 1q incluant le gène *FH* dans 42% (26/62) de la série ; 2) la perte de 17p avec *TP53* dans 29% (18/62) et 3) la perte de 13q incluant *RB1* dans 43% (27/62), homozygote dans 41% (11/27) et hétérozygote dans 59% (16/27). Vingt-deux pourcent de la série (14/62) comportait contemporainement la délétion de *TP53* et *RB1*.

Nous avons identifié trois types distincts de LM-BN avec caractéristiques cliniques, morphologiques, immunohistochimiques et moléculaires différentes : le LM-BN *FH*-déficient et le LM-BN associé aux altérations de *TP53* et un groupe sans altérations des gènes *FH et TP53*. Le LM-BN *FH*-déficient intéresse des femmes plus jeunes (environ 10 ans plus jeunes par rapport au groupe *TP53* altéré), des tumeurs de plus grande taille, montrant des caractéristiques morphologiques associées aux LM *FH*-déficients, perte immunohistochimique de FH et un profil génomique plus simple. Le LM-BN associé aux altérations de *TP53* intéresse des patientes 10 ans plus âgées, le LM a une petite taille, une densité de BN forte (aspect morphologiquement inquiétant), des altérations de *TP53* et un GI plus élevé. C'est ce groupe de LM-BN qui nous pose plus de problèmes diagnostiques aussi bien en morphologie qu' en CGH. Quid du GI au seuil de 10 ? est-il toujours d'actualité ? Dans ce contexte le GI au seuil de 10 n'est pas diagnostique. Les résultats de ce papier nous amènent à deux conclusions. Tout d'abord les informations génomiques doivent être intégrées au contexte clinique, hormonal de l'hôte et à l'histologie de la tumeur analysée. Deuxièmement les LM-BN représentent une entité à part intermédiaire entre le LM et le LMS et qui, pour des raisons encore inconnues n'évoluent pas.

New insights in uterine bizarre-nuclei leiomyoma: a distinct entity genomically different from leiomyoma and leiomyosarcoma of usual type

Quitterie Fontanges[1,2], Tom Lesluyes[3], *Laizet Y[4], Velasco V[5],* Meléndez B[1], D'Haene N[1], Oliva E[6], Young RH[6], Laetitia Mayeur[5], Flora Rebier[5], Claire Larmonier[5], Mojgan Devouassoux-Shisheboran[7], Laurent Arnould[8], Isabelle Soubeyran[5], Camille Chakiba[9], Anne Floquet[9], Guillaume Babin[10], Frédéric Guyon[10], Eliane Merry[12], Sophie Le Guellec[12], Jean-Christophe Noël[1], Sabrina Croce[5,11]* and Frédéric Chibon[3,12]*

*These authors contributed equally to this work

1. Department of Pathology, Gynecopathology and Senology Clinic, Erasme University Hospital, Brussels, Belgium
2. Department of Pathology, Charleroi Hospital, Belgin Department of Biopathology;
3. Oncosarc, INSERM UMR1037, Cancer Research Center, Toulouse, France
4. Department of Bioinformatics, Institut Bergonié, Comprehensive Cancer Center, Bordeaux, France.
5. Department of Biopathology, Institut Bergonié, Comprehensive Cancer Center, Bordeaux, France
6. James Homer Wright Pathology Laboratories, Massachusetts General Hospital, Harvard Medical School, Boston, MA
7. Department of Pathology, CHU Lyon Sud, Pierrebenite, France
8. Department of Pathology, JF Leclerc Center, Comprehensive Cancer Center, F-Dijon, France
9. Department of Oncology, Institut Bergonié, Comprehensive Cancer Center, Bordeaux, France
10. Department of Surgery, Institut Bergonié, Comprehensive Cancer Center, Bordeaux, France
11. INSERM U1218, Bordeaux
12. Department of Pathology, Institut Claudius Regaud, IUCT-Oncopole, Toulouse France

*Correspondence to: Dr Sabrina Croce, Dpt of Biopathology, Institut Bergonié, 229 cours de l'Argonne, 33000, Bordeaux, +33524071898 (s.croce@bordeaux.unicancer.fr)

Abstract

Bizarre nuclei leiomyoma is a rare variant of uterine leiomyoma showing worrisome morphologic features such as hyperchromatic, multilobulated and karyorrhectic nuclei, which make the differential diagnosis with leiomyosarcoma (LMS) difficult. Transformation to malignancy is exceptional, outcome is usually favorable and the entity is considered benign. Here we provide a clinical, morphological, immunohistochemical, molecular and genomic overview (by array-CGH and NGS analysis) of a series of 69 bizarre nuclei leiomyomas from 68 patients. Among 44/68 patients with clinical follow-up, all are alive without evidence of disease (from 1.2 months to 150 months, mean 38 months). The mean genomic index (GI) value was 18.17 (median 10.6; from 1 to 77), which is significantly lower than that of LMS (mean GI 51.8, $p<0.001$).

Among the 62 interpretable CGH, we identified three subgroups of bizarre nuclei (BN) leiomyoma, including two with distinct clinical, morphologic, immunohistochemical and genomic features: a *FH*-deficient group (40%, 25/62), a *TP53*-deleted group (29%,18/62) and a group lacking *FH* and *TP53* deletions (31%,19/62). The FH-deficient group was associated with younger age at diagnosis, larger tumor size, lower GI, lower BN density and edema. The *TP53*-deleted group was associated with older age, smaller tumor size, higher GI and BN density. The third group did not harbor any genomic events on *FH* or *TP53* genes and was no associated with specific clinico-pathologic features.

These results suggest that BN leiomyoma is an entity distinct from common leiomyomas and LMS and that genomic data (number of alterations and complexity by GI assessment) have a different value and meaning according to the context (age, hormonal status and histologic type). This highlights the importance of combining morphologic, immunohistochemical and clinical data with genomic analysis.

Introduction

Bizarre nuclei leiomyoma (LM-BN) is a rare variant of leiomyoma, and is defined as the presence of cells having bizarrely shaped, hyperchromatic, multilobulated nuclei with nuclear pseudo-inclusions intermixed with otherwise classical spindled smooth muscle cells arranged in a multifocal-to-diffuse distribution in a background of a typical leiomyoma tumor[1, 2 3]. Mitotic activity is low, but karyorrhectic nuclei are common and not infrequently counted as atypical mitoses. Likewise, areas of infarct type necrosis can easily be mistaken for tumor cell necrosis.

In this context, the main differential diagnosis of LM-BN is leiomyosarcoma (LMS), which challenges the purpose and relevance of the Stanford criteria[4]. Despite worrisome morphological features, outcome is usually favorable. In fact, in the available series in the literature encompassing 203 cases, no death or metastasis was observed and recurrences were noted in only 3 % of cases[1, 5-10]. Surrogate immunohistochemical markers have been evaluated to help in diagnosing these challenging lesions. However, p16, p53 and Ki67 have proved to be of limited interest, since the expression of those cell cycle regulatory proteins is heterogeneous and exhibits overlapping with LMS[10, 11].

Based on the observation that genomic complexity correlated with the risk of recurrence in a series of uterine smooth muscle tumors with uncertain malignant potential (STUMP)[12], a finding further validated in a larger series of uterine smooth muscle tumors encompassing LM and LMS[13], the goal of this study is to provide a clinical, morphological, immunohistochemical, molecular and genomic overview of the tumors encompassed within the definition of LM-BN. This should provide better understanding of it, so that it may be compared with LM and LMS, leading to a diagnostic algorithm for routine practice.

Material and Method

Tumor samples and Morphological analysis

Sixty-nine uterine LM-BN formalin-fixed and paraffin-embedded (FFPE) from 68 patients were collected through the French sarcoma network GYN RRePS (Institut Bergonié in Bordeaux, JF Leclerc Center in Dijon, Hôpitaux Universitaires Lyon Sud, IUCT Oncopole Toulouse), from Hôpital Universitaire Erasme in Brussels, Belgium, and from the consultation database of two authors at Massachusetts General Hospital (E.O and R.H.Y). The date of diagnosis was available for 63 patients, ranging from 1997 to 2016. One to 6 slides were available for each patient. All cases were reviewed centrally by two of the authors (Q.F and S.C), and the diagnosis of LM-BN was confirmed according to the Stanford criteria and the 2014 WHO definition (1). Clinical data included patient age, type of surgery and clinical outcome. Follow-up data was obtained by contacting the general practitioner or the patient's gynecologist. Gross pathologic features assessed included tumor size, number of fibroids, location of the tumor and extension beyond uterus. Microscopic features, and in particular the semi-quantitative approach to determine density and distribution of BN, were evaluated as previously described[1].

Immunohistochemistry

Four markers were selected for immunohistochemical analysis and the following antibodies were used: FH (Polyclonal, GeneTex; 1:100), p53 (Clone DO-7; Dako; 1:50). Immunohistochemical analyses were performed on 4-µm-thick whole sections from representative FFPE blocks using the automate Benchmark®ULTRA (ROCHE -VENTANA). All stainings were reviewed by two of the authors (Q.F and S.C) independently and blindly[14 15].

Binary interpretation of FH staining was performed, with complete absence of cytoplasmic staining interpreted as lost, and weak-to-strong cytoplasmic staining interpreted as retained. Adjacent myometrium and/or endothelial cells were used as internal control. p53 staining was interpreted as abnormal (mutation-type) if 1) strong nuclear staining in ≥80 % of tumor cells; 2) complete absence of nuclear staining in tumor cells with a positive internal control; or 3) cytoplasmic expression in ≥80% of tumor cells with variable nuclear staining. p53 staining was interpreted as normal, wild-type when the aforementioned criteria were absent [15]. We further specified abnormal expression as being limited to BN or as diffuse. Adjacent myometrium, endothelial cells and/or inflammatory cells were used as internal control.

DNA extraction

Genomic DNA was extracted from formalin-fixed and paraffin-embedded tissues according to the protocol for DNA isolation from formalin-fixed and paraffin-embedded tissues (http://www.chem-agilent.com/pdf/G441090020v3_1_CGH_ULS_Protocol. pdf) (Agilent Technologies, Santa Clara, CA, USA). A cut-off of 50% of cellularity in tumor samples was set for the analysis.

Array-Comparative Genomic Hybridization Analysis

DNA was hybridized onto 8 x 60 K whole-genome arrays (SurePrint G3 Human CGH 8x60k bundle Agilent G5923A) according to the manufacturer's protocol. Microarray slides were scanned using a DNA Microarray Scanner, images were analyzed by an Agilent DNA Microarray Scanner USK0057446 using Agilent® Cytogenomic software 4.0.3.12. The ADM-2 algorithm of the Comparative Genomic Hybridization Analytics v4.0.76 software (Agilent Technologies) was used to identify the DNA copy number anomalies at the probe level. GI was calculated for each profile as follows: $GI = A^2/C$, where A is the total number of alterations (segmental gains and losses) and C is the number of involved chromosomes[12, 13, 16]. DLRS value had to range between 0 and 0.5 as a prerequisite for GI calculation. In the cases where GI was not interpretable, we analyzed CGH array profiles one by one and listed the segmental alterations that were still easily recognizable. These cases were referred to as partially interpretable.

Next-Generation Sequencing

NGS was performed as formerly described[17] using previously extracted DNA. Briefly, 10 ng of DNA (measured using the Qubit1dsDNA HS assay kit) were amplified (Ion AmpliSeq Library Kit v2.0) for library construction using a custom-made panel including 78 hotspot mutations in 16 genes of interest in gynecological cancers (supplementary data, Table 1). An amplicon library was thus generated and then digested, barcoded, and amplified using the Ion Ampliseq™Library kit 2.0 and Ion Xpress™barcode adapters kit (Life Technologies) according to the manufacturer's instructions. Libraries were multiplexed, submitted to emulsion PCR on the Ion Chef System (Thermo Fisher), and sequenced using an Ion Torrent Personal Genome Machine (Thermo Fisher). The sequences were aligned with the hg19 reference genome, and variant calling was performed using the Torrent Mapping Alignment Program (Torrent Suite v.5.6, Thermo Fisher). The following quality metrics were considered for each sequenced sample: total mapped reads (≥100,000) and average base coverage depth (≥250). Variants were filtered out based on the following criteria: (1) fewer than 100 reads; (2) a location outside of the exonic or splice regions; (3) synonymous/silent variant; (4) variants present in the population with a minor allele frequency (MAF) greater than 0.1 %; a mutant allele coverage of fewer than 30 reads; (6) a mutant allele frequency <5% (unless involving mutant allele with a known clinical impact). Samples

displaying an unusually elevated amount of variants were repeated to rule out sequencing artifacts. All the remaining variants were visualized using the Integrative Genomic Viewer (IGV; Broad Institute) and were manually reviewed in COSMIC (Catalogue of Somatic Mutation in Cancer) and IARC (International Agency for Research on Cancer) databases.

Statistical Analysis

Statistical analysis was performed with the BiostaTGV website (marne.u707.jussieu.fr/biostatgv/). Fisher's test and Wilcoxon-Mann-Whitney's test were performed. To avoid a false discovery effect when conducting multiple statistical tests, p values were adjusted according to the Benjamini-Hochberg procedure. For quantitative data following a normal distribution (Shapiro test < 0.05), Student's t-test was performed.

Results

Clinico-morphologic data

Table 1 summarizes the clinico-pathologic and genomic data.

A total of 69 cases of gynecological LM-BN corresponding to 68 patients were analyzed. Patient age at presentation was available in 63 cases (91%) and ranged from 23 to 82 years old (mean age 46 y). Type of surgical procedure was known for 56/69 cases, hysterectomy was performed in 38 cases (68%), and myomectomy in 18 cases (32%). Most of the tumors were located in the uterine corpus (66/69), one was in the vaginal septum, one in the broad ligament, and one was referred to as pelvic and described as having no direct link with the uterus. One lesion extended beyond the uterus and was described as adhesive to the sigmoid. The number of uterine fibroids was available in 26 cases and ranged from 1 to 20 (mean 2.5) with 11 cases (11/26, 42.3%) harboring multiple leiomyomas. Size of the LM-BN was available in 35 cases and ranged from 10 mm to 150 mm (mean 73 mm).

Clinical data were available for 63 of 68 patients and clinical follow-up was retrieved for 44 of them (from 1.2 months to 150 months, mean 38 months). All patients were alive without evidence of disease (NED). One patient had 2 myomectomies (cases 26 and 26 bis): the first in 2009 and the second in 2012. The two tumors showed different molecular and genomic profiles and the second one was diagnosed as a new primary lesion. We consider them as two different tumors and not as a recurrence.

Morphologic data

In 47/69 samples the tumor borders were evaluable and were well delimited in all cases.

No tumor necrosis was detected and in 19/69 (27,5%) ischemic necrosis was present. Edematous changes and inflammatory infiltrate were detected in 58% (40/69) and in 34.8% (24/69) respectively. The mean mitotic count was 1.5 mitoses/10HPF (high-power field) varying from 0 to 8. Karyorrhectic nuclei were present in 55% of the cases (38/69). Orangeophilic prominent nucleoli with perinucleolar clear halo were detected in 74% of the tumors (51/69), nuclear pseudo-inclusions in 64% (44/69), cytoplasmic rhabdoid inclusions in 59% (41/69) and multinucleated cells in 58% (40/69).

BN density was low in 52.2% (36/69), intermediate in 33.3% (23/69) and high in 14.5% (10/69). In addition to these morphologic criteria, we classified the tumors according to a three-tier picture-based classification (Figure 1). Type 1 tumor were poorly fasciculate at low magnification, having a sheet-like growth pattern, striking staghorn vessels sometimes with a thick wall, areas of pseudoalveolar edema and hemorrhage, with inconspicuous scattered BN. In type 2 tumors, foci of densely packed BN were observed right from low magnification and the interspersed, non-BN tumor cells harbored a fascicular growth pattern. Type 3 tumors were almost entirely composed of densely packed BN, with interspersed cells harboring hyperchromatic elongated nuclei reminiscent of a leiomyoblastoma-like appearance. Thus, 38% (26/69) were classified as type I, 32% (22/69) as type II and 30% (21/69) as type III (Fig 1).

Genomic data

Array-comparative genomic analysis

Among the 69 samples tested, 7 were not interpretable because of poor DNA quality, 7 were partially interpretable (GI was not assessable but it was possible to detect some of the obvious structural alterations) and 55 were interpretable. The mean GI value was 18.1, median 10.6 (from 1 to 77) (Table 1), significantly lower than the mean GI of a series of uLMS which we previously reported [13] (mean GI 51.8, *p<0,001*).

Unlike uLMS, BN-LM genomic profiles did not show amplifications and gains were less frequent than deletions. The most frequent genomic events were the following (figure 2):

-1q loss including *FH* gene (1q42-43) in 42% of the series (26/62) with homozygous deletion in half of the lost cases (13/26).

-17p loss including *TP53* gene in 29% (18/62), without any homozygous deletion.

-13q loss including *RB1* gene in 43% (27/62), with homozygous deletion in 41% (11/27).

By incorporating the morphologic features and array-CGH genomic profiles, three main groups of BN-LM emerged: 1) a group associated with *FH* inactivation (25/62 cases; Figure 2A), 2) a group associated with *TP53* alterations (18/62 cases; Figure 2B) and 3) a group without genomic events on *FH* or *TP53* genes (19/62 cases; Figure 2C).

The loss of *TP53* and *FH* was mutually exclusive except in one tumor (case 5) which harbored both *TP53* and *FH* loss. Because the *TP53* deletion was precise specifically involving the *TP53* gene locus and the FH deletion was part of a large chromosome loss, we included the case in the group associated with *TP53* alterations rather than in the *FH* deleted group. Twenty-two percent of the cases (14/62, all in group 2; figure 2B) harbored concomitant *TP53* and *RB1* deletion (5 heterozygous and 9 homozygous deletion).

RB1 deletion was most likely to be found in association with *TP53* deletion (respectively 77.8% (14/18) in association with -*TP53* losses and 29% (13/44) with intact *TP53* (p=0.0007)). Moreover, *RB1* homozygous deletion was significantly associated with heterozygous loss of *TP53* (p<0.0001).

In 9.7% (6/62) of the tumors, *FH* deletion was associated with *RB1* deletion (5 heterozygous and one homozygous). All 6 cases had a *FH* heterozygous status. Less frequent genomic events included the 7q and 10q deletions involving the *CUX1* and *PTEN* genes, respectively. Only one tumor harbored a heterologous *COL4A5* et *COL4A6* deletion (ch Xq).

P53 mutational status

TP53 mutational status was available for 58 of the 69 samples (the DNA quality or quantity was insufficient in 11 cases). Sixty-four percent of the series (37/58) harbored no variant for *TP53* or for the 16 other genes of our NGS panel. Thirty-six percent of the tumors (21/58) harbored one or more *TP53* variants (14 missense mutations, 1 non-sense, 7 frameshift deletion, 1 non-frameshift deletion and 2 variants with unknown effect) thus distributed: 7/21 in the *FH* deleted group, 6 in the *TP53* deleted group, 7 in the group without *TP53 or FH* alterations and 1 tumor with CGH not interpretable (case 47). Four samples showed multiple *TP53* mutations for a total of 25 *TP53* variants. The allelic frequency of mutations varied from 9.8 to 100% (cf Supplementary data. Table 2). Most of the *TP53* mutations (21/25, 84%) were located in the DNA binding domain of the protein (exons 4 to 8).

Immunohistochemical results

FH immunohistochemical staining was performed on 66 out of 69 samples and was contributive in 64/66 cases. Thirty-seven percent of the samples (24/64) showed loss of cytoplasmic expression. At IHC level all the homozygous deleted tumors showed a complete absence of FH protein expression. Among the *FH* heterozygous cases, 7/12 were FH-negative in IHC and 5/12 were FH-positive.

P53 immunostaining was performed on 48 available tumors and was contributive in all but 2 cases. Twenty-nine out of 46 tumors (63%) showed a “wild-type” staining and 17 (37%) an aberrant expression: 7/17 a strong and diffuse expression, 9/17 a strong expression limited to the BN and wild type in the interspersed normal cell and 1/17 a complete absence of staining (cf Figure 3). Among the 7 tumors

with diffuse p53 overexpression, 4 tumors harbored a *TP53* mutation, one a *TP53* deletion on one allele and a mutation on the other, 1 was not informative for CGH or for NGS, and 1 was discordant because of the absence of *TP53* deletion or mutation (case 46) (Figure 4). The tumor showing a complete absence of p53 expression harbored a *TP53* deletion (case 60). Among 9 tumors with p53 overexpression limited to BN, 3 harbored a *TP53* deletion, 3 had *TP53* mutations, one both, one case was not interpretable at CGH and one was discordant (case 25). Among the 15 tumors with aberrant p53 expression, 9 harbored a *TP53* mutation (cf Figure 3). Four out of the 6 discordant tumors showed aberrant p53 staining limited to BN. Interestingly, the tumors showing p53 overexpression limited to BN harbored a mean allelic frequency of *TP53* mutation that was significantly lower (32%) than the tumors showing a diffuse overexpression of p53 protein (64.8%) (*p=0.038*) (cf Figure 3). This finding suggested that "discrepant" cases might, at least partly, be explained by a technical limitation linked to a low amount of *TP53* mutated cells.

Genomic mutational and immunohistochemical data combined with morphology

By combining the array-CGH genomic profiles together with morphologic features, *TP53* mutational status and FH and p53 expression slightly redefined and strengthened the three groups of BN-LM that emerged from genomic analysis: 1) a group associated with *FH* inactivation (cf Figure 2A and 4), 2) a group associated with *TP53* alterations (mutations and/or deletions) (cf Figure 2B and 4), and 3) a group without genomic events on *FH* or *TP53* genes (cf Figure 2C and 4)). These two events (*FH* deletion and *TP53* deletion) are mutually exclusive in our series with the exception of one case (case 5) (Figure 4). Groups 1 and 2 show distinct morphologic and genomic characteristics (cf Figure 4).

The *FH* inactivated subgroup of BN-LM (group 1: 25/62 cases) compared to the *TP53* deleted subgroup of BN-LM showed: 1) younger age at diagnosis (mean age of *FH* deleted group 44.64 y versus 52.9 in *TP53* deleted group, *p=0.04*), 2) larger tumor size (mean size of *FH* deleted group 92.7 mm versus 45.5 mm in *TP53* deleted group, *p=0.04*), 3) more frequent type 1 morphology (*FH* versus *TP53* deletion group *p=0.045*), 4) more frequent alveolar edema (*FH* deleted group versus *TP53* deleted group, *p=0.04*), 5) low BN density (*p=0.04*) and 6) low GI compared to *TP53* deleted group (mean GI of *FH* deleted group: 13.12 versus 26.03 in *TP53* deleted group, *p=0.04*), (cf Figures 4 and 5). The *FH* homozygous deleted tumors were not associated with *TP53* or *RB1* deletions but harbored 7p deletions (without identified target gene) more frequently than the rest of the series (7/13, 53.8% versus 5/36, 13.8%; p=0.008).

The differences in genomic profile complexity were also observed when comparing the group tumors with *FH heterozygous deletion* with FH retained expression (mean GI 33.2) versus tumors with *FH heterozygous deletion* with loss of cytoplasmic expression (mean GI 5.5; p=0.03). (cf Figure 4).

Two tumors (cases 26 bis and 31) showed a loss of FH expression without deletion on 1q 42.3 locus. Unfortunately, the *FH* gene was not included in the NGS GYN panel and the mutational status is unknown.

Six tumors with *FH* homozygous deletion harbored a *TP53* mutation (detected by NGS analysis). Interestingly, the mean allelic frequency of *TP53* mutation was 35% in the group with *FH* homozygous deletion and was higher (65.2%) (*p=0.018*) in the group with *FH* heterozygous deletion and *FH* intact tumors, suggesting the presence of a subclonal *TP53* mutated cell population in the *FH* homozygous group (cf Figure 3).

The *TP53* inactivated subgroup of BN-LM (Group 2: 18/62 cases)

Eighteen out of 62 array-CGH contributive cases harbored a *TP53* heterozygous deletion and 15 of 39 cases without *TP53* deletion had a *TP53* mutation for a total of 33 LM-BN with *TP53* inactivation (cf Figure 2B). No *TP53* homozygous deletion was recorded in this series.

The *TP53* deleted group showed these features:

1) Older age at diagnosis compared to the *FH* deleted group (mean age 52.9 y versus 44.6 y, p=0.04) as well to the remainder of the series (*p=0.02*) (mean age 52.9 y versus 44.1 y),
2) Smaller tumor size compared to the *FH* deficient group (mean size 45.5 mm versus 92.7 mm, *p=0.04*) but also to the remainder of the series (mean size 54.7 mm *p=0.02*),
3) Higher BN density compared to the *FH* deleted group (*p=0.04*) and to the remainder of the series (*p=0.02*);
4) More frequent type 2 and 3 morphology compared to *FH* deleted tumors (*p=0.04*) and to the remainder of the series (*p=0.02*); *
5) Higher GI compared to the *FH* deleted group (p=0.04), reflecting their higher genomic complexity.

Interestingly, *RB1* homozygous deletions were clustered within *TP53* deleted tumors (p<0.0001).

By combining array-CGH and NGS mutational data, 6 tumors were *TP53* nullizigous (one mutation on one allele and one deletion on the second). Among these 6, 3 samples (8,22,32) harbored the *TP53* mutation at high allelic frequency (>80%). These 3 cases showed a high BN density (type 3). Follow-up was retrieved for 5 out of 6 patients and all were alive without evidence of disease (mean 36.1 months, from 22.3 to 47.6 months). p53 IHC and *TP53* mutational status were available for 39 tumors (cf supplementary data Table 2). Figure 4 summarizes the differences between the *FH*-deficient and *TP53* deficient BN-LM subgroups. Lastly 19 tumors did not harbor any *TP53* or *FH* deletions. Their mean GI was 17.8 (median 13.3, from 1 to 57.8). Morphologically 53% (10/19) of the tumors in the third group showed a low BN density (type 1), 32% (6/19) an intermediate density (type 2) and 15% (3/19) a high density (type 3) (cf Figure 1 and 4).

Discussion

The close link between genomic complexity and clinical evolution in uterine smooth muscle tumors has been demonstrated in large series of conventional (spindle cells) LM, STUMP and LMS, and their genomic complexity has been assessed by using the GI [12, 13] . What emerges from the present analysis is the heterogeneous landscape of BN-LM and the presence of three groups. Two of them are clinically, morphologically and genomically distinct, and the third one results from the absence of the alterations defining the first two. The presence of two distinct types of BN-LM has been described before at morphologic and IHC and mutational level[6, 18]. Here we combine the analysis of genomic profiles with clinical morphological and immunohistochemical data in a large series.

The first group harbors *FH* inactivation (40% of the BN-LM), shows a lower degree of genomic complexity as mirrored by a lower GI when compared to the *TP53* group, and has specific clinical (younger age at diagnosis), macroscopic (higher size of LM) and morphologic features (association with the morphologic type 1, lower BN density and diffuse edema). The second group is associated with *TP53* alterations (29% of the BN-LM), affects older patients (10 years older than group 1), with smaller tumor size, is morphologically more frequently associated with types 2 and 3, and has higher BN density and higher GI compared to group 1. Interestingly this group clustered the *RB1* homologous deletions ($p<0.0001$). The third group is defined by the absence of *FH* and *TP53* alterations (31% of the BN-LM) and shows an intermediate complexity of profiles (mean GI 17.8, median 13.3, from 1 to 57.8). No other recurrent and specific genomic events were detected in this group.

At the biologic and metabolic level, loss of FH activity triggers the accumulation of fumarate in cells, which in turn induces hypoxia inducible factor stabilization, causes posttranslational modifications by succination (as highlighted by 2SC positivity in immunohistochemistry) and generates oncometabolites which activate nuclear factors that potentially promote cell growth and proliferation[19].

Based on the observation that *FH* deleted BN-LM, especially those with *FH* homozygous deletion, have simple genomic profiles, we hypothesize that this metabolic remodeling is a very efficient mechanism to promote the genesis of LM. On the other hand, the *TP53* deleted group harbors more complex genomic profiles and more frequent *RB1* alterations, probably as consequence of the lifting of the action of the *TP53* guardian of the genome. Unfortunately, since we do not have a cellular model, we cannot support this hypothesis experimentally.

In daily practice, group 2 (*TP53* deleted) of BN-LM poses the major diagnostic problem in the differential diagnosis with LMS because of the higher concentration of BN. According to the GI, only about half of the BN-LM series (27/55 interpretable samples) had a GI<10 in the absence of recurrence or clinical events, which raises doubts about the clinical pertinence of GI assessment in BN-LM. Similar observations were reported in a limited series of BN-LM by Liegl-Atzwanger et al,[20] who classified BN-LM in an intermediate group distinct from LM but genetically close to LMS. These findings not surprisingly are not in contradiction with our previous results[12, 13] and lead us to following two conclusions. First, the genomic data (number of alterations and complexity) have a different value and meaning according to the contexts and characteristics of the host (*e.g.* age and sex of patient, hormonal context) and type of tumor. In fact, a degree of variability in the genomic complexity probably does not have the same value in a young patient under hormone impregnation as in a post-menopausal woman. Not surprisingly, patients with BN-LM are 10 years younger than those with LMS. An example among soft tissue sarcomas is synovialosarcoma, a sarcoma with a “simplex genomic” associated with X-18

translocation, where the degree of genomic complexity (GI>1) has a different value and prognosis according to the age of the patient[21, 22]. Moreover, the LMS diagnostic criteria for the trunk and peritoneum include sex and hormonal expression, and the mitotic cut off varies according to the location of the tumor (deep or superficial, proximal to large vessel or not) and to hormonal expression[23].

The second conclusion is that BN-LM is a separate entity, distinct in many aspects from usual type LM and from LMS, and that the GI at the cut off of 10 is not applicable. Clinically the patient's age at diagnosis significantly differs from LMS (mean age 46 y in our series, and 45 and 46 y in two other series[1, 20] respectively). Morphologically, BN-LM differs from usual LMS in the presence of mononucleated or multinucleated giant cells with a paradoxical atypia limited to giant cells with low mitotic activity rarely observed in the majority of LMS. A hallmark of BN-LM is the presence of ischemic changes (fibrinoid necrosis of vessels, eosinophilic and lymphocytic infiltrate often associated with obliteration of vessel lumina) supported by genomic alterations in the hypoxia pathways driven by *FH* inactivation via *HIF1*α and *NRF2* accumulation[24]. Interestingly, the limited number of BN-LM analyzed by array-CGH have shown a genomic instability and some molecular events situated on the continuum between usual LM and LMS[20].

Furthermore, *FH* inactivation was detected in 40% of BN-LM in our series, which is similar to previous reports (from 33.3[18] to 51%[25,5]), versus only 4%[18] and 25%[20] in LMS. Another factor that distinguishes BN-LM from LM and LMS is the frequency of *RB1* deletion, which was 42% in our series (other published data varying from 16.6%[5] to 54%[20]). This is different from the frequency of *RB1* deletion in LMS (79%[20], 84%[13], 94%[26]) as well that of *TP53* deletions, which were 29% in our series versus 41%[13] to 95%[27] of deletions in LMS. *TP53* mutations were 36% in our series, compared to a range varying from 12[7] to 28%[5] in the literature. In our series we did not detect any *TP53* homozygous deletion but we did previously report a case of BN-LM with *TP53* homozygous deletion[13]. While these data point to the premalignant nature of BN-LM and despite the existence of exceedingly rare cases of BN-LM adjacent to an LMS,[28, 29] the clinical outcome suggests the benign nature of BN-LM and that it is a separate entity.

In routine practice, we perform array-CGH on BN-LM. Genomic profile analysis is informative about *FH, TP53* deletions and the genomic complexity of these lesions. In practical terms, we feel comfortable with the diagnosis of BN-LM if GI is <10. If it is>10, we do not change the diagnosis but we combine genomic data with morphologic and clinical observations and analyze the slides more carefully in order to avoid missing an LMS.

A major caveat of our analysis is the absence of allelic status data. In our experience with the Affymetrix CGH platform, the BN-LM we examined are polyploid (data not published). If aneuploidy status is related to cancer progression, it is also true that precancerous lesions are more often polyploid and that the subsequent cancerous lesions become diploid, as described in colonic polyps and adenocarcinomas[30]. These observations suggest the hypothesis that BN-LM is a precancerous lesion which, for reasons and mechanisms that remain unknown, is stopped in its progression. Progression might be arrested because the polyploid status does not give a selective advantage to the cell which controls apoptosis and senescence. Further studies with deeper, more extensive investigation including genomic, expression and methylome analyses and a cellular model are needed in order to solve the BN-LM biologic enigma.

In conclusion, this clinico-morphologic, genomic, immunohistochemical and mutational study on a large series of BN-LM confirms their favorable prognosis. By establishing their heterogeneous genomic

profiles, which are more complex than usual LM but not as complex as the majority of LMS, we have distinguished three main types with genomic, IHC, morphologic and clinical features.

Acknowledgments

We thank Dr Ray Cooke for the medical writing service

Legend

Figure 1. Illustration of three-tier picture-based classification: Type 1 (A1&A2) Type 2 (B1&B2) and Type 3 (C1&C2).

Figure 2. Penetrance plot of 26 cases with homozygous *FH* loss (A) Blue arrows in A highlight chromosome 1 with locus of *FH* (1q43). Penetrance plot of 18 cases with heterozygous loss of *TP53 (*B) Blue rectangle in figure B highlights 13q with *RB1* and red rectangle indicates 17p with *TP53*. Figure C represents penetrance plot in the remaining group without FH or TP53 alterations.

Figure 3. Link between p53 IHC staining pattern and *TP53* allelic frequency: samples with p53 abnormal IHC limited to BN harbor a lower allelic frequency than those with diffuse abnormal p53 IHC. This finding might partly explain the “discordant cases”: p53 abnormal staining limited to BN translates into absence of *TP53* variant due to undetectable subclonal cell population**.**

Figure 4. Synoptic representation CGH-array results with NGS mutations, IHC and morphologic data of 69 samples (A) and of 62 tumors according to the three groups (B).

Table 1. Clinical, morphological, immunohistochemical and genomic findings in LM-BN .

Supplementary data.

Table 1. Catalogue of 78 hotspots tested by NGS in panel of 16 genes.

Figure 1. Distribution of *TP53* mutations on p53 protein of 23/25 mutations with known variant effect, obtained with cBioPortal Mutation Mapper tool.

Table 2. Variants of *TP53* mutations.

Bibliography

[1] Croce S, Young RH, Oliva E: Uterine leiomyomas with bizarre nuclei: a clinicopathologic study of 59 cases. Am J Surg Pathol 2014, 38:1330-9.

[2] PC I: Uterine leiomyoma and leiomyomatosis: IARC Lyon, 2020.

[3] Oliva E CM, Carinelli SG, et al: Leiomyoma. WHO classification of tumours of female reproductive organs. Edited by Kurman RJ CM, Herrington CS, Young RH. IARC Lyon, 2014.

[4] Bell SW, Kempson RL, Hendrickson MR: Problematic uterine smooth muscle neoplasms. A clinicopathologic study of 213 cases. Am J Surg Pathol 1994, 18:535-58.

[5] Bennett JA, Weigelt B, Chiang S, Selenica P, Chen YB, Bialik A, Bi R, Schultheis AM, Lim RS, Ng CKY, Morales-Oyarvide V, Young RH, Reuter VE, Soslow RA, Oliva E: Leiomyoma with bizarre nuclei: a morphological, immunohistochemical and molecular analysis of 31 cases. Mod Pathol 2017.

[6] Ubago JM, Zhang Q, Kim JJ, Kong B, Wei JJ: Two Subtypes of Atypical Leiomyoma: Clinical, Histologic, and Molecular Analysis. Am J Surg Pathol 2016, 40:923-33.

[7] Zhang Q, Ubago J, Li L, Guo H, Liu Y, Qiang W, Kim JJ, Kong B, Wei JJ: Molecular analyses of 6 different types of uterine smooth muscle tumors: Emphasis in atypical leiomyoma. Cancer 2014, 120:3165-77.

[8] Downes KA, Hart WR: Bizarre leiomyomas of the uterus: a comprehensive pathologic study of 24 cases with long-term follow-up. Am J Surg Pathol 1997, 21:1261-70.

[9] Christopherson WM, Williamson EO, Gray LA: Leiomyosarcoma of the uterus. Cancer 1972, 29:1512-7.
[10] Sung CO, Ahn G, Song SY, Choi YL, Bae DS: Atypical leiomyomas of the uterus with long-term follow-up after myomectomy with immunohistochemical analysis for p16INK4A, p53, Ki-67, estrogen receptors, and progesterone receptors. Int J Gynecol Pathol 2009, 28:529-34.
[11] Mills AM, Ly A, Balzer BL, Hendrickson MR, Kempson RL, McKenney JK, Longacre TA: Cell cycle regulatory markers in uterine atypical leiomyoma and leiomyosarcoma: immunohistochemical study of 68 cases with clinical follow-up. Am J Surg Pathol 2013, 37:634-42.
[12] Croce S, Ribeiro A, Brulard C, Noel JC, Amant F, Stoeckle E, Devouassoux-Shisheborah M, Floquet A, Arnould L, Guyon F, Mishellany F, Garbay D, Cuppens T, Zikan M, Leroux A, Frouin E, Duvillard P, Terrier P, Farre I, Valo I, MacGrogan GM, Chibon F: Uterine smooth muscle tumor analysis by comparative genomic hybridization: a useful diagnostic tool in challenging lesions. Mod Pathol 2015, 28:1001-10.
[13] Croce S, Ducoulombier A, Ribeiro A, Lesluyes T, Noel JC, Amant F, Guillou L, Stoeckle E, Devouassoux-Shisheboran M, Penel N, Floquet A, Arnould L, Guyon F, Mishellany F, Chakiba C, Cuppens T, Zikan M, Leroux A, Frouin E, Farre I, Genestie C, Valo I, MacGrogan G, Chibon F: Genome profiling is an efficient tool to avoid the STUMP classification of uterine smooth muscle lesions: a comprehensive array-genomic hybridization analysis of 77 tumors. Mod Pathol 2018.
[14] Oliva E CM, Carinelli SG, et al: Mesenchymal tumours. Smooth muscle tumour of uncertain malignant potential. WHO Classification of Tumours of Female Reproductive Organs. Edited by Kurman RJ CM, Herrington CS, Young RH. 2014. pp. pp 135–47.
[15] Kobel M, Ronnett BM, Singh N, Soslow RA, Gilks CB, McCluggage WG: Interpretation of P53 Immunohistochemistry in Endometrial Carcinomas: Toward Increased Reproducibility. Int J Gynecol Pathol 2019, 38 Suppl 1:S123-S31.
[16] Lagarde P, Perot G, Kauffmann A, Brulard C, Dapremont V, Hostein I, Neuville A, Wozniak A, Sciot R, Schoffski P, Aurias A, Coindre JM, Debiec-Rychter M, Chibon F: Mitotic checkpoints and chromosome instability are strong predictors of clinical outcome in gastrointestinal stromal tumors. Clin Cancer Res 2012, 18:826-38.
[17] D'Haene N, Le Mercier M, De Neve N, Blanchard O, Delaunoy M, El Housni H, Dessars B, Heimann P, Remmelink M, Demetter P, Tejpar S, Salmon I: Clinical Validation of Targeted Next Generation Sequencing for Colon and Lung Cancers. PLoS One 2015, 10:e0138245.
[18] Makinen N, Kampjarvi K, Frizzell N, Butzow R, Vahteristo P: Characterization of MED12, HMGA2, and FH alterations reveals molecular variability in uterine smooth muscle tumors. Mol Cancer 2017, 16:101.
[19] Sajnani K, Islam F, Smith RA, Gopalan V, Laam AK: Genetic alterations in Krebs cycle and its impact on cancer pathogenesis. Biochimie 2017, 135:164-72.
[20] Liegl-Atzwanger B, Heitzer E, Flicker K, Muller S, Ulz P, Saglam O, Tavassoli F, Devouassoux-Shisheboran M, Geigl J, Moinfar F: Exploring chromosomal abnormalities and genetic changes in uterine smooth muscle tumors. Mod Pathol 2016, 29:1262-77.
[21] Lagarde P, Przybyl J, Brulard C, Perot G, Pierron G, Delattre O, Sciot R, Wozniak A, Schoffski P, Terrier P, Neuville A, Coindre JM, Italiano A, Orbach D, Debiec-Rychter M, Chibon F: Chromosome

instability accounts for reverse metastatic outcomes of pediatric and adult synovial sarcomas. J Clin Oncol 2013, 31:608-15.
[22] Orbach D, Mosseri V, Pissaloux D, Pierron G, Brennan B, Ferrari A, Chibon F, Bisogno G, De Salvo GL, Chakiba C, Corradini N, Minard-Colin V, Kelsey A, Ranchere-Vince D: Genomic complexity in pediatric synovial sarcomas (Synobio study): the European pediatric soft tissue sarcoma group (EpSSG) experience. Cancer Med 2018, 7:1384-93.
[23] Miettinen M, Fetsch JF: Evaluation of biological potential of smooth muscle tumours. Histopathology 2006, 48:97-105.
[24] Mehine M, Kaasinen E, Heinonen HR, Makinen N, Kampjarvi K, Sarvilinna N, Aavikko M, Vaharautio A, Pasanen A, Butzow R, Heikinheimo O, Sjoberg J, Pitkanen E, Vahteristo P, Aaltonen LA: Integrated data analysis reveals uterine leiomyoma subtypes with distinct driver pathways and biomarkers. Proc Natl Acad Sci U S A 2016, 113:1315-20.
[25] Zhang Q, Poropatich K, Ubago J, Xie J, Xu X, Frizzell N, Kim J, Kong B, Wei JJ: Fumarate Hydratase Mutations and Alterations in Leiomyoma With Bizarre Nuclei. Int J Gynecol Pathol 2017.
[26] Chudasama P, Mughal SS, Sanders MA, Hubschmann D, Chung I, Deeg KI, Wong SH, Rabe S, Hlevnjak M, Zapatka M, Ernst A, Kleinheinz K, Schlesner M, Sieverling L, Klink B, Schrock E, Hoogenboezem RM, Kasper B, Heilig CE, Egerer G, Wolf S, von Kalle C, Eils R, Stenzinger A, Weichert W, Glimm H, Groschel S, Kopp HG, Omlor G, Lehner B, Bauer S, Schimmack S, Ulrich A, Mechtersheimer G, Rippe K, Brors B, Hutter B, Renner M, Hohenberger P, Scholl C, Frohling S: Integrative genomic and transcriptomic analysis of leiomyosarcoma. Nat Commun 2018, 9:144.
[27] Zhai YL, Nikaido T, Orii A, Horiuchi A, Toki T, Fujii S: Frequent occurrence of loss of heterozygosity among tumor suppressor genes in uterine leiomyosarcoma. Gynecol Oncol 1999, 75:453-9.
[28] Mittal KR, Chen F, Wei JJ, Rijhvani K, Kurvathi R, Streck D, Dermody J, Toruner GA: Molecular and immunohistochemical evidence for the origin of uterine leiomyosarcomas from associated leiomyoma and symplastic leiomyoma-like areas. Mod Pathol 2009, 22:1303-11.
[29] Przybora LA: Leiomyosarcoma in situ of the uterus. Cancer 1961, 14:483-92.
[30] Tomita T: DNA ploidy and proliferating cell nuclear antigen in colonic adenomas and adenocarcinomas. Dig Dis Sci 1995, 40:996-1004.

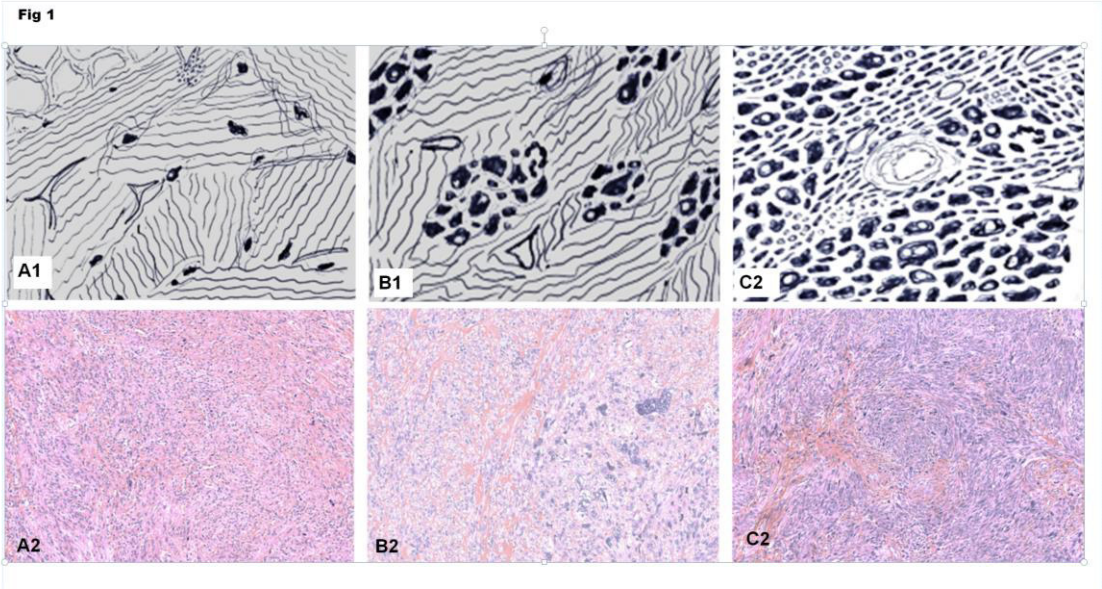

Figure 2

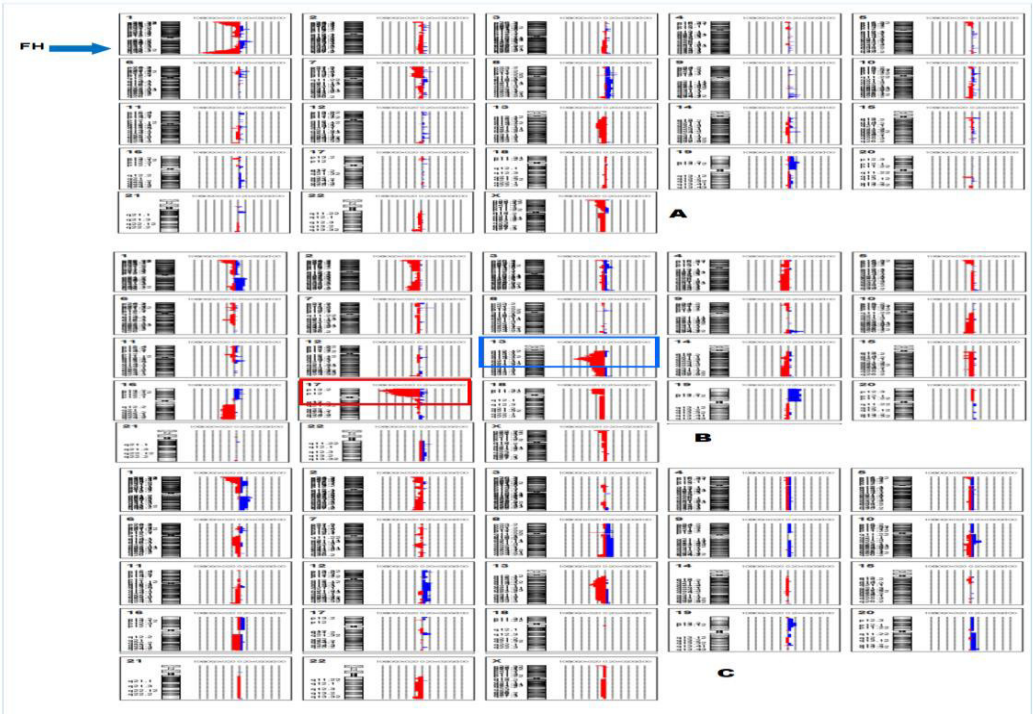

Figure 3

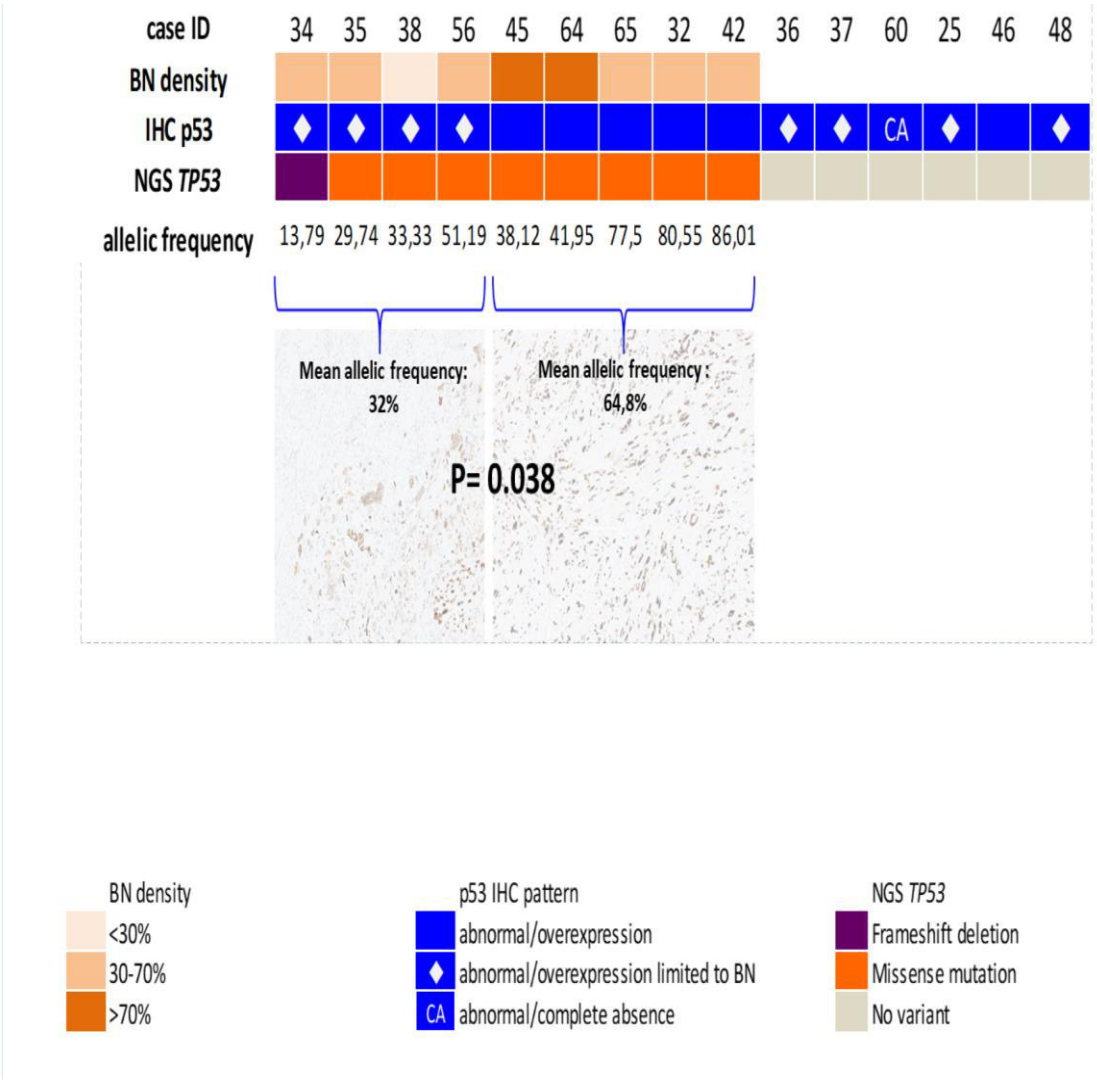
case ID
34 35 38 56 45 64 65 32 42 36 37 60 25 46 48
BN density
IHC p53
CA
NGS TP53
allelic frequency
13,79 29,74 33,33 51,19 38,12 41,95 77,5 80,55 86,01
Mean allelic frequency: 32%
Mean allelic frequency : 64,8%
P= 0.038
BN density
<30%
30-70%
>70%
p53 IHC pattern
abnormal/overexpression
abnormal/overexpression limited to BN
CA
abnormal/complete absence
NGS TP53
Frameshift deletion
Missense mutation
No variant

Figure 4

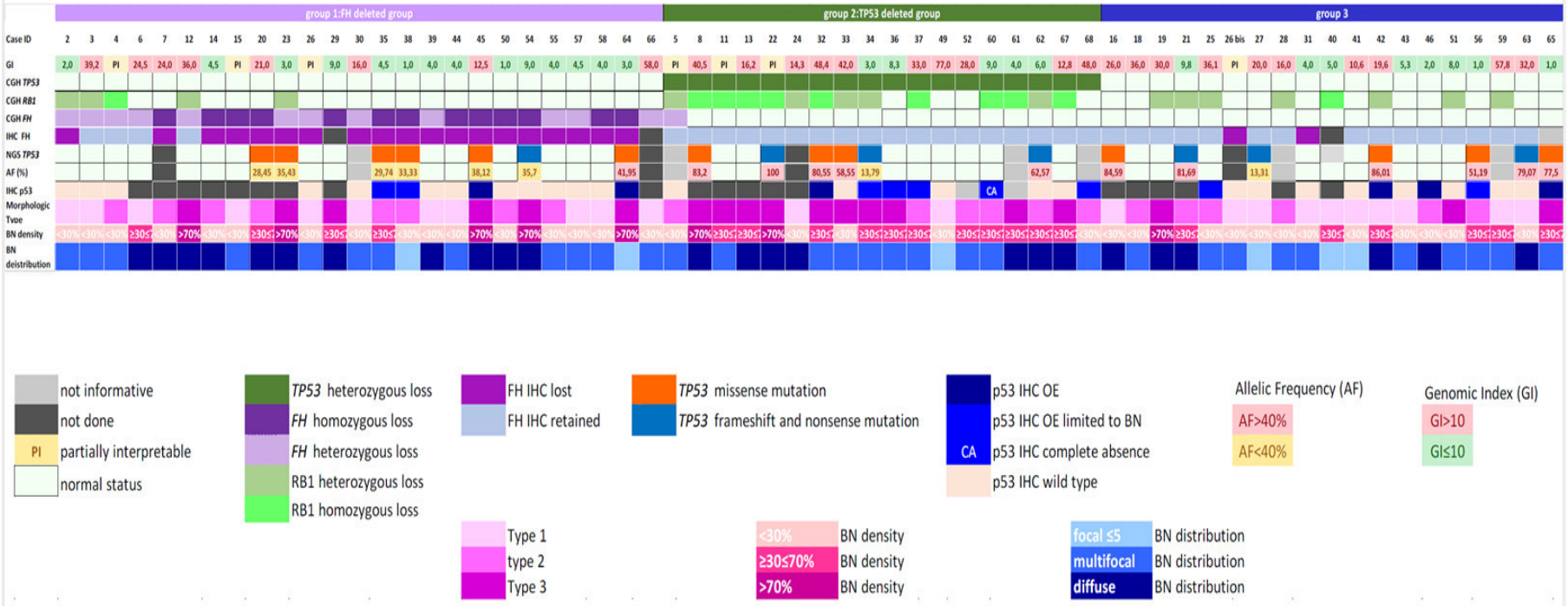
group 1:FH deleted group
group 2:TP53 deleted group
group 3
Case ID
GI
CGH TP53
CGH RB1
CGH FH
IHC FH
NGS TP53
AF (%)
IHC p53
Morphologic Tvoe
BN density
BN deistribution
not informative
not done
PI partially interpretable
normal status
TP53 heterozygous loss
FH homozygous loss
FH heterozygous loss
RB1 heterozygous loss
RB1 homozygous loss
FH IHC lost
FH IHC retained
TP53 missense mutation
TP53 frameshift and nonsense mutation
p53 IHC OE
p53 IHC OE limited to BN
CA p53 IHC complete absence
p53 IHC wild type
Allelic Frequency (AF)
AF>40%
AF<40%
Genomic Index (GI)
GI>10
GI≤10
Type 1
type 2
Type 3
<30% BN density
≥30≤70% BN density
>70% BN density
focal ≤5 BN distribution
multifocal BN distribution
diffuse BN distribution

Supplementary data.

Table 1. Catalogue of 78 hotspots tested by NGS in a panel of 16 genes.

Gene	RefSeq	Exons testés
AKT1	NM_05163	3, 7
BRAF	NM_004333	11, 15
CTNNB1	NM_001904	3
CDKN2A	NM_000077	2
DICER1	NM_030621	25, 26
ERBB2	NM_004448	19-21
FBXW7	NM_033632	5, 8-11
FGFR2	NM_022970	7, 9, 12
FOXL2	NM_023067	1
KRAS	NM_033360	2, 3, 4
PIK3CA	NM_006218	1, 4, 6, 7, 9, 13, 18, 20
PIK3R1	NM_181523	7-13
POLE	NM_006231	9, 13
PTEN	NM_000314	1, 3, 5-8
RB1	NM_000321	4, 6, 10, 11, 14, 17, 18, 20-22
TP53	NM_000546	2, 4-8, 10

Supplementary data. Fig 1

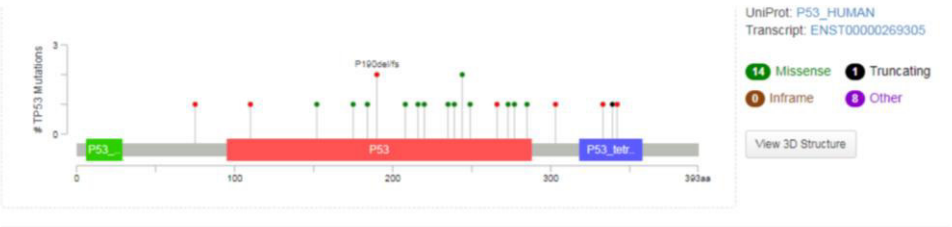

Figure 1. Distribution of *TP53* mutations on p53 protein of the 23/25 mutations with known variant effect, obtained through the cBioPortal Mutation Mapper tool.

4 DISCUSSION ET PERSPECTIVES

Les résultats obtenus au cours de ma thèse ont contribué à démontrer qu'il existe un lien entre le degrés de remaniement du génome, se traduisant dans la complexité génomique d'une tumeur, et l'évolution clinique de la tumeur. Ce lien entre le génome et la clinique (risque de récidive et de décès) peut être également mis à contribution pour le diagnostic.

Du point de vue de l'évolution, le degré de complexité génomique est le reflet des tentatives que la cellule met en place pour lui permettre de survivre et de proliférer.

Dans le vaste panorama de la cancérogenèse, la complexité génomique peut être observée en l'absence d'événement driver spécifique et récurrent à l'image des sarcomes à génomique complexe dont le LMS utérin, ou bien être la conséquence d'une altération qui dérègle le génome. Le carcinome séreux de haut grade de l'ovaire illustre bien ce dernier phénomène. Dans ces carcinomes, une mutation de *TP53* (souvent sur un terrain favorisant comme BRCAness ou les déficiences du système de recombinaison homologue (HRD)) amène à une instabilité chromosomique sans besoin d'autres mutations, comme en témoigne une faible charge mutationnelle[34].

Il existe d'autre part des tumeurs « à génomique simple » qui ne nécessitent pas de complexité chromosomique pour déclencher et promouvoir le processus tumoral puisque l'événement génétique qui les caractérise est nécessaire et suffisant. Les sarcomes associés à translocation (ex synovialosarcome, ou le sarcome de Ewing) ou associés à une mutation activatrice (ex GIST), en sont des exemples typiques.

Néanmoins même pour ces tumeurs, la complexité chromosomique peut influencer le pronostic avec une intensité variable selon l'histotype de la tumeur. On peut citer comme exemple le synovialosarcome où le Genomic Index est pronostique au seuil ≥1[180] ou le GIST, pour lequel le seuil est fixé à 10[153].Les tumeurs qui mieux représentent la complexité génomique sont les sarcomes à génomique complexe, qui ne présentent pas d'événement « driver » actuellement connu, pouvant expliquer à lui seul la cancérogenèse, mais une multitude de réarrangements, délétions et amplifications, le plus souvent « privés », c'est-à-dire propres à chaque tumeur et même à chaque clone de la même tumeur, qui aboutissent à un avantage à la survie et à la prolifération cellulaire (avantage sélectif).

4.1.1 LA SIMPLICITE GENOMIQUE EST-ELLE SYNONYME DE LA BENIGNITE ?

Pas forcément ! Cela dépend de l'histotype et des mécanismes que la cellule a mis en place pour son avantage sélectif. Dans les tumeurs musculaires lisses utérines, un profil simple, peu remanié est synonyme de tumeur bénigne (LM), un profil très remanié est évocateur d'une tumeur maligne (LMS). Cependant, ceci n'est pas confirmé dans tous les types histologiques. En effet, les carcinomes *SMARCA4*-déficients, comme le carcinome à petites cellules hypercalcémiant de l'ovaire[187, 188] et le sarcome utérin SMARCA4-déficient [189] (cf fig 34) ainsi que le tumeurs rhabdoïdes, ont une évolution clinique néfaste nonobstant un état diploïde et un profil génomique très peu remanié. Dans ces tumeurs l'altération génétique (mutation du gène *SMARCA4*) est suffisante en elle-même à la cancérogénèse de la cellule.

Dans les sarcomes gynécologiques à génomique simple, comme par exemple les sarcomes du stroma endométrial de bas grade et de haut grade, où une fusion est le *primum movens* du processus tumoral, il existe un gradient entre des tumeurs bénignes comme le nodule du stroma endométrial (cf fig 34), souvent à profil génomique plat et le sarcome du stroma endométrial de haut grade, avec un *crescendo* d'altérations du bénin au malin [190]. Un autre exemple de relative simplicité du profil génomique nonobstant le pronostic est le sarcome du col utérin associé aux réarrangements *NTRK*, récemment décrit[191](cf Figure 34).

Nous avons également observé une complexité chromosomique accrue entre la tumeur primitive et la métastase, preuve que le degré de complexité est associé également au stade d'évolution de la maladie.

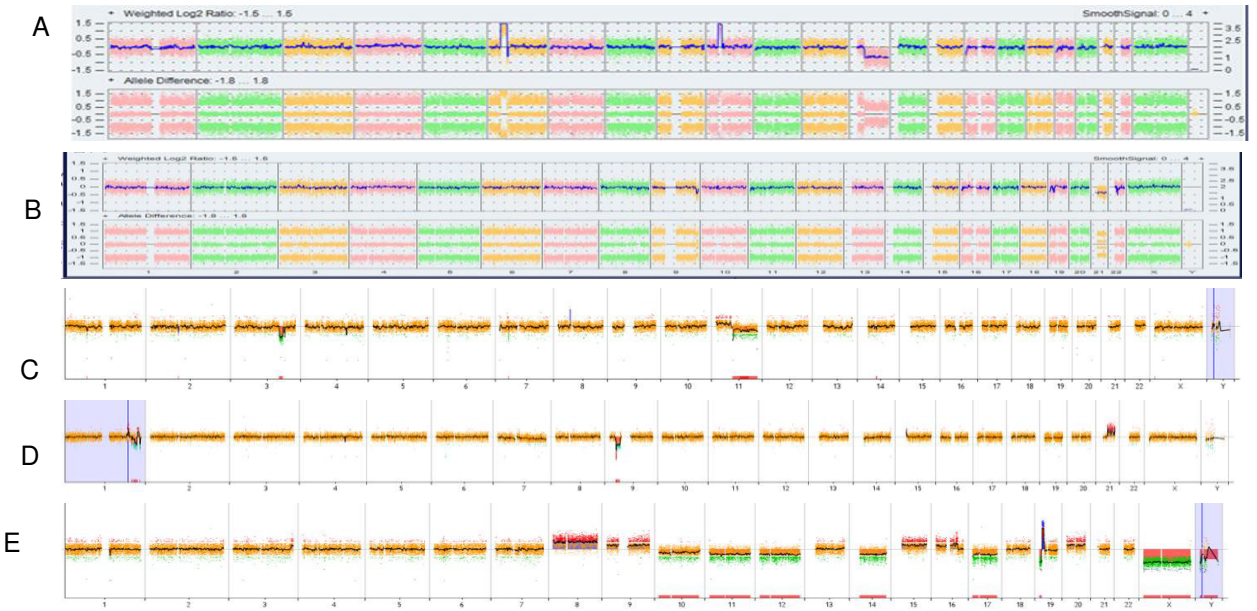

Figure 34. Exemples de profils génomiques dans différents histotypes.

A. Nodule du stroma endométrial (tumeur bénigne). Profil gracieusement fourni par le Dr S Le Guellec. Profil génomique très simple. Ce cas présentait un réarrangement équilibré du gène *PHF1*, non détectable en CGH. B. Sarcome utérin SMARCA4 déficient (sarcome très agressif). C. Sarcome du stroma endométrial de bas grade. D. Fibrosarcome du col utérin avec fusion *EML4-NTRK3*. E. Carcinome séreux de haut grade de l'ovaire.

4.1.2 PEUT-ON APPLIQUER L'ANALYSE DU PROFIL GENOMIQUE AU DIAGNOSTIC DES TUMEURS MUSCULAIRES LISSES DE L'UTERUS ?

Les LMS utérins font partie des sarcomes à génomique complexe et présentent des profils génomiques remaniés voire très remaniés. Les LM de type classique (fusiformes) montrent des profils plats ou très peu remaniés. Nous avons démontré en 2015[74] que l'analyse du profil génomique séparait les STUMP fusiformes en deux groupes distincts : un groupe qui ne montrait pas ou peu d'évènements génomiques, et qui cliniquement ne présentait pas de récidive, proche des LM et un groupe cliniquement malin, avec un profil génomique complexe, semblable aux LMS. Ces deux groupes, indistinguables sur le plan morphologique, étaient séparés par le Genomic Index au seuil de 10. Depuis cette publication[74], le calcul du Genomic Index est appliqué en routine en France dans les principaux centres diagnostiques.

4.1.3 LE CALCUL DU GENOMIC INDEX EST-IL PLATEFORME-DEPENDANT ?

Le calcul du Genomic Index avec les seuils diagnostique de 10 et pronostique de 35 a été mis au point sur une plateforme génomique AGILENT x60K. Depuis, les technologies des arrays ont évolué vers des systèmes d'hybridations plus performants, de plus haute résolution (ex AGILENT x180k) mais surtout avec différentes technologies non plus basées sur l'hybridation physique mais comparée via les algorithmes du logiciel CHAS Affymetrix à des librairies obtenues sur des tissus sains avec une résolution supérieure à la technologie AGILENT. De plus la technologie Affymetrix informe sur le statut allélique, ce qui en pathologie tumorale est très intéressant. Cette technologie est destinée à remplacer de plus en plus, aussi bien en recherche que dans l'activité diagnostique sanitaire la technologie Agilent.

Nous avons réalisé une étude visant à comparer les GI calculés sur deux plateformes AGILENT x60k et 180k, cette dernière étant très utilisée en France. Cette validation

était nécessaire pour confirmer la validité des Genomic Index calculés sur cette plateforme et pouvoir intégrer les données génomiques au diagnostic, quelque soit la plateforme utilisée.

Il existait des différences de sensibilité entre les deux plateformes, essentiellement dans les LMS, qui, en raison de la présence de nombreux événements, montraient plus de variations. Nonobstant les déviations observées entre les deux plateformes, nous n'avons pas relevé des différences qui auraient pu changer le diagnostic dans la série test : les LM testés ont montré un GI<10 et les LMS >10. Pour cela nous avons retenu les même seuils de Genomic Index sur les deux plateformes.

L'étape suivante consistera dans la validation des Genomic Index calculés sur la plateforme Affymetrix, qui est en train de remplacer celle AGILENT à plusieurs centres. Dans ce contexte, un travail de validation sera mis en place dans les plus brefs délais. Une réflexion devra être menée également sur l'intégration de la ploïdie tumorale au Genomic Index afin d'obtenir un score.

4.1.4 PEUT-ON APPLIQUER L'ANALYSE DU PROFIL GENOMIQUE AU DIAGNOSTIC DES TUMEURS MUSCULAIRES LISSES DE TYPE EPITHELIOIDE ?

Les séries publiées en 2015 et 2018[74, 169] essentiellement composées de tumeurs musculaires lisses utérines de type fusiforme ont d'une part confirmé, en analogie à d'autres sarcomes, la corrélation entre la complexité génomique et le pronostic et d'autre part l'utilité diagnostique de son estimation par le calcul du Genomic Index dans les tumeurs musculaires lisses utérines.

Actuellement en France et au sein du réseau RRePS gynécologique, nous intégrons les valeurs des GI des tumeurs musculaires lisses utérines lorsque la morphologie n'est pas conclusive. Cependant, il n'existe aucune donnée génomique inhérente au variant épithélioide, dont peu de séries ont été rapportées dans la littérature[107, 133, 141] et dont les caractéristiques génomiques restent élusives. C'est dans ce contexte que nous avons entrepris de valider le GI dans le sous type épithélioïde des tumeurs musculaires lisses utérines. Notre effectif est faible car il s'agit de tumeurs rares, souvent mal diagnostiquées et non répertoriées comme sous type épithélioïde dans le réseau RRePS. Malgré le faible nombre de cas, nous avons pu confirmer encore une fois l'hypothèse développée dans ma thèse. En effet le GI moyen des E-LM a été de 7.11 (médiane: 7, de 2 à 11.6) alors que le GI moyen des E-LMS était de 69.7 (médiane 36, de 14.4 à 180). Le groupe des E-STUMP a montré des profils génomiques hétérogènes, avec un chevauchement entre les LM et LMS avec un GI moyen de 16.9 (médiane GI: 16,3 ; de 2 to 49). En raison de faible nombre d'événements et d'effectifs l'analyse des courbes de survie a montré une tendance du GI avec l'évolution clinique sans pouvoir être statistiquement significatif.

4.1.5 LE LEIOMYOME A NOYAUX BIZARRE : UNE ENIGME. COMMENT EXPLIQUER L'APPARENTE CONTRADICTION ENTRE LA COMPLEXITE GENOMIQUE ET LA BENIGNITE DE CE VARIANT DE LM ?

En 1961 Przybora publiait 21 cas de tumeurs musculaires lisses utérines arborant les caractéristiques morphologiques de ce que nous nommons actuellement les LM-BN. Six de ces patientes présentaient conjointement des LMS utérins, et les 15 autres étaient significativement plus jeunes que celles présentant une maladie « invasive » (LMS). Devant ces observations cliniques et histologiques, et par analogie avec le carcinome mammaire, Przybora proposa l´hypothèse d´un « sarcome in situ ». Il alimenta ainsi dans la littérature de l´époque les controverses qui perdurent jusqu´à maintenant, opposants les tenants de l´hypothèse «dégénérative» aux partisans de l´hypothèse néoplasique[185]. Les rares séries cliniques disponibles semblaient donner raison aux premiers, les LM-BN présentant dans l´ensemble un comportement

biologique bénin, marqué par un faible taux de récurrence (entre 1,7 et 7%)[2, 99, 102, 174, 192]. Presque 50 ans après Przybora, Mittal et al. décrivaient 26 cas de LMS utérins dont 8 présentaient des territoires de LM-BN. Après analyse comparative des altérations génomiques, détectées par CGH-array, entre le LM et le LMS adjacent, des événements communs entre LM-BN et LMS étaient identifiés, avec une accumulation d'altérations dans le LMS[184]. Si le LM-BN a une évolution favorable et ainsi considéré comme une tumeur bénigne et inclus dans l'OMS 2014 et 2020 dans le chapitre des léiomyomes, les altérations moléculaires et la complexité chromosomique de certains de ces profils, le rapprochent davantage des LMS que des LM.

Sur la base des données moléculaires et immunohistochimiques et à la lumière des résultats de notre travail, nous distinguons trois groupes dans l'hétérogène panorama génomique des LM-BN, avec des caractéristiques cliniques, morphologiques et immunohistochimiques distinctes pour les deux premiers en rejoignant des résultats déjà décrits en littérature[101, 102].

Le LM-BN se décline en un sous-type *FH*-déficient, présentant une inactivation biallélique (délétion homozygote, ou mutation sur un allèle suivie d'une perte de hétérozygotie, ou une délétion/mutation sur un allèle suivi d'une inactivation épigénétique) du gène *FH* (Fumarate Hydratase, situé sur le chromosome 1q43), un sous-type *TP53* délété et un troisième groupe sans altération génomique, ni caractéristique morphologique particulière.

Les patientes du groupe FH déficient sont 10 ans plus jeunes que le groupe *TP53*-délété, les LM ont une plus grande taille et en morphologie la densité des BN est faible. On observe des modifications architecturales et nucléaires décrites dans les LM-FH déficients[101 102]. Ce groupe, surtout quand s'y associe une délétion homozygote de *FH*, présente des profils génomiques plus simples (GI : moyen 3.12, médiane 8.5, de 1 to 58) en particulier en présence d'une délétion homozygote de *FH* (GI moyen: 8.12) et une faible fréquence d'altérations de *TP53* et *RB1*. Le gène Fumarate hydratase code pour une enzyme du cycle de Krebs. Le gène *FH* joue un rôle de suppresseur de tumeur via la production d'espèces réactives de l'oxygène (ROS) induisant des dommages de l'ADN et favorisant l'instabilité génomique[193-195], en provoquant l'accumulation de HIF1a, un facteur de transcription qui favorise le métabolisme cellulaire et l'angiogenèse.

Il est pour cela important d'une part de familiariser le pathologiste avec ces traits morphologiques évocateurs de FH-déficience pour ne pas surdiagnostiquer la lésion en STUMP ou pire en LMS et d'autre part, d'alerter le clinicien de la possibilité d'un syndrome de Reed (léiomyomatose héréditaire et carcinome à cellules rénales), sur la base du jeune âge de la patiente, de la morphologie, de la perte d'expression de FH en immunohistochimie et de la positivité de l'anticorps anti-2SC. Le LM-FH déficient a été d'ailleurs reconnu comme nouveau variant de LM dans le dernier OMS 2020.

Le deuxième groupe est représenté par le LM-BN associé aux altérations de *TP53*. Les patientes sont de 10 ans plus âgées que le groupe *FH*-déficient, la taille des LM est petite et morphologiquement la concentration de BN est plus importante. Ce sous-groupe présente une complexité chromosomique plus importante comme en témoignent des GI plus élevés (GI moyen : 26.03, médiane 16,2, de 3 à 77), et un taux de délétion de *RB1* plus important.

Ce sous-groupe illustre parfaitement les difficultés que pose le diagnostic LM-BN, aussi bien pour le pathologiste que pour le cytogénéticien et le biologiste moléculaire. Sa proximité morphologique, immunophénotypique et moléculaire avec le LMS est plus que troublante, et force est de constater que l´hypothèse de léiomyosarcome in situ de Przybora[185], énoncée il y a près de 60 ans peut-être tentante. Néanmoins seulement une minorité de LMS est associée à un LM-BN.

4.1.6 LEIOMYOMES A NOYAUX BIZARRES ET COMPLEXITE GENOMIQUE. COMMENT EXPLIQUER LA CONTRADICTION ENTRE LA COMPLEXITE CHROMOSOMIQUE ET L'EVOLUTION CLINIQUE FAVORABLE ?

Comme en résulte tout au long de la thèse, l´indice génomique a fait la preuve de son utilité en tant qu´outil diagnostique et pronostique dans les tumeurs musculaires lisses utérines fusiformes. Les résultats de l'étude génomique sur les LM-BN font surgir les questions suivantes : peut-on conclure que les LM-BN sont des LMS mais à pronostic favorable ? ce qui équivaut à redéfinir l'entité de LMS utérin. En effet les critères diagnostiques des LMS utérins (qui pour les tumeurs fusiformes ont été établis à partir de l'étude de Bell[173]) sont très restrictifs car permettent de diagnostiquer les LMS de haut grade. Le taux de récidive et d'évolution défavorable pour ces tumeurs est élevé. Il n'existe pas de LMS de bas grade ou de grade intermédiaire reconnu dans l'utérus et d'ailleurs le grading FNLCC des sarcomes des tissus mous n'est pas pronostique dans les LMS utérins[165]. Les LMS utérins que nous diagnostiquons ainsi pourraient être que la pointe de l'iceberg de la catégorie des LMS utérins avec une évolution différente, rapide et néfaste pour les LMS de la pointe visible et lente et indolente en bas de l'iceberg (LMS de bas grade). Le rationnel de ce changement aurait des bases génomiques (gradient de complexité chromosomique, mutations et délétions de TP53, RB1, ATRX). Néanmoins j'estime que la communauté médicale n'est pas prête à ce changement.

Faut-il établir un seuil différent pour le GI des LM-BN ? Puisque il n'y a pas d'évènement (pas de récidive ou décès dans les séries) ou le taux de récidive est très bas (moins de 7%), il n'y a pas les bases scientifiques pour cela. Néanmoins le GI est informatif, dans le sens rassurant quand il est <10, mais il ne permet pas d'assurer le diagnostic de LMS si >10 dans ce variant. Ces résultats nous amènent à deux conclusions. Tout d'abord les informations génomiques doivent être intégrées au contexte clinique, hormonal de l'hôte et à l'histologie de la tumeur analysée. Plus précisément, la complexité génomique, n'a très vraisemblablement pas la même valeur, la même signification chez une patiente « jeune » (ex patiente pre-ménopausique présentant un LM-BN) sous imprégnation hormonale, que chez une patiente âgée, post-ménopausique. Cette observation a été rapportée également dans les synovialosarcomes où l'impact de la complexité génomique est différent selon l'âge (enfant *versus* adulte). D'autre part dans les tissus mous les critères diagnostiques des LMS profonds, des viscères et du pelvis tiennent en compte le sexe et l'imprégnation hormonale pour le seuil mitotique[182].

Si avec notre étude je n'ai pas pu explorer l'univers de LM-BN quant à leur état de ploïdie, puisque la plateforme CGH-array utilisée ne dispose pas d'évaluation du statut allélique, en l'absence d'une étude mutationnelle à large échelle (whole génome) sur ces tumeurs pour lesquelles le matériel congelé ou frais est rare, voire inexistant, notre travail a toutefois permis, de façon pragmatique de décrire un état des lieux des profils génomiques des LM-BN en précisant que le GI au seuil de 10 n'est pas diagnostique pour ce variant de LM. Notre étude souligne l´importance de déterminer de façon précise le contexte diagnostique morphologique et clinique afin d´utiliser cet outil à bon escient et de conserver sa pertinence. La figure 35 résume l'état des lieux des LM-BN observé dans notre étude et observés au cours de mon expérience diagnostique.

et (cf Fig 35).

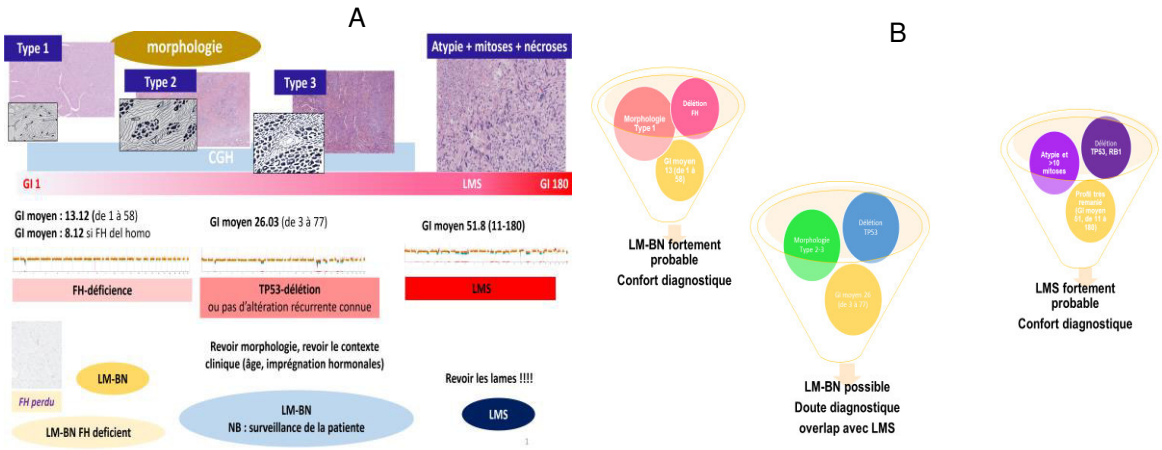

Figure 35. Algorithme diagnostique. Récapitulatif de l'état des lieux des LM-BN et des LMS selon la morphologie et les profils génomiques (A). Trois situations diagnostiques face à une lésion musculaire lisse avec BN. Les deux extrêmes représentent des situations « confort » : d'un côté le LM-BN FH déficient avec une morphologie suggestive de déficit de FH et de l'autre coté la présence d'atypies en dehors des BN, d'un compte mitotique >10 et d'un profil génomique remanié. Entre les deux le groupe de LM-BN avec une morphologie type 2 et 3 (densité moyenne à élevée de BN) et un profil génomique modérément remanié (GI moyen de 26) (B).

Indéniablement les perspectives de recherche concernant les LM-BN devront aller au-delà de l´étude des caractéristiques moléculaires mutationnelles et des anomalies structurelles cytogénétiques. Ces conclusions rejoignent finalement les observations et les démarches actuelles en cancérologie générale, où la caractérisation des éléments inflammatoires observés morphologiquement, l´étude de l´environnement immun ainsi que des phénomènes hypoxiques, constituent des pistes prometteuses pour améliorer la compréhension des processus tumoraux.
Des éléments supplémentaires sont émergés par l'analyse de nouveaux cas de LM-BN dans la routine diagnostique, analysés sur plateforme Affymetrix. Ces tumeurs ont montré un état polyploïde (Fig 36). L'état aneuploïde est considéré comme une des premières étapes, d'au moins une étape favorisante la cancérogenèse. L'aneuploïdie favorise les dommages de l'ADN et agit comme un oncogène[196]. Dans ce cas le LM-BN pourrait représenter une lésion pré-néoplasique, qui dans la majorité des cas n'aboutit pas au LMS. Une piste d'étude suggestive pour expliquer les BN est représentée par la sénescence. En effet les BN expriment fréquemment la protéine p16 qui est, autre qu' une protéine impliquée dans le cycle cellulaire, un marqueur de sénescence[197].

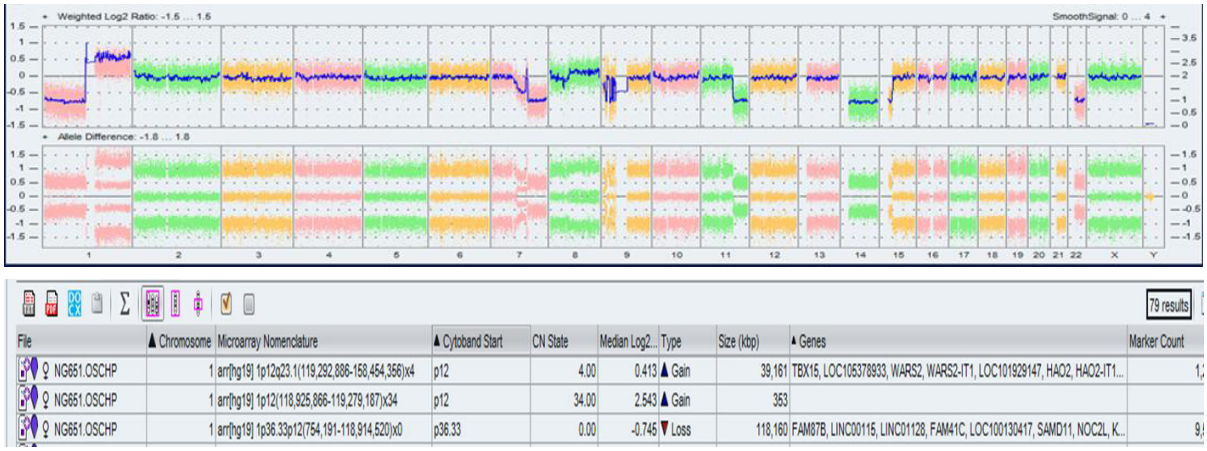

Figure 36. Profil d'un LM-BN. Le profil remanié montre un état polyploïde au niveau du chromosome 1 avec 34 copies du centromère du chromosome 1.

Nous avons testé la signature d'expression CINSARC Nanocind sur une série test de 10 LM-BN et tous ont été classés en C1 (catégorie à faible risque) (cf Fig 37). Néanmoins le groupe C1 comprend également des véritables LMS.

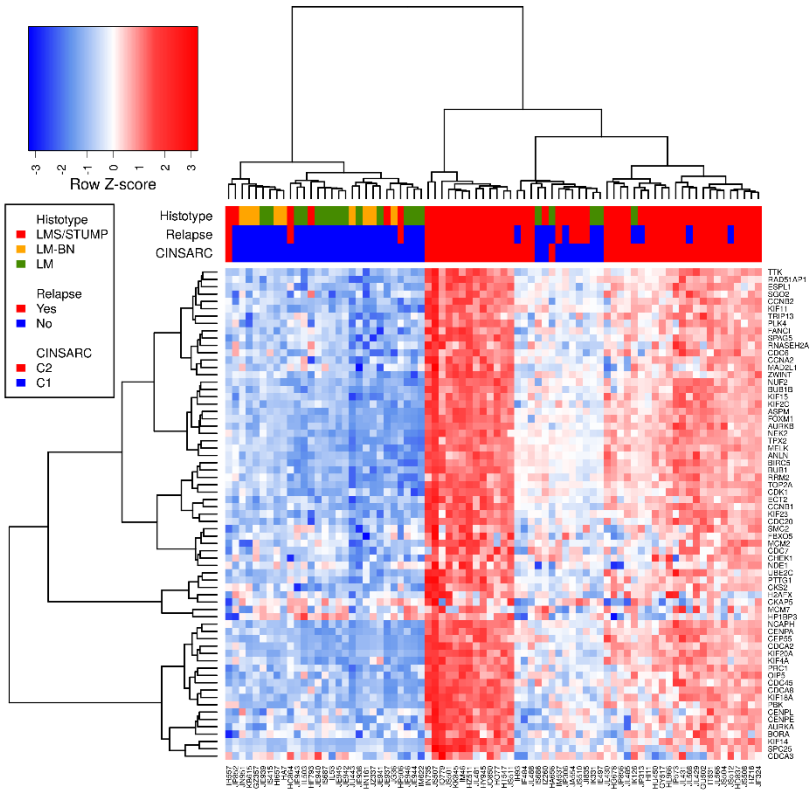

Figure 37. Z score d'une série de LM, LMS, STUMP et LM-BN selon la signature d'expression CINSARC Nanocind.

Le groupe de LM-BN sont clustérisés avec les LM dans le groupe C1.

A ce jour il n´existe pas de modèle biologique de LM-BN du fait de l'absence de matériel tumoral frais, le diagnostic de LM-BN étant un diagnostic fortuit, fait à postériori sur pièce opératoire. Avec la mise en place du diagnostic préopératoire sur microbiopsie, en particulier dans le cadre du protocole Biopsar (Performances diagnostiques de la biopsie utérine echo-guidée pre-chirurgicale dans la prise en charge des tumeurs utérines suspectes de sarcomes), les LM-BN pourront être diagnostiqués ou du moins suspectés en préopératoire et par conséquent il sera possible de congeler et d'obtenir des cultures cellulaires à partir du matériel frais. A partir des modèles cellulaires établis et dans le cadre d'une étude nationale, par exemple au sein du réseau RRePS dans lequel les LM-BN sont recensés, il sera possible de mener une étude par analyse moléculaire par whole génome, et méthylome couplée à une étude fonctionnelle sur les cultures cellulaires établies à partir de LM-BN.

4.1.7 LE CINSARC : UNE EVOLUTION DU GI QUI FAIT MIEUX QUE LE GI DANS LE PRONOSTIC DES LMS

L'estimation du potentiel métastatique dans les sarcomes de l'utérus en particulier et des tissus mous en général, fait partie des critères qui influencent la stratégie thérapeutique (en particulier l'option des traitements adjuvants systémiques). Mis à part le stade qui est le facteur pronostique plus fort[198], le grade histologique, établi sur des critères morphologiques dans la majorité des carcinomes et des sarcomes des tissus mous, est un élément à la base de la décision thérapeutique car il renseigne sur le potentiel métastatique d'une tumeur[199]. Si dans les sarcomes des tissus mous le grade FNLCC[200, 201] a montré sa valeur et il est diffusément employé par les pathologistes au moment du diagnostic et par les cliniciens pour la prise en charge thérapeutique, il n'a pas montré de valeur pronostique dans les LMS utérins[165]. Une des explications possibles est due aux critères diagnostiques restrictifs du LMS utérin,

comme discuté ci-dessus. Ces critères identifiant la pointe de l'iceberg des LMS utérins sélectionnent les LMS de « haut grade ». Pour les LMS au stade FIGO I, qui représentent environ 60% des LMS utérins au diagnostic, la survie globale à 5 ans est estimée entre 50%[136] et 57%[202] et l'indication de la chimiothérapie adjuvante est discutée, son efficacité n'étant pas prouvée[203-205]. Pour répondre au manque de facteurs pronostiques, un nomogramme proposé par le MSK calcule le pourcentage de survie globale à 5 ans pour les LMS utérins[166, 206] . Ce nomogramme évalue des paramètres tels que l'âge au diagnostic, la taille tumorale, le grade (bas et haut grade, sans plus de spécification morphologique), le compte mitotique, l'extension au col utérin, la présence d'extension loco-régionale et à distance (métastases) et produit un rapport avec le pourcentage de survie globale à 5 ans. Néanmoins, deux paramètres sont discutables méthodologiquement : le grade qui par définition est haut si on arrive au diagnostic de LMS selon les critères de Stanford[173] et le compte mitotique sans précision du diamètre de champs.

Dans ce contexte nous avons testé la signature d'expression CINSARC (Complexity Index in SARComa) sur une série de 60 LMS utérins dont 40 au stade FIGO I.

La signature d'expression CINSARC est issue de l'analyse de l'expression génique différentielle, dans une cohorte de 183 sarcomes des tissus mous, entre sarcomes de grade 3 selon FNLCC versus grade 1 et 2 et des tumeurs avec un haut niveau de complexité génomique versus les tumeurs avec un faible niveau de remaniement chromosomique[36]. Les 67 gènes sélectionnés dans la signature sont impliqués dans les mêmes processus biologiques tels que le contrôle de la mitose, le cycle cellulaire et l'intégrité des chromosomes. Ces gènes peuvent être répartis dans cinq groupes majeurs en fonction de leur rôle dans les différentes étapes de la mitose : le cycle cellulaire et les points de contrôle mitotique; la biogenèse des chromosomes, leur condensation et leur ségrégation ; le fuseau mitotique et les centrosomes ; les complexes kinésines et enfin la cytokinèse. Les points forts de la signature sont l'application aux tumeurs fixés en formol (FFPE), se franchissant de la limite du matériel congelé qui n'est pas accessible à tous les laboratoires et la technique relativement simple, par Nanostring, qui a l'avantage d'être reproductible et des plus en plus diffuse dans les laboratoires. L'analyse des résultats obtenus sur les plateformes périphériques sont centralisée, assurant la reproductibilité des résultats.

Nous avons analysé une série de 60 LMS utérins. Dans notre série, la signature CINSARC sépare les tumeurs en deux groupes distincts (C1, de bas risque et C2, de haut risque) avec une survie globale et libre de maladie différentes. De plus, la valeur pronostique de cette signature est confirmée dans les LMS de stade I pour lesquels il n'y pas de véritable facteur pronostique avéré. La valeur pronostique de la signature a également été validée sur une série indépendante (série de 32 LMS utérins publiée dans le consortium international TCGA[60]). Ces résultats indiquent que les mécanismes de contrôle de l'intégrité du génome tumoral sont des éléments majeurs dans l'établissement du potentiel métastatique pour les sarcomes utérins et vraisemblablement pour les autres cancers, et que la mesure de l'expression de ces gènes est un puisant indicateur du pronostic tumoral.

4.2 PERSPECTIVES

Les résultats obtenus au cours de la thèse ont contribué à démontrer le lien entre la complexité génomique et l'évolution tumorale. Pour les tumeurs musculaires lisses utérines, le GI au seuil de 10 représente désormais un outil intégré à l'analyse morphologique et la signature CINSARC Nanocind a démontré sa valeur pronostique dans les LMS utérins et ceci même au stade I, se proposant comme le nouvel outil de randomisation pour les essais thérapeutiques à venir.

L'analyse génomique des LM-BN nous a enseigné la valeur et les limites de l'analyse génomique en suggérant que les données génomiques doivent être intégrées avec le contexte clinique (âge, statut hormonal, localisation tumorale) et histologique (selon le type de tumeur, une tumeur musculaire lisse utérine et une tumeur/sarcome du stroma endométrial) et qui n'ont pas de valeur absolue.

4.2.1 LES LEIOMYOMATOSE UTERINES, INTRAVASCULAIRES ET PERITONEALES : COMPRENDRE LES MECANISMES MOLECULAIRES A LA BASE DE L'ANGIOTROPISME ET DE LA DIFFUSION DANS LA CAVITE PERITONEALE D'UNE TUMEUR MUSCULAIRE LISSE MORPHOLOGIQUEMENT « BENIGNE ».

Pour poursuivre l'étude des tumeurs musculaires lisses utérines et gynécologiques, l'étape suivante est l'analyse des léiomyomatose intravasculaires de l'utérus et les léiomyomatose disséminées du péritoine qui représentent une véritable énigme clinico-biologique. En effet, en l'absence de critères morphologiques de malignité, dans un contexte génomique peu remanié, ces lésions réservent des évolutions cliniques certes le plus souvent lentes mais difficilement contrôlables, au point d'être dénommées « LMS de bas grade ». Nous disposons de 24 échantillons de 13 patientes atteintes de léiomyomatose péritonéale et de 5 échantillons de léiomyomatose utérine en matériel FFPE et pour deux cas du matériel congelé. Nous allons débuter le séquençage par whole génome de deux échantillons congelés avec la finalité de tester les autres cas de la série en paraffine sur la base des altérations que nous aurons observées sur les deux cas princeps. Compte tenu des profils génomiques relativement simples de ces lésions, nous espérons identifier des altérations mutationnelles ou une signature d'expression qui puisse d'une part nous informer sur le potentiel de rechute locale et à distance et d'autre part nous permettre de comprendre les mécanismes moléculaires à la base de l'angiotropisme et de la diffusion dans la cavité péritonéale d'une tumeur musculaire lisse morphologiquement « bénigne ».

4.2.2 LES TUMEURS MESENCHYMATEUSES MYXOÏDES DE L'UTERUS : ANALYSE DE LA COMPLEXITE GENOMIQUE DANS LES LMS MYXOÏDES, LES SARCOMES FIBROMYXOIDES DU STROMA ENDOMETRIAL ET LES TUMEURS MYOFIBROBLASTIQUES INFLAMMATOIRES UTERINES.

Les LMS myxoides de l'utérus sont des tumeurs rares, de diagnostic difficile et probablement mal diagnostiquées. Il existe peu de données moléculaires en littérature dont la présence de réarrangements impliquant le gène *PLAG1*[134], une faible charge mutationnelle et une complexité chromosomique accrue dans les LMS[71]. D'autre part des tumeurs qui rentrent dans le diagnostic différentiel et qui peuvent se présenter au même âge et avec des traits morphologiques superposables sont les tumeurs myofibroblastiques inflammatoires, qui, mise à part l'expression de ALK, peuvent présenter le même phénotype que les LMS myxoïdes et les sarcomes du stroma endométrial de bas et de haut grade, qui, quand ne sont pas associés aux fusions géniques connues, représentent un diagnostic d'exclusion. Si la présence d'un réarrangement ALK nous autorise le diagnostic de tumeur myofibroblastique inflammatoire, environ 2% des LMS arborent un réarrangement de ALK[69]. L'analyse par CGH-array de ces différentes tumeurs myxoïdes, de morphologie semblable mais de pronostic très différent, permettra de mieux les décrire et de mieux les diagnostiquer.

4.2.3 L'ANALYSE DE LA METHYLATION DU GENOME UNE PISTE A SUIVRE ?

La signature sur la base de la méthylation globale du génome a montré dans les sarcomes des tissus mous sa valeur pronostique en survie spécifique identifiant un groupe hypométhylé (MET 1) associé à un meilleur pronostique et un groupe hyperméthylé (MET2) associé à un degré d'instabilité génomique accrue, à une composante inflammatoire moindre[60]. Deux autres études ont montré, bien que sur un

nombre limité d'échantillons, que la signature basée sur la méthylation permet de séparer les LM des LMS utérins[207] et sépare par une analyse non supervisée clustérisée les LMS des sarcomes du stroma endométrial et des carcinomes[208]. L'étude du méthylome pourrait aider le pathologiste dans le diagnostic différentiel de ces tumeurs mésenchymateuses utérines de pronostic radicalement différent.

Les différents sous types histologiques des tumeurs mésenchymateuses de l'utérus peuvent encore poser des problèmes pour le pathologiste dans le diagnostic et par conséquent pour le clinicien pour la prise en charge qui en suit. La classification des tumeurs mésenchymateuses utérines a été jusqu'à maintenant morphologique, complétée par l'immunohistochimie, visant à identifier l'activité mitotique, l'atypie et la nécrose tumorale comme éléments index de la malignité.

De plus en plus les connaissances en biologie moléculaire qui décrivent les caractéristiques génomiques de ces lésions nous apportent des informations que le pathologiste intègre dans son diagnostic. Néanmoins seulement l'analyse intégrée du génome, du transcriptome, du méthylome comparée avec la clinique (évolution, âge et imprégnation hormonale de la patiente) et la morphologie sur un grand nombre de cas, le long des années, associé à la recherche sur des modèles expérimentaux pourra nous permettre de mieux comprendre le développement des lésions mésenchymateuses utérines, de mieux les diagnostiquer et d'améliorer, à long terme, la prise en charge des patientes.

5 ADDENDUM

Durant ces trois années de doctorat j'ai travaillé parallèlement à d'autres sujets toujours focalisés sur les tumeurs mésenchymateuses utérines : les UTROSCT (tumeurs utérines ressemblant les tumeurs des cordons sexuels de l'ovaire) et les sarcomes utérins auparavant classés en fibrosarcomes, associés aux translocations *NTRK* et *COL1A1-PDGFB.*

Il s'agit des tumeurs encore peut caractérisées mais qui de façon de plus en plus évidente sont des sarcomes à génomique simple, drivée par une translocation récurrente.

Received: 18 July 2018 | Revised: 14 October 2018 | Accepted: 16 October 2018
DOI: 10.1002/gcc.22694

WILEY

RESEARCH ARTICLE

GREB1-CTNNB1 fusion transcript detected by RNA-sequencing in a uterine tumor resembling ovarian sex cord tumor (UTROSCT): A novel *CTNNB1* rearrangement

Sabrina Croce[1] | Tom Lesluyes[2,3,4,5] | Lucile Delespaul[3,4] | Benjamin Bonhomme[1] | Gaëlle Pérot[1] | Valérie Velasco[1] | Laetitia Mayeur[1] | Flora Rebier[1] | Houda Ben Rejeb[1] | Frédéric Guyon[6] | W Glenn McCluggage[7] | Anne Floquet[8] | Denis Querleu[3,6] | Camille Chakiba[8] | Mojgan Devouassoux-Shisheboran[9] | Eliane Mery[5] | Laurent Arnould[10] | Gerlinde Averous[11] | Isabelle Soubeyran[1] | Sophie Le Guellec[4,5] | Frédéric Chibon[4,5]

[1]Department of Biopathology, Institut Bergonié, Comprehensive Cancer Center, Bordeaux, France
[2]Comprehensive Cancer Center, INSERM U1218, Institut Bergonié, Bordeaux, France
[3]University of Bordeaux, Bordeaux, France
[4]Cancer Research Center of Toulouse, Oncosarc, INSERM UMR1037, Toulouse, France
[5]Department of Pathology, Institut Claudius Regaud, IUCT-Oncopole, Toulouse, France
[6]Department of Surgery, Institut Bergonié, Comprehensive Cancer Center, Bordeaux, France
[7]Department of Pathology, Belfast Health and Social Care Trust, Belfast, United Kingdom
[8]Department of Oncology, Institut Bergonié, Comprehensive Cancer Center, Bordeaux, France
[9]Department of Pathology, CHU Lyon Sud, Pierrebenite, France
[10]Department of Pathology, Centre JF Leclerc, Comprehensive Cancer Center, Dijon, France
[11]Department of Pathology, CHU Strasbourg, France

Correspondence
Sabrina Croce, Department of Biopathology, Institut Bergonié, Comprehensive anticancer center, 229 cours de l'Argonne, Bordeaux F-33000, France.
Email: s.croce@bordeaux.unicancer.fr

Mutations of *CTNNB1* have been implicated in tumorigenesis in many organs. However, tumors harboring a *CTNNB1* translocation are extremely rare and this translocation has never been reported in a uterine mesenchymal neoplasm. We report a novel translocation t(2;3)(p25;p22) involving the *GREB1* (intron 8) and *CTNNB1* (exon 3) in a uterine tumor resembling ovarian sex cord tumor (UTROSCT), which exhibited extrauterine metastasis. The translocation detected by RNA-sequencing was validated by RT-PCR, and resulted in nuclear expression of β-catenin. Juxtapositioning with *GREB1*, which is overexpressed in response to estrogens, resulted in overexpression of a truncated and hypophosphorylated nuclear β-catenin in the primary and recurrent tumors. This accumulation of nuclear β-catenin results in a constitutive activation of the Wnt/β-catenin signaling pathway with a major oncogenic effect. The *CTNNB1* gene fusion, promoted by an estrogen-responsive gene (*GREB1*), could be a potential driver of tumorigenesis in this case and a therapeutic target with adapted inhibitors. RT-PCR and immunohistochemistry performed on 11 additional UTROSCTs showed no CTNNB1 fusion transcript or nuclear β-catenin immunoreactivity.

KEYWORDS
cytogenetic, molecular biology, pathology, translocation, UTROSCT

1 | INTRODUCTION

Uterine tumor resembling ovarian sex cord tumor (UTROSCT) is a rare mesenchymal neoplasm predominantly arising in perimenopausal and postmenopausal women. The 2014 World Health Organization (WHO) classification of tumors of the female reproductive organs includes these tumors in the category of endometrial stromal and related neoplasms and defines these as "neoplasms that resemble ovarian sex cord tumors without a component of recognizable endometrial stroma".[1] First described in 1976 by Clement and Scully,[2] they

Extraction V10.1.1.1 followed by Agilent Cytogenomic software 4.0. The ADM-2 algorithm of the comparative genomic hybridization (CGH) Analytics v4.0.76 software (Agilent Technologies) was used to identify the DNA copy number anomalies at the probe level. A low-level copy number gain was defined as a log 2 ratio > 0.25 and a copy number loss was defined as a log 2 ratio < −0.25. A high-level gain or amplification was defined as a log 2 ratio > 1.5 and a homozygous deletion was suspected when the ratio was <−1. The range for derivative log ratio spread cut-off was fixed to 0.50.

2.5 | *CTNNB1* exon 3 sequencing

Exon 3 of *CTNNB1* was amplified by PCR; details of the primers are presented in Supporting Information Table S2. The PCR condition included an initial denaturation step at 95°C for 10 minutes, 40 cycles of 95°C denaturation for 30 seconds, 62°C annealing for 45 seconds, 72°C elongation for 45 seconds, and a final elongation step at 72°C for 20 minutes. The quality of the PCR products was analyzed by 2% agarose gel electrophoresis. The PCR products were sequenced using a Big Dye Terminator v3.1 Cycle Sequencing Kit (Applied Biosystems) on a 3130XL Genetic Analyzer (Applied Biosystems) to identify the mutation.

2.6 | β-Catenin immunohistochemistry

Immunohistochemistry was performed on 4 μm thick sections from a representative paraffin block of both the primary and recurrent tumors and on whole tissue sections from the 11 UTROSCTs. Staining was also performed on a tissue microarray (TMA) containing 103 uterine mesenchymal tumors which comprised 31 low-grade ESS, one endometrial stromal nodule, 14 high-grade ESS, 24 undifferentiated uterine sarcomas, 12 leiomyomas, 11 smooth muscle tumors of uncertain malignant potential (STUMP), and 10 leiomyosarcomas. The primary antibody against mouse monoclonal anti-β-catenin (14/β-Catenin clone, from Cell Marque, 760-4242, prediluted) directed against the C-terminus of human β-catenin was incubated for 56 minutes on a Benchmark ULTRA (Roche-Ventana, Tucson, AZ) with detection Kit Optiview DAB IHC (reference: 760-500). Heat-induced antigen retrieval was performed using Cell Ventana Conditioning buffer (CC1 standard), for 64 minutes.

UltraView Ventana was used as revelation system. A desmoid tumor served as a positive external control (nuclear immunoreactivity).

3 | RESULTS

3.1 | Case history and pathological findings

A 70-year-old woman underwent a total hysterectomy with bilateral salpingo-oophorectomy because of a myometrial mass. Gross examination showed a 10 cm yellow, soft and fleshy well-circumscribed myometrial-based mass, which had ruptured the uterine serosa (Figure 1A). Both ovaries and fallopian tubes were grossly normal.

Histologically the myometrial mass comprised a relatively well-circumscribed tumor with a diffuse, tubular, nested, and trabecular growth pattern (Figure 1B). The tumor was composed of epithelioid cells with round to ovoid nuclei and prominent nucleoli. Focally, there was a rhabdoid appearance with eccentric nuclei and abundant eosinophilic cytoplasm (Figure 1C). Elsewhere the tumor cells had clear foamy cytoplasm (Figure 1D). There was little in the way of nuclear atypia and the mitotic rate was low (approximately one mitosis/10 HPF). The tumor cells were set in a fibrous stroma.

The tumor diffusely expressed estrogen receptor (ER), progesterone receptor (PR), and CD10. Desmin, AE1–AE3, epithelial membrane antigen (EMA), CK8/18, calretinin, WT-1, and Melan A were focally positive. H-caldesmon, HMB45, S100, FOXL2, inhibin, myogenin, SALL4, cyclin D1, and BCOR were negative. There was retention of nuclear immunoreactivity with SMARCA4 (BRG1).

The break apart FISH for *JAZF1*, *PHF1*, or *YWHAE* were negative.

The endometrium was atrophic with no hyperplasia or malignancy and the cervix, both ovaries and fallopian tubes were histologically normal.

Based on the morphological features and immunophenotype, a diagnosis of UTROSCT was made.

Seventeen months later, the tumor recurred with widespread pelvic nodules. The patient underwent a posterior exenteration. Morphologically, the tumor was identical to that seen in the original specimen with epithelioid cells in diffuse, corded, and nested arrangements (Figure 1E). The immunophenotype was virtually identical to the original neoplasm. Following the posterior exenteration, the patient was treated with aromatase inhibitors but the tumor did not respond. She developed lung metastases and abdominal peritoneal recurrence a year later.

The original and recurrent neoplasms were reviewed by two gynecological pathologists (SC, WGM) and the diagnosis of UTROSCT confirmed.

The samples from the tumor archives have been declared in the Biological Resources Center of Institut Bergonié, for which the French authorities authorized for scientific research (AC-2008-812) and the patient signed an informed consent for research.

3.2 | RNA-sequencing, CGH analysis and immunohistochemical results

RNA-sequencing on the initial index case identified a fusion transcript *GREB1-CTNNB1* as a product of the translocation t(2;3)(p25; p22). No other in frame rearrangements was detected. This fusion transcript was validated by RT-PCR with specific primers (Table S1, Supporting Information) and was detected in the primary tumor and in the recurrence (Figure 2A). No reciprocal transcript was detected in both (data not shown). The Sanger sequencing analysis of the amplified fusion transcript showed a chimeric transcript consisting of the first eight exons (of 32) plus a small part of intron 8 of *GREB1* gene (NM_014668) and the end of exon 3 of *CTNNB1* gene until its 3′ end. (NM_001098209) (Figure 2B and C). This produces a stop codon in intron 8 of *GREB1*, leading to no or truncated GREB1 protein. It also produces a start codon at the beginning of the exon 4 of *CTNNB1*.The *GREB1-CTNNB1* fusion transcript codes for a truncated form of β-catenin without the 87 N-terminal amino acids that are involved in the protein degradation upon phosphorylation (Refs. 20,21; Figure 2D).

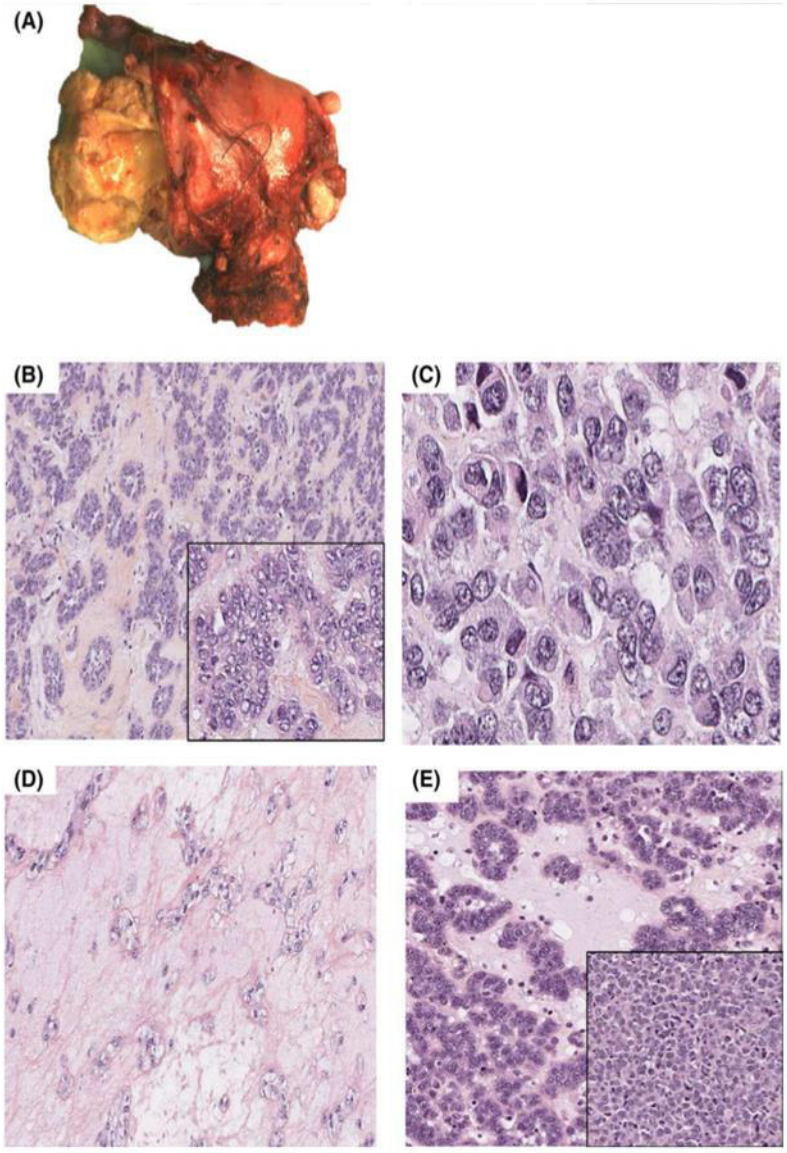

FIGURE 1 A, The UTROSCT comprises a large fleshy soft yellow myometrial mass. B, The primary tumor is composed of epithelioid cells with round nuclei and prominent nucleoli arranged in nested, trabecular, and tubular arrangements. C, Rhabdoid appearance with eccentric nuclei and abundant eosinophilic cytoplasm. D, Occasional cells have foamy cytoplasm. E, Morphologic features of the recurrent tumor that are similar to the primary neoplasm with diffuse, nested, and corded arrangements [Color figure can be viewed at wileyonlinelibrary.com]

Array-CGH performed on the primary tumor and the recurrence showed a very simple profile for the primary tumor (Figure 2E) without evidence of break in chromosome band 2p25 (*GREB1* gene) or in chromosome band 3p22 (*CTNNB1* gene). A more complex genomic profile was observed in the recurrence (Figure 2F) with evidence of breakpoints in chromosome band 3p22 and 2p25 involving both rearranged genes.

Immunohistochemistry was performed to evaluate whether this translocation resulted in overexpression of nuclear β-catenin. This showed strong nuclear positivity in the primary tumor (Figure 3A), as well as in the recurrence (Figure 3B). To rule out the possibility that the nuclear accumulation was caused by *CTNNB1* mutation, we performed Sanger sequencing of exon 3 and observed no β-catenin mutation.

We then performed GSEA between the primary tumor and surrounding normal tissue (adjacent myometrium) (see Section 2). We observed a higher expression of genes belonging to the Wnt/β-catenin signaling pathway in the tumor compared to the surrounding myometrium (FDR q-value = 1.79e-2; Figure 4A). In addition, genes whose proteins interact (selectively and non covalently) with Wnt-protein were also overexpressed in the tumor (FDR q-value = 2.34e-2; Figure 4B). We also observed, using the same method, a lower level

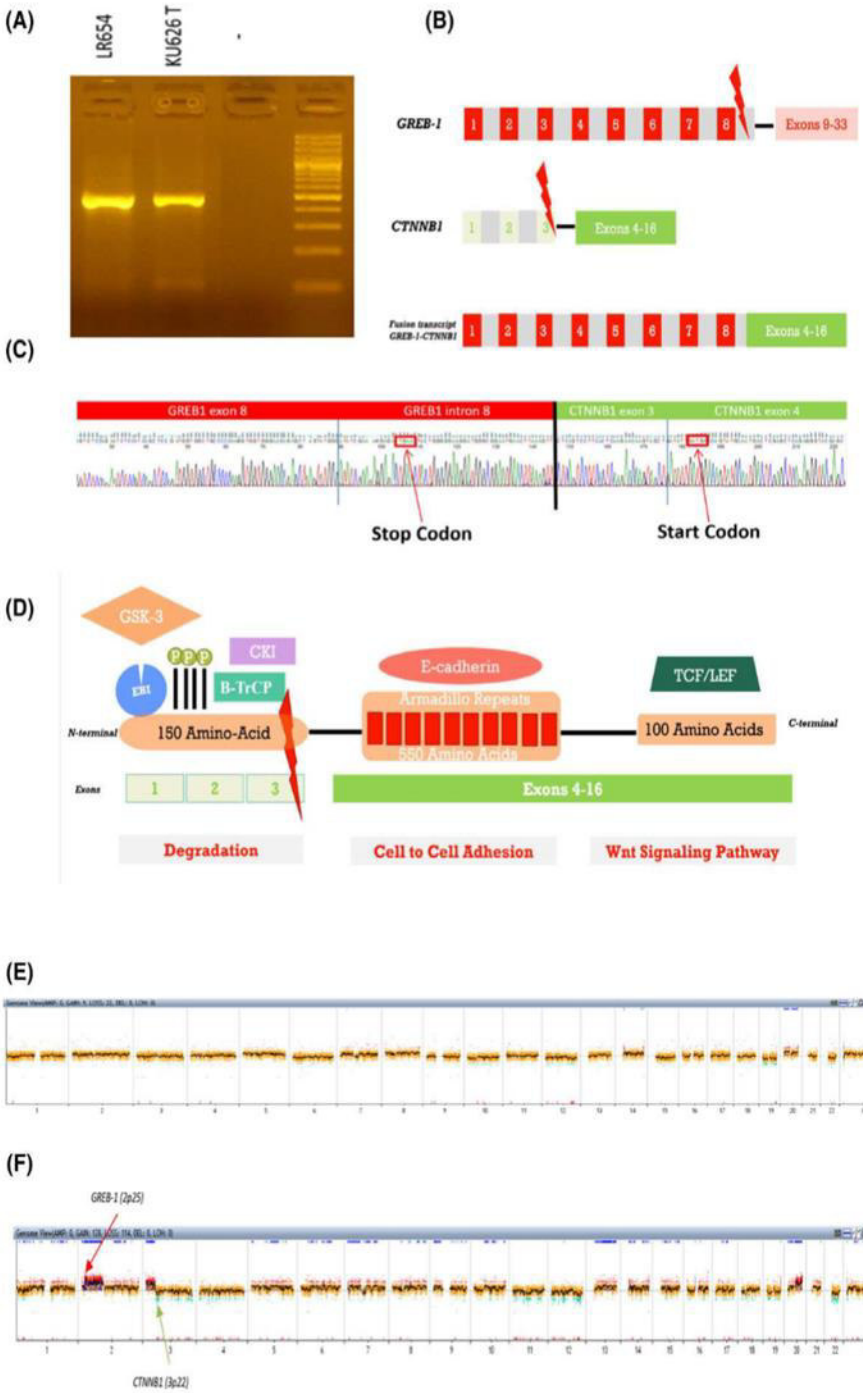

FIGURE 2 A, RT-PCR obtained for GREB1-CTNNB1 chimeric transcript. KU626T: primary tumor; LR 654: recurrence; -: lymphocyte negative control. B, Schematic representation of *GREB1* and *CTNNB1* genes and fusion transcript. *GREB1* and *CTNNB1* exons implicated in translocation are indicated in red and green, respectively. Exons implicated in translocation are shown in light color. Fusion point is represented with a red lightning. C, Partial chromatography electropherogram showing the junction point between intron 8 of *GREB1* gene and exon 4 of *CTNNB1* gene. *GREB1* and *CTNNB1* exons are indicated in red and green, respectively. Point fusion is indicated with black line. D, Primary structure of chimeric protein (*modified from* Ref. 41). Break point is represented with a red lightning. Different partners of *CTNNB1* are indicated. The corresponding exons to different *CTNNB1* domains are represented at bottom of *CTNNB1* protein domains. E, Array-CGH of the primary tumor showing a flat profile. Absence of evidence of breakpoint on *CTNNB1* (Ch 3p22) or *GREB1* (Ch2 p25) genes. F, Array-CGH of recurrence showing a breakpoint on chr 3p22 with *CTNNB1* gene [Color figure can be viewed at wileyonlinelibrary.com]

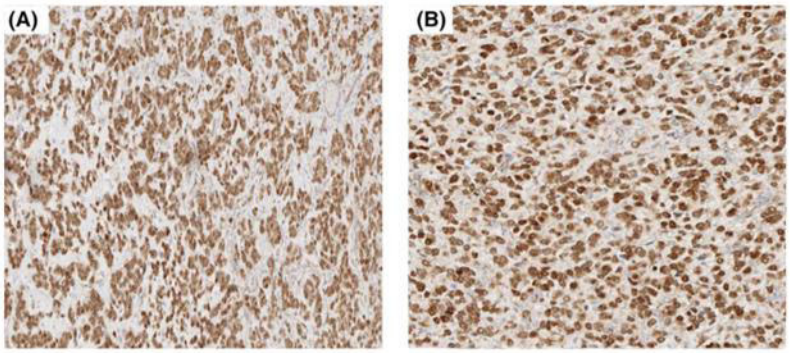

FIGURE 3 A, β catenin nuclear staining in the primary tumor. B, β catenin nuclear staining in the recurrent tumor [Color figure can be viewed at wileyonlinelibrary.com]

of early (Figure 4C) and late (Figure 4D) estrogen response genes (*GREB-1* gene being one of those genes) in the tumor sample as compared with the normal adjacent myometrium.

We performed specific RT-PCR and β-catenin immunohistochemistry in the additional 11 UTROSCTs and observed no fusion transcript or nuclear immunoreactivity (data not shown). In the TMA of 103 uterine mesenchymal tumors, there was no nuclear expression of β-catenin except for a single undifferentiated uterine sarcoma which exhibited nuclear and cytoplasmic immunoreactivity (Supporting Information Figure S1).

4 | DISCUSSION

We report the first case of specific gene fusion in a UTROSCT, namely the *GREB1-CTNNB1* fusion transcript as a product of the translocation t(2;3)(p25;p22). The diagnosis of UTROSCT was established on the basis of the characteristic morphology and a supportive polyphenotypic immunophenotype with expression of CD10, hormone receptors (ER, PR), desmin, epithelial markers and markers which are commonly positive in ovarian sex cord-stromal tumors, including calretinin, WT-1, and Melan A. Inhibin and FOXL2 were negative but these markers are not positive in all UTROSCTs.[10,12]

UTROSCT was originally described as a neoplasm of uncertain but low malignant potential which usually exhibits a benign behavior.[2] In a recent series, one of us (WGM) coauthored the largest published series of cases with follow-up[10]; in that series, 8 of 34 (23.5%) cases, including the index case in this article, exhibited malignant behavior with extrauterine spread. It is possible that the *GREB1-CTNNB1* fusion transcript in this case contributed to the aggressive behavior. Array-CGH showed a very simple genomic profile of the primary tumor and, consonant with the behavior, a more complex profile for the recurrence with evidence of breakpoints in chromosome band 3p22 and 2p25 involving both rearranged genes. This fusion was not found in the series of 11 additional UTROSCTs tested by RT-PCR. There has been limited study of the molecular abnormalities in UTROSCT but in a prior study coauthored by two of us (SC, WGM), mutations in *FOXL2* and *DICER1* were not identified[12]; these mutations are characteristic of ovarian adult granulosa cell tumor and Sertoli-Leydig cell tumor respectively, two neoplasms with morphological and immunophenotypic overlap with UTROSCT.

β-Catenin protein, encoded by the *CTNNB1* gene, is implicated in the canonical Wnt signaling pathway which modulates cell proliferation, cell polarity and differentiation during embryonic development, and regulates the cell-cell adhesion, extra-cellular signals and gene transcription.[21] Wnt-induced β-catenin stabilization and nuclear shuttling results in the T-cell factor/lymphoid enhancer factor (TCF) family of proteins forming a complex with β-catenin, which recruits other coactivators for gene activation via displacement of Groucho.[22,23] β-Catenin acts as a coactivator for TCF and with its transactivation domain activates transcription initiation, histone methyltransferases, histone modification, chromatin modification, and facilitates transcription.[23]

Mutations (in particular in exon 3) are the most frequent mechanisms of alteration in *CTNNB1*, affecting the ubiquitination and resulting in hypophosphorylated β-catenin accumulation and translocation in the nucleus. The resultant effect is the constitutive activation of the Wnt/β-catenin signaling pathway and reprogramming of downstream nuclear transcriptional networks.[24–27] Although some tumors have been reported to harbor 3p21 breakpoints, according to the Mitelman Database of Chromosome Aberrations and Gene Fusions in Cancer (http://cgap.nci.nih.gov/Chromosomes/Mitelman), translocations involving *CTNNB1* are extremely rare[28–30]; the only well-characterized translocation in the literature with *CTNNB1* as a specific partner until now is the t(3;8)(p21;q12) involving *CTNNB1* and *PLAG1* genes in pleomorphic salivary adenoma[31,32]; this translocation results in the activation of *PLAG1* and reduced expression of β-catenin. To our knowledge, t(2;3)(p25;p22) involving *GREB1* and *CTNNB1* has never been reported. Unlike the *CTNNB1-PLAG1* fusion, the chimeric transcript results in the overexpression of β-catenin via excision of the first three exons of *CTNNB1*, wherein the serine phosphorylation sites and the GSK3, CK1 binding sites (Figure 2D), responsible for the degradation of β-catenin, are located.[33] *GREB1* gene, the partner of *CTNNB1* in this fusion, is rearranged in some other types of neoplasia such as T-cell acute lymphoblastic leukemia[34] and prostate carcinoma,[30] and recently rearrangement has been demonstrated in an undifferentiated uterine sarcoma.[35] In our case, given the modality

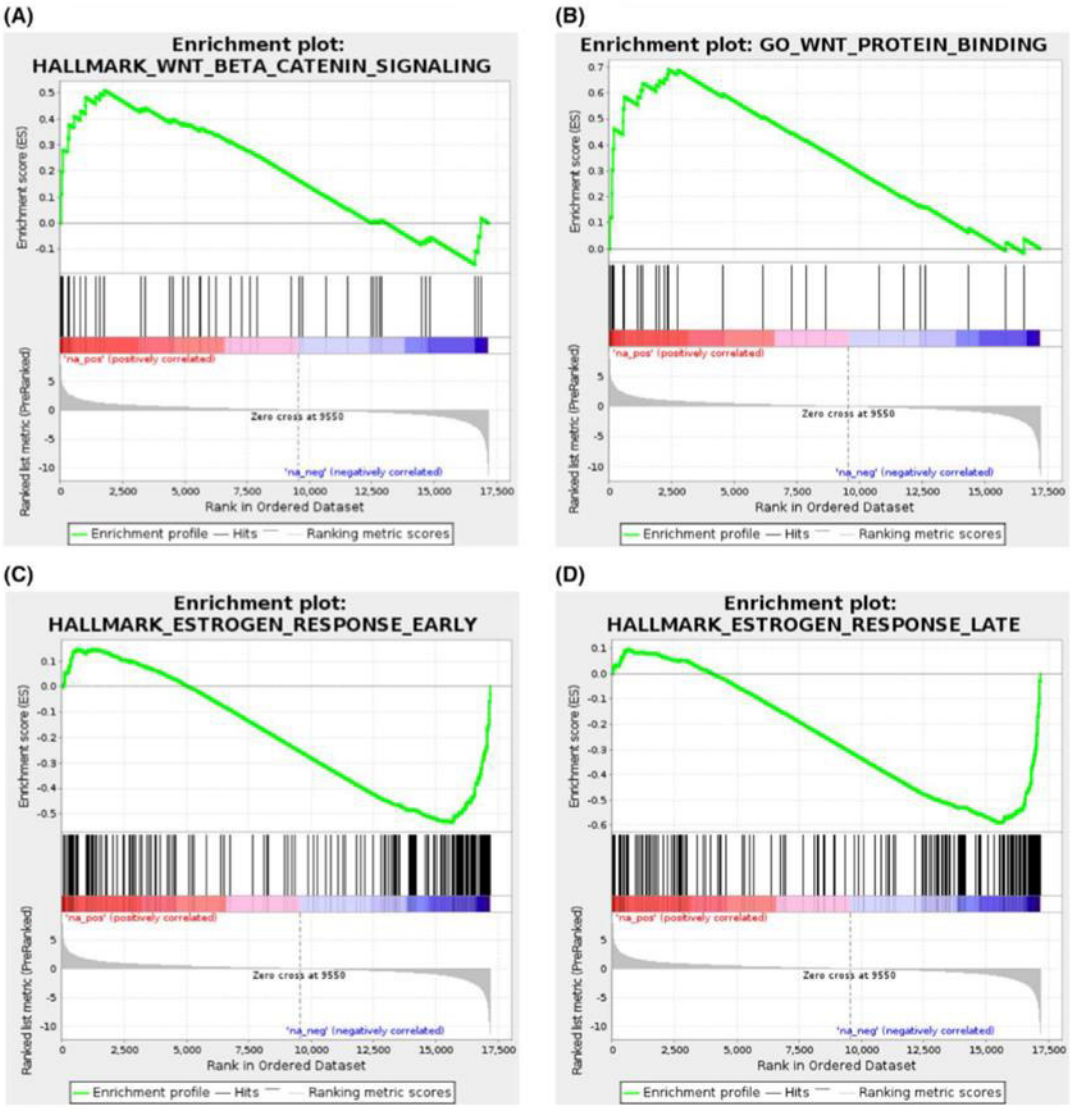

FIGURE 4 A, Gene set enrichment analysis of tumor ("na_pos" on the left side) versus normal adjacent myometrium ("na_neg" on the right side) transcriptomic profiles. This identified an overexpression of genes involved in the Wnt/β-catenin signaling pathway (FDR q-value = 1.79e-2) in the tumor compared to peripheral normal tissues. B, Gene set enrichment analysis of tumor ("na_pos" on the left side) versus normal adjacent myometrium ("na_neg" on the right side) transcriptomic profiles. This indicates an overexpression of genes whose proteins interact (selectively and non covalently) with Wnt-protein (FDR q-value = 2.34e-2) in the tumor compared to peripheral normal tissues. C, Gene set enrichment analysis of normal adjacent myometrium ("na_pos" on the left side) versus tumor ("na_neg" on the right side) transcriptomic profiles. The graph indicates underexpression of genes related to the early response to estrogens in the tumor compared to the peripheral normal tissue. D, Gene set enrichment analysis of normal adjacent myometrium ("na_pos" on the left side) versus tumor ("na_neg" on the right side) transcriptomic profiles. The graph indicates underexpression of genes related to the late response to estrogens in the tumor compared to the peripheral normal tissue [Color figure can be viewed at wileyonlinelibrary.com]

of the rearrangement resulting in a truncated form of *GREB1* in the transcript fusion (Figure 2B), we can assume that GREB1 protein is not synthesized and that the oncogenic effect is driven by truncated β-catenin expression. Nevertheless, this gene has an important role in promoting mRNA expression as it is highly expressed in estrogen-related tissues.[36,37] Furthermore, in our case, we observed that the normal myometrium expressed more of the early (Figure 4C) and late (Figure 4D) estrogen-response genes than the tumor suggesting a

diminution of GREB1 expression. This observation could explain the poor response of the tumor to antihormone therapy (aromatase inhibitors) and the high expression of the translocated β-catenin, under the transcriptomic control of GREB1 promoter.

The nuclear localization of β-catenin as result of *GREB1-CTNNB1* rearrangement was confirmed by immunohistochemistry in the primary tumor and in the recurrence. There was no nuclear expression in the additional 11 UTROSCTs and in the TMA series of 103 uterine mesenchymal tumors with the exception of one undifferentiated uterine sarcoma which exhibited nuclear and cytoplasmic immunoreactivity.

The main limitation of this study is the absence of a cellular model derived from the tumor. Such a model would allow demonstration of the effects of *GREB1-CTNNB1* gene fusion on cellular proliferation and investigation of its driver role in the genesis of this tumor. A possible significance of the *CTNNB1* rearrangement is that β-catenin could be a possible therapeutic target in this tumor. Prior studies have demonstrated inhibition of tumor proliferation in pancreatic neuroendocrine tumors,[38] acute myeloid leukemia,[39] breast and prostate cancer with β-catenin inhibitors.[40]

In summary, we report a novel translocation t(2;3)(p25;p22) involving *GREB1* (intron 8) and *CTNNB1* (exon 3) genes in a UTROSCT. This is the first report of this specific gene fusion in a mesenchymal tumor and in a UTROSCT.

ACKNOWLEDGMENTS

We are grateful to the genotoul bioinformatics platform Toulouse Midi-Pyrenees (Bioinfo Genotoul) for providing help and/or computing and/or storage resources and the "Comité Prévention et Dépistage des Cancers" for founding the purchase of TMA arrayer.

The authors would like to thank Dr Ravi Nookala of Institut Bergonié for the medical writing service.

CONFLICT OF INTEREST

The authors declare that they have no conflict of interests with the contents of this article.

ORCID

Sabrina Croce https://orcid.org/0000-0002-6487-5418
Sophie Le Guellec https://orcid.org/0000-0003-3207-0081
Frédéric Chibon https://orcid.org/0000-0002-6548-2181

REFERENCES

1. Oliva ECM, Carinelli SG, et al. Mesenchymal tumors. Uterine tumour resembling ovarian sex cord tumour. In: CM KRJ, Herrington CS, Young RH, eds. Lyon, France: *WHO Classification of Tumours of Female Reproductive Organs*. 2014:141-147.
2. Clement PB, Scully RE. Uterine tumors resembling ovarian sex-cord tumors. A clinicopathologic analysis of fourteen cases. *Am J Clin Pathol*. 1976;66(3):512-525.
3. Hurrell DP, McCluggage WG. Uterine tumour resembling ovarian sex cord tumour is an immunohistochemically polyphenotypic neoplasm which exhibits coexpression of epithelial, myoid and sex cord markers. *J Clin Pathol*. 2007;60(10):1148-1154.
4. Irving JA, Carinelli S, Prat J. Uterine tumors resembling ovarian sex cord tumors are polyphenotypic neoplasms with true sex cord differentiation. *Mod Pathol*. 2006;19(1):17-24.
5. de Leval L, Lim GS, Waltregny D, Oliva E. Diverse phenotypic profile of uterine tumors resembling ovarian sex cord tumors: an immunohistochemical study of 12 cases. *Am J Surg Pathol*. 2010;34(12):1749-1761.
6. Czernobilsky B. Uterine tumors resembling ovarian sex cord tumors: an update. *Int J Gynecol Pathol*. 2008;27(2):229-235.
7. Krishnamurthy S, Jungbluth AA, Busam KJ, Rosai J. Uterine tumors resembling ovarian sex-cord tumors have an immunophenotype consistent with true sex-cord differentiation. *Am J Surg Pathol*. 1998;22(9):1078-1082.
8. Baker RJ, Hildebrandt RH, Rouse RV, Hendrickson MR, Longacre TA. Inhibin and CD99 (MIC2) expression in uterine stromal neoplasms with sex-cord-like elements. *Hum Pathol*. 1999;30(6):671-679.
9. Bakula-Zalewska E, Danska-Bidzinska A, Kowalewska M, Piascik A, Nasierowska-Guttmejer A, Bidzinski M. Uterine tumors resembling ovarian sex cord tumors, a clinicopathologic study of six cases. *Ann Diagn Pathol*. 2014;18(6):329-332.
10. Moore M, McCluggage WG. Uterine tumour resembling ovarian sex cord tumour (UTROSCT): first report of a large series with follow-up. *Histopathology*. 2017;71:751-759.
11. Chiang S, Staats PN, Senz J, et al. FOXL2 mutation is absent in uterine tumors resembling ovarian sex cord tumors. *Am J Surg Pathol*. 2015;39(5):618-623.
12. Croce S, de Kock L, Boshari T, et al. Uterine tumor resembling ovarian sex cord tumor (UTROSCT) commonly exhibits positivity with sex cord markers FOXL2 and SF-1 but lacks FOXL2 and DICER1 mutations. *Int J Gynecol Pathol*. 2016;35(4):301-308.
13. Wang J, Blakey GL, Zhang L, Bane B, Torbenson M, Li S. Uterine tumor resembling ovarian sex cord tumor: report of a case with t(X;6)(p22.3;q23.1) and t(4;18)(q21.1;q21.3). *Diagn Mol Pathol*. 2003;12(3):174-180.
14. Staats PN, Garcia JJ, Dias-Santagata DC, et al. Uterine tumors resembling ovarian sex cord tumors (UTROSCT) lack the JAZF1-JJAZ1 translocation frequently seen in endometrial stromal tumors. *Am J Surg Pathol*. 2009;33(8):1206-1212.
15. D'Angelo E, Ali RH, Espinosa I, et al. Endometrial stromal sarcomas with sex cord differentiation are associated with PHF1 rearrangement. *Am J Surg Pathol*. 2013;37(4):514-521.
16. McPherson A, Hormozdiari F, Zayed A, et al. deFuse: an algorithm for gene fusion discovery in tumor RNA-Seq data. *PLoS Comput Biol*. 2011;7(5):e1001138.
17. Lesluyes T, Perot G, Largeau MR, et al. RNA sequencing validation of the complexity INdex in SARComas prognostic signature. *Eur J Cancer*. 2016;57:104-111.
18. Subramanian A, Tamayo P, Mootha VK, et al. Gene set enrichment analysis: a knowledge-based approach for interpreting genome-wide expression profiles. *Proc Natl Acad Sci USA*. 2005;102(43):15545-15550.
19. Liberzon A, Subramanian A, Pinchback R, Thorvaldsdottir H, Tamayo P, Mesirov JP. Molecular signatures database (MSigDB) 3.0. *Bioinformatics*. 2011;27(12):1739-1740.
20. Liberzon A, Birger C, Thorvaldsdottir H, Ghandi M, Mesirov JP, Tamayo P. The molecular signatures database (MSigDB) hallmark gene set collection. *Cell Syst*. 2015;1(6):417-425.
21. Logan CY, Nusse R. The Wnt signaling pathway in development and disease. *Annu Rev Cell Dev Biol*. 2004;20:781-810.
22. Daniels DL, Weis WI. Beta-catenin directly displaces Groucho/TLE repressors from Tcf/Lef in Wnt-mediated transcription activation. *Nat Struct Mol Biol*. 2005;12(4):364-371.
23. MacDonald BT, Tamai K, He X. Wnt/beta-catenin signaling: components, mechanisms, and diseases. *Dev Cell*. 2009;17(1):9-26.
24. Korinek V, Barker N, Morin PJ, et al. Constitutive transcriptional activation by a beta-catenin-Tcf complex in $APC^{-/-}$ colon carcinoma. *Science*. 1997;275(5307):1784-1787.
25. Morin PJ, Sparks AB, Korinek V, et al. Activation of beta-catenin-Tcf signaling in colon cancer by mutations in beta-catenin or APC. *Science*. 1997;275(5307):1787-1790.

26. Xia J, Urabe K, Moroi Y, et al. beta-Catenin mutation and its nuclear localization are confirmed to be frequent causes of Wnt signaling pathway activation in pilomatricomas. *J Dermatol Sci*. 2006;41(1):67-75.
27. Lax SF. Molecular genetic pathways in various types of endometrial carcinoma: from a phenotypical to a molecular-based classification. *Virchows Arch*. 2004;444(3):213-223.
28. Guseva NV, Jaber O, Tanas MR, et al. Anchored multiplex PCR for targeted next-generation sequencing reveals recurrent and novel USP6 fusions and upregulation of USP6 expression in aneurysmal bone cyst. *Genes Chromosomes Cancer*. 2017;56(4):266-277.
29. Liu Y, Easton J, Shao Y, et al. The genomic landscape of pediatric and young adult T-lineage acute lymphoblastic leukemia. *Nat Genet*. 2017;49(8):1211-1218.
30. Yoshihara K, Wang Q, Torres-Garcia W, et al. The landscape and therapeutic relevance of cancer-associated transcript fusions. *Oncogene*. 2015;34(37):4845-4854.
31. Kas K, Voz ML, Roijer E, et al. Promoter swapping between the genes for a novel zinc finger protein and beta-catenin in pleiomorphic adenomas with t(3;8)(p21;q12) translocations. *Nat Genet*. 1997;15(2):170-174.
32. Kas K, Voz ML, Hensen K, Meyen E, Van de Ven WJ. Transcriptional activation capacity of the novel PLAG family of zinc finger proteins. *J Biol Chem*. 1998;273(36):23026-23032.
33. Fukuchi T, Sakamoto M, Tsuda H, Maruyama K, Nozawa S, Hirohashi S. Beta-catenin mutation in carcinoma of the uterine endometrium. *Cancer Res*. 1998;58(16):3526-3528.
34. Atak ZK, Gianfelici V, Hulselmans G, et al. Comprehensive analysis of transcriptome variation uncovers known and novel driver events in T-cell acute lymphoblastic leukemia. *PLoS Genet*. 2013;9(12):e1003997.
35. Brunetti M, Panagopoulos I, Gorunova L, Davidson B, Heim S, Micci F. RNA-sequencing identifies novel GREB1-NCOA2 fusion gene in a uterine sarcoma with the chromosomal translocation t(2;8)(p25;q13). *Genes Chromosomes Cancer*. 2018;57(4):176-181.
36. Camden AJ, Szwarc MM, Chadchan SB, et al. Growth regulation by estrogen in breast cancer 1 (GREB1) is a novel progesterone-responsive gene required for human endometrial stromal decidualization. *Mol Hum Reprod*. 2017;23(9):646-653.
37. Pellegrini C, Gori I, Achtari C, et al. The expression of estrogen receptors as well as GREB1, c-MYC, and cyclin D1, estrogen-regulated genes implicated in proliferation, is increased in peritoneal endometriosis. *Fertil Steril*. 2012;98(5):1200-1208.
38. Jiang X, Cao Y, Li F, et al. Targeting beta-catenin signaling for therapeutic intervention in MEN1-deficient pancreatic neuroendocrine tumours. *Nat Commun*. 2014;5:5809.
39. Fiskus W, Sharma S, Saha S, et al. Pre-clinical efficacy of combined therapy with novel beta-catenin antagonist BC2059 and histone deacetylase inhibitor against AML cells. *Leukemia*. 2015;29(6):1267-1278.
40. Lu W, Li Y. Salinomycin suppresses LRP6 expression and inhibits both Wnt/beta-catenin and mTORC1 signaling in breast and prostate cancer cells. *J Cell Biochem*. 2014;115(10):1799-1807.
41. Gao C, Wang Y, Broaddus R, Sun L, Xue F, Zhang W. Exon 3 mutations of CTNNB1 drive tumorigenesis: a review. *Oncotarget*. 2018;9(4):5492-5508.

SUPPORTING INFORMATION

Additional supporting information may be found online in the Supporting Information section at the end of the article.

How to cite this article: Croce S, Lesluyes T, Delespaul L, et al. *GREB1-CTNNB1* fusion transcript detected by RNA-sequencing in a uterine tumor resembling ovarian sex cord tumor (UTROSCT): A novel *CTNNB1* rearrangement. *Genes Chromosomes Cancer*. 2019;58:155–163. https://doi.org/10.1002/gcc.22694

Modern Pathology
https://doi.org/10.1038/s41379-018-0184-6

ARTICLE

Uterine and vaginal sarcomas resembling fibrosarcoma: a clinicopathological and molecular analysis of 13 cases showing common *NTRK*-rearrangements and the description of a *COL1A1-PDGFB* fusion novel to uterine neoplasms

Sabrina Croce[1,2] · Isabelle Hostein[1] · Teri A. Longacre[3] · Anne M. Mills[4] · Gaëlle Pérot[1] · Mojgan Devouassoux-Shisheboran[5] · Valérie Velasco[1] · Anne Floquet[6] · Frédéric Guyon[7] · Camille Chakiba[6] · Denis Querleu[7] · Emmanuel Khalifa[1] · Laetitia Mayeur[1] · Flora Rebier[1] · Sophie Leguellec[8] · Isabelle Soubeyran[1] · W. Glenn McCluggage[9]

Received: 19 September 2018 / Revised: 2 November 2018 / Accepted: 2 November 2018

Abstract

Mesenchymal neoplasms of the uterus (corpus and cervix) encompass a heterogeneous group of tumors with differing morphologies, immunophenotypes and molecular alterations. With the advent of modern molecular techniques, such as next generation sequencing, newly defined genetic abnormalities are being reported in this group of neoplasms. Herein we report the clinicopathological and molecular features of a series of 13 spindle cell sarcomas of the uterus and vagina (10 cervix, 2 uterine corpus, 1 vagina) with morphology resembling fibrosarcoma. After targeted RNA-sequencing, dual FISH fusion and array-CGH analysis, 7 of 13 tumors exhibited *NTRK* rearrangements (6 *TPM3-NTRK1* and 1 *EML4-NTRK3*) and 3 a *COL1A1-PDGFB* fusion; in the other 3 neoplasms, all of which were positive with S100 (2 diffuse, 1 focal), we identified no rearrangement. All the *NTRK* fusion-positive sarcomas were located in the cervix and exhibited diffuse staining with Trk while all the other neoplasms were negative. CD34 was diffusely positive in all 3 of the *COL1A1-PDGFB* fusion sarcomas. The latter molecular abnormality is identical to that commonly found in dermatofibrosarcoma protuberans and has not been reported previously in uterine mesenchymal neoplasms. We suggest that uterine sarcomas with a morphology resembling fibrosarcoma (and in which leiomyosarcoma and the known molecularly confirmed high-grade endometrial stromal sarcomas have been excluded) can be divided into 3 groups:- an *NTRK* fusion group, a *COL1A1-PDGFB* fusion group and a group containing neither of these molecular abnormalities which, on the basis of positive staining with S100, could be tentatively classified as malignant peripheral nerve sheath tumor, although additional molecular studies may identify specific genetic alterations necessitating a nomenclature change. We suggest a diagnostic algorithm when reporting such neoplasms. Identification of these newly described fusion-associated sarcomas is important given the potential for targeted treatments.

Electronic supplementary material The online version of this article (https://doi.org/10.1038/s41379-018-0184-6) contains supplementary material, which is available to authorized users.

✉ W. Glenn McCluggage
glenn.mccluggage@belfasttrust.hscni.net

[1] Department of Biopathology, Institut Bergonié, Comprehensive Cancer Center, Bordeaux, France

[2] Unité INSERM U1218, Bordeaux, France

[3] Department of Surgical Pathology, Stanford University School of Medicine, Stanford, CA, USA

[4] Department of Pathology, University of Virginia School of Medicine, Charlottesville, VA, USA

[5] Department of Pathology, CHU Lyon Sud, Pierrebenite, France

[6] Department of Oncology, Institut Bergonié, Comprehensive Cancer Center, Bordeaux, France

[7] Department of Surgery, Institut Bergonié, Comprehensive Cancer Center, Bordeaux, France

[8] Department of Pathology, Institut Claudius Regaud, IUCT-Oncopole, Toulouse, France

[9] Department of Pathology, Belfast Health and Social Care Trust, Belfast, UK

Published online: 16 March 2019

Introduction

Mesenchymal neoplasms of the uterus (corpus and cervix) encompass a heterogeneous group of tumors with differing morphologies and immunophenotypes. The most common malignant mesenchymal neoplasms are leiomyosarcoma, low-grade and high-grade endometrial stromal sarcoma (*YWHAE or BCOR* rearranged), and undifferentiated sarcoma [1]. A variety of other malignant mesenchymal neoplasms occur rarely within the uterus, including malignant peripheral nerve sheath tumors which are most common in the cervix [2–4]. In 2011, 2 of us (TAL, AMM) coauthored a report of 3 cases of a rare malignant cervical mesenchymal neoplasm which was termed endocervical fibroblastic malignant peripheral nerve sheath tumor (neurofibrosarcoma) [5]; these cervical neoplasms were composed of fascicles of spindle cells arranged in herringbone, fascicular, and storiform patterns and were positive with S100 and CD34 [5].

Recently a series of 4 uterine mesenchymal neoplasms harboring *NTRK (Neurotropic Tyrosine Receptor kinase)* rearrangements was reported [6]. These neoplasms were described as having morphological features resembling fibrosarcoma and exhibited brisk mitotic activity and sometimes focal necrosis; immunohistochemically, there was variable expression of smooth muscle actin and S100, while SOX10, estrogen receptor (ER), progesterone receptor (PR), desmin, and CD34 were negative [6]. The 4 neoplasms expressed Trk (Tropomyosin Related Kinase) and harbored *NTRK* rearrangements (*RBPMS-NTRK3, TPR-NTRK1, LMNA-NTRK1, and TPM3-NTRK1*) [6]. The authors noted that endocervical fibroblastic malignant peripheral nerve sheath tumors bore some morphological and immunohistochemical resemblance to the neoplasms they reported and speculated that the former may represent *NTRK* fusion-positive uterine sarcomas.

Herein we report the clinicopathological and molecular features of a series of 13 spindle cell sarcomas of the uterus and vagina (10 cervix, 2 corpus, 1 vagina) with features resembling fibrosarcoma. We investigated these for *NTRK* abnormalities and show that *NTRK* rearrangements are common in these neoplasms. We also report the *COL1A1-PDGFB* fusion in a subset of these tumors; as far as we are aware, this fusion has not previously been reported in uterine mesenchymal neoplasms.

Materials and methods

Case selection

Thirteen tumors were derived from the in-house material and consultation practice of the pathology departments to which the authors are affiliated. The cases had all been diagnosed as malignant peripheral nerve sheath tumor or as undifferentiated sarcoma composed of uniform cells and resembling fibrosarcoma. The cases included the 3 originally reported endocervical fibroblastic malignant peripheral nerve sheath tumors (neurofibrosarcoma) [5]. Ten tumors were located in the cervix, 2 in the corpus and 1 in vagina. For two cases (10 and 12), we analyzed the primary tumor and the recurrence. Leiomyosarcomas, endometrial stromal sarcomas (low-grade and high-grade) and undifferentiated sarcomas composed predominantly of pleomorphic cells were not included in the study. All available slides were reviewed by two of the authors (SC and WGM); in consultation cases, often all of the slides were not available for examination.

Immunohistochemistry

Immunohistochemistry for Trk was performed on 4 micron thick sections. The primary antibody was a rabbit monoclonal anti- Trk (pan) covering Trk A, B and C (clone A7H6R, 92991 S, Ozyme, Cell Signaling). A dilution of 1/50 was used with 52 min incubation on a Benchmark ULTRA (Roche-Ventana, Tucson, AZ) and detection Kit Optiview DAB IHC (reference: 760-500). Heat-induced antigen retrieval was performed using Cell Ventana Conditioning buffer (CC1 standard) for 64 min. An infantile fibrosarcoma with a known *NTRK* fusion served as a positive external control.

A variety of other immunohistochemical stains were also undertaken. Most of these were performed at the various institutions during the original reporting of the neoplasms while others were undertaken during the preparation of this manuscript.

RNA Extraction and RNA-Sequencing

RNA was extracted from 14 macrodissected formalin fixed paraffin embedded tumor blocks according to the protocol Maxwell® RSC RNA formalin fixed paraffin embedded Kit (Promega®); in 1 case (case 13), sequencing was not performed. Tumor cell percentage varied from 20% to 80% (mean value 72%). Total RNA (200 to 250 ng) was reverse transcribed to cDNA. Libraries were prepared using the CTL FusionPlex Assay for Illumina Platform (ArcherDx®) following the manufacturer's Protocol [7] and sequenced using MiSeq (Illumina, San Diego, CA).

Data were analyzed using the CTL Target Region File and vendor supplied software (Archer Analysis, version 5.0). A minimum of 5 reads with 3 unique sequencing start sites that cross the breakpoints was set as the cutoff value to indicate strong evidence of fusions. The percentage of fusion reads is calculated as following: only reads spanning

Table 1 Primer Sequences for Sanger Sequencing

Sens primer name	Forward	Reverse primer name	Reverse
TPM3_6+	5′-TGAGAGATCGGTAGCCAAGC-3′	*NTRK1-*	5'-AGAAAGGAAGAGGCAGGCAA-3'
TPM3_4+	5′-GAACGCACAGAGAGGAACGAG-3′	*NTRK1-*	5'-AGAAAGGAAGAGGCAGGCAA-3'
EML4-2+	5′-TGATGTTTTGAGGCGTCTTG-3′	*NTRK3_4-*	5'-ACG GAA GTA CTG GGG GTT CT-3'
BETA2m+	5′- TGACTTTGTCACAGCCCAAGATA -3'	*BETA2m-*	5'-AAT CCA AAT GCG GCA TCT TC -3'

the breakpoint are considered to support the fusion/isoform. The percentage is calculated in reference to the total number of reads intersecting the genomic locations on either side of the primary breakpoint, restricted to RNA reads for RNA workflows. Paired reads where both reads completely cover only one of the genes are not considered as supporting a gene fusion. The cutoff is defined as 10%.

Reverse transcriptase PCR (RT-PCR) and sanger sequencing for chimeric transcript validation

From 100 ng to 1 µg RNA were reverse transcribed with the expand reverse transcriptase (Roche) with the specific complementary reverse PCR primers (Table 1). PCR products were then amplified with the Platinum™ Taq DNA Polymerase (Invitrogen™) with the thermal cycling profile of 95 °C for 10 min, then 35 cycles of 95 °C for 30 s, 58 °C for 45 s, 72 °C for 45 s, with a final extension at 72 °C for 10 min. Direct sequencing was performed with the same primers using the Big-Dye DyeDeoxy terminator cycle sequencing kit (Applied Biosystems, Foster City, CA). Sequencing reactions were carried out on the ABI Prism 3100 Genetic Analyzer (Applied Biosystems, Foster City, CA).

DNA extraction and array-comparative genomic hybridization (CGH) analysis

Genomic DNA was extracted from formalin fixed paraffin embedded tissues using QIAmp®DSP DNA formalin fixed paraffin embedded tissue kit according to the manufacturer's protocol for DNA isolation (Qiagen®) after RNAse digestion. A cutoff of 50% of cellularity in tumor samples was set for the analysis. DNA was hybridized onto 8 × 60 K whole-genome arrays (G4450A; Agilent® Technologies) according to the manufacturer's protocol. Microarray Scanner and images were analyzed by Feature Extraction V10.7.3.1 followed by Agilent® Cytogenomic software 4.0.3.12. The ADM-2 algorithm of the CGH Analytics v4.0.76 software (Agilent® Technologies) was used to identify the DNA copy number abnormalities at the probe level. A low-level copy number gain was defined as a log 2 ratio > 0.25 and a copy number loss was defined as a log 2 ratio < −0.25. A high-level gain or amplification was defined as a log 2 ratio > 1.5 and a homozygous deletion was suspected when the ratio was <−1.5. The range for Derivative Log ratio spread cutoff was fixed to 0.50.

The genomic index was calculated for each profile as follows: Genomic Index = A^2/C, where A is the total number of alterations (segmental gains and losses) and C is the number of involved chromosomes [8, 9].

Fluorescence in situ hybridization (FISH)

A *COL1A1-PDGFB* FISH double fusion was performed in order to validate the observation in 2 cases in our series of unbalanced breaks on chromosomes 17 and 22 (involving the genes *COL1A1* and *PDGFB*) by array-CGH analysis as well in 4 other cases (1, 2, 7 and 13).

FISH assay was performed on 4 micron whole tissue sections using a commercially available *COL1A1/PDGFB* dual-fusion probe (ZytoLight® SPEC COL1A1/PDGFB Dual Color Dual Fusion Probe, Zytovision) and the Histology FISH accessory kit (DAKO) according to the manufacturer's instructions. Nuclei were scored for non-translocated patterns (split orange and green signals) and translocated patterns (at least one fusion signal) using a Nikon Eclipse 80i fluorescent microscope with appropriate filters (Nikon). For each case, 50 tumor nuclei were counted, and a come-together signal (orange and green merged signals) in more than 30% of the tumor nuclei was considered a positive result. Pictures were captured using a Pathscan Combi (Excilone).

Results

The clinical and pathological features are presented in Table 2 and the immunohistochemical, RNA-sequencing and genomic data in Table 3.

RNA-sequencing results and sanger sequencing

Seven of the 13 tumors harbored a *NTRK* rearrangement (6 *TPM3-NTRK1* and 1 *EML4-NTRK3*). In 5 tumors (cases 3, 4, 8, 9, 12), the rearrangement was recurrent affecting exon 6 of *TPM3* gene and exon 10 of *NTRK1* gene. In 1 tumor (case 11), the fusion was located between exon 4

Table 2 Clinical and Pathological Features of Cases Included in Study

Case	Age (years)	Size (cm)	Tumor location	Follow-up (months)	Tumor Recurrence	Tumor stage	Predominant degree of nuclear Atypia	Mitoses per 10HPFs	Necrosis	Tumor Border	Lymphocytic Infiltrate	LVSI
1	32	5.5	Cervix	AWD 19	Bone, peritoneal	IB	Moderate	10	Yes	Infiltrating	Yes	No
2	47	5	Corpus/LUS	DOD 11	Adnexa and upper abdomen	IVB	Moderate	50	Yes	Not assessable	No	No
3	39	NA	Cervix	NA	Unknown	NA	Mild	3	Yes	Infiltrating	Yes	No
4	44	4.5	Cervix	NED 2	No	IA	Moderate	3	No	Not assessable	Yes	No
5	26	12	Cervix	AWD 52	Vagina	IB	Moderate	3	Yes	Not assessable	Yes	No
6	82	8.2	Cervix	NED 10	No	IB	Mild	8	Yes	Infiltrating	No	No
7	50	9	Vagina	DOD 34	Pelvis (bladder and rectum)	IIB	Mild	1	No	Infiltrating	Yes	No
8	23	3	Cervix	NED 33	No	IA	Moderate	5	Yes	Not assessable	Yes	No
9	30	2.5	Cervix	NED 12	No	IA	Mild	50	No	Infiltrating	No	No
10	60	5.8	Cervix	DOD 60	Pelvis and bladder	IIIB	Mild	20	No	Infiltrating	No	No
10			Recurrence case 10				Moderate	20	No	Infiltrating	No	No
11	33	5	Cervix	NED 108	No	IA	Mild	1	No	Infiltrating	Yes	No
12	23	2.8	Cervix	AWD 30	Left paracervical and uterovesicle tissue, pelvic gutter, omentum, small bowel, ovary, liver	IIA	Mild	50	Yes	Infiltrating	No	No
12			Recurrence case 12				Marked	32	Yes	Infiltrating	No	No
13	48	12	Corpus	NA-Recent case		IB	Moderate	20	No	NE	No	No

NED no evidence of disease, *DOD* dead of disease; *AWD* alive with disease, *LUS* lower uterine segment, *NA* not available, *NE* not evaluable, *LVSI* lymphovascular invasion

Table 3 Immunohistochemical, RNA-Sequencing and Genomic Data

Case	CD34	S100	Desmin	ER/PR	Trk	Cyclin D1	BCOR	Translocation frequency	ArrayCGH GI	9p21.3 deletion (CDKN2A)
1	N	D	N	N/N	N	80%	< 5%	No	21.4	homozygous 1.3 MB
2	D	F	N	N/N	N	90%	< 5%	No	12.5	no
3	D	D	N	N/N	D	80%	0	*TPM3/NTRK1* 59%	2	heterogyzous 0.5 MB
4	D	D	N	N/N	D	90%	0	*TPM3/NTRK1* 80%	5.3	homozygous 0.1 MB
5	D	D	N	N/N	D	30%	0	*EML4/NTRK3* 90%	21.3	Homozygous 0.3 MB
6	D	N	N	N/N	N	15%	0	*COLA1A/PDGFB* 56%	9.14	no
7	N	D	N	N/N	N	80%	0	No	5.3	heterogyzous 1.6 MB
8	D	D	N	ERN/PR few nuclei positive	D	90%	0	*TPM3/NTRK1* 84%	12.25	Heterozygous 1.6 MB
9	F	D	N	N/N	D	90%	< 5%	*TPM3/NTRK1* 87%	8.3	Homozygous 0.5 MB
10	D	N	ND	N/N	N	10%	0	*TPM3/NTRK1* 6%[a] *COLA1A/PDGFB* 86%	16.2	no
10			N		N	75%	0	*COLA1A/PDGFB* 86%	NI	NI
11	D	D	N	N/N	D	80%	0	*TPM3/NTRK1* 57%	NI	NI
12	D	F and weak	N	N/N	D	20%	0	*TPM3/NTRK1* 86%	6.25	heterozygous 1 MB
12			N		D	30%	0	*TPM3/NTRK1* 85%	20.5	homozygous, 0.9 MB
13	D	N	N	N/N	N	90%	0	*COLA1A/PDGFB* 74%	ND	ND

Other immunohistochemical markers were performed in many of the cases.

MB megabase, *ER* estrogen receptor, *PR* progesterone receptor, *CGH* comparative genomic hybridization, *ND* not done, *F* focal < 50% of tumor cells, *D* diffuse, > 50% of tumor cells, *N* negative, *NI* not Interpretable

[a]Case 10 harbored the *TPM3/NTRK1* fusion in a small percentage (6%) only in the primary tumor and not in the recurrence. As such, it was considered negative for *NTRK* rearrangement.

of *TPM3* and exon 10 of *NTRK1*. The *EML4-NTRK3* fusion involved exon 2 of *EML4* gene and exon 14 of the *NTRK3* gene (case 5). The gene annotation was performed according to the hg19 assembly with the following gene reference: *EML4* NM_001145076.1, *NTRK3* NM_001012338.2, *NTRK1* NM_002529.3 and *TPM3* NM_001278188.1. The specific fusion transcript was confirmed by Sanger sequencing in all positive cases (Fig. 1g).

The *TPM3-NTRK1* fusion transcript (consisting of the *TPM3* exon 6 fusion with the *NTRK1* exon 10) was also detected in case 10 but in a small proportion (6%) and only in the primary tumor and not in the recurrence. The fusion proportion was below the 10% cutoff defined by the supplier. The *TPM3-NTRK1* fusion transcript was confirmed by Sanger sequencing. However, it was considered not relevant since it was only present in the primary tumor and the percentage of the fusion transcript for the positive tumors ranged from 56 to 90%.

Case 7 was not interpretable with ARCHERDX®CTL panel RNA-sequencing. Therefore the tumor was analyzed by Sanger sequencing for *TPM3 (exon 6)-NTRK1 (exon 10)*, *TPM3 (exon 4)-NTRK1 (exon 10)* and *EMLA (exon 2)-NTRK3* (exon 14) fusion transcripts and no specific fusion transcript nor translocation were detected. Case 13 was only tested by Sanger sequencing for the same primers and no fusion was detected. In all cases, β2microglobulin sequence serving as a positive control, was obtained. In those cases where the primary and recurrent tumors were analyzed, an

identical molecular abnormality was found in both neoplasms (with the exception of *TPM3-NTRK1* fusion in case 10, as discussed above).

Array-CGH genomic profile and FISH dual fusion results

Among the 14 available array-CGH profiles, 11 tumors were interpretable (Table 3). The tumors showed low rearranged genomic profiles (mean Genomic Index = 11.7; range from 3 to 21.4). No significant differences were observed in the genomic complexity between the profiles of the *NTRK* rearranged tumors and the other neoplasms ($p = 0.7$). The array-CGH analysis of the *NTRK* rearranged tumors did not show any unbalanced rearrangement of *NTRK1* or *NTRK3*. On the contrary, 2 tumors (cases 6 and 10, primary tumor and recurrence in case 10) showed intrachromosomal breaks involving *COL1A1* on chromosome 17q21.33 and *PDGFB* on chromosome 22q13.1 (Fig. 3e). FISH dual fusion was performed on these 2 tumors (3 samples) with unbalanced 17-22 rearrangement and also on case 13 which morphologically exhibited a pronounced herringbone and storiform architecture and lacked *NTRK*-rearrangements. This analysis showed *COL1A1-PDGFB* fusion in 56%, 86% and 74% of the tumor cells (cases 6, 10 and 13 respectively) (Fig. 3c).

Interestingly among the 12 interpretable tumors at CGH analysis, 9 showed a loss of *CDKN2A* gene (chr 9p21;3), 5 homozygous (cases 1,4,5,9 and the recurrence of case 12) and 4 heterozygous (case 3, 7, 8 and the primary tumor of case 12) (Table 3). The losses were localized, involving short chromosomic regions (between 0.1.and 1.6 Mb) (Fig. 2h).

Trk Immunohistochemistry

Among the 13 tumors, there was diffuse cytoplasmic Trk positivity in 7 (in case 12, both the primary and recurrent tumor were diffusely positive); no nuclear immunoreactivity was observed. All positive tumors harbored a *NTRK* rearrangement.

The single tumor (case 10) which harbored a *TPM3-NTRK1* fusion at low frequency (6%) was negative for Trk. As discussed, the rearrangement was detected in low percentage in the primary tumor only and was absent in the recurrence and the same tumor harbored the *COL1A1/PDGF* translocation.

The other immunohistochemical results are discussed below.

Comparative morphologic, immunohistochemical and molecular data

Taking account of the RNA-sequencing, CGH analysis, morphology and immunohistochemistry, we identified 3 subgroups of "fibroblastic" spindle cell sarcomas of the uterus, namely a subgroup of *NTRK*-rearranged neoplasms, a subgroup harboring *COL1A1-PDGFB* fusions and a subgroup without any known rearrangement that could be tentatively classified as malignant peripheral nerve sheath tumor given that all were S100 positive (see below) and negative for other melanoma markers (HMB45, Melan A, SOX10), except for 1 case where Melan A and SOX10 were focally positive (discussed below). However, it is likely that other molecular abnormalities may be identified in this group of neoplasms which would necessitate a nomenclature change.

NTRK-rearranged sarcomas

In our series, the 7 tumors harboring *NTRK*-rearrangements were all located in the cervix. Patients with *NTRK*-rearranged tumors were significantly younger than the other patients ($p = 0.012$), the mean age at diagnosis being 31 years (median: 30 years, range 23 to 44 years). They generally presented at early stage (4 at stage IA, 1 at stage IB, 1 at stage IIA, 1 stage unknown) (FIGO 2009 staging system for uterine sarcomas). Follow-up was available for all patients except one and 4 of 6 were alive with no evidence of disease (mean follow-up = 39 months, range 2 to 108 months) and 2 were alive with disease (32 and 52 months follow-up). No correlation was observed between the *NTRK* status and clinical outcome when comparing patients alive with alive with no evidence of disease versus patients alive with disease or dead of disease ($p = 0.24$).

The primary tumors ranged in size from 2.5 to 12 cm in those cases where this information was available. When the sections included tumor borders (4 of 7 cases), the neoplasms could be seen to be infiltrating. The neoplasms usually had a predominantly diffuse patternless architecture but in some cases there was a focal or diffuse herringbone pattern with intersecting fascicles of cells. The tumors were predominantly composed of spindle-shaped cells with ovoid nuclei, inapparent nucleoli and scant cytoplasm. In a few cases, small collections of tumor cells with a more epithelioid appearance were present and/or there was focal cytoplasmic vacuolization. Atypia was generally mild to moderate with scattered markedly atypical symplastic-like cells in two tumors and diffuse marked nuclear atypia in the recurrence in case 12. The degree of mitotic activity was highly variable ranging from 1 to 50 per 10 High Power Fields and necrosis was present in 4 of 7 tumors. In 3 of 8 tumors, a focal hemangiopericytoma-like vasculature was present. A prominent lymphocytic infiltrate was observed in 5 of 7 tumors. No lymphovascular invasion was seen. In 1 case (case 3), the tumor infiltrated around pre-existing normal endocervical glands.

Immunohistochemically these tumors were all diffusely positive with CD34 and S100, except for 1 case each where CD34 and S100 exhibited focal immunoreactivity. Trk was diffusely and strongly expressed in all tumors with cytoplasmic positivity. Desmin, ER and PR were negative in all cases with the exception of scattered PR positive cells in case 8. All cases were essentially BCOR negative except for scattered positive nuclei (less than 5%) in some cases. Cyclin D1 was positive in all cases (percentage of positive nuclei ranging from 20 to 90%).

This subgroup showed relatively simple genomic profiles without unbalanced intrachromosomal breaks with a mean Genomic Index of 10.84 (range 2 to 21.3). Among the interpretable profiles (7/8 samples), all *NTRK*-tumors harbored *CDKN2A* loss (4 homozygous and 3 heterozygous, from 0.1 to 1.6 Mb).

Figure 1 illustrates the morphological, immunohistochemical and molecular features of some of these cases.

COL1A1-PDGFB rearranged sarcomas

Three tumors (cases 6, 10 and 13) harbored the *COL1A1-PDGFB* fusion. Two were cervical tumors and one was located in the uterine corpus. The patients were aged 48, 60 and 82 years. The tumors presented at stage IB, IIIB and IB respectively (Table 2). At follow-up, 1 patient was dead of disease after 60 months and 1 was alive with alive with no evidence of disease (10 months follow-up); the third case is recent with no significant follow-up. One of the patients (case 10) had been diagnosed with a Dermatofibrosarcoma Protuberans on her back approximately a year before the cervical lesion was discovered; the lesion on the back had been completely excised and we believe that it is most likely that the cervical tumor represents a separate independent lesion rather than a metastasis.

The tumors measured 5.8, 8.2 and 12 cm. In the 2 tumors with evaluable margins, the borders were infiltrating. Morphologically the tumors were cellular and exhibited a prominent storiform and herringbone architecture and were composed of uniform cells with ovoid to spindle-shaped nuclei, scant cytoplasm and indistinct borders. There was mild to moderate nuclear atypia and mitotic activity ranged from 8 to 20 mitoses/10 High Power Fields. A lymphocytic infiltrate was absent and there was no lymphovascular invasion. Only 1 case exhibited necrosis (case 6).

All tumors diffusely expressed CD34 and were negative for ER, PR, desmin, S100 and Trk when these markers were performed. All cases were essentially BCOR negative except for scattered positive nuclei (less than 5%) in some cases. Cyclin D1 was positive in all cases (percentage of positive nuclei ranging from 10 to 90%).

The two genomic profiles analyzed showed moderately rearranged profiles (Genomic Index = 9.14 and 16.2) with unbalanced 17-22 rearrangements. No *CDKN2A* deletion was detected.

Figure 2 illustrates the morphological, immunohistochemical and molecular features of some of these cases.

Fibroblastic sarcomas with features of malignant peripheral nerve sheath tumor

Three tumors (cases 1, 2, 7) did not harbor any known rearrangement (at Archer® sequencing and after *COL1A1-PDGFB* dual FISH). Although we have tentatively classified these as malignant peripheral nerve sheath tumor predominantly on the basis of S100 positivity and complete loss of staining with H3K27me3 in 2 cases (see below), we recognize that there is limited evidence for this and this classification is likely to change, especially if alternative molecular changes are identified in these neoplasms. None of these patients had a history of neurofibromatosis and in no case was origin from a nerve trunk identified.

The first tumor (case 1) occurred in a 32 year old woman with a 5.5 cm cervical mass which comprised a highly cellular spindle cell neoplasm which was focally well circumscribed with a lobular appearance but elsewhere had infiltrative borders. There was moderate nuclear atypia and 10 mitoses/10 High Power Fields. No lymphovascular invasion was seen. The tumor was ER, PR, desmin, CD34 and Trk negative. S100 was diffusely positive and SOX10 and melan A focally positive but HMB45 and MITF were negative. H3K27me3 was focally positive. Less than 5% of nuclei were BCOR positive and 80% of nuclei were cyclin D1 positive. No recurrent *KIT, BRAF or NRAS* mutations were detected and no NF1 deletion was detected (data not shown). Despite the immunophenotype raising the possibility of a melanocytic neoplasm, the genomic profile was more in favor of a malignant peripheral nerve sheath tumor (see discussion). The tumor recurred with peritoneal and bone metastases 6 months after the primary surgery and the patient was alive 19 months later.

The second tumor (case 2) occurred in a 47 year old woman with a 5 cm mass involving the uterine corpus and lower uterine segment. Metastases to the adnexa and upper abdomen were present at diagnosis and the patient died 11 months after presentation. The tumor was highly cellular and had no particular architectural arrangement and was composed of moderately atypical spindle-shaped cells with vacuolated cytoplasm. There were 50 mitoses/ per 10 High Power Fields. No lymphovascular invasion was seen.The tumor diffusely expressed CD34 and S100 was focally positive. ER, PR, desmin, h-caldesmon, Trk, HMB45, melan A and SOX10 were negative. H3K27me3 was totally negative. Less than 5% of nuclei were BCOR positive and 90% of nuclei were cyclin D1 positive.

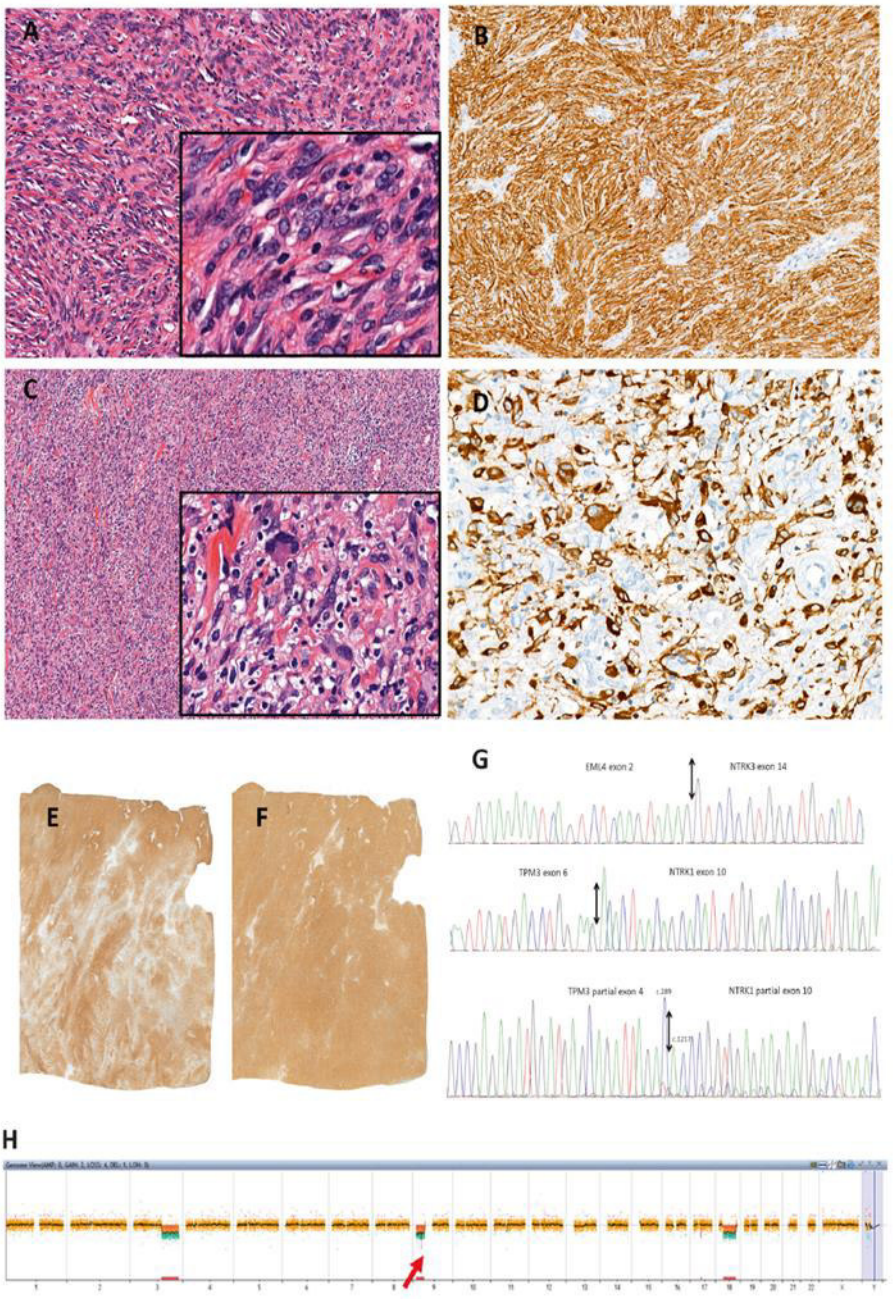

Fig. 1 *NTRK*-rearranged uterine sarcomas. Morphologic features of *NTRK1* rearranged tumors. Fibroblastic appearance with spindle cells exhibiting moderate nuclear atypia (**a**) (case 4). There is diffuse cytoplasmic immunoreactivity with Trk (**b**) (case 4). Prominent inflammatory infiltrate and scattered symplastic nuclei (**c**) (case 8). There is diffuse cytoplasmic immunoreactivity with Trk with a negative stromal background (case 8) (**d**). CD34 (**e**) and S100 (**f**) are diffusely positive (case 5). Sanger sequencing of the transcript fusions detected by RNA-sequencing with the ArcherDX® CTL panel: *EML4 exon 2-NTRK3 exon 14* (**g**) (case 5), *TPM3* exon 6-*NTRK1*exon 10 (3,4,8,9,11 and 12), *TPM3* partial exon4-*NTRK1* partial exon 10). Arrows indicate the point of the junction. Array-CGH genomic profile of a *NTRK1*-rearranged tumor (**h**) (case 4). Note the quite simple genomic profile showing rare genomic events and the homozygous *CDKN2A* loss (arrow)

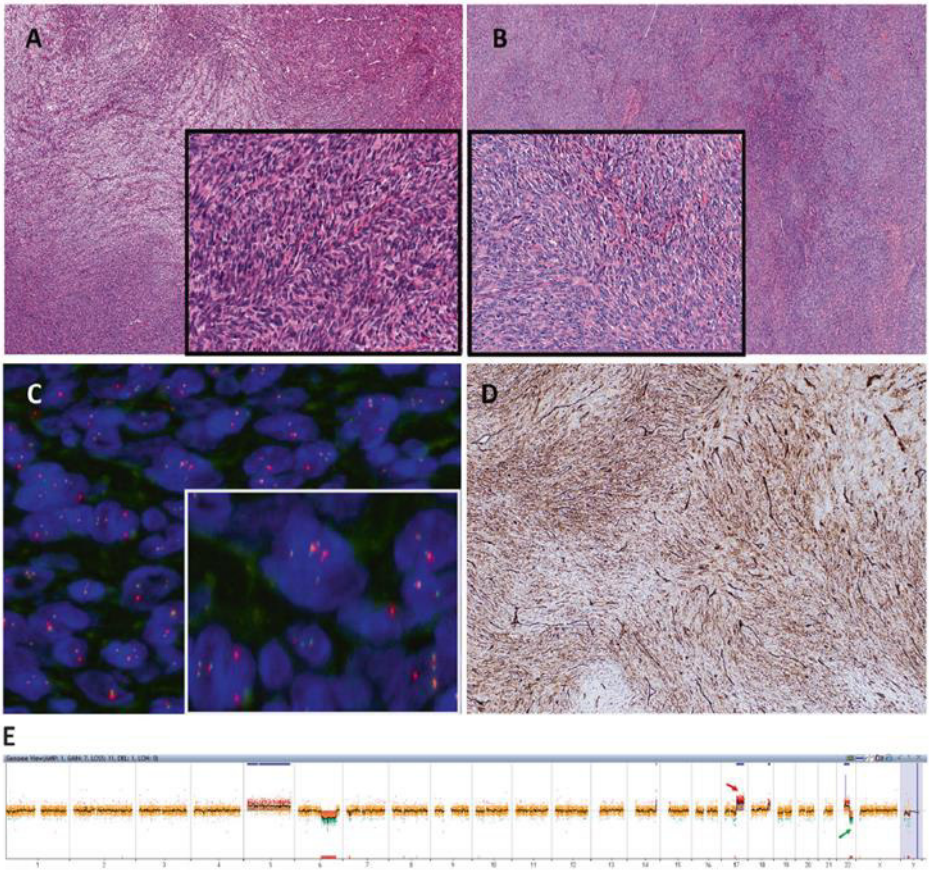

Fig. 2 *COL1A1-PDGFB*-rearranged uterine sarcomas (dermatofibrosarcoma protuberans). Cellular tumors composed of relatively bland spindle-shaped cells with pronounced herringbone pattern of growth (**a**, **b**) (case 6). *COL1A1-PDGFB* dual fusion FISH. Note the presence of two orange/green fusion signals (**c**) (case 10). Diffuse CD34 immunostaining (**d**) (case 13). Array-CGH genomic profile of a *COL1A1-PDGFB* rearranged tumor. Note the unbalanced break-points (arrows) on CH17q (*COL1A1*) and 22q (*PDGFB*) (**e**) (case 10)

The third tumor (case 7) occurred in a 50 year old woman who had undergone a prior hysterectomy for benign reasons. She presented with a mass centered on the vagina which infiltrated the bladder, rectum and other pelvic tissues. She underwent a total pelvectomy. The patient died of disease 34 months following surgery. The tumor had no particular architectural arrangement, exhibited an infiltrative pattern of growth with entrapment of adipose tissue around the periphery and was composed of bland spindle-shaped cells with focal collections of ganglion-like cells with large nuclei, prominent nucleoli and abundant eosinophilic cytoplasm. There was low mitotic activity (1 per 10 High Power Fields) and no necrosis or lymphovascular invasion. There was a prominent lymphocytic infiltrate. S100 was diffusely positive while CD34, HMB45, Melan A, ER, PR, desmin and Trk were negative. H3K27me3 was totally negative. BCOR was negative and 80% of nuclei were cyclin D1 positive.

Two of the cases (cases 2 and 7) showed very simple genomic profiles with a low Genomic Index (12.5 and 5.3 respectively). The other case (case 1) exhibited more intrachromosomal breaks (Genomic Index 21.4). In 2 of the cases, a loss of *CDKN2A* was detected (homozygous in case 1 and heterozygous in case 7).

Figure 3 illustrates the morphological, immunohistochemical and molecular features of some of these cases.

Discussion

A wide range of sarcomas occur within the uterus (corpus and cervix), the most common being leiomyosarcoma, endometrial stromal sarcoma (low-grade and high-grade), and undifferentiated uterine sarcoma. A variety of more uncommon sarcomas have also been reported as primary uterine neoplasms, including rhabdomyosarcoma,

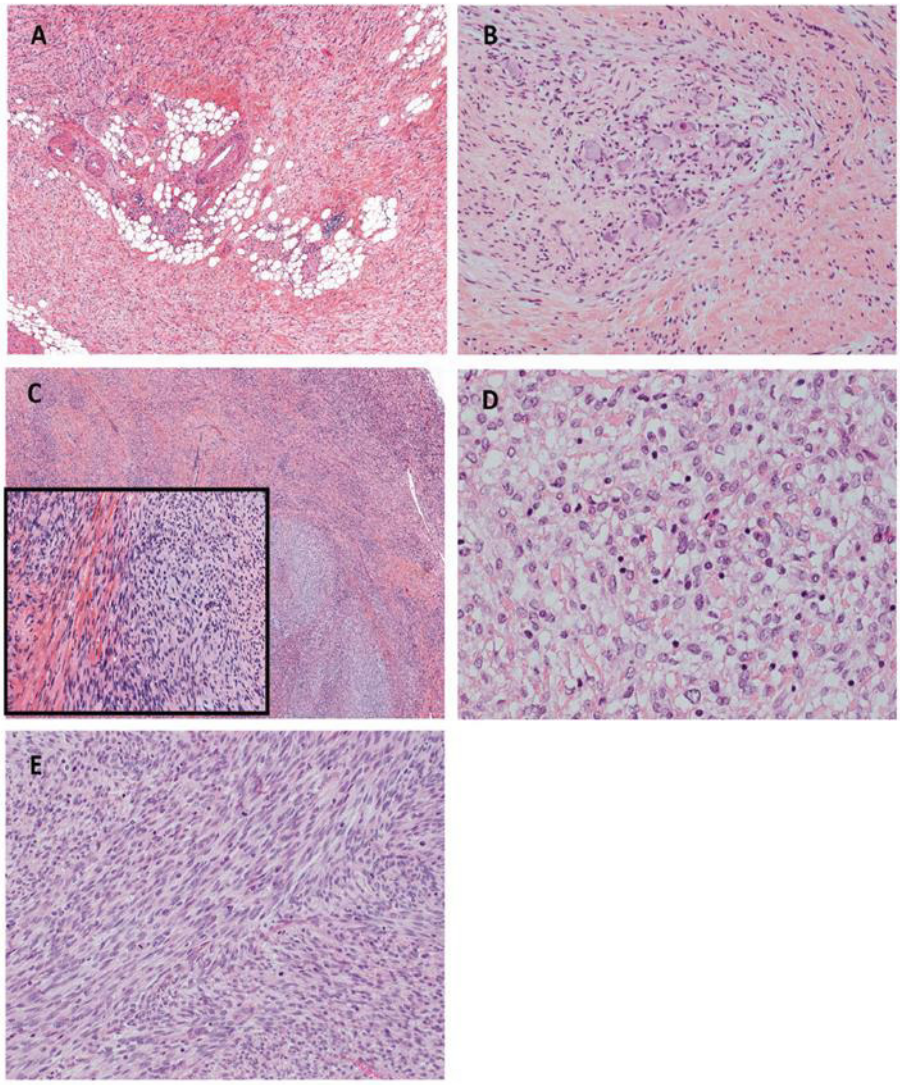

Fig. 3 Malignant Peripheral Nerve Sheath Tumors. Spindle cell tumor infiltrating adipose tissue with mild nuclear atypia and focal collections of ganglion-like cells (**a**, **b**) (case 7). Spindle cell tumor with a focal lobular architecture but elsewhere with infiltrative borders (**c**) (case 1).Cellular tumor composed of spindled and epithelioid cells with focal cytoplasmic vacuolization (**d**) (case 2). Spindle cell tumor with mild nuclear atypia but significant mitotic activity (case 2) (**e**)

angiosarcoma, malignant peripheral nerve sheath tumor, alveolar soft part sarcoma, liposarcoma, malignant solitary fibrous tumor, and Ewing sarcoma. It is clear that the full spectrum of uterine sarcomas has not yet been fully characterized and that so-called undifferentiated uterine sarcomas comprise a morphologically and molecularly heterogeneous group of neoplasms. Modern molecular techniques, such as next generation sequencing, have resulted in the description of new categories of uterine sarcoma, including two which have been classified as high-grade endometrial stromal sarcoma, those associated with *YWHAE* and *BCOR* gene rearrangements [10–14]. Recently, Chiang and coworkers reported a series of 4 uterine mesenchymal neoplasms resembling fibrosarcoma, expressing Trk and harboring *NTRK* rearrangements (*RBPMS-NTRK3, TPR-NTRK1, LMNA-NTRK1* and *TPM3-NTRK1*) [6]. All tumors exhibited brisk mitotic activity with an aggressive clinical outcome in two of four patients [6]. Immunophenotypically all tumors were positive for S100 and negative for CD34, ER, and PR [6]. The authors speculated that so-called endocervical fibroblastic malignant peripheral nerve sheath tumors may represent *NTRK* fusion-

positive uterine sarcomas on the basis of shared morphology and immunophenotype.

In this study, we report the clinicopathological and molecular features of a series of 13 spindle cell sarcomas of the uterus and vagina with morphological features resembling fibrosarcoma, including the 3 originally reported cases of endocervical fibroblastic malignant peripheral nerve sheath tumor and neoplasms diagnosed as malignant peripheral nerve sheath tumor. In reporting these tumors, we propose a diagnostic algorithm when faced with a uterine sarcoma with features resembling fibrosarcoma. The tumors we report were typically infiltrative and composed of spindle-shaped cells exhibiting mild or moderate nuclear atypia, variable but often prominent mitotic activity and a diffuse, herringbone and/ or storiform architecture. The majority (11/13) of the tumors were CD34-positive, S100 was variable, while ER, PR and desmin were typically negative [5].

After transcriptomic and genomic analysis, we identified three subgroups of neoplasms: a subgroup harboring *NTRK*-transcript fusions, a subgroup associated with *COL1A1-PDGFB* fusion and a subgroup without any identified rearrangements. The first group of *NTRK*-rearranged sarcomas, all of which were located within the cervix, corresponds to the tumors recently reported by Chiang et al. [6] and our findings expand on their publication. Three of the neoplasms we report (2 with a cervical and 1 with a corpus location) harbored a *COL1A1-PDGFB* fusion which, as far as we are aware, has never been reported in a uterine neoplasm. The final group comprised 3 S100-positive neoplasms which we currently tentatively suggest to categorize as malignant peripheral nerve sheath tumors (see discussion below).

As discussed, as in the original publication [6], all *NTRK*-associated sarcomas arose in the uterine cervix and generally presented at an early stage. The mean age (31 years) was significantly lower than in the other tumors we report. The tumors recurred in 2 of 6 patients with follow-up and all 6 patients with available follow-up were alive when last seen (2 alive with disease and 4 alive with no evidence of disease). These tumors were generally similar morphologically and immunophenotypically to the other neoplasms we report and we did not identify any specific features which definitively assist in distinguishing these from the other neoplasms. All tumors were positive for CD34 and S100 (usually diffusely) while desmin, ER and PR were negative (except for focal PR positivity in 1 case). The immunophenotype is slightly different from the cases reported by Chiang et al., all of which were CD34 negative [6].

The only feature that reliably identified the *NTRK* rearranged tumors was the Trk positivity with all cases being diffusely positive (except for 1- see below). All of the other neoplasms were Trk negative. This is in keeping with the findings of Hechtman et al. who found Trk expression to be highly concordant with the fusion status detected in tumors of varying histotypes (colorectal, lung, appendiceal and gallbladder adenocarcinomas, secretory-type salivary and breast carcinomas, glioblastomas, melanomas and soft tissue sarcomas) [15]. As discussed, the only *NTRK* rearranged case which was negative for Trk immunohistochemistry harbored a *TPM3-NTRK1* fusion at low frequency (confirmed by Sanger sequencing). The translocation was detected in the primary tumor but not in the recurrence (case 10) and the tumor harbored a *COL1A1-PDGFB* translocation in 74% of the tumor cells. This suggests that the driver genomic event is the *COL1A1-PDGFB* translocation which was present in both the primary and recurrent tumor. We speculate that the*TPM3-NTRK1 fusion* represents a subclonal population which was lost during tumor progression.

Given the immunohistochemical results, Trk immunohistochemistry represents a useful diagnostic tool that reliably identifies *NTRK*-rearranged uterine sarcomas. We suggest to screen all uterine (cervical and corpus) "fibroblastic" spindle cell sarcomas without smooth muscle or endometrial stromal differentiation with Trk. Given the sensitivity and specificity of this antibody for *NTRK* rearrangement [15], positive staining, especially when diffuse, should be followed by molecular testing to prove the presence of a *NTRK* rearrangement. However, we recognize that the specificity of this marker for *NTRK* rearranged neoplasms has not been fully investigated since no study has looked at the full range of uterine mesenchymal neoplasms. In the study of Chiang et al., 2 of 97 uterine leiomyosarcomas showed strong and diffuse pan-Trk expression while 4 of 97 showed diffuse weak TrkA immunoreactivity; this study was performed on tissue microarrays [6].

The Trk A, B and C proteins are encoded by *NTRK1, NTRK2 and NTRK3* respectively [16]. The fusion juxtaposes the kinase domain-containing 3' region of *NTRK* with the 5' region of *NTRKs* gene partner and promotes oncogenesis by constitutive cell proliferation [17]. *NTRK* fusions are relatively rare in tumors but have been identified in < 5% of lung cancers, between 0.5–2% of colorectal cancers, 12% of papillary thyroid carcinomas, 40% of pediatric and 3% of adult brain tumors, 16% of Spitzoid melanomas [18] and 1% of adult soft tissue sarcomas. They have also been identified in 91% of congenital fibrosarcomas and 92–100% of secretory breast carcinomas [17]. Identification of *NTRK* fusions in cancer is important because of a potential effective therapeutic strategy given the durable response to treatment with TRK inhibitors [17].

Interestingly, among the interpretable genomic profiles, all the *NTRK*-rearranged sarcomas in our series harbored a *CDKN2A* deletion (4 homozygous and 3 heterozygous) and

the losses affected short chromosomal segments (from 0.1 to 1.6 Mb). *CDKN2A* deletion has been reported in 50% of *NTRK*-rearranged sarcomas, in 14% of soft tissue sarcomas [19] and in 50% of soft tissue malignant peripheral nerve sheath tumor [20] but in these studies no information was provided regarding the homozygous or heterozygous status of the loss and the biological implications of this deletion. Further investigations are needed in order to understand the role and the effects of *CDKN2A* loss in these sarcomas. No *CDKN2A* loss was detected in the *COL1A1-PDGFB* rearranged sarcomas. In 2 of the 3 malignant peripheral nerve sheath tumors, a loss of *CDKN2A* was detected (homozygous in 1 case 1 and heterozygous in 1).

Among the 13 tumors we studied, we identified 3 cases with a *COL1A1-PDGFB* fusion. This molecular abnormality has not, as far as we are aware, been reported in uterine neoplasms but is characteristic of dermatofibrosarcoma protuberans [21–23] and pediatric giant cell fibroblastoma [24]. These 3 tumors occurred in older patients (48 to 82 years), 2 were located in the cervix and one in the corpus. Morphologically they were cellular with storiform and herringbone architecture and significant mitotic activity. All exhibited diffuse positivity with CD34 and were negative for S100, ER, PR, desmin and Trk. Dermatofibrosarcoma protuberans, the most common dermal sarcoma [25], is a low-grade slow growing tumor with low risk of distant metastases but a significant rate of local recurrence and which may undergo fibrosarcomatous transformation [25]. The tumor characteristically harbors a translocation t(17;22)(q22;q13) resulting in the chimeric fusion transcript *COL1A1-PDGFB* [25]. The trunk and proximal extremities are the most common locations [26–28] but this tumor also occurs on the vulva [29]. Morphologically dermatofibrosarcoma protuberans is composed of spindle-shaped cells arranged in a storiform and herringbone architecture and immunohistochemically there is diffuse expression of CD34 and S100 is negative. *COL1A1-PDGFB* FISH is a useful tool in confirming the diagnosis [22]. While the 3 tumors we report with *COL1A1-PDGFB* translocation could be regarded as dermatofibrosarcoma of the uterus, we prefer not to use this designation given the significant mitotic activity. We prefer to categorize these as *COL1A1-PDGFB* translocation associated fibrosarcomas. Moreover, it should be remembered that different tumor types may exhibit the same molecular abnormality, for example *YWHAE* translocations are found in high-grade endometrial stromal sarcomas and in some clear cell sarcomas of the kidney [10–12, 30, 31]. An interesting observation is that in 1 of our cases harboring a *COL1A1-PDGFB* fusion (case 13), 1 of the tissue blocks was CD34 negative while the others were diffusely positive; CD34 can be focally lost in some cases of dermatofibrosarcoma protuberans, especially in areas of fibrosarcomatous transformation.

The other 3 tumors in our series did not harbor any known rearrangement. Two of them were highly cellular with brisk mitotic activity. These neoplasms were diffusely positive with S100 and generally negative with other melanocytic markers, although SOX10 and melan A were focally positive in 1 case. Although it is difficult to exclude spindle cell malignant melanoma, especially in the case which was focally positive with SOX10 and melan A, we believe these are currently tentatively best categorized as malignant peripheral nerve sheath tumors; no recurrent *KIT, BRAF or NRAS* mutations (molecular abnormalities which are characteristic of malignant melanoma) were detected in the case positive for SOX10 and melan A. However, none of these patients had a history of neurofibromatosis and in no case could origin from a nerve trunk be demonstrated which would have assisted in classifying these neoplasms as malignant peripheral nerve sheath tumors. One of the cases contained a population of ganglion-like cells which may be seen in other "neural" neoplasms, such as ganglioneuroma [32] and gangliocytic paraganglioma [33]. H3K27me3 was completely negative in 2 of these cases and focally positive in the other. While complete loss of H3K27me3 is common in malignant peripheral nerve sheath tumors and could offer some support to this diagnosis [34], a significant number of malignant melanomas also exhibit complete loss. For example, in 1 study, a complete loss of H3K27me3 was found in 37% of all melanomas and partial loss ('mosaic' pattern) in 19% of malignant peripheral nerve sheath tumors and in 51% of melanomas. As such, complete immunohistochemical loss of H3K27me3 is not specific for malignant peripheral nerve sheath tumor and cannot be used reliably in distinguishing this from melanoma [35].

The prognosis of this group was poor; one patient died of disease 11 months after the diagnosis (case 2) and another (case 1) recurred early with local and distant metastases; this patient is alive with disease after 19 months. The third case was a primary vaginal tumor which involved the bladder and rectum. Although the numbers are small, this suggests that these neoplasms have a particular propensity for aggressive behavior. As stated previously, while we currently suggest to tentatively classify these neoplasms as malignant peripheral nerve sheath tumor, it is arguable whether this is an appropriate designation and the nomenclature may change especially if other molecular alterations are identified in this neoplasms.

The differential diagnosis of spindle cell sarcomas of the uterus composed of a uniform population of cells is wide and includes leiomyosarcoma, high-grade endometrial stromal sarcoma, undifferentiated uterine sarcoma (uniform type) and a variety of other uncommon neoplasms including inflammatory myofibroblastic tumor, malignant solitary fibrous tumor [36] and spindle cell malignant melanoma. To that list should be added *NTRK*-rearranged sarcoma,

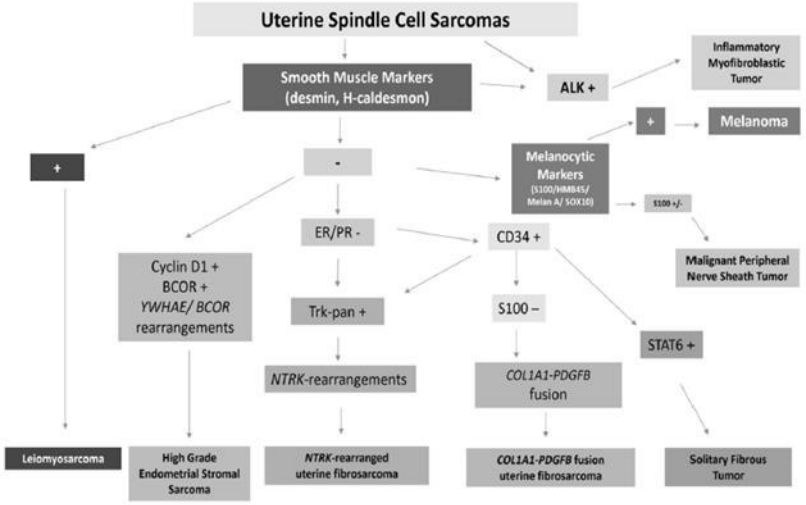

Fig. 4 Diagnostic algorithm for spindle cell sarcomas of the uterus. Although the typical immunophenotypes are listed, in some cases there may be exceptions to these typical staining patterns and other neoplasms may enter into the differential diagnosis

COL1A1-PDGFB fusion-associated fibrosarcoma and malignant peripheral nerve sheath tumor. The differential diagnosis will not be discussed in detail but leiomyosarcoma typically expresses smooth muscle markers including desmin [37], high-grade endometrial stromal sarcomas exhibit high expression of cyclin D1 and BCOR (see below) and the majority of cases harbor *YWHAE* or *BCOR* rearrangements [10, 11, 38, 39].

As discussed, high-grade endometrial stromal sarcomas typically exhibit diffuse expression of cyclin D1 and BCOR. All our cases were BCOR negative except for scattered positive nuclei (less than 5%) in some cases. Cyclin D1 was positive in all of our cases (percentage of positive nuclei ranging from 10 to 90%). This illustrates that cyclin D1 is not a reliable marker in distinguishing *YWHAE* or *BCOR* rearranged high-grade endometrial stromal sarcoma from *NTRK* or *COL1A1-PDGFB* rearranged tumors. This is not surprising since cyclin D1 is a cell cycle related marker rather than a marker of a specific line of differentiation. One of us (WGM) has also observed diffuse cyclin D1 immunoreactivity in a small number of other uterine mesenchymal neoplasms.

Recent studies have emphasized that inflammatory myofibroblastic tumors occur within the uterus and are likely to be misdiagnosed, especially as leiomyomatous neoplasms [40–43]. Inflammatory myofibroblastic tumor is ALK positive and is characterized by genetic fusion of *ALK* with a variety of gene partners [40–43]. Undifferentiated uterine sarcoma is a diagnosis of exclusion and it is likely that cases of *NTRK*-rearranged sarcoma and *COL1A1-PDGFB* fusion-associated fibrosarcoma are currently encompassed into that category [13, 44]. Given the recent identification of *YWHAE* and *BCOR* translocated high-grade endometrial stromal sarcomas and the new entities we describe, it is clear that the category of undifferentiated uterine sarcoma represents a heterogeneous group of neoplasms which will likely significantly decrease with the identification of new molecular entities using modern molecular techniques. We suggest a diagnostic algorithm for uterine spindle cell sarcomas composed of uniform cells resembling fibrosarcoma (Fig. 4); it is stressed that other neoplasms, for example malignant solitary fibrous tumor, may also enter into the differential diagnosis.

In summary, we report the clinicopathological and molecular features of a series of 13 spindle cell sarcomas of the uterus with features resembling fibrosarcoma. We show that *NTRK* rearrangements are common in these neoplasms and describe a novel *COL1A1-PDGFB* fusion which has not previously been reported in uterine mesenchymal neoplasms. Identification of the latter 2 neoplasms is clinically important since these tumors could potentially respond to targeted therapies such as the PDGFβR, KIT, and ABL inhibitor imatinib [45] and anti NTRK inhibitors [17].

Compliance with ethical standards

Conflict of interest The authors declare that they have no conflict of interest.

References

1. Oliva E. CM, Carinelli SG, et al. Endometrial stromal and related tumors. In: Kurman RJ CM, Herrington CS, Young RH, editor. WHO classification of tumors of female reproductive organs. Lyon, IARC; 2014. p. 141–7.
2. Sangiorgio V, Zanagnolo V, Aletti G, Bocciolone L, Bruni S, Landoni F, et al. Fibroblastic malignant peripheral nerve sheath tumour of the uterine cervix: report of a case and literature review with emphasis on possible differential diagnosis. Int J Gynecol Pathol. 2018;37:497–503.

3. Rodriguez AO, Truskinovsky AM, Kasrazadeh M, Leiserowitz GS. Case report: Malignant peripheral nerve sheath tumor of the uterine cervix treated with radical vaginal trachelectomy. Gynecol Oncol. 2006;100:201–4.
4. Bernstein HB, Broman JH, Apicelli A, Kredentser DC. Primary malignant schwannoma of the uterine cervix: a case report and literature review. Gynecol Oncol. 1999;74:288–92.
5. Mills AM, Karamchandani JR, Vogel H, Longacre TA. Endocervical fibroblastic malignant peripheral nerve sheath tumor (neurofibrosarcoma): report of a novel entity possibly related to endocervical CD34 fibrocytes. Am J Surg Pathol. 2011;35:404–12.
6. Chiang S, Cotzia P, Hyman DM, Drilon A, Tap WD, Zhang L, et al. NTRK Fusions Define a Novel Uterine Sarcoma Subtype With Features of Fibrosarcoma. Am J Surg Pathol. 2018;42:791–8.
7. Zheng Z, Liebers M, Zhelyazkova B, Cao Y, Panditi D, Lynch KD, et al. Anchored multiplex PCR for targeted next-generation sequencing. Nat Med. 2014;20:1479–84.
8. Croce S, Ribeiro A, Brulard C, Noel JC, Amant F, Stoeckle E, et al. Uterine smooth muscle tumor analysis by comparative genomic hybridization: a useful diagnostic tool in challenging lesions. Mod Pathol. 2015;28:1001–10.
9. Cuppens T, Moisse M, Depreeuw J, Annibali D, Colas E, Gil-Moreno A, et al. Integrated genome analysis of uterine leiomyosarcoma to identify novel driver genes and targetable pathways. Int J Cancer. 2018;142:1230–43.
10. Lee CH, Marino-Enriquez A, Ou W, Zhu M, Ali RH, Chiang S, et al. The clinicopathologic features of YWHAE-FAM22 endometrial stromal sarcomas: a histologically high-grade and clinically aggressive tumor. Am J Surg Pathol. 2012;36:641–53.
11. Lee CH, Ou WB, Marino-Enriquez A, Zhu M, Mayeda M, Wang Y, et al. 14-3-3 fusion oncogenes in high-grade endometrial stromal sarcoma. Proc Natl Acad Sci USA. 2012;109:929–34.
12. Croce S, Hostein I, Ribeiro A, Garbay D, Velasco V, Stoeckle E, et al. YWHAE rearrangement identified by FISH and RT-PCR in endometrial stromal sarcomas: genetic and pathological correlations. Mod Pathol. 2013;26:1390–400.
13. Hoang L, Chiang S, Lee CH. Endometrial stromal sarcomas and related neoplasms: new developments and diagnostic considerations. Pathology. 2018;50:162–77.
14. Hoang LN, Aneja A, Conlon N, Delair DF, Middha S, Benayed R, et al. Novel high-grade endometrial stromal sarcoma: a morphologic mimicker of myxoid leiomyosarcoma. Am J Surg Pathol. 2017;41:12–24.
15. Hechtman JF, Benayed R, Hyman DM, Drilon A, Zehir A, Frosina D, et al. Pan-Trk immunohistochemistry is an efficient and reliable screen for the detection of NTRK fusions. Am J Surg Pathol. 2017;41:1547–51.
16. Kaplan DR, Martin-Zanca D, Parada LF. Tyrosine phosphorylation and tyrosine kinase activity of the trk proto-oncogene product induced by NGF. Nature. 1991;350:158–60.
17. Kheder ES, Hong DS. Emerging targeted therapy for tumors with NTRK fusion proteins. Clin Cancer Res. 2018.
18. Wiesner T, He J, Yelensky R, Esteve-Puig R, Botton T, Yeh I, et al. Kinase fusions are frequent in Spitz tumours and spitzoid melanomas. Nat Commun. 2014;5:3116.
19. Doebele RC, Davis LE, Vaishnavi A, Le AT, Estrada-Bernal A, Keysar S, et al. An Oncogenic NTRK fusion in a patient with soft-tissue sarcoma with response to the tropomyosin-related kinase inhibitor LOXO-101. Cancer Discov. 2015;5:1049–57.
20. Carroll SL. The challenge of cancer genomics in rare nervous system neoplasms: malignant peripheral nerve sheath tumors as a paradigm for cross-species comparative oncogenomics. Am J Pathol. 2016;186:464–77.
21. Pedeutour F, Simon MP, Minoletti F, Barcelo G, Terrier-Lacombe MJ, Combemale P, et al. Translocation, t(17;22)(q22; q13), in dermatofibrosarcoma protuberans: a new tumor-associated chromosome rearrangement. Cytogenet Cell Genet. 1996;72:171–4.
22. Karanian M, Perot G, Coindre JM, Chibon F, Pedeutour F, Neuville A. Fluorescence in situ hybridization analysis is a helpful test for the diagnosis of dermatofibrosarcoma protuberans. Mod Pathol. 2015;28:230–7.
23. Simon MP, Pedeutour F, Sirvent N, Grosgeorge J, Minoletti F, Coindre JM, et al. Deregulation of the platelet-derived growth factor B-chain gene via fusion with collagen gene COL1A1 in dermatofibrosarcoma protuberans and giant-cell fibroblastoma. Nat Genet. 1997;15:95–8.
24. Maire G, Pedeutour F, Coindre JM. COL1A1-PDGFB gene fusion demonstrates a common histogenetic origin for dermatofibrosarcoma protuberans and its granular cell variant. Am J Surg Pathol. 2002;26:932–7.
25. Thway K, Noujaim J, Jones RL, Fisher C. Dermatofibrosarcoma protuberans: pathology, genetics, and potential therapeutic strategies. Ann Diagn Pathol. 2016;25:64–71.
26. Bowne WB, Antonescu CR, Leung DH, Katz SC, Hawkins WG, Woodruff JM, et al. Dermatofibrosarcoma protuberans: a clinicopathologic analysis of patients treated and followed at a single institution. Cancer . 2000;88:2711–20.
27. Garcia JJ, Folpe AL. The impact of advances in molecular genetic pathology on the classification, diagnosis and treatment of selected soft tissue tumors of the head and neck. Head Neck Pathol. 2010;4:70–6.
28. Chang CK, Jacobs IA, Salti GI. Outcomes of surgery for dermatofibrosarcoma protuberans. Eur J Surg Oncol. 2004;30:341–5.
29. Edelweiss M, Malpica A. Dermatofibrosarcoma protuberans of the vulva: a clinicopathologic and immunohistochemical study of 13 cases. Am J Surg Pathol. 2010;34:393–400.
30. Kao YC, Sung YS, Zhang L, Huang SC, Argani P, Chung CT, et al. Recurrent BCOR internal tandem duplication and YWHAE-NUTM2B fusions in soft tissue undifferentiated round cell sarcoma of infancy: overlapping genetic features with clear cell sarcoma of kidney. Am J Surg Pathol. 2016;40:1009–20.
31. O'Meara E, Stack D, Lee CH, Garvin AJ, Morris T, Argani P, et al. Characterization of the chromosomal translocation t(10;17)(q22;p13) in clear cell sarcoma of kidney. J Pathol. 2012;227:72–80.
32. Scheithauer BW WJ, Erlandson RA. Atlas of tumor pathology: tumors of the peripheral nervous system. 3rd, ed. (AFIP), fascicle 24, Bethesda, MA, 1999.
33. Okubo Y, Yoshioka E, Suzuki M, Washimi K, Kawachi K, Kameda Y, et al. Diagnosis, pathological findings, and clinical management of gangliocytic paraganglioma: a systematic review. Front Oncol. 2018;8:291.
34. Pekmezci M, Cuevas-Ocampo AK, Perry A, Horvai AE. Significance of H3K27me3 loss in the diagnosis of malignant peripheral nerve sheath tumors. Mod Pathol. 2017;30:1710–9.
35. Le Guellec S, Macagno N, Velasco V, Lamant L, Lae M, Filleron T, et al. Loss of H3K27 trimethylation is not suitable for distinguishing malignant peripheral nerve sheath tumor from melanoma: a study of 387 cases including mimicking lesions. Mod Pathol. 2017;30:1677–87.
36. Yang EJ, Howitt BE, Fletcher CDM, Nucci MR. Solitary fibrous tumour of the female genital tract: a clinicopathological analysis of 25 cases. Histopathology. 2018;72:749–59.
37. Oliva E. Practical issues in uterine pathology from banal to bewildering: the remarkable spectrum of smooth muscle neoplasia. Mod Pathol. 2016;29:S104–20.
38. Lee CH, Ali RH, Rouzbahman M, Marino-Enriquez A, Zhu M, Guo X, et al. Cyclin D1 as a diagnostic immunomarker for

endometrial stromal sarcoma with YWHAE-FAM22 rearrangement. Am J Surg Pathol. 2012;36:1562–70.
39. Chiang S, Lee CH, Stewart CJR, Oliva E, Hoang LN, Ali RH, et al. BCOR is a robust diagnostic immunohistochemical marker of genetically diverse high-grade endometrial stromal sarcoma, including tumors exhibiting variant morphology. Mod Pathol. 2017;30:1251–61.
40. Haimes JD, Stewart CJR, Kudlow BA, Culver BP, Meng B, Koay E, et al. Uterine Inflammatory Myofibroblastic Tumors Frequently Harbor ALK Fusions With IGFBP5 and THBS1. Am J Surg Pathol. 2017;41:773–80.
41. Bennett JA, Nardi V, Rouzbahman M, Morales-Oyarvide V, Nielsen GP, Oliva E. Inflammatory myofibroblastic tumor of the uterus: a clinicopathological, immunohistochemical, and molecular analysis of 13 cases highlighting their broad morphologic spectrum. Mod Pathol. 2017;30:1489–503.
42. Pickett JL, Chou A, Andrici JA, Clarkson A, Sioson L, Sheen A, et al. Inflammatory myofibroblastic tumors of the female genital tract are under-recognized: a low threshold for alk immunohistochemistry is required. Am J Surg Pathol. 2017;41:1433–42.
43. Parra-Herran C, Quick CM, Howitt BE, Dal Cin P, Quade BJ, Nucci MR. Inflammatory myofibroblastic tumor of the uterus: clinical and pathologic review of 10 cases including a subset with aggressive clinical course. Am J Surg Pathol. 2015;39:157–68.
44. Kurihara S, Oda Y, Ohishi Y, Iwasa A, Takahira T, Kaneki E, et al. Endometrial stromal sarcomas and related high-grade sarcomas: immunohistochemical and molecular genetic study of 31 cases. Am J Surg Pathol. 2008;32:1228–38.
45. Rutkowski P, Debiec-Rychter M. Current treatment options for dermatofibrosarcoma protuberans. Expert Rev Anticancer Ther. 2015;15:901–9.

[1] Veras E, Zivanovic O, Jacks L, Chiappetta D, Hensley M, Soslow R: "Low-grade leiomyosarcoma" and late-recurring smooth muscle tumors of the uterus: a heterogenous collection of frequently misdiagnosed tumors associated with an overall favorable prognosis relative to conventional uterine leiomyosarcomas. Am J Surg Pathol 2011, 35:1626-37.
[2] Croce S, Young RH, Oliva E: Uterine leiomyomas with bizarre nuclei: a clinicopathologic study of 59 cases. Am J Surg Pathol 2014, 38:1330-9.
[3] Bennett JA, Weigelt B, Chiang S, Selenica P, Chen YB, Bialik A, Bi R, Schultheis AM, Lim RS, Ng CKY, Morales-Oyarvide V, Young RH, Reuter VE, Soslow RA, Oliva E: Leiomyoma with bizarre nuclei: a morphological, immunohistochemical and molecular analysis of 31 cases. Mod Pathol 2017, 30:1476-88.
[4] Liegl-Atzwanger B, Heitzer E, Flicker K, Muller S, Ulz P, Saglam O, Tavassoli F, Devouassoux-Shisheboran M, Geigl J, Moinfar F: Exploring chromosomal abnormalities and genetic changes in uterine smooth muscle tumors. Mod Pathol 2016, 29:1262-77.
[5] Lee-Six H, Olafsson S, Ellis P, Osborne RJ, Sanders MA, Moore L, Georgakopoulos N, Torrente F, Noorani A, Goddard M, Robinson P, Coorens THH, O'Neill L, Alder C, Wang J, Fitzgerald RC, Zilbauer M, Coleman N, Saeb-Parsy K, Martincorena I, Campbell PJ, Stratton MR: The landscape of somatic mutation in normal colorectal epithelial cells. Nature 2019, 574:532-7.
[6] Geigl JB, Obenauf AC, Schwarzbraun T, Speicher MR: Defining 'chromosomal instability'. Trends Genet 2008, 24:64-9.
[7] Bakhoum SF, Ngo B, Laughney AM, Cavallo JA, Murphy CJ, Ly P, Shah P, Sriram RK, Watkins TBK, Taunk NK, Duran M, Pauli C, Shaw C, Chadalavada K, Rajasekhar VK, Genovese G, Venkatesan S, Birkbak NJ, McGranahan N, Lundquist M, LaPlant Q, Healey JH, Elemento O, Chung CH, Lee NY, Imielenski M, Nanjangud G, Pe'er D, Cleveland DW, Powell SN, Lammerding J, Swanton C, Cantley LC: Chromosomal instability drives metastasis through a cytosolic DNA response. Nature 2018, 553:467-72.
[8] Bakhoum SF, Danilova OV, Kaur P, Levy NB, Compton DA: Chromosomal instability substantiates poor prognosis in patients with diffuse large B-cell lymphoma. Clin Cancer Res 2011, 17:7704-11.
[9] Roylance R, Endesfelder D, Gorman P, Burrell RA, Sander J, Tomlinson I, Hanby AM, Speirs V, Richardson AL, Birkbak NJ, Eklund AC, Downward J, Kschischo M, Szallasi Z, Swanton C: Relationship of extreme chromosomal instability with long-term survival in a retrospective analysis of primary breast cancer. Cancer Epidemiol Biomarkers Prev 2011, 20:2183-94.
[10] Zaki BI, Suriawinata AA, Eastman AR, Garner KM, Bakhoum SF: Chromosomal instability portends superior response of rectal adenocarcinoma to chemoradiation therapy. Cancer 2014, 120:1733-42.
[11] Inaki K, Liu ET: Structural mutations in cancer: mechanistic and functional insights. Trends Genet 2012, 28:550-9.
[12] Jackson M, Marks L, May GHW, Wilson JB: The genetic basis of disease. Essays Biochem 2018, 62:643-723.
[13] Mitelman F, Johansson B, Mertens F: The impact of translocations and gene fusions on cancer causation. Nat Rev Cancer 2007, 7:233-45.
[14] Helman LJ, Meltzer P: Mechanisms of sarcoma development. Nat Rev Cancer 2003, 3:685-94.
[15] D'Angelo E, Ali RH, Espinosa I, Lee CH, Huntsman DG, Gilks B, Prat J: Endometrial stromal sarcomas with sex cord differentiation are associated with PHF1 rearrangement. Am J Surg Pathol 2013, 37:514-21.
[16] Koontz JI, Soreng AL, Nucci M, Kuo FC, Pauwels P, van Den Berghe H, Dal Cin P, Fletcher JA, Sklar J: Frequent fusion of the JAZF1 and JJAZ1 genes in endometrial stromal tumors. Proc Natl Acad Sci U S A 2001, 98:6348-53.
[17] Lee CH, Ou WB, Marino-Enriquez A, Zhu M, Mayeda M, Wang Y, Guo X, Brunner AL, Amant F, French CA, West RB, McAlpine JN, Gilks CB, Yaffe MB, Prentice LM, McPherson A, Jones SJ, Marra MA, Shah SP, van de Rijn M, Huntsman DG, Dal Cin P, Debiec-Rychter M, Nucci MR, Fletcher JA: 14-3-3 fusion oncogenes in high-grade endometrial stromal sarcoma. Proc Natl Acad Sci U S A 2012, 109:929-34.
[18] Marino-Enriquez A, Lauria A, Przybyl J, Ng TL, Kowalewska M, Debiec-Rychter M, Ganesan R, Sumathi V, George S, McCluggage WG, Nucci MR, Lee CH, Fletcher JA: BCOR Internal Tandem Duplication in High-grade Uterine Sarcomas. Am J Surg Pathol 2018, 42:335-41.
[19] Croce S, Hostein I, Ribeiro A, Garbay D, Velasco V, Stoeckle E, Guyon F, Floquet A, Neuville A, Coindre JM, MacGrogan G, Chibon F: YWHAE rearrangement identified by FISH and RT-PCR in endometrial stromal sarcomas: genetic and pathological correlations. Mod Pathol 2013, 26:1390-400.
[20] Lewis N, Soslow RA, Delair DF, Park KJ, Murali R, Hollmann TJ, Davidson B, Micci F, Panagopoulos I, Hoang LN, Arias-Stella JA, 3rd, Oliva E, Young RH, Hensley ML, Leitao MM, Jr., Hameed M, Benayed R, Ladanyi M, Frosina D, Jungbluth AA, Antonescu CR, Chiang S: ZC3H7B-

BCOR high-grade endometrial stromal sarcomas: a report of 17 cases of a newly defined entity. Mod Pathol 2018, 31:674-84.
[21] Croce S, Lesluyes T, Delespaul L, Bonhomme B, Perot G, Velasco V, Mayeur L, Rebier F, Ben Rejeb H, Guyon F, McCluggage WG, Floquet A, Querleu D, Chakiba C, Devouassoux-Shisheboran M, Mery E, Arnould L, Averous G, Soubeyran I, Le Guellec S, Chibon F: GREB1-CTNNB1 fusion transcript detected by RNA-sequencing in a uterine tumor resembling ovarian sex cord tumor (UTROSCT): A novel CTNNB1 rearrangement. Genes Chromosomes Cancer 2019, 58:155-63.
[22] Lee CH, Kao YC, Lee WR, Hsiao YW, Lu TP, Chu CY, Lin YJ, Huang HY, Hsieh TH, Liu YR, Liang CW, Chen TW, Yip S, Lum A, Kuo KT, Jeng YM, Yu SC, Chung YC, Lee JC: Clinicopathologic Characterization of GREB1-rearranged Uterine Sarcomas With Variable Sex-Cord Differentiation. Am J Surg Pathol 2019, 43:928-42.
[23] Dickson BC, Childs TJ, Colgan TJ, Sung YS, Swanson D, Zhang L, Antonescu CR: Uterine Tumor Resembling Ovarian Sex Cord Tumor: A Distinct Entity Characterized by Recurrent NCOA2/3 Gene Fusions. Am J Surg Pathol 2019, 43:178-86.
[24] Davoli T, Xu AW, Mengwasser KE, Sack LM, Yoon JC, Park PJ, Elledge SJ: Cumulative haploinsufficiency and triplosensitivity drive aneuploidy patterns and shape the cancer genome. Cell 2013, 155:948-62.
[25] Leibowitz ML, Zhang CZ, Pellman D: Chromothripsis: A New Mechanism for Rapid Karyotype Evolution. Annu Rev Genet 2015, 49:183-211.
[26] Drost J, van Jaarsveld RH, Ponsioen B, Zimberlin C, van Boxtel R, Buijs A, Sachs N, Overmeer RM, Offerhaus GJ, Begthel H, Korving J, van de Wetering M, Schwank G, Logtenberg M, Cuppen E, Snippert HJ, Medema JP, Kops GJ, Clevers H: Sequential cancer mutations in cultured human intestinal stem cells. Nature 2015, 521:43-7.
[27] Rajagopalan H, Jallepalli PV, Rago C, Velculescu VE, Kinzler KW, Vogelstein B, Lengauer C: Inactivation of hCDC4 can cause chromosomal instability. Nature 2004, 428:77-81.
[28] Stephens PJ, Greenman CD, Fu B, Yang F, Bignell GR, Mudie LJ, Pleasance ED, Lau KW, Beare D, Stebbings LA, McLaren S, Lin ML, McBride DJ, Varela I, Nik-Zainal S, Leroy C, Jia M, Menzies A, Butler AP, Teague JW, Quail MA, Burton J, Swerdlow H, Carter NP, Morsberger LA, Iacobuzio-Donahue C, Follows GA, Green AR, Flanagan AM, Stratton MR, Futreal PA, Campbell PJ: Massive genomic rearrangement acquired in a single catastrophic event during cancer development. Cell 2011, 144:27-40.
[29] Forment JV, Kaidi A, Jackson SP: Chromothripsis and cancer: causes and consequences of chromosome shattering. Nat Rev Cancer 2012, 12:663-70.
[30] Mehine M, Kaasinen E, Makinen N, Katainen R, Kampjarvi K, Pitkanen E, Heinonen HR, Butzow R, Kilpivaara O, Kuosmanen A, Ristolainen H, Gentile M, Sjoberg J, Vahteristo P, Aaltonen LA: Characterization of uterine leiomyomas by whole-genome sequencing. N Engl J Med 2013, 369:43-53.
[31] Zack TI, Schumacher SE, Carter SL, Cherniack AD, Saksena G, Tabak B, Lawrence MS, Zhsng CZ, Wala J, Mermel CH, Sougnez C, Gabriel SB, Hernandez B, Shen H, Laird PW, Getz G, Meyerson M, Beroukhim R: Pan-cancer patterns of somatic copy number alteration. Nat Genet 2013, 45:1134-40.
[32] Olaharski AJ, Sotelo R, Solorza-Luna G, Gonsebatt ME, Guzman P, Mohar A, Eastmond DA: Tetraploidy and chromosomal instability are early events during cervical carcinogenesis. Carcinogenesis 2006, 27:337-43.
[33] Hieronymus H, Schultz N, Gopalan A, Carver BS, Chang MT, Xiao Y, Heguy A, Huberman K, Bernstein M, Assel M, Murali R, Vickers A, Scardino PT, Sander C, Reuter V, Taylor BS, Sawyers CL: Copy number alteration burden predicts prostate cancer relapse. Proc Natl Acad Sci U S A 2014, 111:11139-44.
[34] Cancer Genome Atlas Research N: Integrated genomic analyses of ovarian carcinoma. Nature 2011, 474:609-15.
[35] Cancer Genome Atlas Research N, Kandoth C, Schultz N, Cherniack AD, Akbani R, Liu Y, Shen H, Robertson AG, Pashtan I, Shen R, Benz CC, Yau C, Laird PW, Ding L, Zhang W, Mills GB, Kucherlapati R, Mardis ER, Levine DA: Integrated genomic characterization of endometrial carcinoma. Nature 2013, 497:67-73.
[36] Chibon F, Lagarde P, Salas S, Perot G, Brouste V, Tirode F, Lucchesi C, de Reynies A, Kauffmann A, Bui B, Terrier P, Bonvalot S, Le Cesne A, Vince-Ranchere D, Blay JY, Collin F, Guillou L, Leroux A, Coindre JM, Aurias A: Validated prediction of clinical outcome in sarcomas and multiple types of cancer on the basis of a gene expression signature related to genome complexity. Nat Med 2010, 16:781-7.
[37] Mas A, Cervello I, Gil-Sanchis C, Faus A, Ferro J, Pellicer A, Simon C: Identification and characterization of the human leiomyoma side population as putative tumor-initiating cells. Fertil Steril 2012, 98:741-51 e6.

[38] Canevari RA, Pontes A, Rosa FE, Rainho CA, Rogatto SR: Independent clonal origin of multiple uterine leiomyomas that was determined by X chromosome inactivation and microsatellite analysis. Am J Obstet Gynecol 2005, 193:1395-403.
[39] Hashimoto K, Azuma C, Kamiura S, Kimura T, Nobunaga T, Kanai T, Sawada M, Noguchi S, Saji F: Clonal determination of uterine leiomyomas by analyzing differential inactivation of the X-chromosome-linked phosphoglycerokinase gene. Gynecol Obstet Invest 1995, 40:204-8.
[40] Mehine M, Heinonen HR, Sarvilinna N, Pitkanen E, Makinen N, Katainen R, Tuupanen S, Butzow R, Sjoberg J, Aaltonen LA: Clonally related uterine leiomyomas are common and display branched tumor evolution. Hum Mol Genet 2015, 24:4407-16.
[41] Holdsworth-Carson SJ, Zaitseva M, Girling JE, Vollenhoven BJ, Rogers PA: Common fibroid-associated genes are differentially expressed in phenotypically dissimilar cell populations isolated from within human fibroids and myometrium. Reproduction 2014, 147:683-92.
[42] Mehine M, Kaasinen E, Heinonen HR, Makinen N, Kampjarvi K, Sarvilinna N, Aavikko M, Vaharautio A, Pasanen A, Butzow R, Heikinheimo O, Sjoberg J, Pitkanen E, Vahteristo P, Aaltonen LA: Integrated data analysis reveals uterine leiomyoma subtypes with distinct driver pathways and biomarkers. Proc Natl Acad Sci U S A 2016, 113:1315-20.
[43] Makinen N, Kampjarvi K, Frizzell N, Butzow R, Vahteristo P: Characterization of MED12, HMGA2, and FH alterations reveals molecular variability in uterine smooth muscle tumors. Mol Cancer 2017, 16:101.
[44] Makinen N, Mehine M, Tolvanen J, Kaasinen E, Li Y, Lehtonen HJ, Gentile M, Yan J, Enge M, Taipale M, Aavikko M, Katainen R, Virolainen E, Bohling T, Koski TA, Launonen V, Sjoberg J, Taipale J, Vahteristo P, Aaltonen LA: MED12, the mediator complex subunit 12 gene, is mutated at high frequency in uterine leiomyomas. Science 2011, 334:252-5.
[45] Perot G, Croce S, Ribeiro A, Lagarde P, Velasco V, Neuville A, Coindre JM, Stoeckle E, Floquet A, MacGrogan G, Chibon F: MED12 alterations in both human benign and malignant uterine soft tissue tumors. PLoS One 2012, 7:e40015.
[46] Croce S, Chibon F: MED12 and uterine smooth muscle oncogenesis: State of the art and perspectives. Eur J Cancer 2015, 51:1603-10.
[47] Nibert M, Heim S: Uterine leiomyoma cytogenetics. Genes Chromosomes Cancer 1990, 2:3-13.
[48] Rein MS, Friedman AJ, Barbieri RL, Pavelka K, Fletcher JA, Morton CC: Cytogenetic abnormalities in uterine leiomyomata. Obstet Gynecol 1991, 77:923-6.
[49] Meloni AM, Surti U, Contento AM, Davare J, Sandberg AA: Uterine leiomyomas: cytogenetic and histologic profile. Obstet Gynecol 1992, 80:209-17.
[50] Kampjarvi K, Makinen N, Mehine M, Valipakka S, Uimari O, Pitkanen E, Heinonen HR, Heikkinen T, Tolvanen J, Ahtikoski A, Frizzell N, Sarvilinna N, Sjoberg J, Butzow R, Aaltonen LA, Vahteristo P: MED12 mutations and FH inactivation are mutually exclusive in uterine leiomyomas. Br J Cancer 2016, 114:1405-11.
[51] McGuire MM, Yatsenko A, Hoffner L, Jones M, Surti U, Rajkovic A: Whole exome sequencing in a random sample of North American women with leiomyomas identifies MED12 mutations in majority of uterine leiomyomas. PLoS One 2012, 7:e33251.
[52] Je EM, Kim MR, Min KO, Yoo NJ, Lee SH: Mutational analysis of MED12 exon 2 in uterine leiomyoma and other common tumors. Int J Cancer 2012, 131:E1044-7.
[53] Mehine M, Makinen N, Heinonen HR, Aaltonen LA, Vahteristo P: Genomics of uterine leiomyomas: insights from high-throughput sequencing. Fertil Steril 2014, 102:621-9.
[54] Matsubara A, Sekine S, Yoshida M, Yoshida A, Taniguchi H, Kushima R, Tsuda H, Kanai Y: Prevalence of MED12 mutations in uterine and extrauterine smooth muscle tumours. Histopathology 2013, 62:657-61.
[55] Makinen N, Vahteristo P, Kampjarvi K, Arola J, Butzow R, Aaltonen LA: MED12 exon 2 mutations in histopathological uterine leiomyoma variants. Eur J Hum Genet 2013, 21:1300-3.
[56] Taylor BS, Barretina J, Maki RG, Antonescu CR, Singer S, Ladanyi M: Advances in sarcoma genomics and new therapeutic targets. Nat Rev Cancer 2011, 11:541-57.
[57] Italiano A, Lagarde P, Brulard C, Terrier P, Lae M, Marques B, Ranchere-Vince D, Michels JJ, Trassard M, Cioffi A, Piperno-Neumann S, Chevreau C, Blay JY, Delcambre C, Isambert N, Penel N, Bay JO, Bonvalot S, Le Cesne A, Coindre JM, Chibon F: Genetic profiling identifies two classes of soft-tissue leiomyosarcomas with distinct clinical characteristics. Clin Cancer Res 2013, 19:1190-6.
[58] Chibon F, Darbo E, Perot G: Leiomyosarcomas: whole genome sequencing for a whole biology characterization. Curr Opin Oncol 2019, 31:317-21.
[59] Chudasama P, Mughal SS, Sanders MA, Hubschmann D, Chung I, Deeg KI, Wong SH, Rabe S, Hlevnjak M, Zapatka M, Ernst A, Kleinheinz K, Schlesner M, Sieverling L, Klink B, Schrock E, Hoogenboezem RM, Kasper B, Heilig CE, Egerer G, Wolf S, von Kalle C, Eils R, Stenzinger A, Weichert W, Glimm H, Groschel S, Kopp HG, Omlor G, Lehner B, Bauer S, Schimmack S, Ulrich A, Mechtersheimer G, Rippe K, Brors B, Hutter B, Renner M, Hohenberger P, Scholl C, Frohling S: Integrative genomic and transcriptomic analysis of leiomyosarcoma. Nat Commun 2018, 9:144.

[60] Cancer Genome Atlas Research Network. Electronic address edsc, Cancer Genome Atlas Research N: Comprehensive and Integrated Genomic Characterization of Adult Soft Tissue Sarcomas. Cell 2017, 171:950-65 e28.
[61] Perot G, Chibon F, Montero A, Lagarde P, de The H, Terrier P, Guillou L, Ranchere D, Coindre JM, Aurias A: Constant p53 pathway inactivation in a large series of soft tissue sarcomas with complex genetics. Am J Pathol 2010, 177:2080-90.
[62] Leiserson MD, Vandin F, Wu HT, Dobson JR, Eldridge JV, Thomas JL, Papoutsaki A, Kim Y, Niu B, McLellan M, Lawrence MS, Gonzalez-Perez A, Tamborero D, Cheng Y, Ryslik GA, Lopez-Bigas N, Getz G, Ding L, Raphael BJ: Pan-cancer network analysis identifies combinations of rare somatic mutations across pathways and protein complexes. Nat Genet 2015, 47:106-14.
[63] Chibon F, Mairal A, Freneaux P, Terrier P, Coindre JM, Sastre X, Aurias A: The RB1 gene is the target of chromosome 13 deletions in malignant fibrous histiocytoma. Cancer Res 2000, 60:6339-45.
[64] Zhang Q, Ubago J, Li L, Guo H, Liu Y, Qiang W, Kim JJ, Kong B, Wei JJ: Molecular analyses of 6 different types of uterine smooth muscle tumors: Emphasis in atypical leiomyoma. Cancer 2014, 120:3165-77.
[65] Bertsch E, Qiang W, Zhang Q, Espona-Fiedler M, Druschitz S, Liu Y, Mittal K, Kong B, Kurita T, Wei JJ: MED12 and HMGA2 mutations: two independent genetic events in uterine leiomyoma and leiomyosarcoma. Mod Pathol 2014, 27:1144-53.
[66] Perot G, Derre J, Coindre JM, Tirode F, Lucchesi C, Mariani O, Gibault L, Guillou L, Terrier P, Aurias A: Strong smooth muscle differentiation is dependent on myocardin gene amplification in most human retroperitoneal leiomyosarcomas. Cancer Res 2009, 69:2269-78.
[67] Du KL, Ip HS, Li J, Chen M, Dandre F, Yu W, Lu MM, Owens GK, Parmacek MS: Myocardin is a critical serum response factor cofactor in the transcriptional program regulating smooth muscle cell differentiation. Mol Cell Biol 2003, 23:2425-37.
[68] Guo X, Jo VY, Mills AM, Zhu SX, Lee CH, Espinosa I, Nucci MR, Varma S, Forgo E, Hastie T, Anderson S, Ganjoo K, Beck AH, West RB, Fletcher CD, van de Rijn M: Clinically Relevant Molecular Subtypes in Leiomyosarcoma. Clin Cancer Res 2015, 21:3501-11.
[69] Davis LE, Nusser KD, Przybyl J, Pittsenbarger J, Hofmann NE, Varma S, Vennam S, Debiec-Rychter M, van de Rijn M, Davare MA: Discovery and Characterization of Recurrent, Targetable ALK Fusions in Leiomyosarcoma. Mol Cancer Res 2019, 17:676-85.
[70] Bennett JA, Nardi V, Rouzbahman M, Morales-Oyarvide V, Nielsen GP, Oliva E: Inflammatory myofibroblastic tumor of the uterus: a clinicopathological, immunohistochemical, and molecular analysis of 13 cases highlighting their broad morphologic spectrum. Mod Pathol 2017, 30:1489-503.
[71] Yoon JY, Marino-Enriquez A, Stickle N, de Borja RJ, Ismiil N, Djordjevic B, Virtanen C, Ravat A, Nucci MR, Mirkovic J, Parra-Herran C: Myxoid smooth muscle neoplasia of the uterus: comprehensive analysis by next-generation sequencing and nucleic acid hybridization. Mod Pathol 2019.
[72] Parra-Herran C, Quick CM, Howitt BE, Dal Cin P, Quade BJ, Nucci MR: Inflammatory myofibroblastic tumor of the uterus: clinical and pathologic review of 10 cases including a subset with aggressive clinical course. Am J Surg Pathol 2015, 39:157-68.
[73] Parra-Herran C, Howitt BE: Uterine Mesenchymal Tumors: Update on Classification, Staging, and Molecular Features. Surg Pathol Clin 2019, 12:363-96.
[74] Croce S, Ribeiro A, Brulard C, Noel JC, Amant F, Stoeckle E, Devouassoux-Shisheborah M, Floquet A, Arnould L, Guyon F, Mishellany F, Garbay D, Cuppens T, Zikan M, Leroux A, Frouin E, Duvillard P, Terrier P, Farre I, Valo I, MacGrogan GM, Chibon F: Uterine smooth muscle tumor analysis by comparative genomic hybridization: a useful diagnostic tool in challenging lesions. Mod Pathol 2015, 28:1001-10.
[75] Schwetye KE, Pfeifer JD, Duncavage EJ: MED12 exon 2 mutations in uterine and extrauterine smooth muscle tumors. Hum Pathol 2014, 45:65-70.
[76] Teixeira J, Rueda BR, Pru JK: Uterine stem cells. StemBook. Cambridge (MA), 2008.
[77] Commandeur AE, Styer AK, Teixeira JM: Epidemiological and genetic clues for molecular mechanisms involved in uterine leiomyoma development and growth. Hum Reprod Update 2015, 21:593-615.
[78] Oliva E CM, Carinelli SG, et al: Mesenchymal tumours. Smooth muscle tumour of uncertain malignant potential. WHO Classification of Tumours of Female Reproductive Organs. Edited by Kurman RJ CM, Herrington CS, Young RH. 2014. pp. pp 135–47.
[79] PC I, JB B, SC C, KG G, BY Y: Mesenchymal Tumors Specific to the uterus. Female Genital Tumors-WHO. Edited by E O. YARC, 2020.
[80] Baird DD, Dunson DB, Hill MC, Cousins D, Schectman JM: High cumulative incidence of uterine leiomyoma in black and white women: ultrasound evidence. Am J Obstet Gynecol 2003, 188:100-7.
[81] Prat J, Mbatani: Uterine sarcomas. Int J Gynaecol Obstet 2015, 131 Suppl 2:S105-10.
[82] Brosens J, Campo R, Gordts S, Brosens I: Submucous and outer myometrium leiomyomas are two distinct clinical entities. Fertil Steril 2003, 79:1452-4.

[83] Kayser K, Zink S, Schneider T, Dienemann H, Andre S, Kaltner H, Schuring MP, Zick Y, Gabius HJ: Benign metastasizing leiomyoma of the uterus: documentation of clinical, immunohistochemical and lectin-histochemical data of ten cases. Virchows Arch 2000, 437:284-92.
[84] Ross RK, Pike MC, Vessey MP, Bull D, Yeates D, Casagrande JT: Risk factors for uterine fibroids: reduced risk associated with oral contraceptives. Br Med J (Clin Res Ed) 1986, 293:359-62.
[85] Fields KR, Neinstein LS: Uterine myomas in adolescents: case reports and a review of the literature. J Pediatr Adolesc Gynecol 1996, 9:195-8.
[86] Cramer SF, Patel A: The frequency of uterine leiomyomas. Am J Clin Pathol 1990, 94:435-8.
[87] Baird DD, Dunson DB: Why is parity protective for uterine fibroids? Epidemiology 2003, 14:247-50.
[88] Laughlin SK, Herring AH, Savitz DA, Olshan AF, Fielding JR, Hartmann KE, Baird DD: Pregnancy-related fibroid reduction. Fertil Steril 2010, 94:2421-3.
[89] Cesen-Cummings K, Houston KD, Copland JA, Moorman VJ, Walker CL, Davis BJ: Uterine leiomyomas express myometrial contractile-associated proteins involved in pregnancy-related hormone signaling. J Soc Gynecol Investig 2003, 10:11-20.
[90] Kashtan CE: Alport syndrome. An inherited disorder of renal, ocular, and cochlear basement membranes. Medicine (Baltimore) 1999, 78:338-60.
[91] Cohen MM, Jr.: Proteus syndrome: an update. Am J Med Genet C Semin Med Genet 2005, 137C:38-52.
[92] Pilarski R, Eng C: Will the real Cowden syndrome please stand up (again)? Expanding mutational and clinical spectra of the PTEN hamartoma tumour syndrome. J Med Genet 2004, 41:323-6.
[93] Launonen V, Vierimaa O, Kiuru M, Isola J, Roth S, Pukkala E, Sistonen P, Herva R, Aaltonen LA: Inherited susceptibility to uterine leiomyomas and renal cell cancer. Proc Natl Acad Sci U S A 2001, 98:3387-92.
[94] Kiuru M, Launonen V, Hietala M, Aittomaki K, Vierimaa O, Salovaara R, Arola J, Pukkala E, Sistonen P, Herva R, Aaltonen LA: Familial cutaneous leiomyomatosis is a two-hit condition associated with renal cell cancer of characteristic histopathology. Am J Pathol 2001, 159:825-9.
[95] Sanz-Ortega J, Vocke C, Stratton P, Linehan WM, Merino MJ: Morphologic and molecular characteristics of uterine leiomyomas in hereditary leiomyomatosis and renal cancer (HLRCC) syndrome. Am J Surg Pathol 2013, 37:74-80.
[96] Eggert SL, Huyck KL, Somasundaram P, Kavalla R, Stewart EA, Lu AT, Painter JN, Montgomery GW, Medland SE, Nyholt DR, Treloar SA, Zondervan KT, Heath AC, Madden PA, Rose L, Buring JE, Ridker PM, Chasman DI, Martin NG, Cantor RM, Morton CC: Genome-wide linkage and association analyses implicate FASN in predisposition to Uterine Leiomyomata. Am J Hum Genet 2012, 91:621-8.
[97] Cha PC, Takahashi A, Hosono N, Low SK, Kamatani N, Kubo M, Nakamura Y: A genome-wide association study identifies three loci associated with susceptibility to uterine fibroids. Nat Genet 2011, 43:447-50.
[98] Oliva E: Practical issues in uterine pathology from banal to bewildering: the remarkable spectrum of smooth muscle neoplasia. Mod Pathol 2016, 29 Suppl 1:S104-20.
[99] Downes KA, Hart WR: Bizarre leiomyomas of the uterus: a comprehensive pathologic study of 24 cases with long-term follow-up. Am J Surg Pathol 1997, 21:1261-70.
[100] Bennett JA, Weigelt B, Chiang S, Selenica P, Chen YB, Bialik A, Bi R, Schultheis AM, Lim RS, Ng CKY, Morales-Oyarvide V, Young RH, Reuter VE, Soslow RA, Oliva E: Leiomyoma with bizarre nuclei: a morphological, immunohistochemical and molecular analysis of 31 cases. Mod Pathol 2017.
[101] Reyes C, Karamurzin Y, Frizzell N, Garg K, Nonaka D, Chen YB, Soslow RA: Uterine smooth muscle tumors with features suggesting fumarate hydratase aberration: detailed morphologic analysis and correlation with S-(2-succino)-cysteine immunohistochemistry. Mod Pathol 2014, 27:1020-7.
[102] Ubago JM, Zhang Q, Kim JJ, Kong B, Wei JJ: Two Subtypes of Atypical Leiomyoma: Clinical, Histologic, and Molecular Analysis. Am J Surg Pathol 2016, 40:923-33.
[103] Mills AM, Ly A, Balzer BL, Hendrickson MR, Kempson RL, McKenney JK, Longacre TA: Cell cycle regulatory markers in uterine atypical leiomyoma and leiomyosarcoma: immunohistochemical study of 68 cases with clinical follow-up. Am J Surg Pathol 2013, 37:634-42.
[104] Chen L, Yang B: Immunohistochemical analysis of p16, p53, and Ki-67 expression in uterine smooth muscle tumors. Int J Gynecol Pathol 2008, 27:326-32.
[105] Sun X, Mittal K: MIB-1 (Ki-67), estrogen receptor, progesterone receptor, and p53 expression in atypical cells in uterine symplastic leiomyomas. Int J Gynecol Pathol 2010, 29:51-4.
[106] Gannon BR, Manduch M, Childs TJ: Differential Immunoreactivity of p16 in leiomyosarcomas and leiomyoma variants. Int J Gynecol Pathol 2008, 27:68-73.
[107] Prayson RA, Goldblum JR, Hart WR: Epithelioid smooth-muscle tumors of the uterus: a clinicopathologic study of 18 patients. Am J Surg Pathol 1997, 21:383-91.
[108] Evans HL, Chawla SP, Simpson C, Finn KP: Smooth muscle neoplasms of the uterus other than ordinary leiomyoma. A study of 46 cases, with emphasis on diagnostic criteria and prognostic factors. Cancer 1988, 62:2239-47.

[109] Parra-Herran C, Schoolmeester JK, Yuan L, Dal Cin P, Fletcher CD, Quade BJ, Nucci MR: Myxoid Leiomyosarcoma of the Uterus: A Clinicopathologic Analysis of 30 Cases and Review of the Literature With Reappraisal of Its Distinction From Other Uterine Myxoid Mesenchymal Neoplasms. Am J Surg Pathol 2016, 40:285-301.
[110] Busca A, Parra-Herran C: Myxoid Mesenchymal Tumors of the Uterus: An Update on Classification, Definitions, and Differential Diagnosis. Adv Anat Pathol 2017, 24:354-61.
[111] Ip PPC, Lim D, Cheung ANY, Oliva E: Immunoexpression of p16 in uterine leiomyomas with infarct-type necrosis: an analysis of 35 cases. Histopathology 2017.
[112] Miettinen M, Felisiak-Golabek A, Wasag B, Chmara M, Wang Z, Butzow R, Lasota J: Fumarase-deficient Uterine Leiomyomas: An Immunohistochemical, Molecular Genetic, and Clinicopathologic Study of 86 Cases. Am J Surg Pathol 2016, 40:1661-9.
[113] Harrison WJ, Andrici J, Maclean F, Madadi-Ghahan R, Farzin M, Sioson L, Toon CW, Clarkson A, Watson N, Pickett J, Field M, Crook A, Tucker K, Goodwin A, Anderson L, Srinivasan B, Grossmann P, Martinek P, Ondic O, Hes O, Trpkov K, Clifton-Bligh RJ, Dwight T, Gill AJ: Fumarate Hydratase-deficient Uterine Leiomyomas Occur in Both the Syndromic and Sporadic Settings. Am J Surg Pathol 2016, 40:599-607.
[114] Joseph NM, Solomon DA, Frizzell N, Rabban JT, Zaloudek C, Garg K: Morphology and Immunohistochemistry for 2SC and FH Aid in Detection of Fumarate Hydratase Gene Aberrations in Uterine Leiomyomas From Young Patients. Am J Surg Pathol 2015, 39:1529-39.
[115] Bennett JA, Morales-Oyarvide V, Campbell S, Longacre TA, Oliva E: Mismatch Repair Protein Expression in Clear Cell Carcinoma of the Ovary: Incidence and Morphologic Associations in 109 Cases. Am J Surg Pathol 2016, 40:656-63.
[116] Zhang Q, Poropatich K, Ubago J, Xie J, Xu X, Frizzell N, Kim J, Kong B, Wei JJ: Fumarate Hydratase Mutations and Alterations in Leiomyoma With Bizarre Nuclei. Int J Gynecol Pathol 2017.
[117] Roth LM, Reed RJ: Dissecting leiomyomas of the uterus other than cotyledonoid dissecting leiomyomas: a report of eight cases. Am J Surg Pathol 1999, 23:1032-9.
[118] Roth LM, Reed RJ, Sternberg WH: Cotyledonoid dissecting leiomyoma of the uterus. The Sternberg tumor. Am J Surg Pathol 1996, 20:1455-61.
[119] Buza N: Intravenous Leiomyomatosis. Female Genital Tumours. Edited by E O. IARC, Lyon, 2020.
[120] Clement PB, Young RH: Diffuse leiomyomatosis of the uterus: a report of four cases. Int J Gynecol Pathol 1987, 6:322-30.
[121] Mulvany NJ, Ostor AG, Ross I: Diffuse leiomyomatosis of the uterus. Histopathology 1995, 27:175-9.
[122] Clement PB, Young RH, Scully RE: Intravenous leiomyomatosis of the uterus. A clinicopathological analysis of 16 cases with unusual histologic features. Am J Surg Pathol 1988, 12:932-45.
[123] Carr RJ, Hui P, Buza N: Intravenous leiomyomatosis revisited: an experience of 14 cases at a single medical center. Int J Gynecol Pathol 2015, 34:169-76.
[124] Wu RC, Chao AS, Lee LY, Lin G, Chen SJ, Lu YJ, Huang HJ, Yen CF, Han CM, Lee YS, Wang TH, Chao A: Massively parallel sequencing and genome-wide copy number analysis revealed a clonal relationship in benign metastasizing leiomyoma. Oncotarget 2017, 8:47547-54.
[125] Nucci M: Metastasizing leiomyoma. Female Genital tumours. Edited by oliva E LA. Iarc, Lyon, 2020.
[126] Fukunaga M: Benign "metastasizing" lipoleiomyoma of the uterus. Int J Gynecol Pathol 2003, 22:202-4.
[127] Nucci MR, Drapkin R, Dal Cin P, Fletcher CD, Fletcher JA: Distinctive cytogenetic profile in benign metastasizing leiomyoma: pathogenetic implications. Am J Surg Pathol 2007, 31:737-43.
[128] Esteban JM, Allen WM, Schaerf RH: Benign metastasizing leiomyoma of the uterus: histologic and immunohistochemical characterization of primary and metastatic lesions. Arch Pathol Lab Med 1999, 123:960-2.
[129] Rivera JA, Christopoulos S, Small D, Trifiro M: Hormonal manipulation of benign metastasizing leiomyomas: report of two cases and review of the literature. J Clin Endocrinol Metab 2004, 89:3183-8.
[130] Longacre T: Uterine Leiomyosarcoma. Female Genital Tumours. Edited by Oliva E LA. IARC Lyon, 2020.
[131] Lin JF, Slomovitz BM: Uterine sarcoma 2008. Curr Oncol Rep 2008, 10:512-8.
[132] Devereaux KA, Schoolmeester JK: Smooth Muscle Tumors of the Female Genital Tract. Surg Pathol Clin 2019, 12:397-455.
[133] Chiang S, Samore W, Zhang L, Sung YS, Turashvili G, Murali R, Soslow RA, Hensley ML, Swanson D, Dickson BC, Stewart CJR, Oliva E, Antonescu CR: PGR Gene Fusions Identify a Molecular Subset of Uterine Epithelioid Leiomyosarcoma With Rhabdoid Features. Am J Surg Pathol 2019, 43:810-8.

[134] Arias-Stella JA, 3rd, Benayed R, Oliva E, Young RH, Hoang LN, Lee CH, Jungbluth AA, Frosina D, Soslow RA, Antonescu CR, Ladanyi M, Chiang S: Novel PLAG1 Gene Rearrangement Distinguishes a Subset of Uterine Myxoid Leiomyosarcoma From Other Uterine Myxoid Mesenchymal Tumors. Am J Surg Pathol 2019, 43:382-8.
[135] Burghaus S, Halmen S, Gass P, Mehlhorn G, Schrauder MG, Lux MP, Renner SP, Beckmann MW, Hein A, Thiel FC: Outcome and prognosis in uterine sarcoma and malignant mixed Mullerian tumor. Arch Gynecol Obstet 2016, 294:343-51.
[136] Abeler VM, Royne O, Thoresen S, Danielsen HE, Nesland JM, Kristensen GB: Uterine sarcomas in Norway. A histopathological and prognostic survey of a total population from 1970 to 2000 including 419 patients. Histopathology 2009, 54:355-64.
[137] Ip P: Smooth muscle tumour of uncertain malignant potential Female Genital Tumours. Edited by E O. IARC, Lyon, 2020.
[138] Gupta M, Laury AL, Nucci MR, Quade BJ: Predictors of adverse outcome in uterine smooth muscle tumours of uncertain malignant potential (STUMP): a clinicopathological analysis of 22 cases with a proposal for the inclusion of additional histological parameters. Histopathology 2018, 73:284-98.
[139] Ip PP, Cheung AN, Clement PB: Uterine smooth muscle tumors of uncertain malignant potential (STUMP): a clinicopathologic analysis of 16 cases. Am J Surg Pathol 2009, 33:992-1005.
[140] Ip PP, Cheung AN: Pathology of uterine leiomyosarcomas and smooth muscle tumours of uncertain malignant potential. Best Pract Res Clin Obstet Gynaecol 2011, 25:691-704.
[141] Kurman RJ, Norris HJ: Mesenchymal tumors of the uterus. VI. Epithelioid smooth muscle tumors including leiomyoblastoma and clear-cell leiomyoma: a clinical and pathologic analysis of 26 cases. Cancer 1976, 37:1853-65.
[142] Atkins KA, Arronte N, Darus CJ, Rice LW: The Use of p16 in enhancing the histologic classification of uterine smooth muscle tumors. Am J Surg Pathol 2008, 32:98-102.
[143] Slatter TL, Hsia H, Samaranayaka A, Sykes P, Clow WB, Devenish CJ, Sutton T, Royds JA, Pc P, Cheung AN, Hung NA: Loss of ATRX and DAXX expression identifies poor prognosis for smooth muscle tumours of uncertain malignant potential and early stage uterine leiomyosarcoma. J Pathol Clin Res 2015, 1:95-105.
[144] Ahvenainen TV, Makinen NM, von Nandelstadh P, Vahteristo MEA, Pasanen AM, Butzow RC, Vahteristo PM: Loss of ATRX/DAXX expression and alternative lengthening of telomeres in uterine leiomyomas. Cancer 2018, 124:4650-6.
[145] Beroukhim R, Mermel CH, Porter D, Wei G, Raychaudhuri S, Donovan J, Barretina J, Boehm JS, Dobson J, Urashima M, Mc Henry KT, Pinchback RM, Ligon AH, Cho YJ, Haery L, Greulich H, Reich M, Winckler W, Lawrence MS, Weir BA, Tanaka KE, Chiang DY, Bass AJ, Loo A, Hoffman C, Prensner J, Liefeld T, Gao Q, Yecies D, Signoretti S, Maher E, Kaye FJ, Sasaki H, Tepper JE, Fletcher JA, Tabernero J, Baselga J, Tsao MS, Demichelis F, Rubin MA, Janne PA, Daly MJ, Nucera C, Levine RL, Ebert BL, Gabriel S, Rustgi AK, Antonescu CR, Ladanyi M, Letai A, Garraway LA, Loda M, Beer DG, True LD, Okamoto A, Pomeroy SL, Singer S, Golub TR, Lander ES, Getz G, Sellers WR, Meyerson M: The landscape of somatic copy-number alteration across human cancers. Nature 2010, 463:899-905.
[146] Pandis N, Bardi G, Sfikas K, Panayotopoulos N, Tserkezoglou A, Fotiou S: Complex chromosome rearrangements involving 12q14 in two uterine leiomyomas. Cancer Genet Cytogenet 1990, 49:51-6.
[147] Pandis N, Heim S, Bardi G, Floderus UM, Willen H, Mandahl N, Mitelman F: Parallel karyotypic evolution and tumor progression in uterine leiomyoma. Genes Chromosomes Cancer 1990, 2:311-7.
[148] Pandis N, Heim S, Bardi G, Mandahl N, Mitelman F: High resolution mapping of consistent leiomyoma breakpoints in chromosomes 12 and 14 to 12q15 and 14q24.1. Genes Chromosomes Cancer 1990, 2:227-30.
[149] Cho YL, Bae S, Koo MS, Kim KM, Chun HJ, Kim CK, Ro DY, Kim JH, Lee CH, Kim YW, Ahn WS: Array comparative genomic hybridization analysis of uterine leiomyosarcoma. Gynecol Oncol 2005, 99:545-51.
[150] Meadows KL, Andrews DM, Xu Z, Carswell GK, Laughlin SK, Baird DD, Taylor JA: Genome-wide analysis of loss of heterozygosity and copy number amplification in uterine leiomyomas using the 100K single nucleotide polymorphism array. Exp Mol Pathol 2011, 91:434-9.
[151] Raish M, Khurshid M, Ansari MA, Chaturvedi PK, Bae SM, Kim JH, Park EK, Park DC, Ahn WS: Analysis of molecular cytogenetic alterations in uterine leiomyosarcoma by array-based comparative genomic hybridization. J Cancer Res Clin Oncol 2012, 138:1173-86.
[152] Shinawi M, Cheung SW: The array CGH and its clinical applications. Drug Discov Today 2008, 13:760-70.
[153] Lartigue L, Neuville A, Lagarde P, Brulard C, Rutkowski P, Dei Tos P, Wardelmann E, Debiec-Rychter M, Italiano A, Coindre JM, Chibon F: Genomic index predicts clinical outcome of intermediate-risk gastrointestinal stromal tumours, providing a new inclusion criterion for imatinib adjuvant therapy. Eur J Cancer 2015, 51:75-83.

[154] Lagarde P, Perot G, Kauffmann A, Brulard C, Dapremont V, Hostein I, Neuville A, Wozniak A, Sciot R, Schoffski P, Aurias A, Coindre JM, Debiec-Rychter M, Chibon F: Mitotic checkpoints and chromosome instability are strong predictors of clinical outcome in gastrointestinal stromal tumors. Clin Cancer Res 2012, 18:826-38.
[155] Chibon F, Lesluyes T, Valentin T, Le Guellec S: Cinsarc Signature as a Prognostic Marker for Clinical Outcome in Sarcomas and Beyond. Genes Chromosomes Cancer 2018.
[156] Gatta R, Mantovani R: NF-Y affects histone acetylation and H2A.Z deposition in cell cycle promoters. Epigenetics 2011, 6:526-34.
[157] Lesluyes T, Delespaul L, Coindre JM, Chibon F: The CINSARC signature as a prognostic marker for clinical outcome in multiple neoplasms. Sci Rep 2017, 7:5480.
[158] Lesluyes T, Perot G, Largeau MR, Brulard C, Lagarde P, Dapremont V, Lucchesi C, Neuville A, Terrier P, Vince-Ranchere D, Mendez-Lago M, Gut M, Gut I, Coindre JM, Chibon F: RNA sequencing validation of the Complexity INdex in SARComas prognostic signature. Eur J Cancer 2016, 57:104-11.
[159] Geiss GK, Bumgarner RE, Birditt B, Dahl T, Dowidar N, Dunaway DL, Fell HP, Ferree S, George RD, Grogan T, James JJ, Maysuria M, Mitton JD, Oliveri P, Osborn JL, Peng T, Ratcliffe AL, Webster PJ, Davidson EH, Hood L, Dimitrov K: Direct multiplexed measurement of gene expression with color-coded probe pairs. Nat Biotechnol 2008, 26:317-25.
[160] Le Guellec S, Lesluyes T, Sarot E, Valle C, Filleron T, Rochaix P, Valentin T, Perot G, Coindre JM, Chibon F: Validation of the Complexity INdex in SARComas prognostic signature on formalin-fixed, paraffin-embedded, soft-tissue sarcomas. Ann Oncol 2018, 29:1828-35.
[161] D'Angelo E, Prat J: Uterine sarcomas: a review. Gynecol Oncol 2010, 116:131-9.
[162] Toro JR, Travis LB, Wu HJ, Zhu K, Fletcher CD, Devesa SS: Incidence patterns of soft tissue sarcomas, regardless of primary site, in the surveillance, epidemiology and end results program, 1978-2001: An analysis of 26,758 cases. Int J Cancer 2006, 119:2922-30.
[163] Skorstad M, Kent A, Lieng M: Uterine leiomyosarcoma - incidence, treatment, and the impact of morcellation. A nationwide cohort study. Acta Obstet Gynecol Scand 2016, 95:984-90.
[164] Brooks SE, Zhan M, Cote T, Baquet CR: Surveillance, epidemiology, and end results analysis of 2677 cases of uterine sarcoma 1989-1999. Gynecol Oncol 2004, 93:204-8.
[165] Pautier P, Genestie C, Rey A, Morice P, Roche B, Lhomme C, Haie-Meder C, Duvillard P: Analysis of clinicopathologic prognostic factors for 157 uterine sarcomas and evaluation of a grading score validated for soft tissue sarcoma. Cancer 2000, 88:1425-31.
[166] Zivanovic O, Jacks LM, Iasonos A, Leitao MM, Jr., Soslow RA, Veras E, Chi DS, Abu-Rustum NR, Barakat RR, Brennan MF, Hensley ML: A nomogram to predict postresection 5-year overall survival for patients with uterine leiomyosarcoma. Cancer 2012, 118:660-9.
[167] Hensley ML, Ishill N, Soslow R, Larkin J, Abu-Rustum N, Sabbatini P, Konner J, Tew W, Spriggs D, Aghajanian CA: Adjuvant gemcitabine plus docetaxel for completely resected stages I-IV high grade uterine leiomyosarcoma: Results of a prospective study. Gynecol Oncol 2009, 112:563-7.
[168] Silva EG, Deavers MT, Bodurka DC, Malpica A: Uterine epithelioid leiomyosarcomas with clear cells: reactivity with HMB-45 and the concept of PEComa. Am J Surg Pathol 2004, 28:244-9.
[169] Croce S, Ducoulombier A, Ribeiro A, Lesluyes T, Noel JC, Amant F, Guillou L, Stoeckle E, Devouassoux-Shisheboran M, Penel N, Floquet A, Arnould L, Guyon F, Mishellany F, Chakiba C, Cuppens T, Zikan M, Leroux A, Frouin E, Farre I, Genestie C, Valo I, MacGrogan G, Chibon F: Genome profiling is an efficient tool to avoid the STUMP classification of uterine smooth muscle lesions: a comprehensive array-genomic hybridization analysis of 77 tumors. Mod Pathol 2018.
[170] Croce S, Lesluyes T, Valle C, M'Hamdi L, Thebault N, Perot G, Stoeckle E, Noel JC, Fontanges Q, Devouassoux-Shisheboran M, Querleu D, Guyon F, Floquet A, Chakiba C, Mayeur L, Rebier F, MacGrogan GM, Soubeyran I, Le Guellec S, Chibon F: The Nanocind Signature Is an Independent Prognosticator of Recurrence and Death in Uterine Leiomyosarcomas. Clin Cancer Res 2019.
[171] PC I: Uterine leiomyoma and leiomyomatosis: IARC Lyon, 2020.
[172] Oliva E CM, Carinelli SG, et al: Leiomyoma. WHO classification of tumours of female reproductive organs. Edited by Kurman RJ CM, Herrington CS, Young RH. IARC Lyon, 2014.
[173] Bell SW, Kempson RL, Hendrickson MR: Problematic uterine smooth muscle neoplasms. A clinicopathologic study of 213 cases. Am J Surg Pathol 1994, 18:535-58.
[174] Christopherson WM, Williamson EO, Gray LA: Leiomyosarcoma of the uterus. Cancer 1972, 29:1512-7.
[175] Sung CO, Ahn G, Song SY, Choi YL, Bae DS: Atypical leiomyomas of the uterus with long-term follow-up after myomectomy with immunohistochemical analysis for p16INK4A, p53, Ki-67, estrogen receptors, and progesterone receptors. Int J Gynecol Pathol 2009, 28:529-34.
[176] Kobel M, Ronnett BM, Singh N, Soslow RA, Gilks CB, McCluggage WG: Interpretation of P53 Immunohistochemistry in Endometrial Carcinomas: Toward Increased Reproducibility. Int J Gynecol Pathol 2019, 38 Suppl 1:S123-S31.

[177] Dreux N, Marty M, Chibon F, Velasco V, Hostein I, Ranchere-Vince D, Terrier P, Coindre JM: Value and limitation of immunohistochemical expression of HMGA2 in mesenchymal tumors: about a series of 1052 cases. Mod Pathol 2010, 23:1657-66.
[178] D'Haene N, Le Mercier M, De Neve N, Blanchard O, Delaunoy M, El Housni H, Dessars B, Heimann P, Remmelink M, Demetter P, Tejpar S, Salmon I: Clinical Validation of Targeted Next Generation Sequencing for Colon and Lung Cancers. PLoS One 2015, 10:e0138245.
[179] Sajnani K, Islam F, Smith RA, Gopalan V, Lam AK: Genetic alterations in Krebs cycle and its impact on cancer pathogenesis. Biochimie 2017, 135:164-72.
[180] Lagarde P, Przybyl J, Brulard C, Perot G, Pierron G, Delattre O, Sciot R, Wozniak A, Schoffski P, Terrier P, Neuville A, Coindre JM, Italiano A, Orbach D, Debiec-Rychter M, Chibon F: Chromosome instability accounts for reverse metastatic outcomes of pediatric and adult synovial sarcomas. J Clin Oncol 2013, 31:608-15.
[181] Orbach D, Mosseri V, Pissaloux D, Pierron G, Brennan B, Ferrari A, Chibon F, Bisogno G, De Salvo GL, Chakiba C, Corradini N, Minard-Colin V, Kelsey A, Ranchere-Vince D: Genomic complexity in pediatric synovial sarcomas (Synobio study): the European pediatric soft tissue sarcoma group (EpSSG) experience. Cancer Med 2018, 7:1384-93.
[182] Miettinen M, Fetsch JF: Evaluation of biological potential of smooth muscle tumours. Histopathology 2006, 48:97-105.
[183] Zhai YL, Nikaido T, Orii A, Horiuchi A, Toki T, Fujii S: Frequent occurrence of loss of heterozygosity among tumor suppressor genes in uterine leiomyosarcoma. Gynecol Oncol 1999, 75:453-9.
[184] Mittal KR, Chen F, Wei JJ, Rijhvani K, Kurvathi R, Streck D, Dermody J, Toruner GA: Molecular and immunohistochemical evidence for the origin of uterine leiomyosarcomas from associated leiomyoma and symplastic leiomyoma-like areas. Mod Pathol 2009, 22:1303-11.
[185] Przybora LA: Leiomyosarcoma in situ of the uterus. Cancer 1961, 14:483-92.
[186] Tomita T: DNA ploidy and proliferating cell nuclear antigen in colonic adenomas and adenocarcinomas. Dig Dis Sci 1995, 40:996-1004.
[187] Ramos P, Karnezis AN, Craig DW, Sekulic A, Russell ML, Hendricks WP, Corneveaux JJ, Barrett MT, Shumansky K, Yang Y, Shah SP, Prentice LM, Marra MA, Kiefer J, Zismann VL, McEachron TA, Salhia B, Prat J, D'Angelo E, Clarke BA, Pressey JG, Farley JH, Anthony SP, Roden RB, Cunliffe HE, Huntsman DG, Trent JM: Small cell carcinoma of the ovary, hypercalcemic type, displays frequent inactivating germline and somatic mutations in SMARCA4. Nat Genet 2014, 46:427-9.
[188] Ramos P, Karnezis AN, Hendricks WP, Wang Y, Tembe W, Zismann VL, Legendre C, Liang WS, Russell ML, Craig DW, Farley JH, Monk BJ, Anthony SP, Sekulic A, Cunliffe HE, Huntsman DG, Trent JM: Loss of the tumor suppressor SMARCA4 in small cell carcinoma of the ovary, hypercalcemic type (SCCOHT). Rare Dis 2014, 2:e967148.
[189] Kolin DL, Dong F, Baltay M, Lindeman N, MacConaill L, Nucci MR, Crum CP, Howitt BE: SMARCA4-deficient undifferentiated uterine sarcoma (malignant rhabdoid tumor of the uterus): a clinicopathologic entity distinct from undifferentiated carcinoma. Mod Pathol 2018, 31:1442-56.
[190] Flicker K, Smolle E, Haybaeck J, Moinfar F: Genomic characterization of endometrial stromal sarcomas with array comparative genomic hybridization. Exp Mol Pathol 2015, 98:367-74.
[191] Croce S, Hostein I, Longacre TA, Mills AM, Perot G, Devouassoux-Shisheboran M, Velasco V, Floquet A, Guyon F, Chakiba C, Querleu D, Khalifa E, Mayeur L, Rebier F, Leguellec S, Soubeyran I, McCluggage WG: Uterine and vaginal sarcomas resembling fibrosarcoma: a clinicopathological and molecular analysis of 13 cases showing common NTRK-rearrangements and the description of a COL1A1-PDGFB fusion novel to uterine neoplasms. Mod Pathol 2019, 32:1008-22.
[192] Ly A, Mills AM, McKenney JK, Balzer BL, Kempson RL, Hendrickson MR, Longacre TA: Atypical leiomyomas of the uterus: a clinicopathologic study of 51 cases. Am J Surg Pathol 2013, 37:643-9.
[193] Kaelin WG, Jr.: SDH5 mutations and familial paraganglioma: somewhere Warburg is smiling. Cancer Cell 2009, 16:180-2.
[194] Sourbier C, Valera-Romero V, Giubellino A, Yang Y, Sudarshan S, Neckers L, Linehan WM: Increasing reactive oxygen species as a therapeutic approach to treat hereditary leiomyomatosis and renal cell carcinoma. Cell Cycle 2010, 9:4183-9.
[195] Sudarshan S, Sourbier C, Kong HS, Block K, Valera Romero VA, Yang Y, Galindo C, Mollapour M, Scroggins B, Goode N, Lee MJ, Gourlay CW, Trepel J, Linehan WM, Neckers L: Fumarate hydratase deficiency in renal cancer induces glycolytic addiction and hypoxia-inducible transcription factor 1alpha stabilization by glucose-dependent generation of reactive oxygen species. Mol Cell Biol 2009, 29:4080-90.
[196] Chunduri NK, Storchova Z: The diverse consequences of aneuploidy. Nat Cell Biol 2019, 21:54-62.
[197] Salama R, Sadaie M, Hoare M, Narita M: Cellular senescence and its effector programs. Genes Dev 2014, 28:99-114.

[198] Giuntoli RL, 2nd, Metzinger DS, DiMarco CS, Cha SS, Sloan JA, Keeney GL, Gostout BS: Retrospective review of 208 patients with leiomyosarcoma of the uterus: prognostic indicators, surgical management, and adjuvant therapy. Gynecol Oncol 2003, 89:460-9.
[199] Wright JR, Jr.: Albert C. Broders' paradigm shifts involving the prognostication and definition of cancer. Arch Pathol Lab Med 2012, 136:1437-46.
[200] Trojani M, Contesso G, Coindre JM, Rouesse J, Bui NB, de Mascarel A, Goussot JF, David M, Bonichon F, Lagarde C: Soft-tissue sarcomas of adults; study of pathological prognostic variables and definition of a histopathological grading system. Int J Cancer 1984, 33:37-42.
[201] Coindre JM: Grading of soft tissue sarcomas: review and update. Arch Pathol Lab Med 2006, 130:1448-53.
[202] Zivanovic O, Leitao MM, Iasonos A, Jacks LM, Zhou Q, Abu-Rustum NR, Soslow RA, Juretzka MM, Chi DS, Barakat RR, Brennan MF, Hensley ML: Stage-specific outcomes of patients with uterine leiomyosarcoma: a comparison of the international Federation of gynecology and obstetrics and american joint committee on cancer staging systems. J Clin Oncol 2009, 27:2066-72.
[203] Ricci S, Stone RL, Fader AN: Uterine leiomyosarcoma: Epidemiology, contemporary treatment strategies and the impact of uterine morcellation. Gynecol Oncol 2017.
[204] Amant F, Coosemans A, Debiec-Rychter M, Timmerman D, Vergote I: Clinical management of uterine sarcomas. Lancet Oncol 2009, 10:1188-98.
[205] Amant F, Lorusso D, Mustea A, Duffaud F, Pautier P: Management Strategies in Advanced Uterine Leiomyosarcoma: Focus on Trabectedin. Sarcoma 2015, 2015:704124.
[206] Iasonos A, Keung EZ, Zivanovic O, Mancari R, Peiretti M, Nucci M, George S, Colombo N, Carinelli S, Hensley ML, Raut CP: External validation of a prognostic nomogram for overall survival in women with uterine leiomyosarcoma. Cancer 2013, 119:1816-22.
[207] Miyata T, Sonoda K, Tomikawa J, Tayama C, Okamura K, Maehara K, Kobayashi H, Wake N, Kato K, Hata K, Nakabayashi K: Genomic, Epigenomic, and Transcriptomic Profiling towards Identifying Omics Features and Specific Biomarkers That Distinguish Uterine Leiomyosarcoma and Leiomyoma at Molecular Levels. Sarcoma 2015, 2015:412068.
[208] Kommoss FKF, Stichel D, Schrimpf D, Kriegsmann M, Tessier-Cloutier B, Talhouk A, McAlpine JN, Chang KTE, Sturm D, Pfister SM, Romero-Perez L, Kirchner T, Grunewald TGP, Buslei R, Sinn HP, Mechtersheimer G, Schirmacher P, Schmidt D, Lehr HA, Sahm F, Huntsman DG, Gilks CB, Kommoss F, von Deimling A, Koelsche C: DNA methylation-based profiling of uterine neoplasms: a novel tool to improve gynecologic cancer diagnostics. J Cancer Res Clin Oncol 2020, 146:97-104.